Genome instability induced by structured DNA and replication fork restart

Stephanie Schalbetter

Submitted for the degree of Doctor of Philosophy

University of Sussex

January 2012

Declaration

I hereby declare that this thesis has not been and will not be submitted in whole or in part to another University for the award of any other degree.

Signature:

Stephanie Schalbetter

Acknowledgements

I would like to thank Tony Carr for the opportunity to do my PhD in his lab and for his continuous support and very good cooking. Many thanks also to Jo Murray who has supported my work with helpful discussions, good advice and many hours of reading the first drafts of my thesis. Many thanks to Tony and Jo for their kindness and never-ending patience (or high threshold).
Many thanks to my co-supervisor Jessica Downs for helpful discussions and suggestions and to all previous and current members of the Carr, Murray and O'Driscoll labs for an enjoyable time and a good working environment.

I would like to acknowledge two project students, Sarah Curry and Rebecca Haigh, and a summer student, Sina-Maria Schalbetter, who have worked on the Mus81 and the BirA projects with a lot of motivation and enthusiasm. Many thanks to our collaborators at the LRI, Neil McDonald, Andrew Fadden and Maureen Biggerstaff for sharing their results and knowledge about Mus81.

I am obliged to many of my colleagues who taught me scientific techniques in the lab and helped me setting up my experiments. Special thanks to Valerie, Yasu, Ken'Ichi, Izumi, Adam, Edgar, Rolf, Takashi, Chris, Amal and Kostas for supervision and critical discussions. I am grateful to Ann-Sofie and Chieh-Ju for their help with the microscopy imaging and to Tony Oliver for his supervision and advice for the CD measurements. Many thanks to Yari for his friendship and company as a co-PhD student, starting at the same time in the lab and to Ellen for critical reading of my thesis.

I am thankful to all the GDSC staff for their support. I am especially grateful to Gee (Mother Gnome), Graham, Marie and Bernie for their help and to Bob for the jokes even I can understand.

Ganz speziell möchte ich meiner Familie danken für deren Unterstützung, Verständnis und die Ermöglichung meines Studiums. Vielen Dank an Niki für seine Liebe und Geduld, speziell während dieser Zeit. Ohne euch alle hätte ich das nicht geschafft.
Merci villmal!

UNIVERSITY OF SUSSEX

Stephanie Schalbetter

A thesis submitted for the degree of Doctor of Philosophy

Genome instability induced by structured DNA and replication fork restart

DNA replication is a central mechanism to all forms of life. Errors occurring during DNA replication can result in mutagenesis and genome rearrangements, which can cause various diseases. In this work I have investigated the stability of direct tandem repeats (TRs) in the context of replication and replication-associated repair mechanisms. During DNA replication the replication fork encounters many obstacles, such as DNA-protein barriers, secondary DNA structures and DNA lesions. How and if replication resumes or restarts in these circumstances in order to complete genome replication is not well understood and the fidelity of replication in response to such obstacles remains unclear. I have developed TR assays to assess replication errors in the context of replication fork restart and secondary structures. The results suggest that structured DNA (G4) can cause instability of TRs in the context of normal replication and that restarted replication can be intrinsically error-prone. Surprisingly, the mutagenic effect of G4-DNA on TR stability was not elevated in the context of replication fork restart. Therefore, deletions of TRs containing G4-DNA are not more susceptible to the compromised fidelity of a restarted replication fork.

Structures such as stalled replication forks can induce checkpoint responses to maintain genome stability. The stabilisation of replication forks is central in the response to replication stress. These protective mechanisms include the regulation of enzymatic activities. Mus81-Eme1 is a structure-specific endonuclease which is regulated by the DNA replication checkpoint, but has also been shown to be required for replication fork restart in certain circumstances. In collaboration with Professor Neil McDonald I analysed a novel domain identified in Mus81-Eme1. Mutagenesis of key residues deduced from the protein structure and comparison of their genetic analysis to known phenotypes of Mus81-Eme1 suggests distinct requirements for this domain.

Contents

List of Tables xi

List of Figures xiv

1 Introduction 1

1.1 The model organism *Schizosaccharomyces pombe* . . . 1

1.1.1 A brief history . . . 2

1.1.2 *S. pombe* characteristics . . . 2

1.2 The cell cycle and its regulation . . . 2

1.3 Eukaryotic DNA replication . . . 3

1.3.1 Initiation of DNA replication . . . 3

1.3.1.1 Formation of the pre-replication complex (pre-RC) . . . 4

1.3.1.2 Maturation of the pre-RC . . . 4

1.3.2 Regulation of DNA replication in the cell cycle . . . 6

1.3.3 Progression of DNA replication . . . 6

1.3.3.1 Unwinding of the DNA . . . 7

1.3.3.2 DNA synthesis . . . 7

1.3.3.3 Lagging strand DNA synthesis . . . 8

1.4 Checkpoint activation in response to DNA damage and replication stress . . . 11

1.4.1 Early observations defining the checkpoint concept . . . 11

1.4.2 DNA damage and replication checkpoints: an overview . . . 12

1.4.3 Sensing DNA perturbations . . . 13

1.4.4 Checkpoint mediators . . . 15

1.4.5 Responses to replication stress and DNA damage . . . 16

1.5 DNA repair and genome integrity . . . 18

1.5.1 The role of mismatch repair (MMR) in the fidelity of DNA replication . . . 18

1.5.2 Base excision repair (BER) and nucleotide excision repair (NER) . . . 19

1.5.2.1 Base excision repair . . . 19
1.5.2.2 Nucleotide Excision Repair . . . 20
1.5.3 Nonhomologous end joining (NHEJ) and HR in DSB repair . . . 20
1.5.3.1 Nonhomologous end joining . . . 21
1.5.3.2 Homologous recombination . . . 21
1.5.3.3 Single-strand annealing (SSA) . . . 25
1.5.3.4 Recombination products: gene conversion (GC) and loss of heterozygosity (LOH) . . . 26
1.5.4 Recombination and replication . . . 26
1.5.5 Postreplication repair (PRR) . . . 28
1.6 Replication fork barriers (RFBs) . . . 30
1.6.1 Structured DNA: G-quadruplex DNA (G4-DNA) . . . 30
1.6.1.1 Structure of G4-DNA . . . 30
1.6.1.2 Conservation and localisation of G4-DNA . . . 30
1.6.1.3 G4-DNA and telomeres . . . 32
1.6.1.4 G4-DNA, transcription and translation . . . 33
1.6.1.5 Genome instability associated with G4-DNA . . . 33
1.6.2 rDNA RFB . . . 35
1.6.3 Replication termination sequence 1 (RTS1) . . . 37
1.7 Analysis of site-specific replication fork arrest using DNA-protein RFBs . . . 39
1.8 Aims of this work . . . 42

2 Materials and Methods **43**
2.1 Abbreviations, contents and information of frequently used solutions and chemicals 43
2.2 Media . . . 43
2.2.1 Yeast Extract (YE), rich media . . . 43
2.2.2 YE agar plates (YEA) . . . 43
2.2.3 Edinburgh Minimal Media (EMM) . . . 43
2.2.3.1 20x EMM2 salts . . . 44
2.2.3.2 10000x Trace elements . . . 44
2.2.3.3 1000x Vitamins . . . 44
2.2.4 Drugs and chemicals used for selection . . . 45
2.3 List of strains . . . 46
2.4 List of oligonucleotides . . . 51
2.5 Molecular cloning techniques . . . 53

2.5.1 Restriction digests . . . 53
2.5.2 Ligation . . . 53
2.5.3 Fusion PCR . . . 53
2.5.4 *E. coli* transformation . . . 54
2.5.5 Plasmid extraction from *E. coli* cells (Miniprep, Midiprep) . . . 54
2.5.6 Site-directed mutagenesis . . . 54
2.6 Yeast techniques . . . 55
2.6.1 *S. pombe* genetic crosses . . . 55
2.6.1.1 Random spore analysis . . . 55
2.6.1.2 Tetrad dissection . . . 55
2.6.2 *S. pombe* transformation . . . 55
2.6.3 Gene disruption . . . 55
2.6.4 Construction of base strains . . . 56
2.6.5 RMCE . . . 56
2.6.6 Chromosomal DNA preparation . . . 56
2.6.7 Yeast colony PCR . . . 57
2.6.8 Fluctuation analysis . . . 57
2.6.9 Restriction fragment length analysis (RFLA) by Southern blotting . . . 58
2.6.10 Whole cell protein extracts using TCA extraction . . . 59
2.6.11 Protein analysis by Immunostaining (Western blot) . . . 60
2.6.11.1 Specifications of antibodies used in this thesis and dilution factors 61
2.6.12 Microscopy . . . 61
2.7 Additional information - Materials and Methods - Chapter 3 . . . 61
2.7.1 Circular dichroism (CD) spectroscopy . . . 61
2.8 Additional information - Materials and Methods - Chapter 4 . . . 62
2.8.1 Agarose plugs for restriction digest and RFLA . . . 62
2.8.2 Restriction digest of DNA embedded in agarose plugs . . . 62
2.8.3 DNA separation using agarose plugs . . . 63
2.8.4 Alkaline gel electrophoresis . . . 63
2.9 Additional information - Materials and Methods - Chapter 5 . . . 63
2.9.1 RMCE in the ura4 base strain . . . 63
2.9.2 pAW8-ruraR plasmid and *arg3 82TR* constructs . . . 64
2.10 Additional information - Materials and Methods - Chapter 6 . . . 64
2.10.1 Mus81 mutants . . . 64

2.10.2 Colony mismatch PCR for the detection of point mutations 65
2.10.3 Chromatin binding assay (fractionation) 66
2.11 Additional information - Materials and Methods - Appendix I 67
2.11.1 Whole protein extracts (native conditions) 67
2.11.2 Dialysis 67
2.11.3 Pulldown experiments using Dynabeads MyOne Streptavidin T1 (Invitrogen, 65601) 67
2.11.4 Immunoprecipitation (IP) using antibody-coated magnetic beads 68

3 Effects of replication fidelity and replication-associated repair processes on the stability of small direct tandem repeats 69

3.1 Introduction 69
3.2 Aim of the project and summary 70
3.3 Characterisation of TR deletions by fluctuation analysis, PCR and sequencing . . 72
3.4 TR deletion events are independent of homologous recombination, postreplication repair and mismatch repair 77
3.5 DNA damage induced by ultraviolet (UV) radiation and methyl methanesulfonate (MMS) do not increase TR deletion rates 79
3.6 Mutations compromising the replisome and the replication checkpoint increase TR deletion rates 82
3.7 *nat1 101TR* contains a putative G4-motif 84
3.8 Conclusion and discussion 87

4 Genomic instability after replication fork collapse and restart 91

4.1 Introduction 91
4.2 Aim of the project and summary 93
4.3 Constructs, rura(dir)R and rura(inv)R, for analysis of error-prone replication after restart 95
4.4 Replication fork collapse at RTS1 in rura(dir)R and rura(inv)R induces rearrangements restoring *ura4*$^+$ 95
4.5 PCR analysis of the rearrangements restoring *ura4*$^+$ 97
4.6 Restriction fragment length analysis (RFLA) of ura+ cells after replication fork collapse 100
4.7 Detection of dicentric and acentric chromosomes after replication fork collapse in rura(inv)R by RFLA of bulk DNA 103

4.8 Analysis of bulk DNA after replication fork collapse by a different method of DNA preparation . . . 107
4.9 Microscopy of rura(dir)R and rura(inv)R cells before and after replication fork collapse . . . 110
4.10 Conclusion and discussion . . . 110

5 TR instability induced by G4-DNA and erroneous replication after fork restart 114
5.1 Introduction . . . 114
5.2 Aim of the project and summary . . . 115
5.3 Overview of *arg3 82TR* constructs . . . 116
5.4 Effect of HR, MMR, PRR and *mrc1*$^{+}$ on TR deletions in the absence of G4-DNA 118
5.5 The effect of G4-DNA on TR deletions . . . 120
5.6 The effect of *rev1*$^{+}$ on *G4 TR* stability on the leading and the lagging strand . . . 123
5.7 TR instability and HR-dependent replication fork restart . . . 124
5.8 Genetic analysis of a restarted replication fork . . . 126
5.9 Conclusion and discussion . . . 128

6 *In vivo* analysis of the *S. pombe* Mus81 winged helix domain 131
6.1 Introduction and background . . . 131
6.1.1 Structural characterisation of Mus81-Eme1/Eme2/Mms4 . . . 132
6.1.2 *In vitro* substrate specificity of Mus81-Eme1/Mms4 . . . 133
6.1.3 Roles of Mus81-Eme1/Mms4 in HR, at broken forks and its regulation by Cds1 . . . 136
6.1.4 Implications of Mus81-Eme1/Mms4 in HR in the context of replication . 137
6.1.5 Mus81-Eme1/Mms4 in meiosis and the role of *scYEN1* . . . 140
6.1.6 Mus81-Eme1 in higher organisms . . . 141
6.2 Background and aim of the project . . . 142
6.3 Mutations of the winged helix domain of Mus81 in *S. pombe* . . . 143
6.4 Effects of WH mutations on protein localisation . . . 146
6.5 The *mus81-KE* mutant: a separation of function? . . . 149
6.6 Conclusion and discussion . . . 153

7 Final discussion and conclusions 156
7.1 The importance of studying DNA replication and genome rearrangements . . . 156
7.2 TR deletions in the context of their sequence content . . . 158
7.3 Why is replication restarted at RTS1 error-prone? . . . 160

7.4 Which function of Mus81-Eme1 is defective in the *Mus81-KE* mutant? 163
7.5 A biochemical assay for proximity-dependent protein modification 166

Bibliography **168**

A Proximity-dependent protein biotinylation **217**
A.1 Introduction and background 217
A.2 Initial protein tagging and expression of candidates (work done by R. Haigh) . . 219
A.3 Biotinylation of the Rad4 interaction partner Rad9 220
A.4 Overexpression of BirA and R118G in *E. coli* and *S. pombe* 223
A.5 Discussion 228

B Analysis of the short PCR product amplified from rura(inv)R **229**

List of Tables

2.1 List of frequently used chemicals and solutions 44
2.2 List of DNA damaging agents and drugs used for selection 45
2.3 List of strains 50
2.4 List of oligonucleotides 53
2.5 List of antibodies 61
2.6 List of primers used to generate Mus81 mutants 65

List of Figures

1.1 **Eukaryotic DNA replication** . . . 5
1.2 **Replication perturbations and its consequences** . . . 10
1.3 **The DNA damage and replication checkpoints** . . . 13
1.4 **Pathway overview of homologous recombination** . . . 22
1.5 **Postreplication repair initiated by ubiquitylation of PCNA** . . . 29
1.6 **G-quadruplex structure** . . . 31
1.7 **Protein-DNA replication fork barriers (RFBs)** . . . 36
1.8 **RFB systems** . . . 40

3.1 **Rearrangements in tandem repeat sequences due to replication errors or associated repair pathways** . . . 71
3.2 **Cloning of a tandem repeat assay in *Schizosaccharomyces pombe*** . . . 73
3.3 **Fluctuation analysis of TR deletion rates of 101bp, 41bp and 251bp** . . . 76
3.4 **TR deletions are not dependent on homologous recombination or postreplication repair and not suppressed by mismatch repair** . . . 78
3.5 **Treatment with DNA damaging agents does not increase PRR-dependent deletion events** . . . 80
3.6 **Replication mutants increase TR deletion events, independently of PRR** . . . 83
3.7 **The *nat1 TR* sequence contains a putative G4 motif** . . . 85

4.1 **Schematics of RTS1 and rDNA RFB constructs at the *ura4* locus** . . . 93
4.2 **Replication fork collapse at RTS1 induces rearrangements in rura(dir)R and rura(inv)R which restore *ura4*$^+$** . . . 96
4.3 **PCR analysis confirms the expected rearrangements in rura(dir)R and rura(inv)R to restore *ura4*$^+$** . . . 98
4.4 **Confirmation of *ura4* rearrangements by Restriction Fragment Length Analysis (RFLA) using *Ase*I** . . . 101

4.5 Confirmation of orientation switch in rura(inv)R by RFLA using *Ase*I and *Sca*I . . 102
4.6 RFLA of bulk DNA reveals the formation of palindromic chromosomes in RuiuR and rura(inv)R . . . 105
4.7 RFLA of bulk DNA detects an orientation switch rura(inv)R . . . 106
4.8 RFLA of bulk DNA using DNA plugs instead of phenol extracted genomic DNA reduced the amounts of half fragments 'a/2' and 'd/2' in RuiuR . . . 108
4.9 RFLA of bulk DNA using DNA plugs and *Hind*III to visualise the orientation switch in 'c' . . . 109
4.10 Aberrant mitosis in cells containing an inverted repeat nearby an active RTS1 . . . 111

5.1 Overview of the *arg 82TR* constructs in the rDNA RFB-*ura4*$^{+}$-RTS1 locus . . . 117
5.2 Genetic dependency of TR deletions in the *arg3 TR* assay . . . 119
5.3 The intrinsic instability of TRs is higher in the presence of a G4 motif . . . 121
5.4 Effect of transcription direction on TR deletions . . . 122
5.5 G4 TR deletions in *rev1*△ cells . . . 123
5.6 TR instability induced by replication fork collapse and restart . . . 125
5.7 Genetic analysis of a restarted replication fork . . . 127

6.1 Identification of a winged helix (WH) domain in the N-terminus of human MUS81 . 134
6.2 DNA damage sensitivity of conserved residues in the *S. pombe* Mus81 WH domain . 144
6.3 Localisation of Mus81 WH mutant proteins . . . 147
6.4 *Mus81-KE* is proficient in meiosis and sister-chromatid recombination . . . 150
6.5 Genetic interactions of *mus81-KE* with *rad2*△, *rqh1*△ and mutant alleles of the Smc5/6 complex . . . 152

7.1 Overview of RTS1 constructs and the replication restart model . . . 162
7.2 Role of Mus81 in the processing of collapsed and broken replication forks and defects in *mus81-KE* cells . . . 165
7.3 Overview of RTS1 constructs and the replication restart model . . . 167

A.1 A novel method for identification of interaction partners . . . 218
A.2 Pulldown of Rad4-R118G by streptavidin-coated beads . . . 221
A.3 Pulldown by streptavidin-coated beads and immunoprecipitation (IP) of Rad9-HA . 223
A.4 Overexpression of BirA and R118G in *E. coli* and *S. pombe* cells . . . 225
A.5 Random biotinylation is dependent on the presence of additional biotin . . . 226
A.6 IP of Rad9-HA and detection with streptavidin-HRP conjugate . . . 227

B.1 **Analysis of the short PCR fragment resulting from rura(inv)R PP5** 230

Chapter 1

Introduction

The genome of a cell consists of deoxyribonucleic acid (DNA) and carries the hereditary information essential to all forms of life. In order to transmit this information to the next generation, it needs to be duplicated and segregated to the daughter cells. This process is the key to cell proliferation and is described as the cell cycle. The integrity of the genome needs to be preserved throughout the cell cycle to avoid mutations, which can result in uncontrolled cell proliferation and disease.

Sources of mutagenesis can be DNA replication itself or DNA damage. In this introduction I will give insights into the fundamental processes of DNA replication, DNA checkpoints and DNA repair that detect DNA damage and replication stress and coordinate cellular responses. In particular I want to emphasise consequences and sources of DNA replication perturbations. In more detail I will summarise the knowledge about the structure-specific endonuclease Mus81-Eme1, which was implicated in replication fork restart and DNA repair. I will also give some background information about *S. pombe*, which was used as a model organism for this work. Throughout the introduction I will refer to human proteins using *h* as a prefix and similarly for *Schizosaccharomyces pombe sp* and *Saccharomyces cerevisiae sc*.

1.1 The model organism *Schizosaccharomyces pombe*

The fission yeast *Schizosaccharomyces pombe* (*S. pombe*) is a valuable model organism to investigate biological questions and its easy access for molecular and genetic methods enables researchers to gain insight into biological mechanisms. In this work, I have used *S. pombe* as a model to study DNA replication and repair.

1.1.1 A brief history

S. pombe is a unicellular eukaryote belonging to the family of ascomycetous fungi. The widely used laboratory strains 968, 972 and 975 originate from a culture isolated from french wine by A. Osterwalder in 1924 in Switzerland (PombeNet http://www-bcf.usc.edu/∼forsburg/main.html). In the 1940s Urs Leupold started to characterise the isolated strains used today and build up the genetic infrastructure of *S. pombe* as a model organism (Leupold, 1949). Independently, Murdoch Mitchison started to investigate the physiology of cell division using a different isolate of *S. pombe* as a model organism in the early 1950s (Mitchison, 1957).

1.1.2 *S. pombe* characteristics

S. pombe is distantly related to the budding yeast *Saccharomyces cerevisiae* (*S. cerevisiae*), however evolutionarily the yeasts are as diverged from each other as from mammals (Sipiczki, 2000). *S. pombe* cells grow vegetatively as haploids, but can also be grown as diploids under selection. A haploid cell is 12-15μm long (at division) and 3-4 μm wide and the doubling time ranges from 2-5 hours, depending on the media (PombeNet http://www-bcf.usc.edu/∼forsburg). The 13.8Mb genome of *S. pombe* is divided into three chromosomes (Kohli et al., 1977). The genome sequence was published in 2002 by Wood et al. (2002) and 4940 protein coding genes were predicted. The mitotic cell cycle of *S. pombe* cells is characteristic in its predominant G2 phase, followed by M, G1 and S, where the G1 phase is very short. The relatively long G2 phase might reflect the preference of two genome copies rather than one. This is compared to the yeast *S. cerevisiae* which preferentially grows as a diploid and the cell cycle is dominated by G1 (Egel et al., 1980; Herskowitz, 1988).

1.2 The cell cycle and its regulation

The cell cycle is divided into four phases; G1, S, G2 and M. Central to this process is the replication of the genome in S-phase (S for synthesis) and its segregation to the daughter cells in M-phase (M for mitosis) before cell division. S- and M-phases are divided by two gap phases, G1 and G2 (Nurse, 1991). In eukaryotes, cyclin-dependent kinases (CDKs) control the progression through the cell cycle. Changes in CDK activity during the cell cycle and the resulting phosphorylation of target proteins are crucial for the regulation of cellular processes like DNA replication, segregation and repair (Nurse, 1997; Branzei and Foiani, 2008).

Higher eukaryotes express several CDKs, whereas the yeasts *S. pombe* and *S. cerevisiae* express only one counterpart, Cdc2 and Cdc28, respectively (Cdc, for cell division cycle) (Nurse,

1997). The activity of CDKs is dependent on their association with cyclins. Cyclins are specific to each cell cycle phase and their levels oscillate throughout the cell cycle, whereas the level of CDKs remains fairly constant (Alberts et al., 2002). Full activation of the CDK-cyclin complexes requires its phosphorylation by a CDK activating kinase (CAK) and CDK activity can be further regulated by inhibitory phosphorylation and association with inhibitory proteins (CKIs) (Alberts et al., 2002; Nurse, 1991). The CDK inhibitory kinase Wee1 and the activating phosphatase Cdc25 play important roles in the regulation of CDK by inhibitory phosphorylation and activating dephosphorylation of the catalytic subunit of CDK, respectively (Thuriaux et al., 1978; Russell and Nurse, 1986; Nurse, 2002).

CDK activity is high during S-phase and early mitosis to initiate replication and chromosome segregation (Nurse, 1991). In late M-phase, CDKs are inactivated and activity stays low during G1-phase until the next S-phase. The low levels of CDK from late M- to early S-phase is due to CDK inhibitors and cyclin proteolysis initiated by the APC/C (anaphase promoting complex or cyclosome) and its regulatory subunits Cdc20 and Cdh1 (Diffley, 2004). The APC/C is a E3 ubiquitin ligase, which targets many regulatory mitotic proteins for degradation (Alberts et al., 2002). Increasing activity of CDKs at the onset of S-phase requires the degradation of CKIs by SCF, another E3 ubiquitin ligase (Diffley, 2004).

1.3 Eukaryotic DNA replication

In the process of DNA replication, the parental DNA needs to be separated and copied by DNA polymerisation reactions (Aves, 2009). DNA synthesis mainly occurs in S-phase and the whole process of DNA replication can be separated into different steps that follow one another through the cell cycle in a distinct manner, so that the genome is duplicated only once per cell cycle. Although the proteins acting in DNA replication are highly conserved, the mechanisms of regulation can vary between different organisms (Kearsey and Cotterill, 2003). An overview of the establishment of replication forks is shown in Figure 1.1A and described in more detail below.

1.3.1 Initiation of DNA replication

Whereas replication of the circular genomes of prokaryotes is initiated from a single origin, eukaryotic genomic replication is initiated from multiple origins on the chromosomes (Aves, 2009). Origins in *S. cerevisiae* consist of a small conserved sequence essential for origin function (Kearsey, 1984; Palzkill and Newlon, 1988). However, in *S. pombe* as well as in higher eukaryotes, the origin sequences are generally larger and less well defined (Aves, 2009). *S. pombe* origins were found to be 500bp to 1500bp in size, containing AT-rich sequences, but, unlike in *S.*

cerevisiae, lacking an essential motif (Maundrell et al., 1988; Clyne and Kelly, 1995).

1.3.1.1 Formation of the pre-replication complex (pre-RC)

The formation of replication complexes at origins and their activation is essential for DNA replication (Aves, 2009). Stepwise accumulation of proteins at origins establish the pre-RC, that can mature into a functional replisome progression complex (RPC), which actively replicates the genome once per cell cycle. Pre-RC formation is also referred to as "licensing", which describes the loading of the 6-subunit origin recognition complex (ORC, Orc1-6) and the putative replicative helicase hexamer Mcm2-7 (MCM, for minichromosome maintenance) by Cdt1 and Cdc18 (*sc*Cdc6) at origins (Araki, 2011). ORC binds to origins in an ATP-dependent manner continuously during the cell cycle in *S. cerevisiae* and in late M-/G1-phase in *S. pombe* (Bell and Stillman, 1992; Wu and Nurse, 2009). Interestingly, *S. pombe* Orc4 was shown to contain an AT-hook which binds to AT-rich regions, including the autonomously replicating sequence 1 (ars1) (Lee et al., 2001). In order to establish a bidirectional replication fork (Figure 1.1B), at least two copies of the MCM complex have to be loaded onto origins (Remus et al., 2009; Evrin et al., 2009).

1.3.1.2 Maturation of the pre-RC

Once the pre-RC is formed in late M-/G1-phase, its maturation and the activation of the MCM helicase is dependent on two essential kinases, *sc*Cdc7-Dbf4 or DDK for Dbf4-dependent kinase (*sp*Hsk1-Dfp1/Him1) and the S-phase cyclin-dependent kinase CDK (*sp*Cdc2 and *sc*Cdc28), which are active in S-phase (Labib, 2010). The activity of these two kinases is crucial for the assembly of replication factors and the activation of the replicative helicase (Labib, 2010).

Sld2 and Sld3 were shown to be the minimal requirement of S-CDK substrates for initiation of DNA replication in *S. cerevisiae* (Zegerman and Diffley, 2007). Sld (sld for synthetically lethal with dpb11-1) proteins were initially identified by a screen for factors that genetically interact with *DPB11* (*sp*Rad4 and *h*TopBP1), an essential gene for DNA replication (Kamimura et al., 1998). The phosphorylation of Sld2 and Sld3 by CDK creates binding sites for Dpb11 (Tak et al., 2006; Zegerman and Diffley, 2007). Sld3 further interacts with Cdc45 (Sld4) and they associate with origins (Kamimura et al., 2001). Recently it was discovered that Sld3 exists in a complex with Sld7 (Tanaka et al., 2011). Sld2 forms a fragile complex with GINS (Sld5, Psf1-3), the replicative polymerase ε (Pol ε) and Dpb11 in a CDK-dependent manner (Muramatsu et al., 2010). These interactions assemble key factors of the RPC at origins; Cdc45, MCM, GINS and Pol ε. The main targets of the Cdc7-Dbf4 kinase seem to be five out of six MCM proteins (Lei et al., 1997; Weinreich and Stillman, 1999). Importantly, in eukaryotes, the MCM complex loaded at pre-RCs

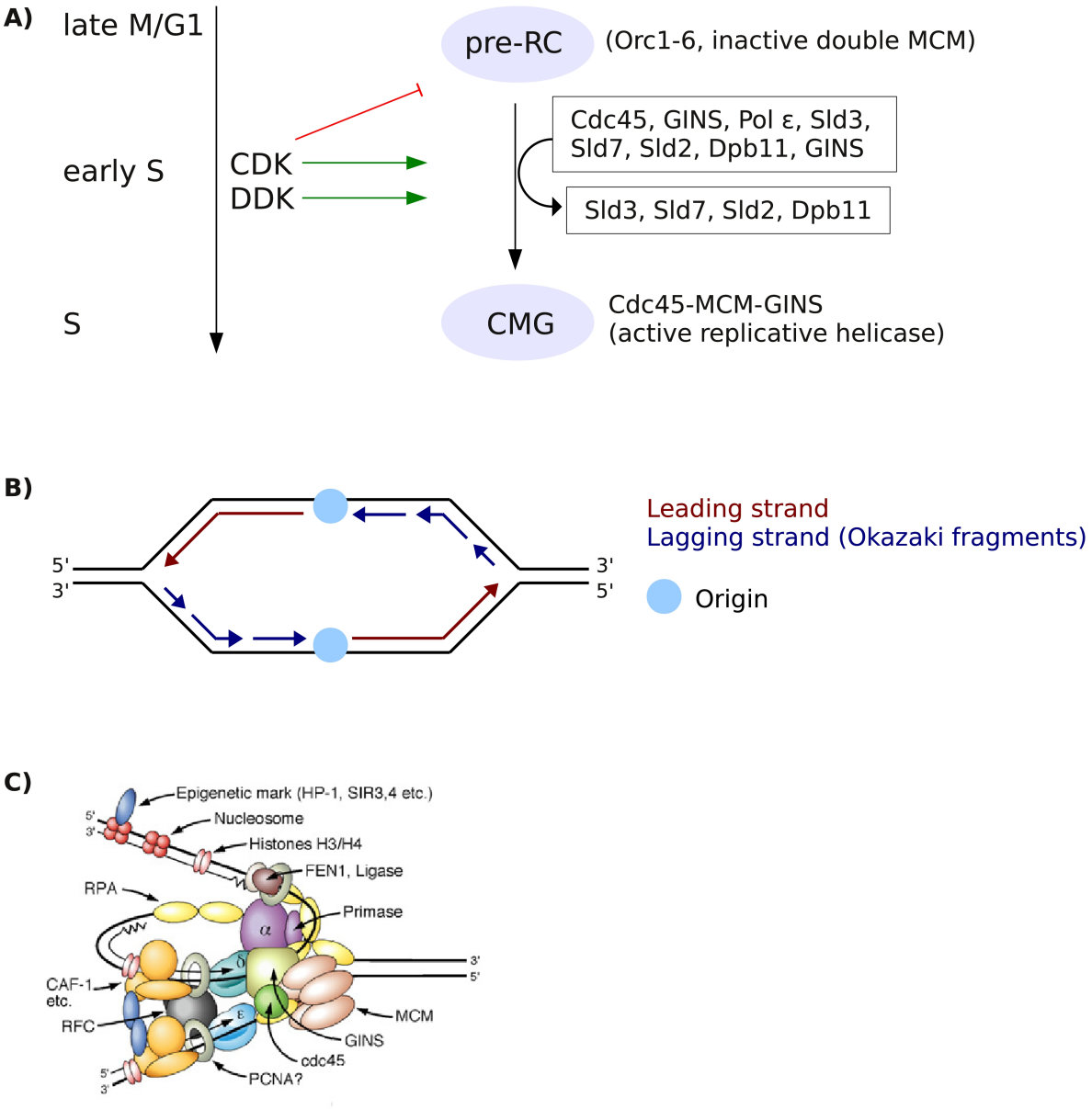

Figure 1.1: Eukaryotic DNA replication
A) Establishment of active replication forks. Pre-replication complex (pre-RC) formation describes the loading of the inactive MCM helicase at origins and is restricted to late M- and G1-phase. Increasing CDK activity at early S-phase catalyses the loading of additional factors important for replication. GINS and Cdc45 are recruited to the pre-RC through interactions with Sld2 and Sld3, respectively, which bind to Dpb11 (*sp*Rad4). Cdc45, MCM and GINS (CMG) are thought to form the active replicative helicase complex. DDK targets the MCM complex and is, together with CDK, required for activation of replication (origin firing).
B) Progression of DNA replication. DNA consists of two paired anti-parallel strands of bases with a sugar (deoxyribose)-phosphate backbone. The sugars are linked through the phosphate group at the 3'- and the 5'-position. This gives DNA strands a direction, 5' to 3' or 3' to 5'. DNA is synthesised in the 5' to 3' direction. This is expected to result in semi-discontinuous replication; continuous replication of the leading strand (red) and discontinuous replication of the lagging strand (blue). The discontinuous replication of the lagging strand forms Okazaki fragments that require further processing. The blue circle represents the origin recognition complex at the origin.
C) Eukaryotic replication fork. The directionality (see B) of replication leads to the formation of loops on the lagging strand and discontinuous replication. This model was suggested according to the "trombone model" in bacteria. Unwinding of the DNA by the CMG (Cdc45-MCM-GINS) complex is followed by DNA synthesis by Pol ε on the leading strand and Pol δ on the lagging strand. Pol α/primase is required to initiate replication once on the leading strand and for each Okazaki fragment on the lagging strand. Okazaki fragment processing involves the Fen1 endonuclease and DNA ligase. Replication proceeds in the context of chromatin which is disassembled and reassembled in a controlled manner. This figure was adapted from (Stillman, 2008).

is inactive and CDK and DDK are required for its activation (Remus and Diffley, 2009). While Dpb11, Sld2, Sld3-Sld7 and ORC are left behind, once an origin is fired (activation of replication), Cdc45, MCM and GINS (CMG complex) form an active helicase at the replication fork (Figure 1.1A) (Gambus et al., 2006; Moyer et al., 2006).

1.3.2 Regulation of DNA replication in the cell cycle

Genome replication is tightly controlled and takes place only once per cell cycle, so two genomes of the same size can be distributed faithfully to daughter cells. Pre-RC assembly is restricted to late M-/G1-phase when CDK activity is low, while the activation of replication (origin firing) requires CDK and DDK activity and is therefore limited to S-phase (Labib, 2010). In yeast, CDK activity inhibits Cdc6, ORC, MCM and Cdt1 association and in metazoans inhibition of Cdt1 by geminin adds an additional level of regulation (Diffley, 2004; Kearsey and Cotterill, 2003). Therefore the oscillation of CDK activity during the cell cycle ensures the temporal order of replication events. In order to avoid re-replication, origins can only fire once per cell cycle and new pre-RC formation is prevented until the end of M-phase (Diffley, 2004). Firing does not occur at the same time at every origin, and can be early or late (Aves, 2009). Origins can also be dormant and are replicated passively or can play a role in the response to replication stress (Ge and Blow, 2010; Kawabata et al., 2011).

1.3.3 Progression of DNA replication

The progression of the replication fork - separating, synthesising and reassembling the DNA strands - is an interplay between multiple mechanisms. DNA unwinding and DNA synthesis occurs in the context of chromatin, which requires coordinated transition of nucleosomes to ensure the inheritance of epigenetic marks (Sarkies and Sale, 2011). The topology of DNA is adjusted during replication and cohesion needs to be established (Bermejo et al., 2008). The coordination of factors present at a replication fork is depicted in Figure 1.1C and discussed in detail below. DNA replication progression can be perturbed by other DNA transactions, such as transcription and DNA repair. Protein-DNA complexes, DNA secondary structures and DNA damage also represent possible obstacles for a replication fork (Lambert and Carr, 2005). Checkpoint mechanisms are coupled to DNA replication, sensing perturbations and initiating responses to coordinate replication fork stability, DNA repair and cell cycle progression (Segurado and Tercero, 2009).

In the following paragraphs, I will first discuss the process of DNA replication, the checkpoint cascades in response to DNA perturbations, DNA repair pathways and finally sources of DNA

replication perturbations and their consequences.

1.3.3.1 Unwinding of the DNA

As mentioned above, the MCM helicase is a component of the pre-RC and required for replication initiation (Remus and Diffley, 2009). The CMG complex has been identified at RPC's and is thought to be the replicative helicase (Moyer et al., 2006; Gambus et al., 2006). Experiments using temperature-sensitive mutants in yeast identified a function for MCM proteins for replication initiation, rather than elongation (Nasmyth and Nurse, 1981; Hennessy et al., 1990). However, using inducible protein degradation in *S. cerevisiae*, Labib et al. (2000) demonstrated that MCM is required for replication elongation as well as initiation. MCM is therefore considered to be the best candidate for the replicative helicase. Other helicases, such as Dna2, Pif1 (*sp*Pfh1), Rrm3 and RecQ helicases (*sc*Sgs1, *sp*Rqh1) have been implicated in DNA replication, but do not fully correspond to the description of a replicative helicase and are involved in replication related functions (Labib and Diffley, 2001). Some of these helicases will be revisited below.

Importantly, single stranded DNA (ssDNA) resulting from the unwinding process is covered by replication protein A (RPA) (Fanning et al., 2006). The heterotrimer RPA, has been implicated in cellular processes such as DNA replication, repair and checkpoint signalling (Fanning et al., 2006).

1.3.3.2 DNA synthesis

As the substrate for DNA synthesis, the production of dNTPs and its regulation play a crucial role not only in DNA replication, but also in DNA repair (Mathews, 2006). Defects in the regulation of dNTP pools can lead to mutagenesis (Weinberg et al., 1981; Mathews, 2006).

Once the DNA is unwound, DNA synthesis can start. The genome is replicated bidirectionally in a 5'-3' direction (Figure 1.1B). Because the DNA strands are antiparallel, replication is a semi-discontinuous process (Alberts et al., 2002). Replication is initiated by Pol α/primase and elongation is carried out mainly by Pol ε, continuously replicating the leading strand, and Pol δ, discontinuously replicating the lagging strand (Nick McElhinny et al., 2008; Miyabe et al., 2011). The "trombone" model describes the coordination of leading and lagging strand synthesis (Figure 1.1C). In this model the association of the polymerases with the replisome and the directionality of replication leads to the formation of loops on the lagging strand, which are replicated as Okazaki fragments (Stillman, 2008).

Pol α/primase, but not Pol δ or ε can initiate de novo DNA synthesis (Muzi-Falconi et al., 2003). Pol α/primase firstly starts leading strand replication by the synthesis of RNA (10 nu-

cleotides) and a stretch of DNA (20 nucleotides) (Hübscher, 2009). This is repeated on the lagging strand for the initiation of each Okazaki fragment. The clamp loader RF-C (replication factor C) seems to play an important role in the switching from Pol α to the replicative polymerases δ or ε. It has been shown *in vitro* that RF-C can inhibit the activity of Pol α, and this inhibition is reversed upon loading of proliferating cell nuclear antigen (PCNA) (Maga et al., 2000). PCNA would then allow for the loading of Pol δ or ε. PCNA, loaded by RF-C, is a processivity factor for polymerases and has multiple functions in DNA replication and repair (Moldovan et al., 2007). Replicative polymerases are essential for cell viability, but intriguingly it has been shown, that in yeast the catalytic domain of Pol ε is dispensable for viability, but required for normal replication (Dua et al., 1999; Kesti et al., 1999; Feng and D'Urso, 2001; Ohya et al., 2002).

1.3.3.3 Lagging strand DNA synthesis

The discontinuity of lagging strand replication results in an array of nascent DNA stretches of 200-1000bp called Okazaki fragments (Figure 1.1B), which require further factors for processing to form a continuous DNA strand (Okazaki et al., 1968; Miyabe et al., 2011). Pol α/primase synthesises the RNA primer and a stretch of DNA before handing over to DNA Pol δ. When Pol δ arrives at the 5'-end of the preceding Okazaki fragment, it displaces it, exposing a short 5'-flap. This flap is processed by the flap-endonuclease Fen1 (*sc*Rad27 and *sp*Rad2) and Dna2 and the Okazaki fragments are ligated by DNA ligase 1 (Burgers, 2009). It was shown that the proofreading function of Pol δ, 3' to 5'-exonuclease activity, can lead to the polymerase retreating backwards to leave a ligatable nick for DNA ligase 1, a process called "idling" (Garg et al., 2004). Interestingly, the preferred substrate of *sc*Rad27 was shown to contain a double-flap (5' and short 3'), which could arise from such a process (Kao et al., 2002). Other factors implicated in the processing of Okazaki fragments are the helicase/nuclease Dna2 and the RNA-specific endonuclease RNase H2. Dna2 is thought to preferably cleave long flaps that are coated with RPA, which are inhibitory for cleavage by Fen1 (Stewart et al., 2008). Dna2 has been shown to genetically and physically interact with RPA, which stimulates cleavage by Dna2 (Bae et al., 2001, 2003). Furthermore, Dna2 was implicated in the processing of structured DNA, which could occur during replication of sequences prone to form secondary structures (Stewart et al., 2010). PCNA is thought to play a very central role in lagging strand DNA synthesis by acting as a platform for multiple factors required for the processing (Beattie and Bell, 2011). Several factors involved in lagging strand processing (DNA ligase 1, Pol δ, FEN1) were shown to interact with PCNA through their PIP (PCNA-binding peptide) motifs (Hübscher, 2009).

It is important to note that Pol α/primase does not have proofreading activity like the poly-

merases δ and ε. Therefore, it is favourable that the RNA and DNA synthesised by Pol α/primase is replaced by Pol δ (Beattie and Bell, 2011). Indeed, it was shown that the proofreading activity of Pol δ, but not Pol ε affects a mutator phenotype of Pol α (Pavlov et al., 2006), suggesting the replacement of Pol α DNA by Pol δ DNA.

Apart from the discussed enzymatic reactions at the replication fork, such as DNA unwinding and DNA synthesis, several accessory factors are necessary for efficient DNA replication. Mrc1 (*sp*/*sc*Mrc1, *h*Claspin) is one such factor. Mrc1 functions as a mediator in the replication checkpoint, which will be discussed below (Alcasabas et al., 2001; Tanaka and Russell, 2001). In *S. cerevisiae*, Mrc1 is also required for normal rates of replication fork progression (Tourrière et al., 2005; Szyjka et al., 2005; Hodgson et al., 2007). Lou et al. (2008) have shown that Mrc1 physically interacts with Pol ε. This makes it a candidate to physically link DNA unwinding and DNA synthesis, as it has also been shown to interact with the MCM complex (Nedelcheva et al., 2005; Gambus et al., 2006; Komata et al., 2009). The coupling of the helicase to the polymerase by Mrc1 would support the observation of slower fork progression in *mrc1*Δ cells.

*sc*Ctf4 (*sp*Mcl1) has been shown to be important for the coupling of Pol α to the MCM complex (Gambus et al., 2009). It is interesting to note that *ctf4*Δ *mrc1*Δ cells are inviable (Warren et al., 2004). Gambus et al. (2009) showed that depletion of Ctf4 in *mrc1*Δ cells severely affects replication and prevents the completion of the cell cycle and this is independent of the checkpoint function of Mrc1. This suggests that these factors are important for the coordination of replication, which only allows for limited perturbations. *mrc1*$^+$ and *CTF4* have also been implicated in establishing sister chromatid cohesion (Hanna et al., 2001; Williams and McIntosh, 2002; Xu et al., 2004). Other factors that were shown to associate with MCM are the histone chaperone FACT, topoisomerase 1 (Top1) and Mcm10 (Gambus et al., 2006). Mcm10 is required for the association of Pol α with replication forks (Ricke and Bielinsky, 2004). Several components of the replication fork are involved in checkpoint activation or are targets of the checkpoint response (Tercero et al., 2003; Zegerman and Diffley, 2009). It is vital for the cell to monitor and regulate replication forks to maintain genome integrity. Interferences with replication can lead to replication fork arrest. I would like to introduce three different terms to describe the physiology of an arrested replication fork (Figure 1.2A). Replication perturbations can inhibit replisome progression with the replisome staying associated with the DNA, resulting in a "stalled fork", or cause the disassembly of the replisome and exposure of nascent DNA ("collapsed fork"). A stalled fork can be rescued by the approaching replication fork, fired from a neighbouring origin or, if kept in a stable conformation, can resume DNA replication. Collapsed replication forks can be fur-

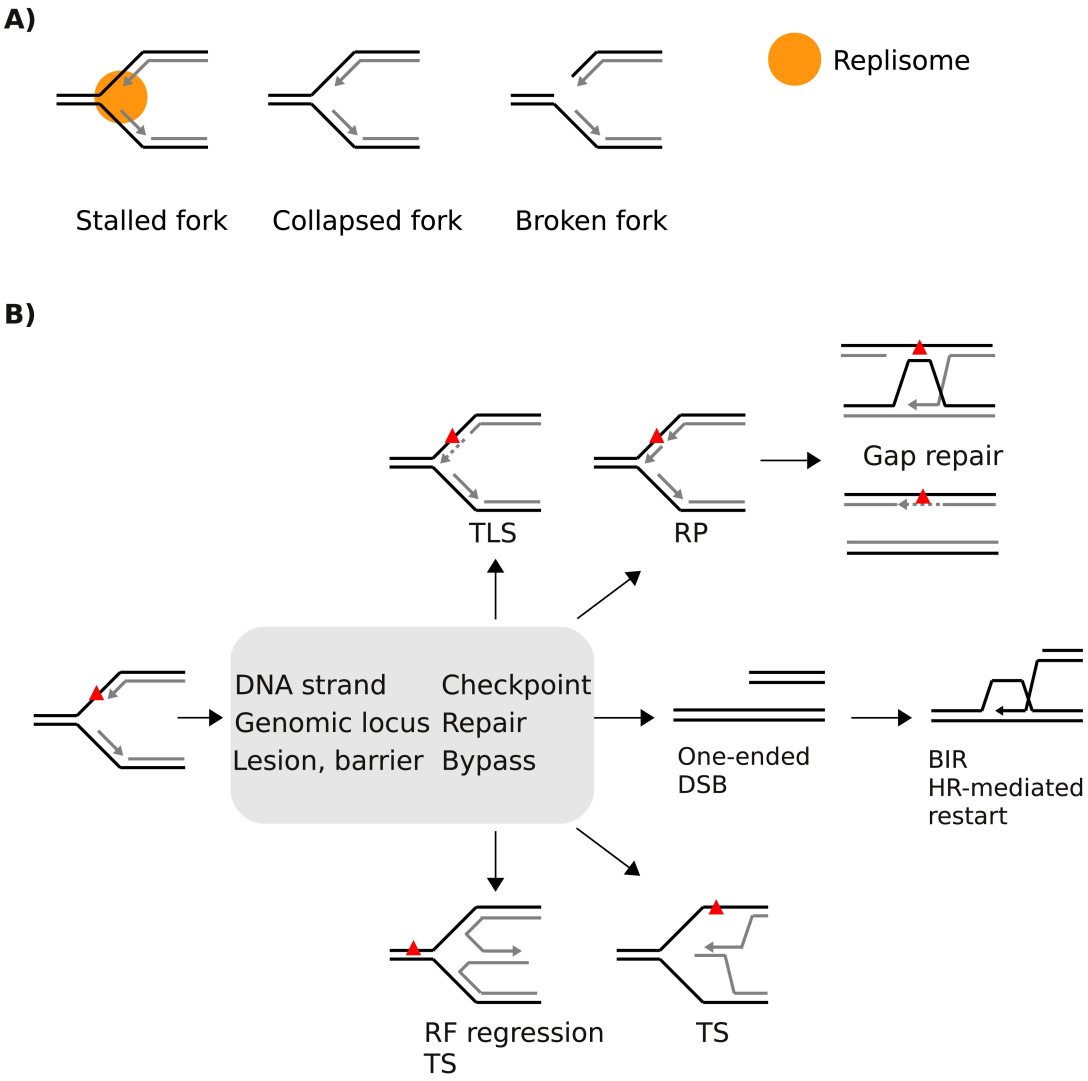

Figure 1.2: Replication perturbations and its consequences
A) Replication fork physiology. At a stalled replication fork the replisome components remain associated with the DNA and the ends of the nascent strands are therefore protected. In contrast, at a collapsed fork, where the replisome disassembles, the ends of the nascent DNA are exposed. A broken fork can arise by endonucleolytic processing or replication of a nicked template, where the replisome could "run-off" the DNA. Fork breakage leads to the formation of a one-ended DSB. Nascent strands are shown in grey and parental strands are shown in black.
B) Perturbation of replication and possible responses. As an example, replication fork arrest at a DNA lesion (red triangle) is shown. The parental template strands are shown in black and the nascent strands in grey. The responses to replication fork arrest can be influenced by several factors. The type of the lesion might trigger checkpoint activation and DNA repair. The checkpoint response in S-phase is important for the stabilisation of replication forks and regulation of origin firing. A lesion on the lagging strand might not be as inhibitory as on the leading strand, simply because of discontinuous replication. Repriming (RP) on the leading strand leaves a gapped substrate containing the lesion, which could be filled-in and repaired later. A replication blocking lesion might be bypassed by postreplication repair (PRR) involving translesion synthesis (TLS) or template switching (TS). This could happen at the replication fork or during gap repair behind the fork. Replication fork (RF) regression by reannealing the nascent strands changes the context of the lesion (from ssDNA to dsDNA) and therefore the possibility of detection. Also it provides an alternative template for strand elongation (template switching). RF regression forms a cruciform structure (holliday junction) which could be processed by enzymatic activities such as Mus81-Eme1. A broken fork exposing a one-ended DSB can be used for reinitiation of replication by break-induced replication (BIR). Homologous recombination (HR)-mediated restart pathways however do not absolutely require the formation of a DSB.

ther processed by endonucleolytic activities leading to fork breakage ("broken fork") leaving a one-ended (polar) double strand break (DSB). Or the unprotected nascent 3'-end at a collapsed fork is available for strand invasion and replication restart without creating a DSB. Examples for different fork structures and their processing are recombination-dependent fork restart by break-induced replication (BIR) which requires a polar DSB (Llorente et al., 2008) and strand invasion at a collapsed fork by homologous recombination without creating a DSB (Lambert et al., 2005; Mizuno et al., 2009; Lambert et al., 2010). Inhibition of DNA synthesis by damaged DNA can also be overcome by postreplication repair, which enables the fork to bypass a lesion (Lehmann, 2003; Ulrich, 2011). Figure 1.2B shows an example of possible consequences in response to a replication blocking lesion and what might determine these outcomes.

So far I have only discussed the establishment of replication forks in the context of the cell cycle and the replication process. In order to understand more about replication perturbations and resulting cellular responses, as mentioned above, I will discuss individual aspects of the overview shown in Figure 1.2B in the remaining paragraphs of this introduction. Firstly, I will explain the concept of DNA checkpoints and focus in particular on responses to DNA replication stress (Paragraph 1.4). Then I will summarise the main DNA repair pathways (Paragraph 1.5). DNA damage can interfere with DNA replication and therefore its removal prior to S-phase facilitates replication progression. Also DNA repair pathways are involved in the response to replication stress and enzymatic activities of these pathways are important for the recovery of collapsed and broken replication forks. Obstacles interfering with replication can be caused by DNA damage, but also by protein-DNA complexes or DNA secondary structures. I will give an overview of characterised protein-DNA replication fork barriers (RFBs) in *S. cerevisiae* and *S. pombe* and G-quadruplexes as an example of structured DNA (Paragraph 1.6). Finally, I will summarise what is known so far about the responses to replication fork stalling/collapse from studies using RFB systems in yeast (Paragraph 1.7).

1.4 Checkpoint activation in response to DNA damage and replication stress

1.4.1 Early observations defining the checkpoint concept

Important observations leading to the concept of DNA checkpoints emerged from the analysis of human cells from patients suffering from ataxia telangiectasia (AT), and *rad9* mutant cells in *S. cerevisiae* (Callegari and Kelly, 2007). AT cells showed a defect in mitotic delay in response to X-rays compared to cells from normal donors and it was suggested that the DNA damage

sensitivity of these cells is due to the missing delay allowing time for repair rather than a defect in damage repair directly (Painter and Young, 1980; Zampetti-Bosseler and Scott, 1981). Similarly, *S. cerevisiae rad9* mutant cells were defective in damage-induced cell cycle delay. Importantly, artificially induced delay of mitosis allowing for repair rescued the sensitivity phenotype (Weinert and Hartwell, 1988). Weinert and Hartwell (1988) introduced the term "checkpoint" to describe this damage-induced cell cycle delay.

1.4.2 DNA damage and replication checkpoints: an overview

Problems affecting the DNA metabolism can evoke checkpoints that initiate diverse responses to allow for efficient repair and prevent the entry into mitosis in the presence of DNA damage (DNA damage checkpoint), but also slow down S-phase and stabilise replication forks (S-phase checkpoint) (Caspari and Carr, 1999; Segurado and Tercero, 2009). The substrates for checkpoint activation are DSBs and ssDNA (Cimprich and Cortez, 2008). DNA damage and S-phase checkpoints can be overlapping responses, as for example replication stress can result in DNA damage and processing of DNA damage (e.g. DSBs) can lead to ssDNA (Carr, 2002; Cimprich and Cortez, 2008). However, the initiation of the S-phase checkpoint requires established replication forks and ssDNA and results in replication fork stabilisation (Lupardus et al., 2002; Stokes et al., 2002; Tercero et al., 2003). ssDNA is bound by the ssDNA binding protein RPA, which is important for the detection by checkpoint sensors (Zou et al., 2003; Zou and Elledge, 2003). Accumulation of ssDNA at replication forks is believed to be a consequence of additional DNA unwinding by the replicative helicase after uncoupling from the polymerase. Indeed, it has been shown by electron microscopy that additional ssDNA accumulates at replication forks when DNA synthesis is inhibited by depletion of dNTPs by hydroxyurea (HU), which could serve as the checkpoint signal (Sogo et al., 2002). Experiments in *Xenopus* egg extracts suggest that the uncoupling of the replicative helicase and polymerase activities results in checkpoint activation (Byun et al., 2005). After the detection of the ssDNA, the signal is transduced from the sensors to mediator proteins, which activate effector kinases. Phosphorylation of various target proteins by these kinases then leads to the observed cell cycle delay and initiates responses to maintain genome stability. The function of the checkpoints and proteins involved in these cascades are widely conserved in different organisms (Boye et al., 2009). Figure 1.3 shows a simplified overview of the checkpoint model in humans, *S. cerevisiae* and *S. pombe*.

In *S. cerevisiae*, Rad53 is the main effector kinase, which is activated by the mediator protein Rad9 in response to DNA damage (Weinert, 1998) and by Mrc1 upon replication stress (Alcasabas et al., 2001). In *S. pombe*, activation of the sensor Rad3-Rad26 can result in transduction of the

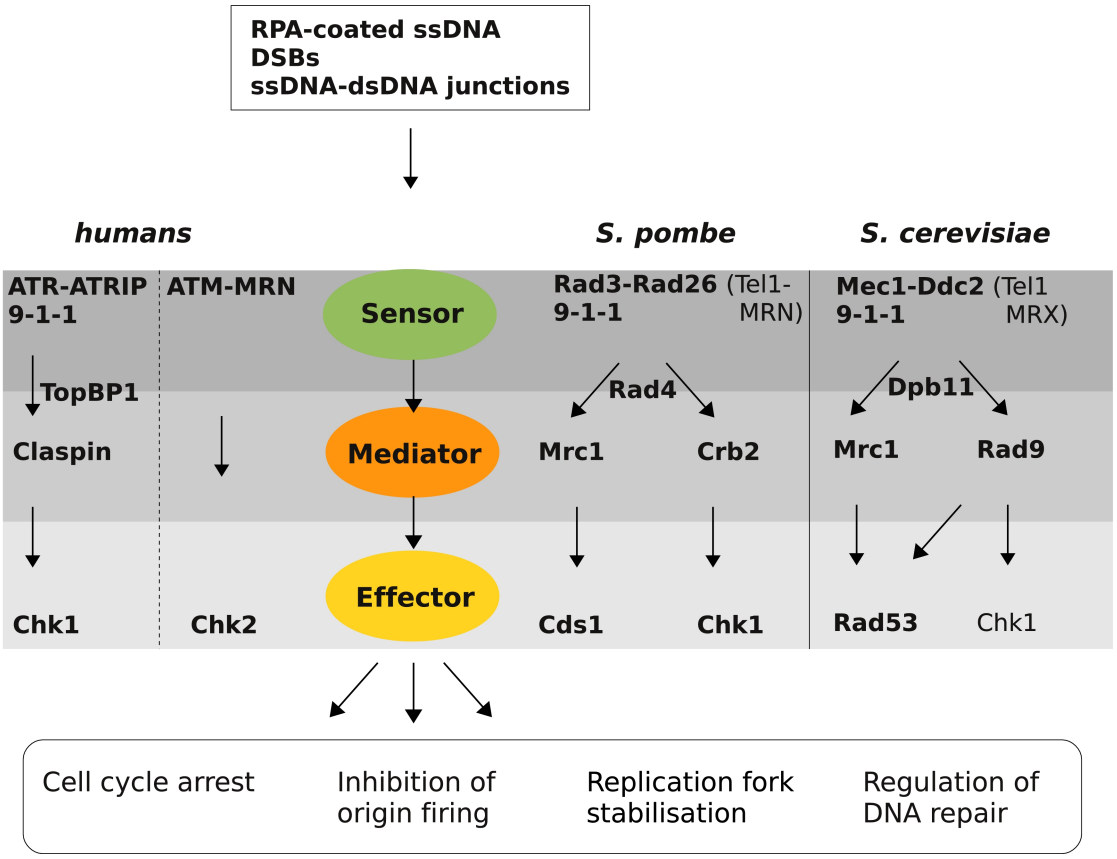

Figure 1.3: The DNA damage and replication checkpoint
A general overview of checkpoint signalling. RPA-coated ssDNA, dsDNA-ssDNA junctions and DSBs can be exposed after DNA damage or due to replication stress. These substrates are recognised by the checkpoint sensors, which through mediators activate effector kinases by phosphorylation events. The effector kinases transmit the signal to their target proteins and initiate the full checkpoint response (as shown in the box at the bottom). Factors involved in the DNA damage and replication checkpoints in humans, *S. pombe* and *S. cerevisiae* are shown. The main factors are printed in bold.

---

signal to Cds1 (*sc*Rad53) by Mrc1 (Xu et al., 2006) or to Chk1 by Crb2 (*sc*Rad9) (Carr, 2002). In mammalian cells, ATR signals for the activation of Chk1 in response to replication stress, whereas the main effector kinase in response to activation of ATM by DSBs is Chk2 (Cimprich and Cortez, 2008). The effector kinases are responsible for the subsequent phosphorylation of target proteins involved in cell cycle control, origin firing, DNA replication and repair and replication fork stabilisation to initiate the full checkpoint response (Branzei and Foiani, 2008; Segurado and Tercero, 2009). I will now discuss individual steps of the checkpoint cascades in more detail.

1.4.3 Sensing DNA perturbations

DNA structures activating the checkpoint response include RPA-coated ssDNA, DSBs and ssDNA-dsDNA junctions (Cimprich and Cortez, 2008). The phosphoinositide 3-kinase (PI3K)-related kinase ATM (ataxia-telangiectasia mutated) is recruited to DSBs by interactions with the Mre11-

Rad50-Nbs1 (MRN) complex (Branzei and Foiani, 2008). The yeast homologs of ATM, *sc*/*sp*Tel1, are involved in telomere maintenance and play a minor role in the checkpoint response (Greenwell et al., 1995; Boye et al., 2009). The PI3K-related kinase ATR (*sp*Rad3 and *sc*Mec1) associates with sites of DNA damage and replication stress via its activating unit ATRIP (*sp*Rad26 and *sc*Ddc2), which binds RPA-coated ssDNA (Edwards et al., 1999; Cortez et al., 2001). Importantly, ATM and MRN are required for ATR activation in response to DSBs, suggesting the conversion of a DSB to a ssDNA checkpoint substrate (Myers and Cortez, 2006; Adams et al., 2006; Jazayeri et al., 2006). This shows that perturbations of the DNA are not static and their processing can create new substrates, inducing dynamics into the checkpoint response.

Full activation of ATR requires the PCNA-like 9-1-1 complex (*sp*/*h*Rad9-Rad1-Hus1, *sc*Ddc1-Rad17-Mec3), which is loaded onto chromatin independently of ATR (Parrilla-Castellar et al., 2004). This complex is loaded onto 5'-ssDNA/dsDNA junctions by its clamp loader Rad17-RFC (RFC2-5) (Caspari et al., 2000; Bermudez et al., 2003; Ellison and Stillman, 2003; Majka and Burgers, 2005; Majka et al., 2006). The 9-1-1 complex is essential for the ATR pathway and has also been shown to be involved in the regulation of DNA repair (Helt et al., 2005; Kai et al., 2007). Interestingly, artificial co-localization of the ATR homolog and the 9-1-1 complex in *S. cerevisiae* has been shown to be sufficient for checkpoint activation in the absence of DNA damage (Bonilla et al., 2008).

A conserved function of the 9-1-1 complex in checkpoint activation is its interaction with TopBP1 (*sc*Dpb11, *sp*Rad4), which is important for checkpoint activation (Cimprich and Cortez, 2008). ATR-dependent phosphorylation of the C-terminus of the 9-1-1 component Rad9 creates binding sites for the BRCT-domains of TopBP1 (Furuya et al., 2004; Lee et al., 2007a; Delacroix et al., 2007). In *S. pombe*, Rad9 is phosphorylated (T412/S423) in S-phase, after S-phase arrest and after DNA damage and Rad4 (*h*TopBP1) was shown to interact with phosphorylated Rad9 (Furuya et al., 2004). This interaction is required for the activation of the DNA damage effector kinase Chk1, but not the replication checkpoint kinase Cds1 (Furuya et al., 2004). Rad4 and Rad3 co-precipitate when Rad9 is phosphorylated, suggesting close proximity of these three components (Furuya et al., 2004). In *S. pombe*, a Rad9 hypershift dependent on T225 was observed in response to DNA damage in G2 and replication fork collapse (Furuya et al., 2004). Phosphorylation of T225 has been shown to promote error-free repair pathways and to suppress translesion synthesis and strand invasion by Rad51 (Kai et al., 2007). More recent work has shown that the T225-dependent hypershift is also dependent on DDK and results in the release of Rad9 from chromatin, possibly to facilitate DNA repair (Furuya et al., 2010).

An ATR activating domain (AAD), which is required for and capable of ATR activation *in vivo*

and *in vitro*, was found in human and *Xenopus* TopBP1 (Kumagai et al., 2006). A functionally conserved domain was also identified in *sc*Dpb11 (Mordes et al., 2008; Navadgi-Patil and Burgers, 2008). The homolog of Rad9 in *S. cerevisiae*, Ddc1, can also directly stimulate Mec1 activation (Navadgi-Patil and Burgers, 2008). The different Mec1 activation mechanisms play distinct roles dependent on the cell cycle phases (Navadgi-Patil and Burgers, 2008). A corresponding AAD domain was found in *S. pombe* Rad4 and characterised, suggesting that the AAD plays a role in chromatin-dependent checkpoint amplification, especially in G1/S, when resection, and therefore ssDNA, is limited (Lin et al. in preparation).

1.4.4 Checkpoint mediators

The activation of checkpoint effector kinases requires the transduction of the initial signal by mediator proteins. While the mediator BRCT-domain protein *sc*Rad9 (*sp*Crb2, *h*53BP1) is crucial for the activation of the DNA damage checkpoint responses, *sc/sp*Mrc1 (*h*Claspin) is central for the response to replication stress (Carr, 2002; Segurado and Tercero, 2009).

In *S. cerevisiae*, Rad9 has been shown to be a target of Mec1 phosphorylation, which results in the activation of the effector kinase Rad53 (Vialard et al., 1998; Emili, 1998). Similarly, in *S. pombe*, Crb2 is required for the checkpoint response to DNA damage (Willson et al., 1997; Saka et al., 1997). Crucial for the response to DNA damage are its BRCT domains, which can bind to phosphorylated proteins (Manke et al., 2003; Mochida et al., 2004; Kilkenny et al., 2008). Crb2 is recruited to the associated Rad4/Rad9/Rad3 complex and is required for activation of Chk1 (Saka et al., 1997; Mochida et al., 2004).

The mediator protein Mrc1 in yeast and Claspin in mammals is a component of the replisome and is required for checkpoint activation by ATR in response to replication stress (Kumagai and Dunphy, 2000; Alcasabas et al., 2001). Mrc1 is phosphorylated by Mec1 and Tel1 in response to replication stress in *S. cerevisiae* (Zhao et al., 2003). It has been shown that phosphorylated Mrc1 recruits *sp*Cds1/*sc*Rad53, for activation by *sp*Rad3/*sc*Mec1 (Alcasabas et al., 2001; Zhao et al., 2003; Xu et al., 2006). Work in *S. pombe* suggests a model in which phosphorylated Mrc1 recruits Cds1 to stalled replication forks, where it can be phosphorylated by Rad3, which allows dimerisation and autophosphorylation of Cds1 (Xu et al., 2006; Xu and Kelly, 2009).

Mrc1 in *S. cerevisiae* is required in unperturbed replication progression (Alcasabas et al., 2001; Osborn and Elledge, 2003). Mutating the Mec1 phosphorylation sites in Mrc1 (*mrc1-AQ*) allowed the separation of the replication and the checkpoint function of Mrc1 (Osborn and Elledge, 2003). A similar mutant has been described in *S. pombe* (*mrc1-T645A/T653A*), however, whether this mutant separates a replication and a checkpoint function of Mrc1 has not yet been characterised

(Xu et al., 2006). Mrc1 has been suggested to be important for the coupling of the replicative helicase and DNA polymerase upon replication fork stalling which enables a stalled fork to resume or restart DNA synthesis once the obstacle is removed (Katou et al., 2003). In *S. cerevisiae*, association of Mrc1 with the fork is dependent on Tof1-Csm3 (*sp*Swi1-Swi3) (Katou et al., 2003) and also in *S. pombe*, Swi1-Swi3 are required for the association of Mrc1 with chromatin (Shimmoto et al., 2009). In both yeasts, Tof1-Csm3 (*sp*Swi1-Swi3), but not Mrc1, are required for replication fork arrest at protein-DNA barriers (Dalgaard and Klar, 2000; Calzada et al., 2005). *sp*Swi1-Swi3 and *sc*Tof1-Csm3 were characterised as checkpoint mediators and components of the replisome (Katou et al., 2003; Noguchi et al., 2003, 2004; Gambus et al., 2006) .

In higher eukaryotes, the Mrc1 homolog Claspin has been identified in *Xenopus* as a factor required for activation of the replication checkpoint (Kumagai and Dunphy, 2000). *h*Claspin is also required for efficient replication fork progression (Petermann et al., 2008). The human homologs of *sp*Swi1-Swi3, Timeless-Tipin, are involved in DNA replication and activation of the replication checkpoint (Unsal-Kaçmaz et al., 2005; Chou and Elledge, 2006; Yoshizawa-Sugata and Masai, 2007). They have further been implicated in sister-chromatid cohesion and in maintaining the stability of the replication fork (Leman et al., 2010).

1.4.5 Responses to replication stress and DNA damage

Checkpoint activation results in multiple responses, such as the delay of cell cycle progression, regulation of DNA repair, stabilisation of replication forks and up-regulation of dNTPs (Cimprich and Cortez, 2008; Zegerman and Diffley, 2009). A hallmark of checkpoint mutants is their inability to induce a cell cycle arrest in the presence of DNA damage and therefore they fail to prevent entry into mitosis (Carr, 2002). In *S. pombe*, the checkpoint kinases Chk1 and Cds1 were identified as components necessary for cell cycle arrest after DNA damage and replication stress, respectively (Walworth et al., 1993; Murakami and Okayama, 1995). The targets of the checkpoint kinases to control cell cycle progression include the CDK inhibitory kinases Wee1 and Mik1 and the activating phosphatase Cdc25 (Furuya and Carr, 2003). In *S. pombe*, Cdc25 and Wee1 are phosphorylated in response to DNA damage, which results in a G2/M arrest (Raleigh and O'Connell, 2000).

The levels of dNTPs are also regulated in a checkpoint-dependent manner. Ribonucleotide reductase (RNR) catalyses the synthesis of dNTPs, required for DNA synthesis, and its regulation is important to cover the requirement of dNTPs for DNA repair (Niida et al., 2010). In *S. cerevisiae*, the RNR inhibitor Sml1 has been identified as a target of Rad53 (Zhao et al., 2001). Importantly, the lethality of the deletion of *MEC1* and *RAD53* can be rescued by increasing dNTP levels (De-

sany et al., 1998; Zhao et al., 1998). In *S. pombe*, Chk1 is involved in the regulation of degradation of the RNR inhibitor Spd1 after DNA damage (Liu et al., 2003). Although *rad3*$^+$ is not essential, its deletion is lethal when checkpoint-independent degradation of Spd1 is impaired (*csn1*Δ) (Liu et al., 2003). Liu et al. (2003) showed that this lethality can be rescued by overexpression of the RNR subunit *suc22*$^+$ or loss of the RNR inhibitor *spd1*$^+$.

Another conserved effect of checkpoint activation is the inhibition of origin firing (Zegerman and Diffley, 2009). It was shown in *S. cerevisiae*, that origin firing is regulated by Rad53-dependent phosphorylation of the DDK kinase and the CDK substrate Sld3 (Zegerman and Diffley, 2010). In addition to the inhibition of origin firing, the S-phase checkpoint is required for the stabilisation of replication forks (Segurado and Tercero, 2009). Interestingly, a separation of function allele of *MEC1* (*mec1-100*), which is defective in the prevention of late origin firing, has given insight into the weight of different checkpoint responses. Comparison of *mec1*Δ cells and *mec1-100* cells in DNA damage sensitivity assays has shown that the inhibition of late origin firing contributes to cell viability only in a minor way, whereas the stabilisation of replication forks seems to be crucial (Paciotti et al., 2001; Tercero et al., 2003). The importance of the checkpoint for stabilisation of replication forks was suggested from observations in experiments monitoring the replication of alkylated DNA in checkpoint mutants (*MEC1* or *RAD53*) in *S. cerevisiae* which unlike wild-type cells were unable to finish replication (Tercero and Diffley, 2001). Furthermore, dNTP depletion by hydroxyurea (HU) in *RAD53* deficient cells, resulted in the accumulation of aberrant DNA structures at stalled replication forks, which persisted after release from the replication block (Lopes et al., 2001).

In *S. pombe*, HU treatment results in the dissociation of the site-specific endonuclease Mus81-Eme1, after phosphorylation by the S-phase effector kinase Cds1 (Kai et al., 2005). Activity of Mus81-Eme1 on replication fork-like structures was shown *in vitro* (Doe et al., 2002; Gaillard et al., 2003). The recombination protein Rad60 is excluded from the nucleus upon phosphorylation by Cds1 (Boddy et al., 2003) and recently the helicase/endonuclease Dna2 has been identified as a candidate of Cds1-dependent regulation (Hu et al., submitted). In *S. cerevisiae*, the deletion of the exonuclease *EXO1* rescues the DNA damage sensitivity of *rad53* mutants and prevents irreversible replication fork collapse in these mutants (Segurado and Diffley, 2008). These examples demonstrate that the checkpoint response employs multiple mechanisms to ensure replication fork integrity.

1.5 DNA repair and genome integrity

The integrity of the genome depends on multiple factors and is continuously challenged by the introduction of damage by endogenous and exogenous agents (Friedberg et al., 2004). Several repair and surveillance mechanisms are employed in order to repair DNA damage and coordinate repair with other forms of DNA metabolism (Branzei and Foiani, 2008). Different DNA repair pathways remove lesions throughout the cell cycle. However, lesions that remain, are introduced or only detected in S-phase can interfere with replication. In this case, the damage needs to be repaired but also DNA replication has to be completed before mitosis. The following paragraphs will describe the major DNA repair and damage bypass pathways in eukaryotes and their contribution to genome integrity with emphasis on homologous recombination (HR) and postreplication repair (PRR).

1.5.1 The role of mismatch repair (MMR) in the fidelity of DNA replication

The accuracy with which the genome is replicated depends on several factors. The intrinsic fidelity of the replicative polymerases α, δ and ε, as well as the 3'-5'-exonuclease (proofreading) activity of Pol δ and Pol ε make significant contributions (Arana and Kunkel, 2010). Furthermore, defects in the regulation of dNTP pools can also lead to mutagenesis (Weinberg et al., 1981; Mathews, 2006). Another level of counteracting replication infidelity is the detection and repair of mismatches, small insertions and deletion loops occurring during replication by the mismatch repair (MMR) components (Arana and Kunkel, 2010; Preston et al., 2010). Together, these mechanisms ensure an error-rate lower than 1 in 1 x 10^9 base pairs copied (McCulloch and Kunkel, 2008).

MMR involves mismatch recognition, recruitment of repair factors, sensing and degrading of the newly synthesised mismatch and re-synthesis of the correct sequence (Hoeijmakers, 2001). MMR is highly conserved from bacteria to humans (Li, 2008). In eukaryotes the recognition step of MMR is carried out by the two heterodimers Msh2-Msh6 and Msh2-Msh3 (Acharya et al., 1996). Msh2-Msh6 preferably binds base mismatches and small insertions or deletions (loops) and Msh2-Msh3 detects larger loops resulting from deletions and insertions, although the spectra of substrates can be overlapping (Habraken et al., 1996; Palombo et al., 1996; Umar et al., 1998). MMR proteins also play important roles in HR repair and can prevent pairing of homeologous sequences (Saparbaev et al., 1996; Lovett and Feschenko, 1996; Sugawara et al., 1997). The importance of the MMR pathway to preserve genome integrity is underlined by the development of cancers, such as the hereditary non-polyposis colorectal cancer as a result of mutations in components involved in the MMR pathway (Hoeijmakers, 2001).

1.5.2 Base excision repair (BER) and nucleotide excision repair (NER)

BER and NER share several features as the detection of DNA damage is followed by excision, DNA synthesis and ligation (Alberts et al., 2002). BER is a major repair pathway responsible for the removal of base damages from endogenous sources, like alkylation, deamination or oxidation (Hoeijmakers, 2001). NER repairs preferentially bulky lesions that distort the DNA double helix as well as lesions that physically block the transcription machinery (Hoeijmakers, 2001).

1.5.2.1 Base excision repair

BER is widely conserved and functions by similar mechanisms in different organisms (Robertson et al., 2009). The central substrates in BER are apurinic/apurimidinic (AP) sites, which are either created by DNA glycosylases acting on damaged bases or occur spontaneously (Mol et al., 1999). AP sites are then processed by either a DNA AP endonuclease or DNA AP lyase, that incise the DNA 5' or 3' to the AP site, respectively (Robertson et al., 2009). From here two pathways can be chosen for subsequent repair; short-patch or long-patch BER (Dianov et al., 2003). These two pathways differ in the factors involved as well as the length of DNA sequence that is replaced. In the short-patch pathway only one nucleotide is replaced, whereas in the long-patch pathway at least two nucleotides or more are replaced (Frosina et al., 1996; Robertson et al., 2009). Short-patch repair was shown to require the human DNA polymerase β (Pol β) for the filling reaction as well as the processing of the nick (the 5'-deoxyribophosphate) for efficient subsequent ligation by DNA ligase 3 (Matsumoto and Kim, 1995; Kubota et al., 1996). *h*XRCC1, which lacks enzymatic activity, is also required for short-patch BER and interacts with Pol β and DNA ligase 3 (Caldecott et al., 1994; Kubota et al., 1996).

Long-patch repair involves Pol δ or Pol β, as well as the flap endonuclease Fen1 and DNA ligase 1 (Frosina et al., 1996; Klungland and Lindahl, 1997). A patch longer than one nucleotide is displaced in a PCNA-dependent manner by the polymerase during the polymerisation reaction. The resulting flap is cleaved by the flap endonuclease Fen1 and ligated by DNA ligase 1 (Robertson et al., 2009). It was suggested that the decision between the two pathways depends on the efficient removal of the 5'-deoxyribophosphate by Pol β (Klungland and Lindahl, 1997).

BER can indirectly lead to single strand breaks (SSBs) and many of the enzymes involved in BER are involved in SSB repair (SSBR) (Hoeijmakers, 2001). SSBs arising directly by sugar damage are detected by PARP1, a major player in SSBR (Caldecott, 2008). Often, unligatable DNA-ends need to be processed by additional enzymatic activities before ligation can take place (Dianov and Parsons, 2007). Important factors in the end-processing step of SSBR are APE1, PNKP and APTX (Caldecott, 2008). After the processing, repair can proceed via the short-patch

or long-patch repair pathways involving gap filling and ligation.

1.5.2.2 Nucleotide Excision Repair

Although the NER pathway is widely conserved, it requires only three enzymes in prokaryotes (UvrA, UvrB and UvrC), but many more in eukaryotes (Guo et al., 2010). NER is divided into two sub-pathways; global genome repair (GGR) and transcription coupled repair (TCR) (Fleck and Nielsen, 2004). Both pathways catalyse the excision of a lesion, DNA synthesis and ligation. However a main difference lies in the recognition of the DNA lesions (Sugasawa, 2011). TCR is specialised for the repair of the transcribed strand of active genes and relies on RNA Pol 2 for the recognition of a substrate. In humans the factors CSA and CSB are required for this subpathway (Venema et al., 1990; van Hoffen et al., 1993). The recognition step in GGR involves DDB1 and DDB2 (UV-DDB) and XPC-HR23B (Sugasawa et al., 1998; Moser et al., 2005). The subsequent processing steps are similar in both pathways and involve DNA unwinding by the transcription factor TFIIH, XPB and XPD and stabilisation of the resulting bubble by XPA, XPG and RPA. Subsequent incision by the endonucleases XPG and ERCC1-XPF removes the damage and leaves a gap, which is filled by a DNA polymerase and ligated by a DNA ligase activity (Sugasawa, 2011). It was shown *in vitro* that DNA polymerases δ or ε and DNA ligase 1 could catalyse these reactions (Araújo et al., 2000). Alternatively, DNA Pol κ and XRCC1-ligase 3 have also been suggested (Ogi and Lehmann, 2006; Moser et al., 2007). The diseases xeroderma pigmentosum, Cockayne syndrome and trichothiodystrophy are all associated with mutations in NER factors (Hoeijmakers, 2001).

1.5.3 Nonhomologous end joining (NHEJ) and HR in DSB repair

Two-ended DSBs arise during meiosis as a result of a regulated enzymatic activity, but can also arise after treatment with ionizing radiation or chemical agents. NHEJ and HR are involved in the repair of DSBs. Whereas HR uses the sister-chromatid for repair and is mainly error-free, NHEJ rejoins two double-stranded ends, which might involve the loss of several nucleotides due to processing (Fleck and Nielsen, 2004). HR requires a homologous sequence. The availability of homology is influenced by the cell cycle stage and the compaction of the chromatin, which can therefore affect the choice of repair (Branzei and Foiani, 2008). NHEJ seems to be the predominant pathway for DSB-repair in mammals (Hefferin and Tomkinson, 2005) and recently it was shown that HR is important for the repair of DSBs in heterochromatin in G2 (Beucher et al., 2009). This is surprising as homology-directed repair in heterochromatic regions, which often contain repetitive sequences, might lead to rearrangements. Although both pathways are conserved in yeast, HR is

mainly used for DSB repair (Prudden et al., 2003; Hefferin and Tomkinson, 2005). The G2 phase is the longest phase in the *S. pombe* cell cycle and therefore a homologous sequence is available for repair at most times.

1.5.3.1 Nonhomologous end joining

NHEJ involves the binding of the two DSB ends, recruitment of bridging factors, which tether the ends together, processing of DSB ends and rejoining followed by ligation (Hefferin and Tomkinson, 2005). After DSB formation, both ends are bound by the heterodimer Ku70/80 with high affinity, which is important for the recruitment of other factors and might play a role in tethering the two ends together (Mahaney et al., 2009). The complex then slides inwards making the DSB ends available for the loading of the catalytic subunit of DNA-PK (DNA-PKcs) (Yoo and Dynan, 1999). DNA-PK takes part in the regulation of the processing of the DSB ends, which likely leads to the loss of a few nucleotides and therefore results in error-prone repair (Mahaney et al., 2009). The main factors involved in the processing step are the endo-/exonuclease Artemis, DNA polymerases μ and λ, the 3'-DNA phosphatase/5'-DNA kinase PNK, the endo-/exonuclease APLF and the RecQ helicase WRN, which exhibits DNA helicase, exonuclease and strand annealing activities (Mahaney et al., 2009). Finally the re-ligation of the DNA is catalysed by XRCC4/Ligase4 and XLF (Ahnesorg et al., 2006). Besides the classical NHEJ pathway described here, there is also an alternative pathway (alt-EJ, backup-NHEJ or MMEJ for microhomology-mediated end joining) (Lieber and Wilson, 2010). The MRN complex in *Xenopus laevis* has been shown to play a role in MMEJ, which is independent of DNA-PK and Ku70 (Taylor et al., 2010). Interestingly, DNA-PK is not conserved in yeast and it has been proposed that in *S. cerevisiae* the MRX (Mre11-Rad50-Xrs2) complex plays a role in the tethering of the two ends of DSBs (Hefferin and Tomkinson, 2005).

1.5.3.2 Homologous recombination

HR is the major pathway for DSB-repair in yeast (Raji and Hartsuiker, 2006). The classical steps of HR were described by Szostak et al. (1983) and involve the 5' to 3' resection of both DSB ends leaving a 3'-ssDNA overhang, invasion by this overhang into the homologous template, D-loop formation, repair synthesis and holliday junction (HJ) formation and resolution. The main factors involved in HR are members of the Rad52 epistasis group which are conserved in *S. cerevisiae* and *S. pombe*, as well as in higher organisms (Symington, 2002). I will explain the model using the *S. cerevisiae* protein names. Figure 1.4 shows an overview of the different HR pathways. The classic HR model from Szostak is underlayed with grey background.

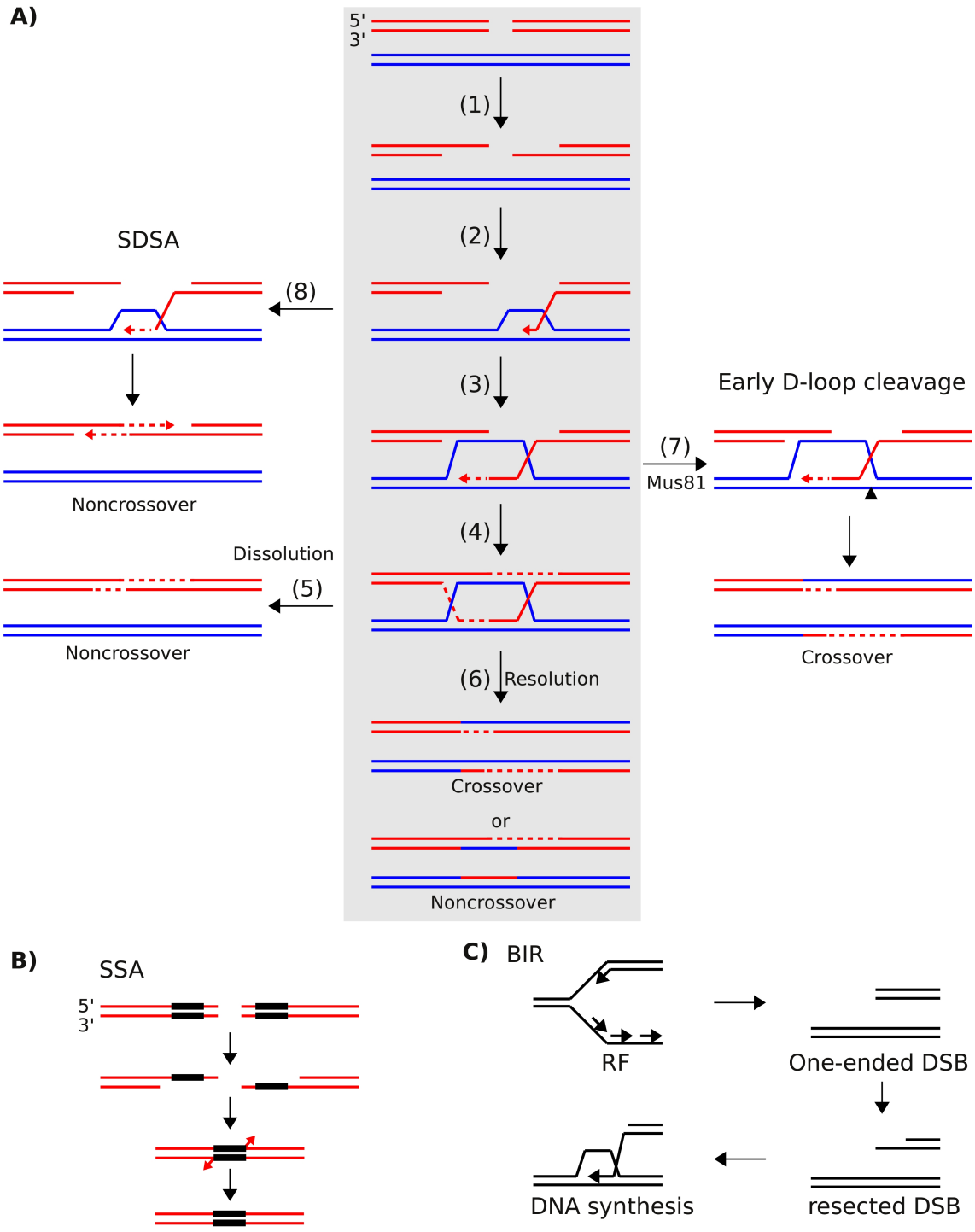

Figure 1.4: Pathway overview of homologous recombination
A) The classic HR pathway model by Szostak (Szostak et al., 1983) is underlayed in grey. Two homologous dsDNA strands are shown in red and blue. The numbers correspond to the following steps of the reaction; (1) DSB resection and Rad51 filament formation, (2) strand invasion and D-loop formation, (3) strand extension and second end capture, (4) double HJ formation, (5) dissolution of the double HJ by Sgs1-Top3-Rmi1 resulting in noncrossover, (6) resolution of the double HJ by endonucleolytic cleavage resulting in either noncrossover or crossover, (7) cleavage of the D-loop by the structure-specific endonuclease Mus81-Eme1/Mms4 prior to double HJ formation, resulting in crossover formation, (8) synthesis-dependent strand annealing (SDSA), resulting in noncrossover formation. For further details see text.
B) Single strand annealing (SSA). A DSB formed between two homologous sequences (black boxes) is resected and exposes single stranded homologous ends that reanneal. Processing of the flaps and ligation of the DNA results in repair of the DSB as well as in the deletion of the intervening sequence.
C) Break-induced replication (BIR). Processing of a collapsed replication fork (RF) can result in a one-ended DSB. Strand resection and invasion of the homologous duplex DNA can establish repair synthesis and restoration of a replication fork.

5'-3' resection of DSB ends The resection of the DSB ends is a two-step process involving the MRX (*sp*MRN) complex together with the endonuclease Sae2 (*sp*Ctp1), followed by the exonucleolytic activity of Exo1 or Sgs1-Top3-Rmi1 and Dna2 (Zhu et al., 2008; Mimitou and Symington, 2008). DNA end resection is important for the initiation of HR and concomitant inhibition of NHEJ and there is evidence that the process of resection is cell cycle regulated, as CDK activity is required for DSB-end resection (Aylon et al., 2004; Huertas et al., 2008).
See step (1) in Figure 1.4.

Rad51 filament formation and strand invasion The 3'-overhang resulting from DSB-end resection is immediately coated with the ssDNA binding protein RPA, which is subsequently replaced by the RecA-homolog Rad51 (Sugiyama et al., 1997; Sugiyama and Kowalczykowski, 2002; Sugiyama and Kantake, 2009). Rad51-filament formation by displacement of RPA is facilitated by the mediator protein Rad52 (Sugiyama and Kantake, 2009; Mazón et al., 2010). Rad52 was shown to interact with Rad51 and RPA (Song and Sung, 2000; Sugiyama and Kowalczykowski, 2002). Rad55 and Rad57 play a role in Rad51 filament stabilisation and strand exchange (Sung, 1997; Fortin and Symington, 2002). Once the Rad51 filament is assembled, the 3'-end can invade a homologous dsDNA strand, forming a displacement loop (D-loop) (Mazón et al., 2010). Rad54 (*sp*Rhp54), a member of the Swi2/Snf2 family, has DNA-dependent ATPase activity and was shown to be important for the homologous pairing of the Rad51-filament with the donor strand (Petukhova et al., 1998, 1999). Rad54 is also important for the extension of the invaded strand (Solinger and Heyer, 2001).
See step (2) in Figure 1.4.

Strand extension, second end capture and double HJ formation After strand invasion of the homologous duplex, DNA synthesis is required for strand extension. Li et al. (2009) could show in a reconstituted system, that Pol δ is targeted to the D-loop by PCNA, where it can extend the invading 3'-end using the donor DNA as a template. In the classic HR model, the other 3'-overhang of the resected DSB is annealed to the D-loop (second end capture) and can then be extended using the D-loop as a template (Szostak et al., 1983). Rad52 was shown *in vitro* to promote the annealing reaction between the D-loop and the second end (Nimonkar et al., 2009). Rejoining of the extended invading 3'-end and the 5'-end of the DSB leads to the formation of a double HJ (Szostak et al., 1983).
See steps (3) and (4) in Figure 1.4.

HJ resolution and dissolution The resulting double HJ is either dissolved or resolved to separate the entangled molecules into individual DNA duplexes (Mazón et al., 2010). The RecQ helicase Sgs1 (*sp*Rqh1, *h*BLM) together with Top3 and Rmi1 exhibits branch migration activity and can dissolve HJs resulting in two intact dsDNA molecules (Wu and Hickson, 2003; Cejka et al., 2010; Ashton et al., 2011). The alternative pathway to the dissolution reaction by Sgs1-Top3-Rmi1 was suggested to be HJ resolution by the structure-specific endonuclease Mus81-Mms4 (*sp*/*h*Mus81-Eme1) (Ashton et al., 2011). This is supported by the synthetic lethality of these two enzymes in several organisms (Boddy et al., 2000; Kaliraman et al., 2001; Hartung et al., 2006; Trowbridge et al., 2007). Resolution of a double HJ can give rise to crossover products versus non-crossover products, depending on the cutting site of the endonuclease. In *S. cerevisiae* and human cells, a novel structure-specific endonuclease has been identified recently, *sc*Yen1 and *h*GEN1 (Ip et al., 2008). Yen1 and Mus81-Mms4 are regulated by phosphorylation during meiosis, which ensures their sequential activation (Matos et al., 2011). An assay using plasmid-substrates showed that Mus81 and Yen1 have redundant functions in HJ resolution and are not the only HJ resolving activities, as in *yen1*Δ *mus81*Δ cells 50% of the HJ-substrate is still resolved (Tay and Wu, 2010). *In vitro* studies established the preferred substrate for Mus81 complexes as nicked HJs, D-loops, 3'-flaps and replication fork-like structures, rather than intact HJs (Ciccia et al., 2003; Gaillard et al., 2003; Whitby et al., 2003; Osman et al., 2003; Fricke et al., 2005). In agreement with this, it has been suggested that *sp*Mus81-Eme1 prefers to cleave an early intermediate of meiotic DSB repair before the double HJ formation and direct repair to form crossovers (Osman et al., 2003). See steps (5), (6) and (7) in Figure 1.4.

In addition to mitotic and meiotic recombination, the heterodimer Mus81-Eme1 has been shown to be involved in replication and the tolerance of replication perturbations (Osman and Whitby, 2007). In *S. pombe*, Mus81 is required for the repair of a replication-associated polar DSB at the mating type locus (Roseaulin et al., 2008). Furthermore, Mus81 is synthetically lethal with the flap-endonuclease *sprad2*$^{+}$ and *scRAD27* (*h*Fen1) (Tong et al., 2001; Osman and Whitby, 2007). I will explain the structure and function of Mus81-Eme1/Mms4 in more detail in Chapter 6.

Other models or mechanisms of HR have been established that share similarities in several steps or factors involved in the classic HR model.

Synthesis-dependent strand annealing (SDSA) SDSA differs from classic HR after the invasion of the Rad51-coated 3'-end of the resected DSB and its extension on the homologous donor. In SDSA, strand displacement of the extended strand and reannealing with the exposed

3'-overhang from the other DSB-end results in two intact duplex DNA molecules without forming crossovers (Mazón et al., 2010). The helicases *SRS2* and *SGS1* were found to suppress crossovers during DSB repair likely by promoting SDSA and double HJ dissolution, respectively (Ira et al., 2003). In agreement with this, *in vitro* studies showed that Srs2 promotes SDSA by translocating along the displaced strand (ssDNA) and unwinding dsDNA coated with Rad51 (the invading strand annealed to the new template) (Dupaigne et al., 2008). Interestingly, the helicase *fbh1*$^+$ in *S. pombe* was identified as a suppressor mutation in *rad22*Δ cells, counteracting *rhp51*$^+$-dependent recombination in the absence of *rad22*$^+$ (encoding Rad52) (Osman et al., 2005). Whether *fbh1*$^+$ is also involved in SDSA is not known.

See step (8) in Figure 1.4.

1.5.3.3 Single-strand annealing (SSA)

SSA is an error-prone repair pathway and can act when a DSB is introduced in between two homologous sequences (Raji and Hartsuiker, 2006). Recombination between the direct repeats leads to the deletion of the intervening sequence. SSA has been well characterised in *S. cerevisiae*. This pathway does not require *RAD51* for strand invasion, but does require *RAD52* for strand annealing (Krogh and Symington, 2004). A system using a site-specific DSB, introduced by the HO-endonuclease, flanked by direct repeats was used to study SSA (Rudin and Haber, 1988; Fishman-Lobell et al., 1992). Using this setup, Rudin and Haber (1988) showed that DSB-repair between two repeats is almost exclusively carried out by SSA and is dependent on *RAD52*. Fishman-Lobell et al. (1992) demonstrated that a DSB between two homologous sequences can be repaired by two competing independent mechanisms, SSA and gene conversion and ssDNA formation in the homologous regions is crucial for SSA, i.e. deletion formation. In addition to *RAD52*, *RAD59*, the flap endonuclease *RAD1-RAD10* and the MMR components *MSH2* and *MSH3* were identified to be required for SSA (Fishman-Lobell and Haber, 1992; Sugawara et al., 1997, 2000). SSA can be initiated between homologies as small as 29bp and probably less, however it increases in efficiency between homologies of up to 400bp (Sugawara et al., 2000).

A SSA-assay developed in *S. pombe* has shown that this mechanism is independent of *rhp51*$^+$, but dependent on *rad22*$^+$, and the endonucleases *rad16*$^+$ (*scRAD1*) and *swi10*$^+$ (*scRAD10*) (Raji and Hartsuiker, 2006; Watson et al., 2011).

See Figure 1.4B.

1.5.3.4 Recombination products: gene conversion (GC) and loss of heterozygosity (LOH)

HR is also described as gene conversion in the sense that the sequence of a particular locus is replaced by copying the sequence of a homologous locus (Haber, 2000a). If there are multiple copies of the same allele in a cell, which differ slightly in sequence, a gene conversion event could result in LOH. LOH describes the loss of an allele which was heterozygous, i.e. is now homozygous, so that only one version of this allele remains (Alberts et al., 2002). LOH is a hallmark of cancer and is of great importance to consider in diploid heterozygous organisms, like mammals (Alberts et al., 2002). HR is a vital repair process and its importance is underlined by the many severe phenotypes of HR mutants in different organisms (Haber, 2000b). However, recombination between homologous sequences can also result in gross chromosomal rearrangements (GCRs) and therefore be a source of genome instability (Lambert et al., 2005; Mizuno et al., 2009; Lambert et al., 2010).

RAD51 deficient mice are embryonic lethal suggesting HR to be vitally important (Lim and Hasty, 1996; Tsuzuki et al., 1996). However, in mice, *RAD52* is not essential (Rijkers et al., 1998). Mouse embryonic cells deficient in *RAD52* show no increased sensitivity to DNA damaging agents, but exhibit a reduction in HR, suggesting a functional redundancy with other factors (Rijkers et al., 1998). Depletion of RAD52 in *BRCA2* deficient human cells is synthetically lethal (Feng et al., 2011). BRCA2 (Breast cancer susceptibility gene 2) was identified by Wooster et al. (1995) and is a major regulator of HR in mammals (Wooster et al., 1995; Thorslund and West, 2007). A study by Feng et al. (2011) suggests that RAD52 plays an important role in HR in the absence of BRCA2. In yeast, where BRCA2 is not present, *RAD52* (*sprad22*$^{+}$) is required for HR and *rad52*Δ cells (*sprad22*Δ) show severe phenotypes and are HR-deficient (Haber, 2000b). Rad52 is the main regulator of HR in yeast and can function in a Rad51-dependent and -independent manner (Symington, 2002; Doe et al., 2004).

1.5.4 Recombination and replication

Recombination proteins were implicated in the replication process in many organisms (Haber, 1999; Lambert et al., 2007; Allen et al., 2011). Recombination is important in the repair or restart of collapsed or broken replication forks (McGlynn and Lloyd, 2002; Mizuno et al., 2009; Lambert et al., 2010). It is well established that in bacteria, the Rad51 homolog RecA plays a major role in replication fork restart (Kowalczykowski, 2000). The circular bacterial genome is replicated from one origin. Therefore, if both replication forks stall, replication needs to be restarted in order to be completed. Replication fork restart models in bacteria suggest that recombination-dependent resumption of replication is initiated from a collapsed fork (inactive, nascent DNA ends exposed

due to replisome disassembly) rather than a stalled fork (nascent ends protected, replication proteins stay associated with the fork) (Lambert et al., 2007). In eukaryotes, multiple origins fire in S-phase and a stalled fork can be rescued by an approaching fork and dormant origins can be activated to increase the number of replication forks in order to complete replication (Blow et al., 2011). However, if two converging forks arrest and there is no origin left to fire in between them, there is a need for replication fork restart to complete replication. A system in *S. pombe* was designed to mimic this situation (Lambert et al., 2005). Two copies of the RTS1 barrier (replication termination sequence 1) were introduced upstream and downstream of *ura4*$^{+}$ to prevent its replication. Analysis of this system suggested that the arrested replisome disassembles (fork collapse) and HR is required for replication fork restart, which can result in GCRs (Lambert et al., 2005). A more detailed analysis suggests a homology-dependent restart mechanism by strand invasion of the nascent 3'-end, facilitated by Rad52 (Lambert et al., 2010). A similar system using a palindromic sequence in between two RTS1 sequences also requires HR-dependent fork restart (Mizuno et al., 2009). Induction of fork arrest at a single copy of RTS1 surrounded by direct repeats resulted in recombination between the homologous sequences surrounding RTS1 (Ahn et al., 2005).

In eukaryotes, stalled replication forks are stabilised by the replication checkpoint response (Segurado and Tercero, 2009). Several experiments, including analysis by 2D-gel electrophoresis and electron microscopy have shown that in the absence of the checkpoint aberrant structures (such as regressed forks, termed "chicken foot") can form, which interfere with the completion of genome replication (Lopes et al., 2001; Sogo et al., 2002). However, it has been shown that paused forks at the rDNA barrier in *S. cerevisiae* do not require checkpoint or recombination functions to resume replication and replication proteins stay associated with the fork (Calzada et al., 2005). HR-dependent replication fork restart is also important in higher eukaryotes (Allen et al., 2011).

Hashimoto et al. (2010) suggested a more direct role for recombination in replication progression by showing that in *Xenopus* egg extracts Rad51 is required during replication to protect the nascent strand from Mre11-dependent degradation. In this study, Mre11-dependent degradation could be detected in ssDNA gaps behind the fork, but not at the fork. Furthermore, the functional Rad52 homolog BRCA2 in human cells was shown to suppress Mre11-dependent degradation at stalled replication forks (Schlacher et al., 2011).

One-ended DSBs can result from endonucleolytic cleavage of collapsed replication forks or if the replication fork encounters a nick. A one-ended DSB could re-invade the intact double-stranded sister-chromatid and use it as a template for DNA synthesis. This mechanism is described as break-induced replication (BIR) (Llorente et al., 2008). BIR shares the same strand invasion steps

as classic HR, however instead of second end capture and double HJ formation, DNA synthesis is continued and used to re-establish a replication fork (Figure 1.4C) (Llorente et al., 2008). If at a two-ended DSB only one end initiates recombination and repair synthesis, this can also be classified as BIR (Haber, 2000a). Although, BIR can rescue a broken replication fork, it can also lead to LOH and therefore be mutagenic.

1.5.5 Postreplication repair (PRR)

During replication the dsDNA is separated into two single strands. As a consequence, lesions on these strands cannot be detected and repaired by canonical pathways of excision repair and thus inhibit approaching replicative polymerases. Under these circumstances, the bypass of the lesion is required in order to continue replication (Ulrich, 2011). PRR is described as DNA damage avoidance or bypass mechanisms, which already implies that the actual damage is not removed by this process, but overcome. Lesion bypass has been demonstrated in prokaryotes and eukaryotes using alkaline sucrose gradients (Rupp and Howard-Flanders, 1968; Lehmann and KirkBell, 1972; Prakash, 1981). These studies showed that DNA containing UV lesions could be replicated without much delay. Furthermore, replication appeared to be discontinuous at first, leaving gaps, which were converted into large molecular weight DNA later on. These results suggested an accumulation of ssDNA gaps due to UV damage. The nature of continuous and discontinuous DNA synthesis on the leading and lagging strand, respectively, suggests that a lesion on the leading strand might have more severe consequences. Experiments assessing replicated DNA in recombination and PRR mutants demonstrated an accumulation of ssDNA gaps on both strands, suggesting repriming of replication on the leading strand as well as on the lagging strand (Lopes et al., 2006).

PRR is controlled by the Rad6 epistasis group and is mediated by post-translational modification of PCNA by ubiquitin and SUMO (small ubiquitin-like modifier) (Hoege et al., 2002). PCNA is a ring-shaped sliding clamp that interacts with many different proteins involved in DNA replication and repair (Maga and Hubscher, 2003). Ubiquitin is a small 76 residue protein which is covalently linked to specific lysine residues of target proteins by an enzyme cascade (Dubiel and Gordon, 1999). Ubiquitylation of PCNA is mediated by the ubiquitin conjugating (E2) enzymes, *sc*Rad6 (*sp*Rhp6) and *sc*Ubc13/Mms2 (*sp*Ubc13/Mms2) and the ubiquitin ligase (E3) enzymes *sc*Rad18 (*sp*Rhp18) and *sc*Rad5 (*sp*Rad8) (Figure 1.5) (Ulrich, 2005; Frampton et al., 2006). The polyubiquitin chains on PCNA residue K164 are linked by K63 as opposed to the degradation-targeting K48-linkage (Pickart, 2000; Hoege et al., 2002).

Whereas monoubiquitylation by Rad6 and Rad18 initiates a mostly error-prone bypass mechanism involving translesion synthesis (TLS) polymerases, polyubiquitylation by Ubc13-Mms2 and

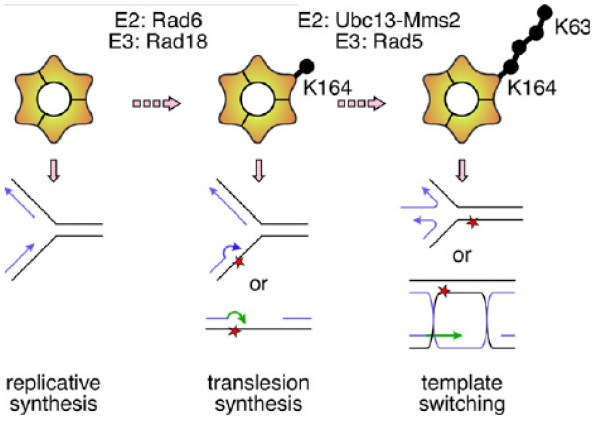

Figure 1.5: Postreplication repair initiated by ubiquitylation of PCNA
Indicated is the monoubiquitylation of PCNA-K164 by the ubiquitin conjugating enzyme (E2) Rad6 (*sp*Rhp6) and the ubiquitin ligase (E3) Rad18 (*sp*Rhp18), which leads to translesion synthesis at the fork or during gap repair. Polyubiquitylation is carried out by the E2 Ubc13-Mms2 and the E3 Rad5 (*sp*Rad8), which results in template switching at the fork or during gap repair. The ubiquitin chains at PCNA-K164 are linked by K63. This figure was adapted from (Ulrich, 2011).

Rad5 activates an error-free mechanism by template switching (Ulrich, 2005). TLS is carried out mostly by Y-family polymerases of low fidelity, which allows the replication of damaged template DNA (Lehmann et al., 2007). In agreement with this, ubiquitin binding domains in these polymerases enable them to interact with monoubiquitylated PCNA (Bienko et al., 2005). Template switching induced by polyubiquitylation of PCNA involves annealing of the nascent DNA strands and copying the information beyond the replication-blocking lesion (Ulrich, 2005; Zhang and Lawrence, 2005).

Figure 1.5 shows an overview of PCNA-ubiquitylation and its associated bypass pathways. Sumoylation of PCNA at K164 was shown to suppress recombination via the anti-recombinase Srs2 in *S. cerevisiae* (Papouli et al., 2005; Pfander et al., 2005). Whereas the role of PCNA-ubiquitylation in PRR is widely conserved, the role of PCNA-sumoylation in different organisms is less clear (Ulrich, 2005). Whether PRR acts at the replication fork or on ssDNA gaps left behind the fork or if there is a preferential pathway for certain substrates is not entirely known. However, two recent studies in *S. cerevisiae* have demonstrated that PRR can be uncoupled from bulk DNA synthesis and act in late S-/G2-phase of the cell cycle (Daigaku et al., 2010; Karras and Jentsch, 2010). Work in DT40 cells has shown that the Y-family polymerase Rev1 is required for efficient fork progression on a damaged template, whereas PCNA ubiquitylation is necessary for post-replicative gap filling (Edmunds et al., 2008). It is important to note that, unlike in DT40 cells, Rev1 belongs to the Rad6 epistasis group in yeast (Kunz et al., 2000).

1.6 Replication fork barriers (RFBs)

DNA replication can be stalled at lesions, because of depletion of dNTPs, secondary structures formed by specific DNA sequences, but also by DNA-protein interactions that form a physical block to the replisome (Lambert and Carr, 2005; Labib and Hodgson, 2007). The best described RFBs in eukaryotes are the rDNA barrier (rDNA RFB) in *S. pombe* and *S. cerevisiae* and the replication termination sequence 1 (RTS1) at the mating type locus in *S. pombe*. Furthermore, structured DNA, such as repetitive sequences forming hairpins or G-quadruplex DNA (G4-DNA) could also interfere with replication fork progression (Lambert and Carr, 2005). In the following paragraphs I will describe the nature and implications of G4-DNA and natural protein-DNA RFBs.

1.6.1 Structured DNA: G-quadruplex DNA (G4-DNA)

1.6.1.1 Structure of G4-DNA

DNA usually forms a right-handed double helix consisting of two antiparallel strands which are held together by the base pairing of complementary bases (adenine, A with thymine, T and cytosine, C with guanine, G), termed Watson-Crick base pairing (Alberts et al., 2002). Certain sequences can give rise to alternative structures and base pairings. G-rich sequences (in particular four separate clusters of two to four Gs) can form G4-DNA (Figure 1.6A) (Sen and Gilbert, 1988). These structures can form in DNA and RNA (Burge et al., 2006). G4-DNA is held together by Hoogsten hydrogen bonding and consists of stacked planar G-quartets (Figure 1.6B and C). G4-structures can form inter- or intra-molecularly and the strands (Figure 1.6C) can be oriented in a parallel or anti-parallel orientation (Burge et al., 2006). Monovalent cations such as K^+ or Na^+ are required for the structure to form (Figure 1.6B). Once formed, G4-DNA is more stable than dsDNA (Lipps and Rhodes, 2009). For the formation of G4-DNA, dsDNA needs to be at least transiently unwound. Hence DNA metabolism such as transcription, replication and DNA repair could theoretically provide a favourable environment for these structures to form.

1.6.1.2 Conservation and localisation of G4-DNA

G4-quadruplexes are widely conserved in prokaryotes and eukaryotes and the first *in vivo* evidence for this structure was gained from immunostaining of telomeric DNA in *Stylonychia lemnae* (Schaffitzel et al., 2001; Lipps and Rhodes, 2009). The repetitive G-overhangs in telomeres mostly fulfil the sequence requirement for G4-DNA and, because of their single-strandedness, are potential sites of G4-DNA formation. Analyses of bacterial and eukaryotic genomes for potential G4-DNA forming sequences have been carried out. Potential loci for these structures cor-

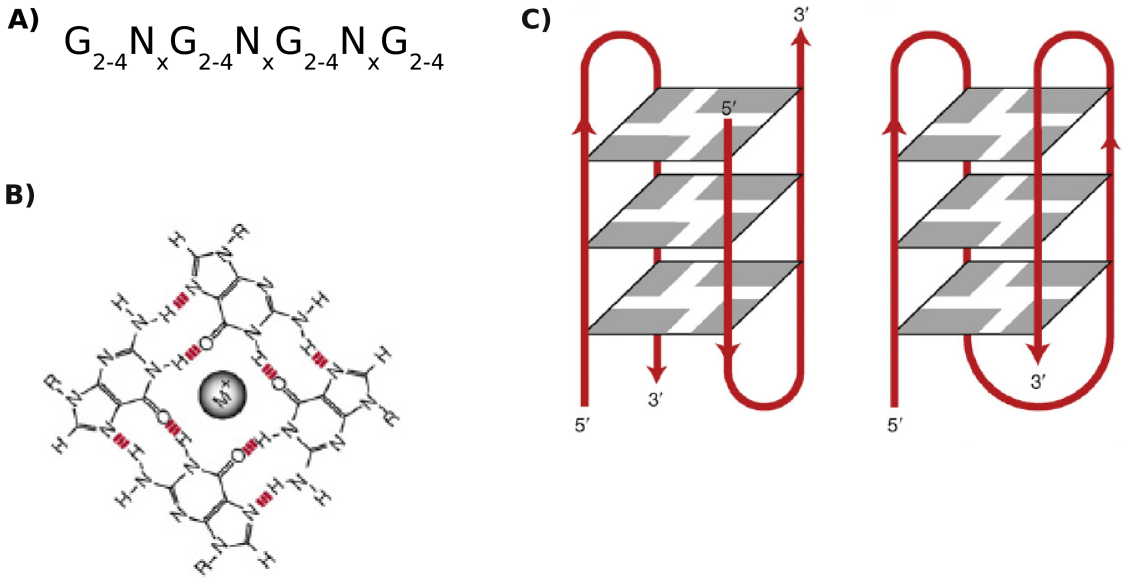

Figure 1.6: G-quadruplex structure
A) Typical sequence of a putative G4-DNA. Four repeats of 2-4 Guanines (G) are separated by loops of variable length (N).
B) Hoogsten hydrogen bonding of a G-quartett stabilised by a monovalent cation (M^+). Adapted from (Lipps and Rhodes, 2009).
C) Intermolecular folding of G4-DNA (left); two individual strands contribute to the structure. Intramolecular folding of G4-DNA (right); only one strand contributes to the structure. Adapted from (Lipps and Rhodes, 2009).

---

related with telomeres, promoters, rDNA and also with minisatellites and the immunoglobulin (Ig) heavy chain switch region (Rawal et al., 2006; Johnson et al., 2008; Hershman et al., 2008; Eddy and Maizels, 2009). A recent study by Capra et al. (2010) showed that G4-DNA motifs are conserved between seven yeast species and furthermore the conservation on the nucleotide level suggests evolutionary pressure on the capacity to form G4-DNA. In the same study a more detailed analysis of G4-DNA sequences in *S. cerevisiae* shows that non-telomeric conserved motifs are preferentially found in the rDNA, promoters, transcription factor binding sites and "dubious" open reading frames (ORFs). Interestingly, an opposite relationship was observed for ORFs in essential genes. There was also a correlation between the non-conserved G4-DNA sequences in *S. cerevisiae* and sites of frequent mitotic and meiotic DSB formation. *S. cerevisiae* mitochondrial DNA was enriched in G4-DNA sequences compared to nuclear DNA (Capra et al., 2010). In the human genome, G4-DNA motifs are enriched in the regulatory 5' regions of genes as compared to downstream regions (Eddy and Maizels, 2009). Independent of this feature, G4-DNA motifs were enriched in proto-oncogenes and of very low abundance in tumor suppressor genes (Eddy and Maizels, 2006, 2009).

1.6.1.3 G4-DNA and telomeres

As telomeres are associated with G-rich sequences and also a single-stranded overhang, a connection between G4-DNA structures and these genomic loci seems feasible. Immunostaining in the ciliate *Stylonychia lemnae* with antibodies raised against different G4-DNA conformations formed by the telomeric G-overhang of this organism, provided direct *in vivo* evidence for G4-DNA (Schaffitzel et al., 2001; Lipps and Rhodes, 2009). Detection of these structures was possible because of the high concentration of telomeres in this organism. Importantly, replication takes place in the "replication band", which is a morphologically separated region (Prescott, 1994). This allowed for the observation that G4-DNA was absent during replication (Schaffitzel et al., 2001).

Even though several groups have shown that telomeric DNA from different organisms have the capacity to form G4-DNA *in vitro*, it is difficult to demonstrate this capability *in vivo*. Parkinson et al. (2002) crystallised G4-DNA structures formed by human telomeric DNA. A recent study has compared the capacity of telomeric repeats from different species to form G4-DNA *in vitro* (Tran et al., 2011). Interestingly, the telomeric sequences in *S. pombe* and *S. cerevisiae* are heterogeneous. While *S. pombe* telomeres contain G_2 motifs in $(GGTTAC)_3GG$ or $(GGTTACA)_3GG$ repeats, *S. cerevisiae* repeats consist of $(GGGTGT)_3GGG$. Tran et al. (2011) showed *in vitro* that *S. pombe* telomeric sequences were not prone to form G4-DNA compared to *S. cerevisiae* sequences. It is worth noting that a separate study using more heterogenous telomeric repeat sequences for *S. pombe* (G_{1-8}) came to the conclusion that these sequences do form G4-DNA *in vitro* (Torigoe and Furukawa, 2007). However, consistent with Tran et al. (2011), the capacity to form G4-structures was minor in repeats containing G_2 and gradually increased with increasing amount of Gs per repeat (Torigoe and Furukawa, 2007; Tran et al., 2011).

In vivo evidence of a role for these structures in telomere maintenance has emerged from studies of the *Stylonychia lemnae* proteins TEPBα and TEPBβ. These two proteins are required for G4-DNA formation, where TEPBα binds to the G-rich sequence and interaction with TEPBβ catalyses G4-DNA formation (Paeschke et al., 2005). In replication, G4-DNA structures have to be removed to allow access to the G-overhang by telomerase for telomere synthesis. Paeschke et al. (2008) could further demonstrate that phosphorylation of TEPBβ regulates G4-DNA unfolding as well as telomerase recruitment. Treatment of cells with a G4-DNA stabilising agent in telomerase expressing tumor cells resulted in the activation of a DNA damage response and cell apoptosis, suggesting an interference of G4-DNA with the replication and extension of telomeres (Salvati et al., 2007). Proteins required for telomere maintenance have been shown to bind and process G4-DNA. Among these are members of the human RecQ helicases and also the yeast helicase *sc*Sgs1, as well as *h/sc*Pif1, *h*Pot1 and *sc*Mre11 (MRX complex) (Ghosal and Muniyappa, 2005;

Johnson et al., 2008; Lipps and Rhodes, 2009).

1.6.1.4 G4-DNA, transcription and translation

The occurrence of G4-forming sequences in promoters and also in ORFs together with the possibility that G4-structures can form in RNA, which is single-stranded, led to the model that G4-motifs can regulate transcription and translation. One example of the effect of G4-DNA on gene expression is the human c-Myc promoter. The G-rich promoter sequence of c-Myc can form G4-DNA *in vitro* (Siddiqui-Jain et al., 2002). The same study has shown that a single point mutation can destabilise this structure and furthermore, that a G4-DNA binding ligand was sufficient to suppress c-Myc transcription, suggesting that stabilisation of the G4-motif negatively regulates transcription. A genome-wide analysis in *S. cerevisiae* has shown that treatment with a G4-stabilising ligand (NMM) leads to up-regulation of genes that have a putative G4-DNA motif in their promoters (Hershman et al., 2008). This seems to contrast the results seen for the c-Myc expression regulation (Siddiqui-Jain et al., 2002). However, it should be noted that the changes in expression levels could be an indirect effect rather than a direct result due to G4-DNA stabilisation in each particular promoter. Hershman et al. (2008) further demonstrated that the same expression study in a *sgs1*Δ background led to a down-regulation of the same genes. This is surprising, as Sgs1 was shown *in vitro* to unwind G4-DNA (Huber et al., 2002) and therefore G4-DNA could be expected to be more stable in this background. However, other helicases like Pif1 have been implicated in G4-DNA unwinding and in fact, a recent study which directly compared the two helicases (Sgs1 and Pif1) showed that Pif1 family helicases are much more efficient in G4-DNA unwinding as compared to RecQ helicases (Ribeyre et al., 2009, Bochman et al., personal communication).

The role of G4-RNA in translational regulation is not well characterised. Kumari et al. (2007) have identified a G4-motif in the 5'-UTR of the human proto-oncogene NRAS and *in vitro* analysis showed that this motif can form G4-RNA and repress translation *in vitro*.

1.6.1.5 Genome instability associated with G4-DNA

Occurrence of G4-DNA in the genome poses a theoretical threat to DNA replication. As several helicases were described to be capable of unwinding G4-DNA, it was suggested that these helicases might be required to ensure progression of replication (Johnson et al., 2008; Lipps and Rhodes, 2009). Several reports have associated genomic rearrangements with G4-DNA sequences. Cahoon and Seifert (2009) reported that a G4-DNA containing motif was required for pilin antigenic variation in *Neisseria gonorrhoeae*. Interestingly, mutations in this sequence that destabilise the G4-DNA prevented nick-formation and subsequent recombination required for antigenic vari-

ation (Cahoon and Seifert, 2009). Ribeyre et al. (2009) analysed the stability of the human minisatellite CEB1 in *S. cerevisiae*. They confirmed that this sequence forms G4-DNA *in vitro* and also used a mutated sequence where G4-structure formation was abolished. A change in genomic rearrangements in a wild-type background could not be detected between the two sequences. However, in a *pif1*Δ or *rad27*Δ (Fen1 homolog) background, rearrangements were increased in the G4-DNA construct. Stability of CEB1 containing the mutated G4 sequence was not affected in *pif1*Δ cells, but was increased in *rad27*Δ cells, suggesting a role for Pif1, but not for Rad27 in the stability of G4-containing sequences (Ribeyre et al., 2009). A different study using the CEB1 sequence demonstrated that treatment of *S. cerevisiae* cells with the G4-interacting compound Phen-DC3 resulted in minisatellite instability (Piazza et al., 2010).

Bochman et al. (personal communication) assayed the ability of RecQ and Pif1 helicases for G4-DNA unwinding and also effects on GCRs related to G4-DNA. They found that Pif1 helicases were most efficient in unwinding G4-structures. Introducing a G4-motif (and also a mutated G4-motif) into a *S. cerevisiae* chromosome carrying selectable markers enabled them to assay G4-related GCRs in mutant backgrounds. While *sgs1*Δ cells showed a minor change in instability, *pif1*Δ cells had elevated levels of GCRs. Interestingly, genomic instability in *pif1*Δ cells was increased by the deletion of *RRM3*, the second member of the Pif1 helicase family in *S. cerevisiae*. This suggests a certain redundancy between these helicases, which was further confirmed by chromatin immunoprecipitation (ChIP): enrichment of Pif1 at G4-DNA sequences and also an enrichment of Rrm3 at these sites in *pif1*Δ cells was detected (Bochman et al., personal communication).

The semi-discontinuous replication of genomic DNA suggests that G4-DNA might be a more severe obstacle for the continuous leading strand synthesis, but ssDNA, favourable for G4-DNA formation, would be more abundant on the lagging strand during replication. Studies as to whether G4-DNA has a strand-specific effect on replication were carried out in human and chicken DT40 cells. A plasmid containing G4-DNA (human telomeric DNA) on either the leading or lagging strand was replicated in human cells and assayed for mutagenesis (Damerla et al., 2010). This analysis showed that G4-DNA on the leading strand had a more mutagenic effect as compared to G4-DNA on the lagging strand. In DT40 cells, the Y-family DNA polymerase REV1 is required for efficient replication of G4-DNA specifically on the leading strand template (Sarkies et al., 2010).

1.6.2 rDNA RFB

The rDNA locus consists of multiple copies of tandem repeats encoding the ribosomal genes. RFBs enforce unidirectional replication in this locus to prevent a possible collision with the transcription machinery. Therefore stalled forks accumulate in the rDNA locus (Tsang and Carr, 2008). Recovery of replication perturbations in a unidirectional locus is of pronounced importance because a stalled fork cannot be rescued by a fork approaching from the other direction (Murray and Carr, 2008). Furthermore, because of its repetitive nature, defective HR can lead to contraction or expansion of the rDNA locus (Tsang and Carr, 2008).

The rDNA locus is best characterised in *S. cerevisiae*. In this locus, the activity of transcription, replication and recombination are highly regulated. Recombination activity in the rDNA is essential to maintain the copy number of repeats (Labib and Hodgson, 2007). The rDNA consists of multiple copies of ribosomal genes (35S and 5S), which are transcribed in opposite directions by RNA polymerase 1 (Pol 1) and RNA Pol 3, respectively (Tsang and Carr, 2008). The spacers in between the coding sequences contain functional elements (cis-acting factors), like origins of replication and RFBs (Figure 1.7A) (Tsang and Carr, 2008; Dalgaard et al., 2009). The rDNA RFB elements, RFB 1, 2 and 3 function as polar replication fork arrest sites and interact with the trans-acting factors Fob1 and Reb1 (Dalgaard et al., 2009).

Whereas Fob1 regulates replication termination, Reb1 was shown to be important for transcription termination (Dalgaard et al., 2009). Fob1 binds the rDNA RFBs, RFB1 and 2, and stalls replication in a polar manner (Kobayashi, 2003; Mohanty and Bastia, 2004). This arrest ensures unidirectional replication of the rDNA locus (Brewer and Fangman, 1988; Linskens and Huberman, 1988). HOT1 consists of two elements, the Pol 1 promoter of 35S and the polar RFB and was shown to be a hotspot for recombination (Figure 1.7A) (Keil and Roeder, 1984). Fob1 as well as RNA Pol 1 transcription of the recombining sequences are required for HOT1 activity (Voelkel-Meiman et al., 1987; Labib and Hodgson, 2007). A model in which replication fork arrest induces recombination could explain the interplay of the elements of the rDNA. However, it was shown that recombination induced by HOT1 placed in an ectopic position is dependent on Fob1 and RNA Pol 1, but not on replication fork arrest (Ward et al., 2000).

In *S. pombe*, rDNA units consist of only one coding sequence, 35S, which is post-transcriptionally processed into smaller units (Dalgaard et al., 2009). The origin *ars3001* and the RNA Pol 1 promoter are located in the non-transcribed spacer and RFBs direct replication in the same direction as transcription (Figure 1.7B) (Linskens and Huberman, 1988). There are four polar RFBs in the *S. pombe* rDNA (RFB1-4/Ter1-4), of which only Ter1-3 also function on plasmids (Krings and Bastia, 2004). The essential gene $sap1^{+}$ is required for replication fork stalling at Ter1 (Mejía-

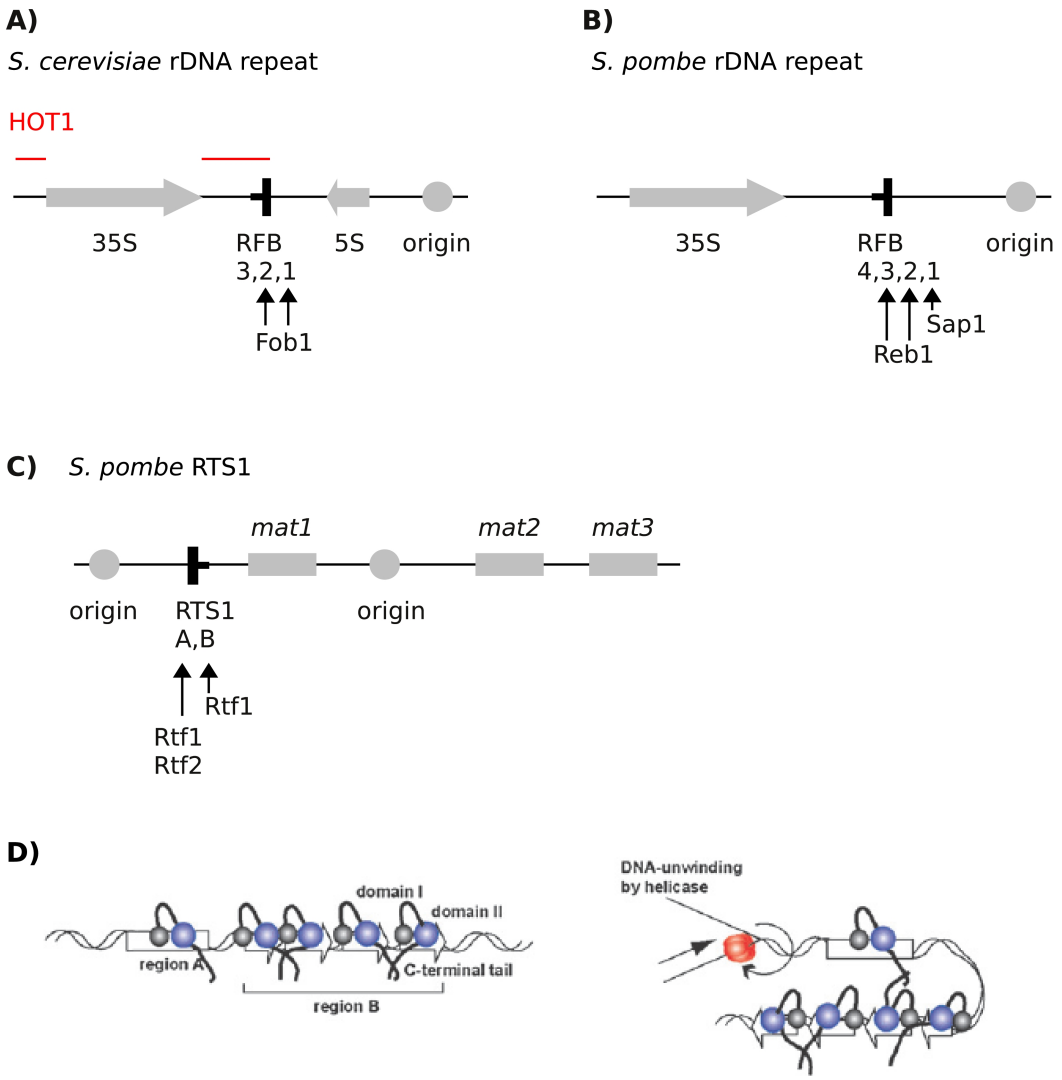

Figure 1.7: Protein-DNA replication fork barriers (RFBs)
A) One repeat of the rDNA repeat in *S. cerevisiae*. The ribosomal genes 35S and 5S are represented by grey arrows indicating the direction of transcription. The origin is shown as a grey circle. RFB1-3 are shown and arrows indicate binding sites of Fob1. The RFB blocks replication from the right. Elements contained in HOT1 are shown in red.
B) One repeat of the rDNA repeat in *S. pombe*. As described in A. The trans-acting factors Sap1 and Reb1 are required for replication fork stalling and their binding sites are indicated by arrows.
C) Replication termination sequence 1 (RTS1) in the *S. pombe* mating type locus. The transcriptionally active *mat1* and the silenced donors *mat2* and *mat3* are represented with grey boxes. The RFB blocks replication from the left. Origins are shown as circles. Binding of Rtf1 and Rtf2 in regions A and B is indicated by arrows. While region B is absolutely required for barrier activity, region A acts as an enhancer.
D) Model of Rtf1 binding of RTS1. Left: Domain I and II are shown in grey and blue, respectively. Four molecules of Rtf1 bind to region B and protein-protein interactions facilitate the binding of Rtf1 to region A. Right: DNA looping by protein interactions and DNA binding. This represents a constraint for the replicative helicase (red). This figure was adapted from (Eydmann et al., 2008).

Ramírez et al., 2005; Krings and Bastia, 2005). *sap1*$^+$ was initially shown to be required for mating type switching, as it binds to the element SAS1 (Arcangioli and Klar, 1991). The process of mating type switching is connected to unidirectional replication and DNA modification (imprint). Although *sap1*$^+$ is required for imprinting, it is not required for replication fork pausing at SAS1, like it is at Ter1 (Dalgaard and Klar, 2000). Biochemical analysis of the Sap1 protein structure and its binding capacities to SAS1 and Ter1 have given some insight into its function. Sap1 consists of a C-terminal coiled-coil domain and a N-terminal DNA binding domain and both of these motifs are important for oligomerisation (Ghazvini et al., 1995). In addition to SAS1 and Ter1, Sap1 was shown to bind to the artificial sequence DR2 (Ghazvini et al., 1995). Studies comparing the binding capacities of Sap1 to these three sequences and its effect on replication and conformational changes of the DNA suggest that binding affinity does not correlate with RFB efficiency and that Sap1 binding at these sites introduces local helical distortions which differ between SAS1 and Ter1 and could account for RFB efficiency (Krings and Bastia, 2006). The genes encoding components of the fork protection complex, *swi1*$^+$ and *swi3*$^+$ are required for replication fork stalling at SAS1 and at Ter1-3 and Swi1 was shown to accumulate at the Ter sites (Dalgaard and Klar, 2000; Noguchi et al., 2004; Krings and Bastia, 2004). Reb1 was shown to bind to RFB2 and 3 and is required for polar replication fork stalling and transcription termination at these sites (Sánchez-Gorostiaga et al., 2004; Krings and Bastia, 2004). Reb1 is a paralog of Rtf1, which is required for fork arrest at RTS1 (RFB at the mating type locus) and will be discussed in the next paragraph. RFB4 is only active in its chromosomal context, it is independent of *swi1*$^+$ and *swi3*$^+$ and its activity increases if the other three barriers are not functional (Krings and Bastia, 2004). This increase might reflect collisions between transcription and replication.

1.6.3 Replication termination sequence 1 (RTS1)

RTS1 is a polar RFB located at the mating type locus on chromosome 2 in *S. pombe*, where it is required to coordinate mating type switching (Dalgaard and Klar, 2001). The direction of replication is important for the switching process because of an imprint formed in a replication-dependent manner (Dalgaard and Klar, 1999; Vengrova and Dalgaard, 2004; Kaykov and Arcangioli, 2004). This imprint initiates recombination between the transcriptionally active *mat1* cassette and the silent donor cassettes *mat2* and *mat3* (Beach et al., 1982). Similar to the rDNA barrier, cis-acting sequences and trans-acting factors are involved in the regulation of RTS1 (Dalgaard et al., 2009). The RTS1 element consists of two regions, termed A and B (Figure 1.7C) (Codlin and Dalgaard, 2003). Codlin and Dalgaard (2003) showed that region A is purine-rich and enhances RFB activity of RTS1 four-fold, but has no barrier activity on its own. Furthermore, region B consists of

four imperfect repeats of 55bp and is essential for function. The repeated motifs show sequence similarity to the Reb1 binding site at the rDNA. Rtf1, a paralogue of Reb1, binds to regions A and B and is required for barrier activity (Codlin and Dalgaard, 2003; Eydmann et al., 2008). A genetic screen identified four genes that are important for RTS1 function; *rtf1*$^+$, *rtf2*$^+$, *swi1*$^+$ and *swi3*$^+$ (Dalgaard and Klar, 2000). *swi1*$^+$ and *swi3*$^+$ encode members of the replication fork protection complex (FPC), components of the replisome, which are important for checkpoint activation in S-phase (Noguchi et al., 2003, 2004). Rtf1 belongs to the Rtf1/Reb1/TTF1 family. TTF1 is a mammalian transcription termination factor which causes a polar replication fork arrest in the rDNA (Gerber et al., 1997). Two domains of Rtf1 (domain I and II) have been characterised by mutational and computational analysis (Eydmann et al., 2008). Both are myb-like domains containing three myb motifs in the N-terminal domain I and two myb/SANT motifs in the C-terminal domain II. myb motifs consist of 50 amino acids and are involved in DNA-binding and myb/SANT motifs describe a subclass of these motifs and were suggested to interact with histone tails (Boyer et al., 2002). The C-terminus of Rtf1 was shown to be important for dimerisation or polymerisation and is essential for RTS1 function (Eydmann et al., 2008). While domain I was shown to bind to regions A and B of RTS1 and is important for the polarity of the RFB, domain II binds to region B (Eydmann et al., 2008). Eydmann et al. (2008) suggest a model in which at least five Rtf1 molecules bind to dsDNA of RTS1; four Rtf1 binding sites are in region B and probably region A could be occupied helped by protein-protein interactions. This setup would result in a topological constraint (by DNA looping) interfering with the replicative helicase (Figure 1.7D).

rtf2$^+$ is epistatic to region A of RTS1 and is required for efficient replication termination by preventing replication restart (Codlin and Dalgaard, 2003; Inagawa et al., 2009). Also, Rtf2 was shown to interact with PCNA (Inagawa et al., 2009). Inagawa et al. (2009) established that in the absence of *rtf2*$^+$, slow-moving forks are detectable and these are dependent on the helicase Srs2, but not on the TLS polymerases η, κ and ξ. Furthermore, SUMO (Pmt3) is required for full RFB activity (Inagawa et al., 2009). In their model they suggest that the role of Rtf2 is downstream of Rtf1 by stabilising the stalled replication fork for termination. Computational analysis showed that Rtf2 is conserved in higher eukaryotes and contains RING-finger-like domains, indicative of protein binding (Inagawa et al., 2009; Marchler-Bauer et al., 2011).

1.7 Analysis of site-specific replication fork arrest using DNA-protein RFBs

The rDNA barrier in *S. cerevisiae* and RTS1 in *S. pombe* have been used as site-specific RFBs to study cellular responses to this event (Lambert and Carr, 2005; Labib and Hodgson, 2007). The *S. cerevisiae* rDNA element HOT1 was shown to induce recombination at the rDNA (Kobayashi et al., 1998; Johzuka and Horiuchi, 2002). Insertion of the rDNA barrier at ectopic sites also induces recombination (Keil and Roeder, 1984). HOT1-induced recombination requires Pol 1 transcription (Voelkel-Meiman et al., 1987), but not replication fork stalling (Ward et al., 2000). It has also been shown that RFB-activity is not dependent on Pol 1 transcription (Brewer et al., 1992). Therefore, the induced recombination at the *S. cerevisiae* rDNA RFB was not due to replication fork stalling.

Calzada et al. (2005) created a system in which two rDNA RFBs were place on chromosome 3 in *S. cerevisiae* in such orientation that replication of the intervening sequence is prevented (Figure 1.8A). The construct is flanked by two highly active origins and the activity of the RFBs was regulated by controlled expression of FOB1. Replication forks were shown to arrive at the RFBs with similar kinetics and would resume replication and pass the barrier after a period of pausing. ChIP analysis established that fork pausing at the RFBs did not cause the replisome to disassemble and the helicase Rrm3 was specifically recruited to paused forks. Although Mrc1 and Tof1 were present at the paused forks, only Tof1 (and Csm3) seemed to be important for pausing. Furthermore, pausing and recovery of the replication fork were independent of *MEC1*, *RAD53* and *RAD52*. These data suggest that the paused replisome can resume replication independently of the checkpoint and HR (Calzada et al., 2005).

The polar barrier RTS1 has been used as a site-specific RFB. Three studies in fission yeast have shown that replication fork arrest at an ectopic RTS1 site induced chromosomal rearrangements (Ahn et al., 2005; Lambert et al., 2005; Mizuno et al., 2009). Ahn et al. (2005) inserted a copy of RTS1 in different orientations at the *ade6* locus on chromosome 3 (Figure 1.8B). In this assay, RTS1 is flanked by two copies of mutant adenine alleles. Recombination between the mutant alleles can give rise to a functional *ade6*$^+$ allele resulting from gene conversion or deletion dependent on HR (Doe et al., 2004). Ahn et al. (2005) showed that replication fork arrest induced recombination between the direct repeats and gave rise to *ade6*$^+$ cells. The recombination events induced by RTS1 were dependent on *rhp51*$^+$ and *rad22*$^+$. The viability of HR-deficient cells was not compromised in the presence of blocked replication forks at RTS1. As expected, the orientation of RTS1 such that most approaching replication forks are blocked was most efficient in the induction of recombination (Ahn et al., 2005).

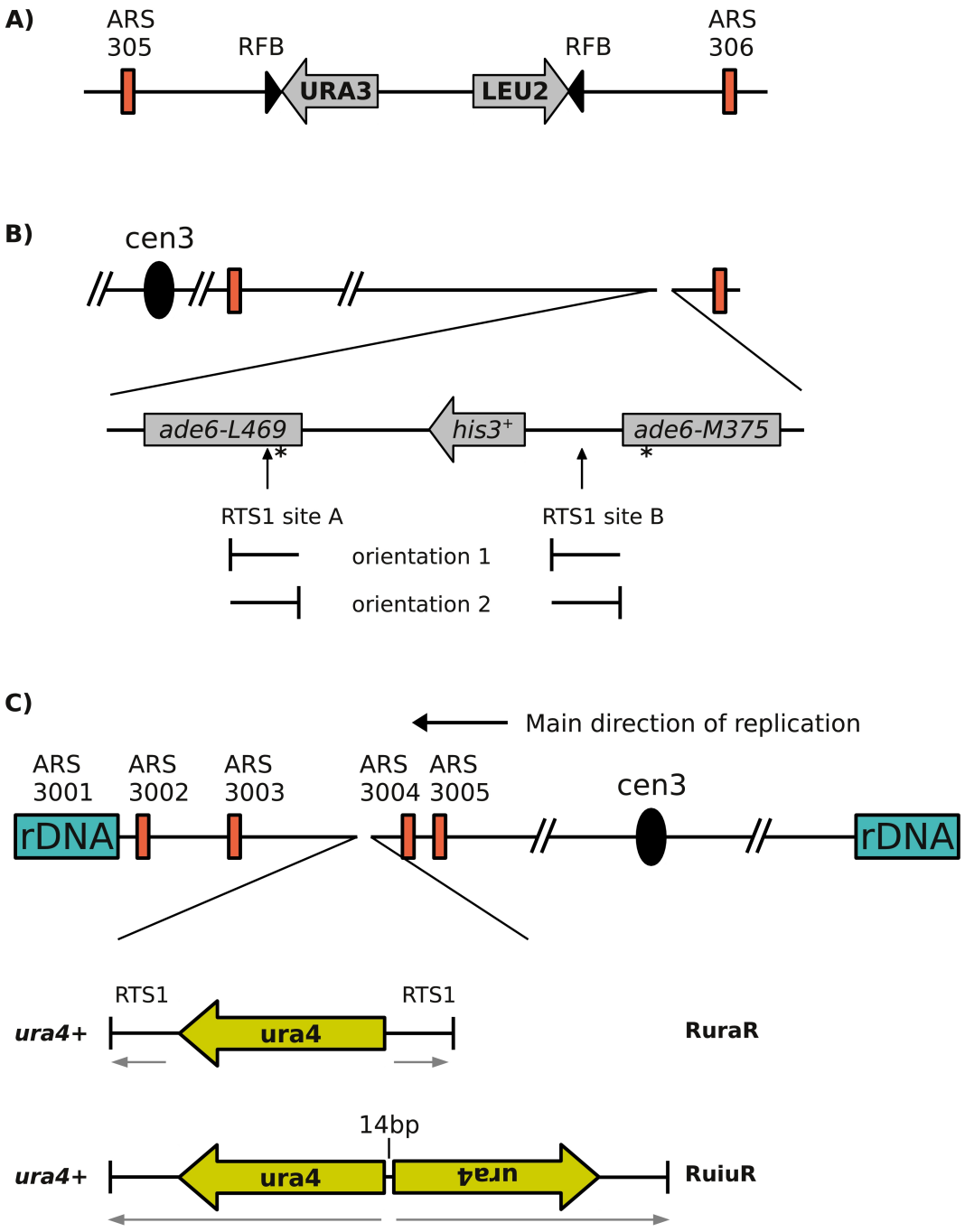

Figure 1.8: RFB systems
A) *S. cerevisiae* rDNA RFB system. Two rDNA barriers (RFBs) were integrated on chromosome 3 to block replication forks approaching from the flanking origins *ARS305* and *ARS306*. The two marker genes *LEU2* and *URA3* are indicated with grey arrows showing their transcription direction. Modified from (Calzada et al., 2005).
B) *S. pombe* RTS1 direct repeat assay. Depicted is chromosome 3 in *S. pombe*, where the RTS1 barrier was integrated upstream (site B) or downstream (site A) of *his3*$^{+}$ in both orientations (1 and 2). Two mutant alleles of *ade6*$^{+}$ (*ade6-L469* and *ade6-M375*) are flanking RTS1. The positions of the mutations are indicated by "*". ARS are shown in red boxes. Modified from (Ahn et al., 2005).
C) *S. pombe* RTS1 inverted repeat (RuraR) and palindrome (RuiuR) assay. Chromosome 3 is shown and ARS are indicated in red boxes (ARS numbers as in (Segurado et al., 2003). The main direction of replication is from the centromere. For RuraR, two copies of RTS1 were integrated flanking *ura4*$^{+}$. Grey arrows indicate homologous sequences. Modified from (Lambert et al., 2005). For RuiuR, two copies of RTS1 are flanking an inverted repeat of *ura4*$^{+}$ (RuiuR) separated by a 14bp spacer. Modified from (Mizuno et al., 2009).

Lambert et al. (2005) introduced two copies of RTS1 at the *ura4* locus on chromosome 3 in *S. pombe* (Figure 1.8C). The copies are flanking *ura4*$^+$ (RuraR) in a manner such that replication is blocked from both directions and the cell is confronted with a non-replicated stretch of DNA. The two RTS1 elements form inverted repeats with a 1.7kb spacer (*ura4*$^+$). Constructs with only one repeat of RTS1 upstream or downstream of *ura4*$^+$ were also analysed (Rura and uraR). RTS1 is controlled by the *nmt41*$^+$ promoter in this system and expression can be induced by the removal of thiamine from the media. Replication fork arrest at RTS1 is most effective when placed such as to inhibit replication forks approaching from the most active origin for this region, which is situated centromere-proximal of RuraR (Segurado et al., 2003; Lambert et al., 2005). Induction of replication fork arrest showed an increase in GCRs, namely, orientation switch of *ura4*$^+$ and translocations between the RTS1 sequences at *ura4*$^+$ and the endogenous RTS1 sequence at the mating type locus on chromosome 2. The orientation switch of *ura4*$^+$ was not observed in Rura or uraR indicating the requirement of two RTS1 sequences. Optimal viability of cells carrying one or two copies of RTS1 at *ura4*$^+$ required HR, but not the DNA damage or replication checkpoint. These results suggest that firstly, the replisome, arrested at RTS1, is not stabilised and therefore disassembles (fork collapse) and secondly, HR is important for recovery after replication fork collapse at RTS1 and also for replication termination between an arrested fork at RTS1 and a fork approaching from the opposite direction. Rad51 and Rad52 foci accumulated after induction of RTS1 activity and Rad52 was enriched at the site of fork collapse in RuraR as well as in uraR, suggesting that recombination proteins associate with these fork structures (Lambert et al., 2005).

A more recent study, using the same systems (RuraR and uraR), identified replication and recombination intermediates after replication fork collapse at RTS1 (Lambert et al., 2010). This study suggests that recombination intermediates are formed during replication fork restart at RTS1. The intermediates are dependent on *rad22*$^+$, but can occur in the absence of *rhp51*$^+$, though at a lower frequency. The RecQ helicase *rqh1*$^+$ limits the *rhp51*$^+$-dependent pathway, although this does not affect replication fork restart and the helicase *srs2*$^+$ promotes replication fork restart. In agreement with the previous study (Lambert et al., 2005), these results show that replication fork collapse and recombination-dependent restart causes chromosomal rearrangements (Lambert et al., 2010).

A different study employed two RTS1 sequences flanking two inverted copies of *ura4*$^+$, resulting in a large palindrome only separated by a 14bp spacer (RuiuR) (Figure 1.8D) (Mizuno et al., 2009). Replication fork collapse at RuiuR induced the formation of acentric (no centromere) and dicentric (two centromeres) chromosomes in a high percentage of cells. These palindromic chromosomes are also formed in RuraR upon replication fork collapse, however, about 10-fold less

than compared to RuiuR. The formation of these palindromic chromosomes coincided with a loss of viability, which correlates with a mitotic catastrophe phenotype in 20-25% of cells. A construct using two RTS1 sites where the orientation was inverted (oRuiuRo), leads to replication of the *ura4*$^{+}$ palindrome from the centromere and fork collapse only at the second (telomere-proximal) RTS1. This construct also formed palindromic chromosomes, suggesting that one collapsed fork within a palindromic sequence is sufficient for these rearrangements to occur. DSBs were not detected at this locus upon replication fork collapse in any genetic background. As observed in RuraR (Lambert et al., 2005), HR proteins were required for these rearrangements to occur (Mizuno et al., 2009). Importantly, genetic analysis revealed that the formation of palindromic chromosomes was independent of NHEJ, SSA or of proteins proposed to cleave an extrusion of the palindrome.

All these studies suggest that a HR-dependent restart mechanism at RTS1 can lead to chromosomal rearrangements at repetitive sequences. It is important to note that this event occurs in the absence of a detectable DSB and is therefore distinct from BIR.

1.8 Aims of this work

Genomic instability that is caused by replication perturbations underlay many diseases. How genome instability is related to DNA replication and replication-associated repair pathways is not fully understood. In this work I have developed assays, which enable the detection of TR deletions. I have used these assays to measure TR deletions in the context of G4-DNA and also to investigate erroneous replication after replication fork collapse and HR-dependent restart at RTS1.

Enzymatic activities, such as the structure-specific endonuclease Mus81-Eme1, play important roles in DNA replication and repair. In collaboration with Professor Neil McDonald I have characterised a novel domain in Mus81. This characterisation should give further insight into the importance of this enzyme and its specific functions.

Finally, I aimed to develop a biochemical assay, which could potentially be used for proximity-dependent protein purification. This technique would open new possibilities in the identification of factors associated with DNA repair and replication fork restart.

Chapter 2

Materials and Methods

2.1 Abbreviations, contents and information of frequently used solutions and chemicals

2.2 Media

2.2.1 Yeast Extract (YE), rich media

0.5% w/v (5g/l)	yeast extract
3.0% w/v (30g/l)	glucose

2.2.2 YE agar plates (YEA)

YE with 12.5g/l Difco Bacto Agar

Yeast Nitrogen Base (YNB) without Thiamine or Edinburgh Minimal Media (EMM) was used for growth in minimal media.

2.2.3 Edinburgh Minimal Media (EMM)

50.0ml/l	20x EMM2 salts (see below)
25.0ml/l	20% NH_4Cl
25.0ml/l	0.4M Na_2HPO_4
50.0ml/l	40% Glucose
1.0ml/l	1000x Vitamins
0.1ml/l	10000x Trace elements

PBS	Phosphate buffered saline (137mM NaCl, 2.7mM KCl, 10mM Na_2HPO_4, 1.76mM KH_2PO_4)
PBST	PBS with 0.1% Tween 20 (Sigma, P7949)
BSA	Albumin from bovine serum (Sigma, A9647)
SDS	Sodium dodecyl sulfate
EDTA	Ethylenediaminetetraacetic acid
SSC	20x SSC (0.15M NaCl, 0.015M Sodium citrate pH 7.0)
Denhardt's reagent	100x (20g/l Polyvinylpyrrolidone pH 7.0, 20g/l BSA, 20g/l Ficoll 400)
TBE	0.5x (44mM Tris base, 44mM Boric acid, 1mM EDTA pH 8.0)
Lauryl sarcosine	(Sigma, 61747)
Proteinase K	(Sigma, P2308)
RibonucleaseA	(Sigma, R4875)
TE	1x (10mM Tris-HCl, 1mM EDTA pH 7.5)

Table 2.1: List of frequently used chemicals and solutions

2.2.3.1 20x EMM2 salts

61.20g/l	Potassium hydrogen phthallate
20.00g/l	KCl
21.40g/l	$MgCl_2$ x $6H_2O$
0.20g/l	Na_2SO_4
0.26g/l	$CaCl_2$ x $2H_2O$

2.2.3.2 10000x Trace elements

5.0g/l	H_3BO_3
4.0g/l	$MnSO_4$
4.0g/l	$ZnSO_4$ x $7H_2O$
2.0g/l	$FeCl_3$ x $6H_2O$
1.5g/l	Na_2MoO_4
1.0g/l	KI
0.4g/l	$CuSO_4$ x $5H_2O$
10.0g/l	Citric acid

2.2.3.3 1000x Vitamins

1.0g/l	Pantothenic acid
10.0g/l	Nicotinic acid
10.0g/l	Inositol
0.01g/l	d-Biotin

Unless stated otherwise the yeast minimal media YNB and EMM were supplemented with adenine hydrochloride, histidine, leucine, uracil and lysine hydrochloride at a final concentration of 100mg/l.

Luria-Bertani (LB) media was used to grow *E. coli*.

2.2.4 Drugs and chemicals used for selection

Hydroxy Urea (HU)	Sigma, H8627
Methyl Methanesulfonate (MMS)	Sigma, 129925
Camptothecin (CPT)	Acros Organics, 27672
nourseothricine (NAT)	Werner BioAgents, clonNAT, 51000
4-Nitroquinoline 1-oxide (4-NQO)	Sigma, N8141
5-Fluoroorotic acid (5-FOA)	Melford, F5001
Geneticin disulphite (G-418)	Melford, G0175
Hygromycin B	Melford, H7502)
Kanamycin monosulfate	Melford, Kanamycin A, K0126
Ampicillin sodium salt	Sigma, A9518

Table 2.2: List of DNA damaging agents and drugs used for selection

2.3 List of strains

The numbers of the strains listed below refer to the SAS collection unless stated otherwise.

48	mus81::loxP_ura4$^+$_loxM3 ade6-704 ura4-D18 leu1-32 h$^-$
61	ura4::nat1(101TR) h$^-$
63	ura4::nat1(101TR) h$^+$
70	mus81::loxP_mus81$^+$_loxM3 ade6-704 ura4-D18 leu1-32 h$^-$
72	mus81::loxP_mus81-WHΔ_loxM3 ade6-704 ura4-D18 leu1-32 h$^-$
74	mus81::loxP_mus81-K176,181A_loxM3 ade6-704 ura4-D18 leu1-32 h$^-$
81	ura4::nat1(41TR) h$^+$
83	ura4::nat1(41TR) h$^-$
84	ura4::nat1(251TR) h$^-$
85	ura4::nat1(251TR) h$^+$
141	ura4::nat1(251TR) rhp51::kanMX6 h$^-$
197	ura4::nat1(101TR) h$^-$ smt0
198	ura4::nat1(41TR) h$^-$ smt0
199	ura4::nat1(251TR) h$^-$ smt0
229	ura4::nat1(101TR) pcn1-K164R::ura4$^+$ h$^-$
239	ura4::nat1(101TR) pcn1-K164R::ura4 h$^+$
240	mus81::loxP_mus81-D395,396A_loxM3 ade6-704 ura4-D18 leu1-32 h$^-$
243	mus81::loxP_mus81-R165,168A_loxM3 ade6-704 ura4-D18 leu1-32 h$^-$
260	mus81::loxP_mus81-R165,168A/K176,181A_loxM3 ade6-704 ura4-D18 leu1-32 h$^-$
271	rad22::kanMX6 ura4::nat1(101TR) h$^-$ smt0
272	rad22::kanMX6 ura4::nat1(101TR) h$^-$ smt0
293	mus81::loxP_mus81-K176,181E_loxM3 ade6-704 ura4-D18 leu1-32 h$^-$
296	mus81::loxP_mus81-H189A/K192A_loxM3 ade6-704 ura4-D18 leu1-32 h$^-$
315	rhp51::hphMX6, ura4::nat1(101TR), h$^-$ smt0
323	rad8::kanMX6 ura4::nat1(101TR) h$^-$ smt0
337	mus81::loxP_mus81-R165,168A/K176,181E_loxM3 ade6-704 ura4-D18 leu1-32 h$^-$
340	mus81::loxP_mus81-Y122A/R123A_loxM3 ade6-704 ura4-D18 leu1-32 h$^-$
344	ubc13::kanMX6 ura4::nat1(101TR) h$^-$ smt0
345	ubc13::kanMX6 ura4::nat1(101TR) h$^-$ smt0
362	urg1::loxP_hphMX6_loxM3 leu1-32 ade6-704 h$^-$

372	urg1::loxP_rad4-BirA-R118G_loxM3 ura4-D18 leu1-32 ade6-704 h^-
382	ubc13::kanMX6 ura4::nat1(41TR) h^- smt0
384	ubc13::kanMX6 ura4::nat1(251TR) h^- smt0
396	mus81::loxP_mus81-R113A/K114A/R115A/K116A_loxM3 ade6-704 ura4-D18 leu1-32 h^-
410	sws1::hphMX6 ura4::nat1(101TR) h^- smt0
413	msh2::kanMX6 ura4::nat1(101TR) h^- smt0
419	urg1::rad4-BirA-R118G rad9-cHA:natMX6 ade6-704 h^+
424	pREP1 ade6-704 ura4-D18 leu1-32 h^-
426	pREP1:6Flag:BirA-R118G ade6-704 ura4-D18 leu1-32 h^-
433	rhp51::hphMX6 rad22::ura4$^+$ ura4::nat1(101TR) leu1-32 h^- smt0
456	PRRX3AS-ura4$^+$-RTS1 rtf1:nmt41:sup3.5 ade6-704 leu1-32 h^- smt0
461	RuiuR rtf1:nmt41:sup3.5 ade6-704 leu1-32 h^- smt0
462	PRRX3AS-ura4(dup)-RTS1 rtf1:nmt41:sup3.5 ade6-704 leu1-32 h^- smt0
465	PRRX3AS-ura4(inv)-RTS1 rtf1:nmt41:sup3.5 ade6-704 leu1-32 h^- smt0
469	mus81::loxP_mus81-T275A_loxM3 ura4-D18 ade6-704 leu1-32 h^-
471	mus81::loxP_mus81-T275A/K176,181E_loxM3 ura4-D18 ade6-704 leu1-32 h^-
477	pREP1-BirA-c6His ade6-704 ura4-D18 leu1-32 h^-
478	pREP1-BirA-R118G-c6His ade6-704 ura4-D18 leu1-32 h^-
479	pREP1-SPBC30D10.07c-R396G-c6His ade6-704 ura4-D18 leu1-32 h^-
480	pREP1-SPBC30D10.07c-c6His ade6-704 ura4-D18 leu1-32 h^-
488	PRRX3AS-ura4(dup)-RTS1 rtf1::natMX6 ade6-704 leu1-32 h^- smt0
492	PRRX3AS-ura4(inv)-RTS1 rtf1::natMX6 ade6-704 leu1-32 h^- smt0
501	rad62-1 ade6-704 leu1-32 ura4-D18 h^+
502	rad62-1 ade6-704 leu1-32 ura4-D18 h^+
507	smc6-X ura4-D18 ade6-704 h^+
512	smc6-n74 leu1-32 ade6-704 ura4-D18 h^+
509	ura4::nat1(101TR) mrc1::ura4$^+$ ade6-704 h^- smt0
510	ura4::nat1(101TR) swi1::kanMX6 h^- smt0
514	pRep1-gBirA-R118G-6xFlag ade6-704 ura4-D18 leu1-32 h^-
515	pRep1-gBirA-R118G-6xFlag ade6-704 ura4-D18 leu1-32 h^-
523	ade6-704 leu1-32 ura4-D18 pREP1-gBirA h^-
524	ade6-704 leu1-32 ura4-D18 pREP1-gBirA h^-
525	ade6-704 leu1-32 rad9-cHA:kanMX6 ura4-D18 pRep1-gBirA-R118G-6xFlag h^-

526	ade6-704 leu1-32 rad9-cHA:kanMX6 ura4-D18 pRep1-gBirA-R118G-6xFlag h^-
527	ade6-704 leu1-32 rad9-cHA:kanMX6 ura4-D18 pRep1-gBirA-R118G-6xFlag-Rad4 h^-
528	ade6-704 leu1-32 rad9-cHA:kanMX6 ura4-D18 pRep1-gBirA-R118G-6xFlag-Rad4 h^-
558	M 2,3Δ::Leu2 ade6-210 ura4-D18 leu1-32 h^- (Klar and Miglio, 1986)
564	mus81::loxP_ura4$^+$_loxM3 Pdelta17::LEU2 ade6-M210 leu1-32 h^+
567	mus81::loxP_mus81$^+$_loxM3 Pdelta17::LEU2 ade6-M210 leu1-32 ura4-D18 h^+
573	mus81::loxP_mus81-K176,181E_loxM3 Pdelta17::LEU2 ade6-M210 leu1-32 h^+
711	ade6-704 leu1-32 ubc13::kanMX6 cdc6::loxP_cdc6$^+$_loxM3 ura4::nat1(101TR) h^+
714	ubc13::kanMX6 cdc6::loxP_cdc6-L591M_loxM3 ura4::nat1(101TR) ade6-704 leu1-32 h^+
718	rhp18::kanMX6 cdc6::loxP_cdc6$^+$_loxM3 ura4::nat1(101TR) h^+
719	rhp18::kanMX6 cdc6::loxP_cdc6-L591M_loxM3 ura4::nat1(101TR) ade6-704 leu1-32 h^-
732	ura4::loxM3_kanMX6_loxP rtf1::hphMX6 h^- leu1-32 ade6-704 arg3-D4 smt0
749	ura4::loxP_RFB:ura4$^+$:arg3(G4top_82TR_o1):RTS1_loxM3 rtf1::hphMX6 leu1-32 ade6-704 arg3-D4 h^- smt0
751	ura4::loxP_RFB:ura4$^+$:arg3(G4top_82TR_o2):RTS1_loxM3 rtf1::hphMX6 leu1-32 ade6-704 arg3-D4 h^- smt0
753	ura4::loxP_RFB:ura4$^+$:arg3(G4m_82TR_o1):RTS1_loxM3 rtf1::hphMX6 leu1-32 ade6-704 arg3-D4 h^- smt0
756	ura4::loxP_RFB:ura4$^+$:arg3(82TR_o1):RTS1_loxM3 rtf1::hphMX6 leu1-32 ade6-704 arg3-D4 h^- smt0
758	ura4::loxP_RFB:ura4$^+$:arg3(82TR_o2):RTS1_loxM3 rtf1::hphMX6 leu1-32 ade6-704 arg3-D4 h^- smt0
760	ura4::loxP_RFB:ura4$^+$:arg3(G4_82TR_o2):RTS1_loxM3 rtf1::hphMX6 leu1-32 ade6-704 arg3-D4 h^- smt0
762	ura4::loxP_RFB:ura4$^+$:arg3(G4_82TR_o1):RTS1_loxM3 rtf1::hphMX6 leu1-32 ade6-704 arg3-D4 h^- smt0
778	mus81::loxP_mus81-K176,181E_loxM3 leu-132 ade6-704 ura4-D18 h^- smt0
873	ura4::loxP_RFB:ura4$^+$:arg3(G4top_82TR_o2):RTS1_loxM3 rtf1:nmt41:sup3.5 leu1-32 ade6-704 arg3-D4 h^- smt0

881	ura4::loxP_RFB:ura4$^+$:arg3(82TR_o1):RTS1_loxM3 rtf1::hphMX6 cdc27-D1 leu1-32 ade6-704 arg3-D4 h$^-$ smt0
910	ura4::loxP_RFB:ura4$^+$:arg3(G4mtop_82TR_o1):RTS1_loxM3 rtf1::hphMX6 leu1-32 ade6-704 arg3-D4 h$^-$ smt0
911	mrc1::ura4$^+$ ura4::loxP_RFB:ura4$^+$:arg3(82TR_o1):RTS1_loxM3 rtf1::hphMX6 leu1-32 ade6-704 arg3-D4 h$^+$
914	mrc1::ura4 ura4::loxP_RFB:ura4$^+$:arg3(82TR_o1):RTS1_loxM3 leu1-32 ade6-704 arg3-D4 h$^-$ smt0
919	rev1::kanMX6 ura4::loxP_RFB:ura4$^+$:arg3(G4_82TR_o1):RTS1_loxM3 rtf1::hphMX6 leu1-32 ade6-704 arg3-D4 h$^-$ smt0
929	rev1::kanMX6 ura4::loxP_RFB:ura4$^+$:arg3(G4top_82TR_o1):RTS1_loxM3 rtf1::hphMX6 ade6-704 leu1-32 arg3-D4 h$^-$ smt0
973	mus81::loxP_mus81-CTAP_loxM3 ura4-D18 ade6-704 leu1-32 h$^-$
975	mus81::loxP_mus81-WHΔ-CTAP_loxM3 ura4-D18 ade6-704 leu1-32 h$^-$
977	mus81::loxP_mus81-K176,181E-CTAP_loxM3 ura4-D18 ade6-704 leu1-32 h$^-$
979	mus81::loxP_mus81-K176,181E/R165,168A-CTAP_loxM3 ura4-D18 ade6-704 leu1-32 h$^-$
1000	mrc1::ura4 leu1::mrc1(T645,653A)-3HA ade6-M210 ura4::nat1(101TR) h$^-$ smt0
1006	mcl1-101 ura4-D18 leu1-32 ura4::loxP_RFB:ura4$^+$:arg3(82TR_o1):RTS1_loxM3 rtf1::hphMX6 h$^-$ smt0
1007	mcl1-101 ura4-D18 leu1-32 ura4::loxP_RFB:ura4$^+$:arg3(82TR_o1):RTS1_loxM3 h$^+$
1009	leu1-32 arg3-D4 ura4::loxP_RFB:ura4$^+$:arg3(82TR_o1):RTS1_loxM3 h$^-$ smt0
1010	leu1-32 arg3-D4 ura4::loxP_RFB:ura4$^+$:arg3(82TR_o1):RTS1_loxM3 h$^+$
1030	msh2::kanMX6 ura4::loxP_RFB:ura4$^+$:arg3(82TR_o1):RTS1_loxM3 rtf1::hphMX6 leu1-32 ade6-704 arg3-D4 h$^-$ smt0
1050	ura4::loxP_RFB:ura4$^+$:arg3(G4m_82TR_o1):RTS1_loxM3 leu1-32 ade6-704 arg3-D4 h$^-$ smt0
1052	ura4::loxP_RFB:ura4$^+$:arg3(G4top_82TR_o1):RTS1_loxM3 leu1-32 ade6-704 arg3-D4 h$^-$ smt0
1054	ura4::loxP_RFB:ura4$^+$:arg3(G4mtop_82TR_o1):RTS1_loxM3 leu1-32 ade6-704 arg3-D4 h$^+$
1056	ura4::loxP_RFB:ura4$^+$:arg3(G4_82TR_o1):RTS1_loxM3 leu1-32 ade6-704 arg3-D4 h$^+$

1058	rqh1::kanMX6 ade6-704 leu1-32 ura4-D18 h^+
1059	rqh1::kanMX6 ade6-704 leu1-32 ura4-D18 h^-
1122	leu1-32 ade6-704 arg3-D4 ura4::loxP_RFB:ura4$^+$:arg3(82TR_o1):RTS1_loxM3 swi7-H4 h^+
1125	leu1-32 ade6-704 arg3-D4 ura4::loxP_RFB:ura4$^+$:arg3(82TR_o1):RTS1_loxM3 swi7-H4 rtf1::hphMX6 h^- smt0
1144	leu1-32 ade6-704 arg3-D4 ura4::loxP_RFB:ura4$^+$:arg3(82TR_o1):RTS1_loxM3 rad22::natMX6 rhp51::kanMX6 rtf1::hphMX6 h^- smt0
1176	leu1-32 ade6-704 arg3-D4 ura4::loxP_RFB:ura4$^+$:arg3(82TR_o1):RTS1_loxM3 cdc27-D1 h^+
AMC168	rad2::ura4$^+$ ade6-704 leu1-32 ura4-D18 h^+
AMC358	ade6-704 leu1-32 ura4-D18 arg3-D4 h^+
KAF1177	rhp18::kanMX6 ade6-704 leu1-32 ura4-D18 h^+
KAF1166	rad9-cHA:natMX6 h^+

Table 2.3: List of strains

2.4 List of oligonucleotides

3	ATTCAGGCGCCTGACCGTCGAGGACATCGAG
4	ATTGAGGCGCCCCGCTCGCGGGCGAACTC
11	GCGCCTGATGGGGCTCGCGACGGAGTTCGCCCGCGAGCGGG
12	GCGCCCCGCTCGCGGGCGAACTCCGTCGCGAGCCCCATCAG
13	ATTCAGGCGCCTGACCAAGGTGTTCCCCGACGACG
24	ATTGACATATGAATGGGATTTTTCATCCCCTCA
27	TGATATGAGCCCAAGAAGCA
28	GATGCCAGACCGTAATGACA
45	AACTTTCTAAAAATATACCCTAATACACGAGAAACTGTTTTATAATGA TGATAATGATTTTTTATTTTGTTCACCTATAATTGTTTTCTTTATTTTG TTTCGGATCCCCGGGTTAATTAA
46	GCAATTTCCGATGGTAAAGCAAAGGTAAATTAAATATATGGGAAATG ATAAGAAAATTGAATAAATATTATGAATCATAAATAAATAAAAGTTCA AAGGCGAATTCGAGCTCGTTTAAAC
47	AGAAAGAGAAAGCGGAAACATACTGTATCAAACTTTTCTG
48	ACAGTATGTTTCCGCTTTCTCTTTCTTGTAGTCGGTTTTTTAACG
54	ATTCAGCATGCATACTGATCATAAAATCTCGGTTGTCCC
55	ATTGAACTAGTTCAAGATTCTGGAAAGAAAACGCTTG
56	TTCTGCCAAGCAGCTCGAGA
57	CGTGACATGATACAGCAGTTTCA
58	CATGGAGTGCTATGGCGACTTTGATCACAGCAAATTTAGTTTACC
59	GGTAAACTAAATTTGCTGTGATCAAAGTCGCCATAGCACTCCATG
69	GCATCTGGGCAGATGATGTCGA
72	GTTGAAAGGAAAAGATATGCTGCTTTAGTTGCTTCCATTAAGGAC
73	GTCCTTAATGGAAGCAACTAAAGCAGCATATCTTTTCCTTTCAAC
80	CAACCATGGGTACCACTCTTGACG
94	CCTTTGGATCTGCTACAGACGCAAACATGGCTTATACTGCATGGAGT GCTA
95	TAGCACTCCATGCAGTATAAGCCATGTTTGCGTCTGTAGCAGATCCA AAG
102	AAGAGAAAGGTCTATGTTCCGAGCGCTGCTTCTGGTGCATATTCAAT TCT
103	AGAATTGAATATGCACCAGAAGCAGCGCTCGGAACATAGACCTTTCT CTT
104	ATTTAGTTTACCAGACAGGTGCTCCCTCTGCGTACTGCTTGACCGAC GATG
105	CATCGTCGGTCAAGCAGTACGCAGAGGGAGCACCTGTCTGGTAAAC TAAAT

128	GCATGGAGTGCTATGGAGACTTTGATCACAA
129	TTGTGATCAAAGTCTCCATAGCACTCCATGC
130	GCTATGAAGACTTTGATCACAGAAAATTTAGTTTACCA
131	TGGTAAACTAAATTTTCTGTGATCAAAGTCTTCATAGC
163	ATTGAACTAGTGCCATACCAAGTATTACTGTTAGTAG
198	CCTCGAAGCGTTAAAAAACCGACTACAGCAGCGGCAGCGGTCTATGTT CCGAGCTATCGTTCTGGT
199	AACGATAGCTCGGAACATAGACCGCTGCCGCTGCTGTAGTCGGTTTTT TAACGCTTCGAGG
278	TAAACCAAAAGAAATATTGTTAAACTTTGACAGAAGCTTTAAATTTTG ATTCCATACATTAAATGGATAAAACTCCTGAAACGACGGCCAGTGAA TTCGC
279	TTTTCTTAAGAACATGTGATTGGAGCAATTTTAAAACCTATTTGCACCGAT ATTGTGTATTATACTCCGAGAAAAAGTATTTACGCCAAGCTTGCATGGC
280	GGTCTTTGAATCATTGTCGAAA
281	CCTATTGTTAGCAACTTTGGCT
299	GTTTCGGATCCCCGGGTTAATTAACATAACT
300	GCCTGAGAAGGACGATGAAATGTGAT
303	GAACTTGTTTTATGTCAGCTTTTTATTCG
304	GAACTTGTTTTATGTCAGCTTTTTATTCA
313	AGTATATGACAGTGAAAGAGC
314	CGAGCTAGAAAATCCAATGCG
315	CGAGCTAGAAAATCCAATGCA
316	AAAGCCTCAAATACTAATCGCG
317	AAAGCCTCAAATACTAATCGCA
318	GAGATTGTTCCCACAGAAGT
344	ATTCAGCGGCCGCGAACTAGATATCGGCTATATGCA
345	ATTGAGCGGCCGCCTTTTTTAACGTATAAGTACGTCTT
346	ACGTTTTACATGATTTGATGATTGCAAATGCCAAGGTTGGTATTCATACTA GCGTTGCTAAGCCCAAGGACGTCAACGTT CG
347	CGAACGTTGACGTCCTTGGGCTTAGCAACGCTAGTATGAATACCAACCTT GGCATTTGCAATCATCAAATCATGTAAAAC GT
348	CCCACCCAACCCACCCACGTTTTACATGATTTGATGATTGCAAATGCCAA GGTTGGTATTCATACTAGCGTTGCTAAGCC CAAGGACGTCAACGTTCG

349	CGAACGTTGACGTCCTTGGGCTTAGCAACGCTAGTATGAATACCAACCTT
	GGCATTTGCAATCATCAAATCATGTAAAAC GTGGGTGGGTTGGGTGGG
350	CCCACCCAACTCACCCACGTTTTACATGATTTGATGATTGCAAATGCCAA
	GGTTGGTATTCATACTAGCGTTGCTAAGCC CAAGGACGTCAACGTTCG
351	CGAACGTTGACGTCCTTGGGCTTAGCAACGCTAGTATGAATACCAACCTT
	GGCATTTGCAATCATCAAATCATGTAAAAC GTGGGTGAGTTGGGTGGG
352	GGGTGGGTTGGGTGGGACGTTTTACATGATTTGATGATTGCAAATGCCAA
	GGTTGGTATTCATACTAGCGTTGCTAAGCC CAAGGACGTCAACGTTCG
353	CGAACGTTGACGTCCTTGGGCTTAGCAACGCTAGTATGAATACCAACCTT
	GGCATTTGCAATCATCAAATCATGTAAAAC GTCCCACCCAACCCACCC
354	GGGTGGGTTGAGTGGGACGTTTTACATGATTTGATGATTGCAAATGCCAA
	GGTTGGTATTCATACTAGCGTTGCTAAGCC CAAGGACGTCAACGTTCG
355	CGAACGTTGACGTCCTTGGGCTTAGCAACGCTAGTATGAATACCAACCTT
	GGCATTTGCAATCATCAAATCATGTAAAAC GTCCCACTCAACCCACCC

Table 2.4: List of oligonucleotides

2.5 Molecular cloning techniques

2.5.1 Restriction digests

Restriction digests were carried out according to the manufacturer's conditions unless indicated otherwise. Restriction enzymes used were purchased from New England Biolabs, NEB.

2.5.2 Ligation

Cut vector DNA (50ng) was incubated with cut insert DNA in a ratio of fragments 1:2. Buffer and ligase were used as recommended by Fermentas when using the Rapid DNA ligation kit (K1422) or New England Biolabs, when using T4 DNA Ligase (NEB, M0202S).

2.5.3 Fusion PCR

The KOD Hot Start DNA polymerase (Novagen, 424762T) was used for fusion PCR. The reaction mix contained 50-100ng of the two DNA fragments, which were to fuse, 0.2mM dNTPs (of each), 0.3μM of each primer, 1x KOD reaction buffer, 1-6mM $MgSO_4$ and 0.02U/μl KOD polymerase. The PCR programme consisted of:

98°C for 3 minutes, followed by 5 cycles of 98°C for 30 seconds, 50°C for 1 minute, 68°C for 1 minute and 24 cycles of 98°C for 30 seconds, 55°C (or Tm) for 30 seconds and 68°C for the required extension time.

2.5.4 *E. coli* transformation

DH5 alpha cells were thawed on ice, purified plasmid DNA or ligation products were added and incubated for 30 minutes on ice before the heat-shock at 42°C for 90 seconds. Cells were put back on ice for 5 minutes, 1ml LB was added and the reactions were incubated at 37°C for 30-60 minutes (at least 60 minutes for plasmids with kanamycin resistance). 100μl and 900μl (pooled) were plated onto LB plates plus ampicilin (100μg/ml) or kanamycin (30-50μg/ml) and grown over night at 36°C.

2.5.5 Plasmid extraction from *E. coli* cells (Miniprep, Midiprep)

For a Miniprep, 2-5ml *E. coli* cells were grown over night at 37°C in LB supplemented with ampicilin (100μg/ml) or kanamycin (30-50μg/ml), pelleted (1 minute, 13000rpm, room temperature) and resuspended in 200μl P1 (50mM Tris-HCl pH 8.0, 10mM EDTA, 100μg/ml RNaseA). 300μl of P2 (200mM NaOH, 1% (w/v) SDS) were added and samples were incubated at room temperature for 5 minutes. 300μl of P3 (3M KAc pH 5.5) were added, samples were incubated on ice for 10 minutes, pelleted (10 minutes, 13000rpm, 4°C) and the supernatant was transferred to a new tube and mixed with 1 volume of isopropanol. Samples were incubated for 5 minutes at room temperature and pelleted (10 minutes, 13000rpm, 4°C). The pellet was washed with 500μl 70% Ethanol, pelleted as before and resuspended in 19μl of H_2O and 1μl of 10mg/ml RNaseA.

This DNA was subsequently used for restriction digests or if used for sequencing, purified using a QIAprep Spin Column (Qiagen 27104).

For Midipreps, the Qiagen Midiprep Kit (12145) was used and carried out according to the manufacturers instructions.

2.5.6 Site-directed mutagenesis

Primers were designed to enclose one or two base mutations with 15 to 20 nucleotides on each side. The PCR reaction contained; 10ng of Plasmid DNA template, 0.25μM primers 0.2mM dNTPs (of each), 1x PfuTurbo Polymerase buffer, 2.5U PfuTurbo DNA Polymerase (Agilent Technologies, 600250). The cycles of the PCR programme were; 95°C for 2 minutes, followed by 18 cycles of 95°C 30 seconds, 55°C 60 seconds, 68°C 120 seconds/kb of plasmid length. 20U of *Dpn*I

restriction enzyme were added to the reaction mixture and incubated for 1 hour at 37°C. 1-2μl of this reaction were transformed into 100μl DH5 alpha cells as described above.

2.6 Yeast techniques

2.6.1 *S. pombe* genetic crosses

2.6.1.1 Random spore analysis

Fresh cells were mixed together on an ELN plate with a drop of H_2O and incubated at 25°C for 2 days. The efficiency was checked by microscope and a loop of cells was resuspended in 1ml of H_2O. 20μl of a 1:100 dilution of Helix Pomatia Juice were added and the spores were incubated on a wheel over night at room temperature. Spores were counted using a Haemocytometer, diluted and 500-1000 spores were plated onto YEA.

2.6.1.2 Tetrad dissection

Fresh cells were mixed together on an ELN plate with a drop of H_2O and incubated at 25°C for 2 days. A loop of cells were streaked on a YEA plate and incubated at 30°C for 4-6 hours or at 4°C over night. Tetrads were dissected using a Singer MSM System dissection microscope.

2.6.2 *S. pombe* transformation

S. pombe cells were grown to 1x10^7 cells/ml. 10ml (10^8 cells) were used per transformation, pelleted and washed once with 5ml H_2O, 1ml H_2O, 1ml LiAc-TE (0.1M LiAc, 0.01M Tris-HCl, 0.001M EDTA pH 7.5) and resuspended with 100μl LiAc-TE. 2μl of single stranded sperm DNA (Invitrogen Salmon Sperm DNA VX15632011) and 1-10μl plasmid DNA (1μg) or PCR fragment (up to 10μg) were added and incubated for 10minutes at room temperature. 260μl of 40% PEG-LiAc-TE were added and incubated 30-60 minutes at 30°C. 43μl of DMSO were added and the cells were incubated at 42°C for 5 minutes, washed with 1ml H_2O, resuspended in 400μl and 200μl were plated onto selective plates for transformation of plasmids. For integration of antibiotic markers, cells were plated onto YEA plates, grown for 24 hours at 30°C and replica plated onto plates containing the corresponding drugs (100μg/ml clonNAT, Werner BioAgents, 51000; 100μg/ml G-418 disulphate G0175, 200-400μg/ml Hygromycin B, H7502).

2.6.3 Gene disruption

An antibiotic cassette or auxotrophic marker was amplified with primers of 100bp (20bp homology to the cassette and 80bp homology to the targeted locus). The PCR product was purified and

transformed into *S. pombe* cells as described below.

2.6.4 Construction of base strains

Base strains for recombinase mediated cassette exchange (RMCE) were constructed as described (Watson et al., 2008). A plasmid template carrying the *ura4*$^+$ marker gene flanked by loxP and loxM3 sites (pAW1) was used to amplify the deletion fragments for subsequent integration into the *S. pombe* genome (Figure). The primers used for the amplification contained 20bp homology to pAW1 on the 3' end and 80bp homology to the gene of interest as a 5' overhang. The homology was selected directly downstream of the translation stop codon and about 150bp upstream of the ATG start codon, to avoid possible effects of the lox sites on transcription. The primers used for this amplification step are listed in table 1. Integration was checked by PCR and sequencing.

For RMCE, the required gene sequence was cloned into the pAW8 plasmid in between loxP and loxM3 sites. pAW8 carries the LEU2 marker and the Cre recombinase, regulated by the *Pnmt41*$^+$ promoter (induced in the absence on thiamine). The resulting plasmid could then be used for RMCE.

2.6.5 RMCE

The modified pAW8 plasmids were transformed into the *S. pombe* base strains and transformants were selected for the presence of pAW8 (leu+) and the presence of the base strain construct (ura+). These clones were grown in rich YE media (*Pnmt41*$^+$ repressed) over night and 1000-10000 cells were plated onto YEA plates containing 0.1% (w/v) 5-fluoroorotic acid (5-FOA) (Melford, F5001), which allows for the growth of ura- cells. The resulting colonies were re-streaked to single colonies and checked for the absence of the pAW8 plasmid by replica plating onto -leu plates and the absence of *ura4*$^+$ by replica plating onto -ura plates. These steps are indicated in Figure 2.1. Correct integration was checked by PCR and sequencing.

2.6.6 Chromosomal DNA preparation

Cells were grown in 10ml YE at 30°C over night, pelleted (5 minutes, 3000 rpm, room temperature) and resuspended in 1ml buffer SP1 (1.2M sorbitol, 50mM citric acid, 50mM Na_2HPO_4, 40mM EDTA pH 5.6) containing 1mg/ml Zymolyase T20 (Seikagaku, AmsBiotechnology, 120491-1). Cells were incubated at 37°C for 15-30 minutes and spheroplasting was monitored by microscope by adding 5% SDS. After 95% digestion was complete, spheroplasts were pelleted (5 minutes, 3000 rpm, room temperature) and resuspended in 450μl 5xTE (0.05M Tris-HCl, 0.005M EDTA pH 7.5), 50μl of 10% SDS were added and incubated for 5 minutes at room temperature.

150μl of 5M potassium acetate (KAc) were added and the samples were incubated for 10 minutes on ice. Samples were pelleted (10 minutes, 13000 rpm, 4°C) and the supernatant was transferred to a new eppendorf tube. 1 volume of isopropanol was added, incubated on ice for 10 minutes and pelleted again (10 minutes, 13000 rpm, 4°C). The pellet was washed with 500μl 70% ethanol and dried in a speed vacuum dryer. If the samples were used for PCR analysis, the pellet was re-suspended in 250μl 1xTE and 5μl of 10mg/ml RibonucleaseA were added. If the DNA was used for restriction fragment length analysis by Southern blotting, the pellet was resuspended in 250μl 5xTE and 5μl of 10mg/ml RibonucleaseA were added. The pellet was incubated at 37°C for 20 minutes to facilitate resuspending. 2μl of 10% SDS and 20μl of 5mg/ml Proteinase K (Sigma, P2308) were added and the samples were incubated at 55°C for 1 hour. The DNA was extracted twice by Phenol chloroform extraction; 500μl of Phenol:chloroform:isoamyl alcohol (mixture 25:24:1, Sigma 77617) were added and the solution was mixed by gentle vortexing. The DNA was pelleted and the upper phase (aqueous phase containing the DNA) was transferred to a new eppendorf tube. After the second extraction, the DNA was precipitated by adding 1/10 volume of Potassium acetate and 1 volume isopropanol and the mixture was incubated on ice for 10 minutes. The sample was pelleted (15 minutes, 13000 rpm, 4°C), washed with 500μl 70% ethanol, pelleted (15 minutes, 13000 rpm, 4°C) again and the pellet was resuspended in 30μl 1xTE and incubated at 37°C for 20 minutes.

2.6.7 Yeast colony PCR

A tip-full of fresh yeast cells was resuspended in 5μl H_2O and heated to 95°C for 5 minutes in a PCR machine (Biometra T3 Thermocycler). The cells were quickly spun down in a minifuge and 20μl of reaction mix were added, containing 1x Taq Buffer, 2.5mM $MgCl_2$, 0.2mM of each nucleotide, 0.2μM primers, 0.025U Taq DNA polymerase (Thermo Fisher ScientificAB-0192/B) at final concentrations.

2.6.8 Fluctuation analysis

Cells were streaked to single colonies on YEA plates. Single colonies (1-2mm) were excised from the plates and resuspended in 200μl sterile ddH_2O. Appropriate dilutions were plated onto non-selective and selective plates, and grown for 3-4 days at 30°C, unless stated otherwise. The number of colonies grown on each plate were determined, which allowed for the calculation of the number of viable cells and the number of mutants per analysed colony. The m-value was calculated using the formula x = m*(1.24+(ln(m))) (Lea and Coulson, 1949), where x equals the number of mutants per analysed colony. The deletion rate per cell per generation was determined by m/N, where N

equals the number of cells per analysed colony. For statistic analysis, the Mann-Whitney test was applied, and the resulting two-tailed p-value was used (http://faculty.vassar.edu/∼lowry/utest.html) (Putnam et al., 2010). The higher and lower values for the 95% confidence intervals were determined as described in (http://www.math.unb.ca/∼knight/utility/MedInt95.htm). This method was adapted from (Lea and Coulson, 1949; Reenan and Kolodner, 1992; Putnam et al., 2010).

2.6.9 Restriction fragment length analysis (RFLA) by Southern blotting

0.5-5μg of genomic DNA was digested with restriction enzymes in a total volume of 100μl for 3 hours or over night at 37°C. Restriction enzymes were purchased from New England Biolabs and the reaction mixture contained the corresponding buffers. An aliquot of each sample was analysed by agarose gel electrophoresis to verify complete digestion. 1/10 volume of Potassium acetate and 1 volume isopropanol were added and the mixture was incubated on ice for 15 minutes and pelleted (15 minutes, 13000 rpm, 4°C). The pellet was washed with 500μl 70% ethanol and pelleted (15 minutes, 13000 rpm, 4°C). The pellet dried in a speed vacuum dryer and resuspended in 30μl by incubation at 37°C for 20 minutes.

The DNA was separated by agarose gel electrophoresis at 50V constant for about 20 hours in a Biorad SubCell GT gel apparatus in 0.5x TBE. The agarose gel was incubated in depurination solution (0.25 M Hydrochloric acid) for 30 minutes , in denaturation solution (1.5 M NaCl, 0.5 M NaOH) for 30 minutes and neutralised in buffer containing 1M Tris pH 8.0 and 1.5 M NaCl for 30 minutes. The DNA was transferred by capillary transfer over night with 20x SSC (3M NaCl, 300mM Sodium citrate) or with a Amersham Biosciences Vacugene XL apparatus for 2 hours onto a GeneScreen Hybridization Transfer Membrane (Perkin Elmer, NEF983001PK). The membrane was rinsed with 5xSSC, air dried and the the DNA was crosslinked with a Stratagene Stratalinker (1200 J/m^2). For the preparation of the radioactive probe, 47μl H_2O containing 50-150ng/μl of the DNA template was boiled for 5 minutes and subsequently cooled on ice. The template DNA solution was added to the labelling reaction tube (GE Healthcare, Ready-To-Go DNA Labeling Beads (-dCTP), 27-9240-01) and 3μl 32P-α-dCTP (EasyTides, Deoxycytidine, 5'-triphosphate, [alpha-32P]-50mM Tricine (pH 7.6), green, Perkin Elmer, NEG513Z) were added. The reaction was incubated at 37°C for 15 minutes and labelled DNA was purified with G-50 Microspin columns (Illustra Microspin G-50 columns, GZ27533002). Hybridisation buffer (6x SSC, 1x Denhardt's reagent, 1% Sarcosyl (Sigma, 61747), pre-warmed to 65°C) containing 0.1% BSA was added to the membrane in a roller tube and incubated for 30 minutes at 65°C, turning, for pre-hybridisation. The membrane was hybridised at 65°C, turning, over night in hybridisation buffer containing 100μg/ml Salmon sperm DNA (Invitrogen, VX15632011) the radioactively la-

belled DNA probe. The membrane was washed in wash buffer I (2x SSC, 1% SDS, pre-warmed to 65°C), for 10 minutes at 65°C, turning, and again in 200ml wash buffer I (pre-warmed to 65°C) twice for 15 minutes under agitation. Subsequently, the membrane was washed twice in 500ml wash buffer II (0.1x SSC, 0.01% SDS, pre-warmed to 42°C) for 15 minutes at room temperature under agitation. The membrane was air-dried, the signal was detected with a storage phosphor screen (Fuji BAS-MS Imaging Plate) which was scanned using a FujiFilm FLA-5100 Fluorescent Image Analyser or Molecular Dynamics Storm 840 phosphorimager apparatus. The software AIDA Image analyzer v4.27 was used for quantification.

2.6.10 Whole cell protein extracts using TCA extraction

5 ODs or $5x10^7$ cells were pelleted and resuspended in 200μl 20% TCA (20% w/v trichloro acetic acid), approximately 2 eppendorf lids acid-washed glass beads or Zirkonia/Silica beads were added. The cells were lysed in a ryboliser (FastPrep24, MP) for one minute at speed 6.5 m/s, the tube was punctured with a hot needle, placed into a clean tube and the sample was pelleted (5 minutes, 4000 rpm, 4°C) into the clear tube, retaining the beads in the ribolyser tube. All supernatant was removed after centrifugation (5 minutes, 13000 rpm, 4°C), and the pellet was resuspended in 200μl 1x TCA sample buffer, boiled for 5 minutes and frozen at -20°C or pelleted (2 minutes, 13000rpm, room temperature) before analysis on a polyacrylamide gel.

Gels for SDS-PAGE were prepared with ProtoGel (30%, 37.5:1 Acrylamide to Bisacrylamide stabilised solution optimised for SDS-PAGE of proteins, National Diagnostics, ELR-210-010P). The table below shows the compositions of separating gels of different percentages for a volume of 10ml.

	6%	**8%**	**10%**	**12%**	**15%**
H_2O (ml)	5.3	4.6	4.0	3.3	2.3
30% Acrylamide mix (ml)	2.0	2.7	3.3	4.0	5.0
1.5M Tris (pH 8.8) (ml)	2.5	2.5	2.5	2.5	2.5
10% SDS (ml)	0.1	0.1	0.1	0.1	0.1
10% APS (ml)	0.1	0.1	0.1	0.1	0.1
TEMED (ml)	0.008	0.006	0.004	0.004	0.004

TEMED: N, N, N', N'-Tetramethylethylenediamine, APS: Ammonium persulfate

The table below shows the composition of the stacking gel for a volume of 5ml.

H_2O (ml)	3.4
30% Acrylamide mix (ml)	0.83
1M Tris (pH 6.8) (ml)	0.63
10% SDS (ml)	0.05
10% APS (ml)	0.05
TEMED (ml)	0.005

The solution mixtures for polyacrylamide gels were adapted from (Sambrook et al., 1989).

2.6.11 Protein analysis by Immunostaining (Western blot)

Protein samples were separated by SDS-PAGE (SDS for Sodium Dodecyl Sulfate and PAGE for PolyacrylAmide Gel Electrophoresis) using a BIORAD Mini-PROTEAN TetraCell or a C.B.S. Double- or Triple-wide electrophoresis system in 1x running buffer (0.025M Tris base, 0.25M Glycine, 0.1% SDS). Prestained Protein Marker (NEB, P7708) was loaded as a size reference. The samples were run through the stacking gel (see below) at 80V constant and through the separating gel at 80-120V.

Subsequently the gels were transferred onto a Nitrocellulose membrane (GE Healthcare, Nitrocellulose (unsupported), Hybond, RPN3032D) for 2 hours 30 minutes at room temperature at 300mM in transfer buffer (20mM Tris, 20% Methanol, 750mM Glycine). The membranes were stained with Ponceau-S solution (0.2% (w/v) Ponceau S, 3% (w/v) Trichloro acetic acid) to check for protein content and washed in PBS (Phosphate buffered saline) containing 0.1% Tween 20 (Sigma, P7949). The membrane was blocked with 3% milk powder (Marvel dried skimmed milk) in PBST (PBS, 0.1% Tween 20) for at least 1 hour at room temperature or over night at 4°C under agitation. The primary antibody was added at a dilution factor as listed below in PBST including 3% milk and the membrane was incubated for 2 hours at room temperature or over night at 4°C under agitation. The membrane was washed in PBST including 3% milk for 30 minutes at room temperature, changing the solution three times. The secondary antibody was added at a dilution factor as listed below in PBST including 3% milk and the membrane was incubated for 1 hour at room temperature under agitation. The membrane was washed in PBST for 30 minutes, changing the solution three times, and the bound antibody was detected by chemiluminescence (ECL Plus Western Lightning, Perkinelmer, NEL104001EA or ECL Plus Western Blotting Detection Reagents, GE Healthcare, RPN2132). The reaction was detected with GE Healthcare Hyperfilm ECL, GZ28906837. The film was developed with a Xograph Imaging Systems Compact X4.

When using the Streptavidin-HRP conjugate (Amersham Biosciences, RPN1231V) for detection, the membrane was blocked and incubated for detection with 5% BSA (Albumin from bovine serum - lyophilized powder, Sigma A9647) in PBST over night at 4°C. The membrane was incubated with the Streptavidin-HRP conjugate for 1 hour at room temperature under agitation and subsequently washed for 2 hours with PBST, changing the solution every 10-15 minutes.

2.6.11.1 Specifications of antibodies used in this thesis and dilution factors

anti-myc mouse monoclonal IgG1	Santa Cruz, 9E10 sc-40)	1:3000
anti-HA mouse monoclonal IgG2a	Santa Cruz, F-7 sc-7392)	1:3000
anti-FLAG M2 monoclonal	Sigma, F1804	1:4000
Streptavidin-HRP	Amersham Biosciences, RPN1231V	1:30000
Polyclonal Rabbit Anti-Mouse/HRP	DakoCytomation, P0260	1:5000
Polyclonal Swine Anti-Rabbit/HRP	DakoCytomation, P0217	1:5000
Peroxidase Anti-Peroxidase (Rabbit)	Sigma, P1291	1:5000
Rad4 (532) Rabbit polyclonal	provided by V. Garcia	1:1000
anti-histone H3 rabbit polyclonal	Abcam, ab1791	1:4000
anti-α-tubulin mouse monoclonal	Sigma, T5168	1:10000

Table 2.5: List of antibodies

2.6.12 Microscopy

10ml of exponentially growing cells were pelleted, washed in 1ml PBS and resuspended in Methanol. For fluorescence microscopy of EGFP-tagged proteins, cells were spread onto a glass slide and mounted with Vectashield Mounting Medium with DAPI. Alternatively, cells were mounted onto an agarose pad on a glass slide and stained with DAPI (1μg/ml) and Calcofluor (50μg/ml) in 50% Glycerol for analysis. The microscope used for fluorescent analysis was a Delta Vision.

2.7 Additional information - Materials and Methods - Chapter 3

2.7.1 Circular dichroism (CD) spectroscopy

Oligonucleotides were resuspended to 1mM in H_2O and diluted to a final concentration of 10μM in 100mM phosphate buffer pH 7.4 in the presence (red, K^+ or absence (blue, H_2O) of 100mM KCl. The oligonucleotide solutions were heated to 95°C-100°C in a waterbath, cooled down slowly and stabilised at 4°C for 24 hours. CD measurements were recorded with a JASCO J-715

CD spectropolarimeter. A 2mm cell was used and each data set contains three scans from 200-350nm (every 0.1nm). The resulting curves were corrected for the buffer and represented in molar ellipticity [θ] (deg$\times$M$^{-1}\times$m^{-1}).

2.8 Additional information - Materials and Methods - Chapter 4

2.8.1 Agarose plugs for restriction digest and RFLA

Agarose (InCert Agarose, Lonza, 50123) for the plugs was melted in TSE (10mM Tris-HCl pH 7.5; 45mM EDTA pH 8.0, 0.9M sorbitol) and kept at 55°C (final concentration was 0.8%). Exponentially growing cells in the presence or absence of 15μM thiamine were pooled to get 1 x 10^8 cells. After pooling the cells 1/100 volume of 10% NaN_3 and 1/10 volume of 0.5M EDTA pH 8.0 were added to each sample and incubated on ice for 10 minutes or kept at 4°C for longer periods of time. Cells were pelleted (3 minutes, 3500 rpm, swing rotor, room temperature), resuspended with 50ml of H_2O and pelleted again as before. The supernatant was aspirated completely and the pellet was resuspended in 1ml CSE (20mM Citrate/Phosphate pH 5.6, 40mM EDTA, 1.2M sorbitol). 250μl of 5 mg/ml lyticase (Lyticase from Arthrobacter luteus, 200 units/mg, Sigma, L4025) in CSE were added, the solution was mixed and incubated at 37°C for 15-30 minutes (or until about 95% of cells lysis, checked by microscope with 1% SDS). The samples were put on ice and the spheroplasts were pelleted (3 minutes, 1000 g, 4°C). The supernatant was removed completely by aspiration and the pellet was resuspended in 100μl TSE using a sterile loop. The samples were incubated at 37°C for 3 minutes. 133μl of prepared 0.8% agarose were added (use cut pipette tips). The mixture was pipetted up and down 5 times quickly and loaded into a plug mould (closed on one side). The plug mould was then put on ice for 5 minutes and the plugs were pushed out into 5ml of lysis buffer 1 (50mM Tris-HCl pH 7.5, 250mM EDTA, 1% SDS). The samples were incubated at 50°C for 90 minutes. Lysis buffer one was drained off and plugs were hold back with a spatula (Fisherbrand, FB65083) and 3ml of lysis buffer2 (1% lauryl sarcosine, 0.5M EDTA pH 9.5) were added (tubes were put horizontally on bench, so plugs did not deform). 80μl of 20mg/ml Proteinase K were added and incubated at 55°C for 24 hours. Another 80μl 20 mg/ml Proteinase K were added to the tubes and again incubated at 55°C for 24 hours. Samples were stored at 4°C.

2.8.2 Restriction digest of DNA embedded in agarose plugs

A third of a plug was put into a microcentrifuge tube, 1ml of ice-cold 1xTE was added and incubated at 4°C for 30 minutes. The buffer was removed and this was repeated twice. Then, 1ml of

the respective NEB restriction buffer (ice-cold) was added and incubated for 4°C for 60 minutes. The buffer was removed and 400μl of NEB buffer plus 100 units (U) of restriction enzyme were added. The sample was incubated at 37°C for 4 hours and then put on ice.

2.8.3 DNA separation using agarose plugs

A 0.5% solution of agarose (US biological EEO, C8102420) in 0.5% TBE was prepared and kept at 55°C. The agarose plug (after DNA digestion) was washed in 0.5x TBE 3 times for 10 minutes. The fragments were put on a comb, excess liquid was removed and two drops of melted agarose were added onto each plug. An agarose plug containing 0.05μg/μl of DNA ladder (Gene Ruler, Fermentas, SM0331) was used as a marker in the first well. They were left to cool for 1-2 minutes at room temperature (the plugs should stay at the bottom of the well). More agarose was put on, until 3/4 of the well was covered and left to solidify for 10 minutes. The remaining 0.5% agarose was used to poor the gel in the cold room and comb containing the plugs was added into it. The gel was run at 50V constant for about 20 hours in the cold room in 0.5x TBE.

2.8.4 Alkaline gel electrophoresis

To separate DNA samples under denaturing conditions, 6x alkaline loading buffer (300mM NaOH, 6mM EDTA pH 8.0, 18% Ficoll-400, 0.15% bromocresol green, 0.25% xylene cyanol FF) was added to the DNA accordingly. 1.5% agarose gels were prepared in 50mM NaCl and 1mM EDTA pH 8.0. The gel was soaked in alkaline running buffer (50mM NaOH, 1mM EDTA pH 8.0) 3 times for 30 minutes in the cold room and the samples were run in the coldroom over night at 100mA constant in pre-cooled alkaline running buffer. After running, the gel was depurinated in 0.25M HCl for 10 minutes under agitation and incubated in 0.4M NaOH for 30 minutes under agitation. The DNA was transferred onto Genescreen hybridisation membrane (Perkin Elmer, NEF983001PK) by capillary transfer in 0.4M NaOH and subsequently neutralised in 2x SSC twice for 15 minutes under agitation.

2.9 Additional information - Materials and Methods - Chapter 5

2.9.1 RMCE in the ura4 base strain

ura4$^+$ was deleted using a PCR fragment amplified from a modified pAW8 template containing the kanMX6 cassette in between loxP and loxM3 sites using P278 and P279. Tranformants into the ura4 base strain were selected for the presence of the pAW8 plasmid (leu+). Positive transformants were grown in rich YE media (*Pnmt41*$^+$ repressed) over night and 500 cells were plated onto

YEA. Replica plating of the resulting colonies onto YEA plates containing 100μg/ml geneticin disulphite (G-418, Melford, G0175) allowed for selection of loss of the kanMX6 cassette and for successful RMCE. The resulting colonies were re-streaked to single colonies and checked for the absence of the pAW8 plasmid by replica plating onto -leu plates and the absence of kanMX6 by replica plating onto G-418 plates. Correct integration was checked by PCR using P280 and P281 and sequencing. The rtf1::hphMX6 allele was crossed into the ura4 base strain and the resulting strain was frozen as SAS732.

2.9.2 pAW8-ruraR plasmid and *arg3 82TR* constructs

pAW8 containing loxP and loxM3 sequecnes was modified by multiple cloning steps to contain three repeats of the rDNA RFB (Ter2/3), *ura4*$^+$ and RTS1 (pAW8-ruraR). The sequence order and important restriction sites are as follows:

loxP - *Afl*II - rDNA RFB - *Spe*I - 3'-*ura4*$^+$-5' - *Not*I - *Blp*I - RTS1 - *Blp*I - loxM3

arg3$^+$ was amplified using P344 and P345 for integration into the *Not*I site of pAW8-ruraR. The TR inserts were cloned into the *Nru*I site of *arg3*$^+$.

82TR	346, P347
82TR G4 (bottom strand)	P348, P349
82TR G4m (bottom strand)	P350, P351
82TR G4 (top strand)	P352, P353
82TR G4m (top strand)	P354, P355

2.10 Additional information - Materials and Methods - Chapter 6

2.10.1 Mus81 mutants

The mus81 base strain was constructed using P45 and P46 to amplify the *ura4* cassette for integration and checked by PCR using P56 and P57.

mus81$^+$ was amplified from genomic DNA (KOD Hot Start DNA polymerase, Novagen, 424762T) using P54 and P55 and cloned into pAW8 *Sph*I and *Spe*I sites. This construct was used as a template for site-directed mutagenesis as described above. The oligonucleotides used for each mutation are listed below.

mus81-D395A/D396A	P72, P73
mus81-R165A/R168A	P94, P95
mus81-K176A/K181A	P58, P59
mus81-K176E/K181E	P128, P129 and P130, P131
mus81-H189A/K192A	P104, P105
mus81-Y122A/R123A	P102, P103
mus81-R113A/K114A/R115A/K116A	P198, P199

Table 2.6: List of primers used to generate Mus81 mutants

mus81-WHΔ was constructed by fusion PCR. The C-terminal part of Mus81 was amplified (KOD) using P48 and P54. The N-terminal part of Mus81 was amplified using P47 and P55. Fusion of these two fragments resulted in the deletion of the winged helix domain (WHΔ).

2.10.2 Colony mismatch PCR for the detection of point mutations

In order to distinguish between wild-type alleles and point mutations by PCR, oligonucleotides for mismatch PCR have been designed. These the last nucleotide at the 3' end of these oligonucleotides contain the either the wild-type or the mutant base. The PCR is carried out at a high melting temperature and in with Taq DNA polymerase which lacks proof-reading activity. This high stringency results in the amplification of matched bases and in the abortion of reactions containing a mismatch at the 3' end. The PCR reaction mix and the programme used are the same as described above. The respective oligonucleotide pairs are indicated below.

strain	primers	melting temperature
rad62-1:		
rad62$^+$	P163, P304	63°C
rad62-1	P163, P303	65°C
smc6-X:		
smc6$^+$	P313, P314	62.5°C
smc6-X	P313, P315	62.5°C
smc6-n74:		
smc6$^+$	P316, P318	62.5°C
smc6-n74	P317, P318	62.5°C

2.10.3 Chromatin binding assay (fractionation)

0.1% of sodium azide was added to 20-25 OD_{600} of exponentially growing cells. The cells were pelleted (5 minutes, 4000 rpm, room temperature), resuspended in 1.5ml prespheroplasting buffer (100mM PIPES pH 9.4, 10mM DTT 0.1% sodium azide), incubated for 10 minutes at room temperature, pelleted again and resuspended in 1ml spheroplasting buffer (50mM sodium citrate, 40mM EDTA, 1.2M sorbitol). Spheroplasting was monitored by OD_{600} (drop by 90%). 10μl were used immediately to measure OD_{600} in 1ml of H_2O as the starting sample. 50μl of 10mg/ml Zymolyase T100 (final 0.5mg/ml) and 50μl of 20mg/ml lysing enzymes (Sigma, L1412) (final 1mg/ml) were added to the samples and incubated at 35°C with occasional mixing. OD_{600} was monitored as described above every 10-15 minutes until only 10% of the starting value were left. Spheroplasts were harvested (1 minute, 2500 rpm, 4°C), washed with 1ml wash buffer (100mM KCl, 50mM HEPES-KOH pH 7.5, 2.5mM $MgCl_2$, 0.4M sorbitol) and resuspended with 150μl (final volume) extraction buffer (100mM KCl, 50mM HEPES-KOH pH 7.5, 2.5mM $MgCl_2$, 2mM Benzamidine, Roche complete EDTA-free protein inhibitor cocktail). The samples were aliquoted into three microcentrifuge tubes, 50μl each and labelled with W (whole extracts), S (supernatant) and C (chromatin). All samples were lysed by the addition of 0.25% Triton X-100 and incubated on ice for 5 minutes with occasional gentle mixing. The samples C were underlayed with 50μl of 30% sucrose solution (30% w/v in H_2O), pelleted (10 minutes, 13000 rpm, 4°C), the supernatant was aspirated and the pellet was resuspended with 50μl of extraction buffer containing 0.25% Triton X-100. This step was repeated and 1μl of a 1:10 dilution of benzonase (WVR, 71205-3) was added and incubated for 15 minutes on ice. 10μl of 4x SDS loading buffer (20mM Tris pH 6.8, 8% SDS, 20% glycerol, 20% -mercaptoethanol, 0.4% Bromophenol blue) were added.

The samples S were pelleted (10 minutes, 13000 rpm, 4°C), the supernatant was transferred to a new microcentrifuge tube and 10μl of 4x SDS loading buffer were added.

1μl of a 1:10 dilution of benzonase was added to the samples W, incubated for 15 minutes on ice and 10μl of 4x SDS loading buffer were added.

The samples were separated by SDS-PAGE as described above and anti-α-tubulin (Sigma, T5168) was used as a cytoplasmic control and anti-H3 as control for the chromatin fraction. Western blotting was performed as described above with the difference that 0.5% of milk powder was used.

2.11 Additional information - Materials and Methods - Appendix I

2.11.1 Whole protein extracts (native conditions)

5×10^8 cells of an exponentially growing culture were pelleted (5 minutes, 3000 rpm, room temperature) and resuspended in 400μl of lysis buffer (50mM Tris pH 7.5, 250mM NaCl, 50mM NaF, 5mM EDTA, 0.1% NP40) supplemented with Complete Protease Inhibitor Cocktail tablets, EDTA-free (Roche, 11873580001) and 10μg/ml of 4-(2-Aminoethyl)benzenesulfonyl fluoride hydrochloride (AEBSF, Sigma, A8456) and approximately 2-3 eppendorf lids acid-washed glass beads or Zirkonia/Silica beads were added. The cells were lysed in a ryboliser (FastPrep24, MP) three times for 20 econds at speed 6.5 m/s and cooled for 2 minutes between each cycle. Lysis was checked by microscope and the tube was punctured with a hot needle, placed into a clean tube and the sample was pelleted (5 minutes, 4000 rpm, 4°C) into the clear tube, retaining the beads in the ribolyser tube. The supernatant was transferred to a new tube, pelleted (10 minutes, 13000 rpm, 4°C) and the resulting supernatant was used for Bradford (Biorad) analysis and subsequent purification experiments.

2.11.2 Dialysis

Slyde-a-lyzer dialysis cassettes MWCO 3.5kDa 0.1-0.5ml (Pierce, 66333) were used for dialysis. Cell extracts were dialysed against lysis buffer containing 1mM phenylmethanesulfonyl fluoride PMSF. Dialysis was performed in the cold room in the cold room for at least 3 hours, changing the buffer three times. The dialysis buffer volume was always 500 times the volume of the sample.

2.11.3 Pulldown experiments using Dynabeads MyOne Streptavidin T1 (Invitrogen, 65601)

Pulldown experiments were performed with 2-5mg of protein extract in lysis buffer (50mM Tris pH 7.5, 250mM NaCl, 50mM NaF, 5mM EDTA, 0.1% NP40) supplemented with Complete Protease Inhibitor Cocktail tablets, EDTA-free (Roche, 11873580001) and 10μg/ml of 4-(2-Aminoethyl)benzenesulfonyl fluoride hydrochloride (AEBSF, Sigma, A8456). Cell extracts were dialysed and incubated with washed Dynabeads for 2 hours on a wheel in the cold room. The beads were then washed once with lysis buffer, resuspended in 50-100μl 1x sample buffer and subsequently boiled for 5 minutes.

2.11.4 Immunoprecipitation (IP) using antibody-coated magnetic beads

These experiments were carried out as described in the previous paragraph using antibody-coated Dynabeads (Protein G, Invitrogen, Dynal, VX10004D). The beads were washed in PBS + 0.02% Tween20 and coated in PBS + 0.02% Tween20 containing 5μg of anti-HA antibody for 10 minutes on a wheel at room temperature, washed and stored at 4°C. Optional crosslinking of the antibody was performed by washing twice in conjugation buffer (20mM NaPhosphate, 0.15M NaCl pH 7.9) and subsequent incubation in 250μl of conjugation buffer containing 5mM Bis(sulfosuccinimidyl) suberate (BS^3) for 30 minutes on a wheel at room temperature. The beads were washed with lysis buffer 3 times and used for subsequent IP.

Chapter 3

Effects of replication fidelity and replication-associated repair processes on the stability of small direct tandem repeats

3.1 Introduction

Completion and accuracy of DNA replication is important to allow for faithful segregation of the chromosomes and to avoid mutations which could lead to malfunction and disease. Perturbations of the replication process could potentially lead to errors and therefore to mutations. Streisinger et al. (1966) proposed the model of replication slippage to account for deletion or expansion of short tandem repeats (TRs) during DNA replication leading to frameshift mutations. Replication slippage is thought to create rearrangements of repeated DNA sequences in bacteria (Albertini et al., 1982), yeasts (Tran et al., 1995) and humans (Efstratiadis et al., 1980). Repeat rearrangements occur through slipped misalignment of the nascent strand with its template, also called "simple slippage" (Figure 3.1A). A loop formed between the repeats on the template leads to a deletion product and a loop on the nascent strand leads to an expansion product after completion of replication (Figure 3.1A). TR assays in *E. coli* suggested that displacement of the nascent strand may be an active process which is part of a recombinational repair mechanism, initiated when replication is blocked (Lovett et al., 1993). These findings were based on observations that TR rearrangements, independent of the HR protein RecA, resulted in sister chromatid exchanges (SCEs) (Lovett et al., 1993). SCEs would not be expected to occur by "simple slippage" (Fig-

ure 3.1A). However, a template switch during replication or an associated repair pathway could result in the alignment of the nascent DNA strands and the formation of a HJ and therefore explain the occurrence of SCEs (Figure 3.1B).

RecA-independent deletions of TRs were shown to be largely dependent on the chaperone *Dna*K (Goldfless et al., 2006). Goldfless et al. (2006) proposed that *Dna*K facilitates a cross-fork template switching mechanism similar to eukaryotic error-free postreplication repair (PRR). This mechanism could result in rearrangements in repetitive sequences due to misalignment of the nascent strands.

PRR is a DNA damage avoidance mechanism that facilitates the completion of genomic replication despite a damaged template, and the filling of postreplicative gaps without removing the damage (Lehmann and KirkBell, 1972; di Caprio and Cox, 1981; Prakash, 1981). It is not yet clear whether and when PRR functions: at the replication fork or behind the replication fork as a gap-filling mechanism (Ulrich, 2011). In eukaryotes, monoubiquitylation of PCNA on lysine 164 (K164) by the heterodimer Rad6-Rad18 (*sp*Rhp6-Rhp18) activates DNA damage bypass by translesion synthesis (TLS) (Figure 3.1C) (Stelter and Ulrich, 2003). This pathway of PRR involves DNA polymerases of the Y family which can be error-prone (Lehmann et al., 2007). Ubc13-Mms2 and Rad5 (*sp*Rad8) catalyse polyubiquitylation of PCNA, which results in an error-free pathway (Hofmann and Pickart, 1999; Hoege et al., 2002; Brown et al., 2002; Frampton et al., 2006) that is thought to utilise the nascent strand as a template for DNA synthesis by template switching (Zhang and Lawrence, 2005). Plasmid assays in *S. cerevisiae* have produced evidence for template switching, however, the mechanism of this pathway in the context of genomic DNA remains unknown (Zhang and Lawrence, 2005). Figure 3.1C shows an overview of PRR and possible template switch intermediates during error-free repair. The annealing of the nascent strands at the replication fork could lead to TR rearrangements at repetitive sequences (annealing of red and yellow). Whether this process involves fork regression (chickenfoot, shown in brackets) is not known. Although it was shown that *sc*Rad5 can function as a helicase to catalyse fork regression (Blastyák et al., 2007), *in vivo* these structures have only been observed in checkpoint mutant cells and could therefore be classified as pathological rather than intermediates of an active repair process (Sogo et al., 2002).

3.2 Aim of the project and summary

In this chapter I describe the development of a TR system in *S. pombe* which allows us to determine TR deletion rates by fluctuation analysis. This assay was set up to test its suitability as a tool to measure template switching during PRR. Template switching has also been implicated in

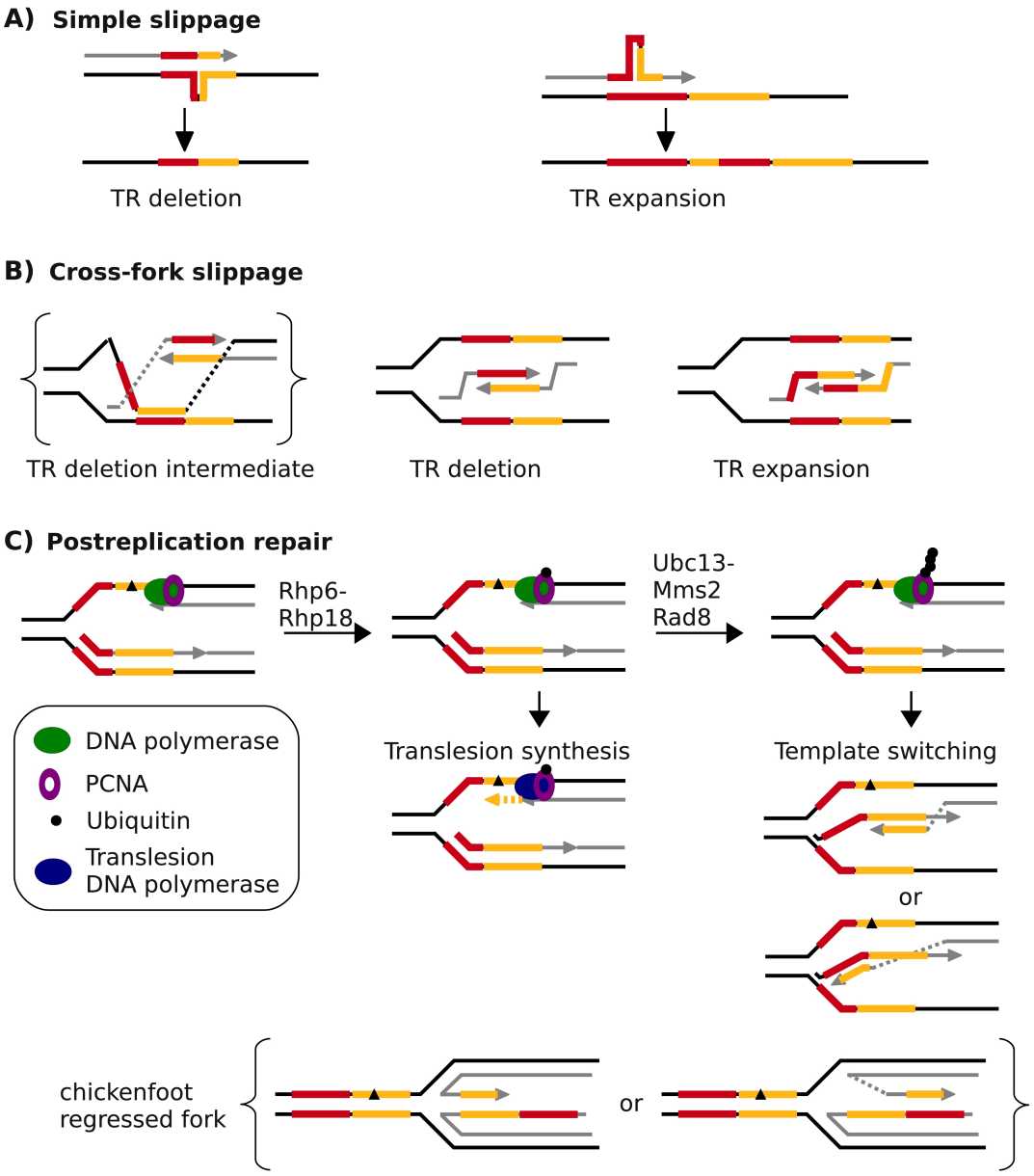

Figure 3.1: Rearrangements in tandem repeat sequences due to replication errors or associated repair pathways

A) Errors during replication of tandem repeats (TRs) can result in deletion or expansion of these sequences. Parental DNA is shown in black, nascent strands are shown in grey and repeated sequences are shown in red and yellow. The term "simple slippage", is used to describe the dislocation of the nascent strand and erroneous reannealing to its template. Misalignment of the first (red) to the second (yellow) repeat results in the deletion of one repeat and misalignment of the second to the first repeat results in the expansion/triplication of the repeated sequence.

B) Dislocation of both nascent strands during replication could result in their annealing. Similar to the "simple slippage" model, this misalignment between nascent strands in a repetitive sequence can lead to deletion or expansion of the repeat. Annealing of the parental strands as well as the nascent strands forms an intermediate containing a HJ (as shown for the deletion event on the left), the resolution of which can result in sister chromatid exchange (SCE).

C) Postreplication repair (PRR) is a DNA damage avoidance pathway, ensuring the progression of replication on a damaged template. In *S. pombe* PRR is mediated by Rhp6-Rhp18, Ubc13-Mms2 and Rad8. Ubiquitylation of PCNA by these enzymes results in translesion synthesis (monoubiquitylation) or template switching (polyubiquitylation). The latter could give rise to TR rearrangements by misalignment of the two nascent strands. Fork regression (chickenfoot) could facilitate the alignment of the two nascent strands. A DNA lesion is shown as a black triangle.

replication fork restart mechanisms and it has been suggested to occur as a result of replication fork collapse and that this can lead to genomic instability (Lambert et al., 2005; Mizuno et al., 2009). Genetic analysis of the assay described here showed that the TR deletions were not dependent on PRR, but were sensitive to aberrant replication. Biochemical characterisation of the repeat sequence suggested the formation of a secondary structure due to its high G-content. This might account for elevated levels of errors by aberrant replication. Depending on the nature of the obstacle and other factors, inhibition of replication can lead to several outcomes, such as replication resumption, replication fork collapse and restart or damage bypass by PRR (Carr et al., 2011). The observations, using my assay, suggest that spontaneous and elevated levels of TR deletions, due to aberrant replication, are independent of PRR in the context of G-rich DNA prone to form secondary structures.

3.3 Characterisation of TR deletions by fluctuation analysis, PCR and sequencing

The *nat1*$^+$ gene from *Streptomyces noursei* (Krügel et al., 1993) was chosen as a marker gene to select for TR deletions in *S. pombe*. *nat1*$^+$ encodes nourseothricin acetyltransferase 1, which gives resistance to the antibiotic nourseothricin (NAT) (Goldstein and McCusker, 1999). A functional copy of *nat1*$^+$ can be selected for by resistance to the drug NAT (100μg/ml clonNAT) (Hentges et al., 2005). First, duplications of 41, 101 and 251bp of the sequence upstream of the *Kas*I restriction site in *nat1*$^+$ were introduced by ligation of amplified fragments (101bp, 251bp) or annealed oligonucleotides (41bp). The plasmid pAG25 (Euroscarf P30104, (Goldstein and McCusker, 1999) containing the *nat1* cassette was used as a template. All three duplications result in a STOP codon after the *Kas*I site.

For integration into the *S. pombe* genome, a targeting vector for the *ura4* locus was constructed. 600bp of the 3'- and 5'-end of *ura4*$^+$ (1.75kb *Hind*III fragment) were amplified with primers containing *Nde*I and *Not*I sites, as indicated in Figure 3.2A (a). Fusion PCR was used to combine these two fragments so that the 3'-end was placed upstream of the 5'-end. The fusion fragment is flanked by *Nde*I sites and the two initial fragments are separated by a *Not*I site. This *ura4* integration fragment and the *nat1 TR* constructs (as shown in Figure 3.2A (b)) were cloned into pUC19 using *Nde*I and *Bam*HI-*Sac*I, respectively. The resulting plasmids were linearised with *Not*I and used for homology-directed integration into the *ura4* locus of the *S. pombe* wild-type strain 972. Successful integration disrupts the *ura4* locus and cells become resistant to 5-fluoroorotic acid (5-FOA). Genomic DNA from selected cells was extracted and analysed by PCR and restriction

fragment length analysis (RFLA). Figure 3.2B shows schematics of the *ura4* loci in 972 and *nat1 TR* integrants. The primers used for PCR analysis are indicated as arrows. Primer pairs P24/P28, P27/P28 and P28/P80 are specific for 972 and *nat1 TR*, 972 only or *nat1 TR* only, respectively. The wild-type strain 972 shows the expected fragments for P24/P28 and P27/P28 and yields no result for P28/P80 (Figure 3.2C). The *nat1 TR* strains show the same fragment size as *972* for P24/P28, no fragment for P27/P28 and a specific fragment for P28/P80, confirming successfull integration.

The same genomic DNA was used for RFLA using *Ava*I as a restriction enzyme (Figure 3.2D). The DNA was separated by agarose gel electrophoresis and fragments were detected by radioactively labelled probes, as indicated in Figure 3.2B. Figure 3.2D shows the same membrane labelled either with probe 'ura' (red) or probe 'nat' (green). The *Ava*I fragment of the *ura4* locus in the wild-type strain 972 is detected with probe 'ura', but not with probe 'nat', as expected. In *nat1 TR* integrants, the *Ava*I fragment is detected with both probes which confirms integration. Detection by 'nat' is specific for cells harbouring *nat1* and the size change of the *ura4* locus after integration is clearly visible when probing with 'ura'. The faint larger band visible for the *nat1 TR* strains when using the 'ura' probe, is likely to show the 4.7kb *Ava*I fragment. A contamination in the 'ura' probe recognising the other arm of the *ura* integration site could explain this hybridisation.

Figure 3.2 *(following page)*: Cloning of a tandem repeat assay in *Schizosaccharomyces pombe*
A) Overview of the cloning of the TR assay. For integration into the genome, a *ura4* integration vector was designed, containing 600bp homology of the 3'- (blue) and 5'- (green) end of *ura4*$^+$ (a). The fragments were assembled by fusion PCR and cloned into pUC19 using *Nde*I (pUC19_Ui). A *Not*I site separating the two *ura4* homology sequences can be used for linearisation and integration of the plasmid into the *ura4* locus. The marker gene *nat1* was selected for the TR assay in *S. pombe*. As a template, pAG25 (euroscarf accession no. P30104) was used, to introduce TRs of 41bp, 101bp and 251bp by duplication of the sequence upstream of the *Kas*I restriction site (b). The primer pairs used for the individual repeats were: 41bp; P11/P12, 101bp; P3/P4, 251bp; P13/P4, as listed in Materials and Methods. The *nat1* cassettes containing the TRs were subcloned into pUC19_Ui using *Bam*HI and *Sac*I (c). The repeated sequences in *nat1* are indicated by brown boxes. The resulting vector, pUC19_Ui_N, was linearised by *Not*I and integrated into the *ura4* locus of wild-type *S. pombe* 972.
B) The *ura4* locus before (972 wt) and after integration (*nat1 101/41/251TR*). For simplicity only *nat1 101TR* is shown in the schematic. Probes 'ura' (red) and 'nat' (green) are indicated with boxes. Primers used for PCR are indicated with numbered arrows and listed in Materials and Methods, P28, P24, P27, P80. 'A' indicates *Ava* I restriction sites.
C) Correct integration of pUC19_Ui_N was confirmed by PCR. Genomic DNA was isolated and used as a template for PCR analysis. The numbers of the primers correspond to the arrows in A. As control DNA wild-type 972 (wt) was used and also a reaction without template (no). Two clones of each repeat size (101bp, 41bp, 251bp) were used. The reaction products were separated by agarose gel electrophoresis. Expected fragment sizes are shown in kb. The size marker of the agarose gels is indicated on the left in kb. Strain genotypes are listed in Materials and Methods. Strains used: SAS61/63 (101TR), SAS81/83 (41TR) and SAS84/85 (251TR).
D) The integration of the *nat1 TR* constructs was further confirmed by restriction fragment length analysis (RFLA). Genomic DNA was digested with *Ava*I, separated by agarose gel electrophoresis, transferred to a membrane and fragments were detected with radiolabelled probes 'ura' and 'nat', as indicated in **B**. Fragment sizes are shown on the left in kb.

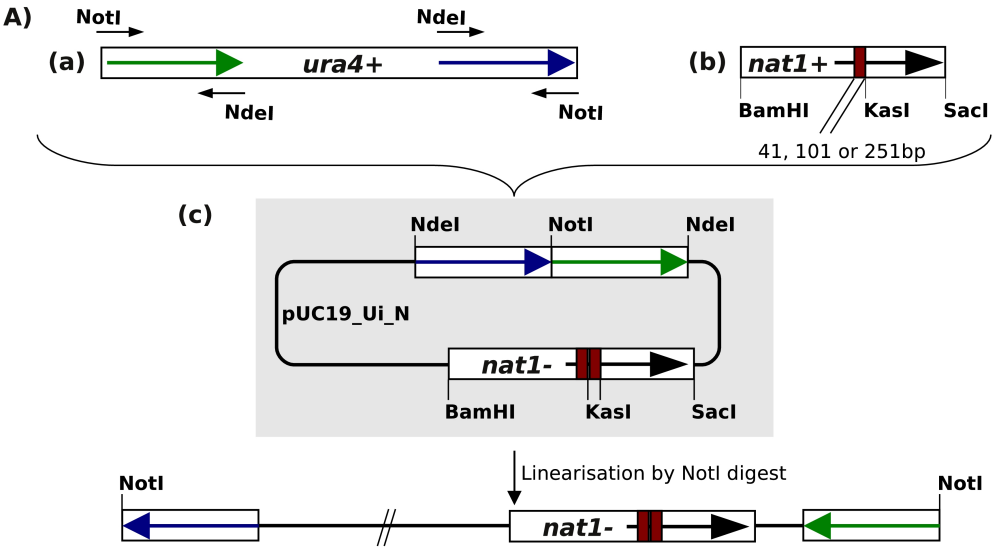

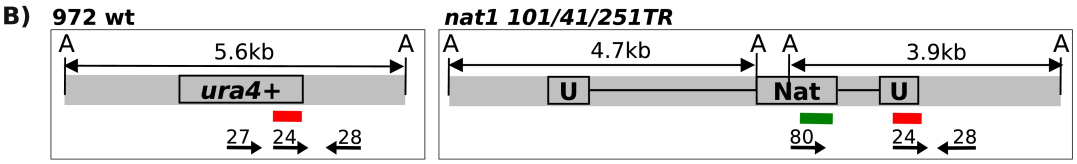

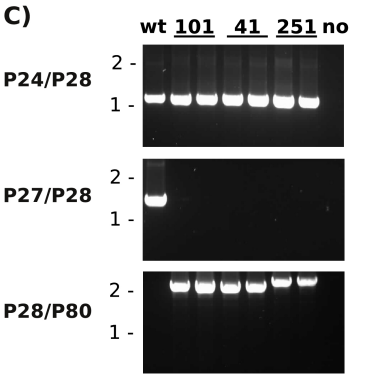

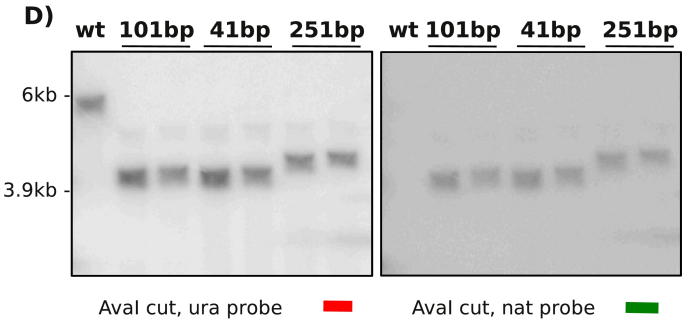

Expected fragment sizes (in kb)

	wt	nat1 101TR
PP1	1.07	1.07
PP2	1.37	-
PP3	-	2.26

Expected fragment sizes (in kb)

	wt	nat1 101TR
ura	5.6	3.9
nat	-	3.9

The strains containing the *nat1 41TR, 101TR* and *251TR* constructs were characterised for the rate of loss of one repeat, i.e. deletion events by fluctuation analysis. For this analysis, the number of mutants is determined in several colonies originating from a single cell and the deletion rate is calculated according to the Method of the Median (Lea and Coulson, 1949). This analysis allows calculation of mutation events per cell per generation. This is important because rare mutation events can lead to very different rates dependent on whether they occur early or late during colony growth. The deletion rates of all three constructs yielded similar results, 3.21-4.25 x10^{-5} (Figure 3.3A). Colonies fromlancing, u non-selective (N) YEA and selective (S) YEA+NAT (100μg/ml clonNAT) plates were analysed by colony PCR to confirm the TR deletions. A primer pair flanking the TR was used to amplify the repeat fragment and therefore visualise the loss of one repeat by agarose gel electrophoresis (Figure 3.3B). PCR reactions for all colonies grown on selective plates resulted in the expected 1213bp fragment corresponding to a functional *nat1*$^{+}$ (Figure 3.3B, Lane C+). All colonies grown on non-selective plates yielded fragments corresponding to the respective repeat size. In total, 83 colonies from two different series of experiments were analysed and 23 were sequenced confirming the deletion of the TR as cause of the restoration of *nat1*$^{+}$ and resistance to NAT (data not shown). Since the deletion rates of the three different constructs showed similar results, further experiments were mainly carried out with the *nat1 101TR* allele.

A)

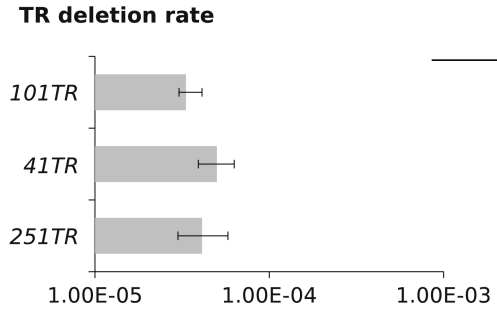

genotype	n	deletion rate x 10^{-5} (95% ci)	p
101TR	44	3.3 (3.0-4.1)	
41TR	22	5.0 (3.9-6.3)	0.0027
251TR	22	4.1 (3.0-5.8)	0.1902

B)

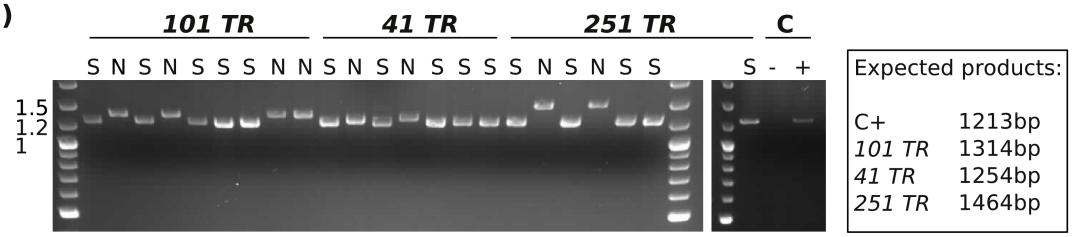

Figure 3.3: Fluctuation analysis of TR deletion rates of 101bp, 41bp and 251bp

A) Cells were streaked to single colonies on non-selective media. Colonies were excised from the plate, resuspended in 200μl water, serially diluted and plated onto non-selective and selective (YEA + 100 μg/ml NAT) plates. Deletion rates were calculated by the Method of the Median (Lea and Coulson, 1949). The graph on the left shows the median deletion rates on a logarithmic scale. Error bars represent 95% confidence intervals (ci). The table on the right lists the genotypes, number of colonies analysed (n), deletion rates with 95% ci and the p-value for statistical significance (p). Two-tailed p-values were calculated using the Mann-Whitney Test as described in Materials and Methods. The p-value was determined for the deletion rates of *nat1 41TR* and *251TR* in comparison to *101TR*. Strain genotypes are listed in Materials and Methods. Strains used: *101TR*; SAS197, *41TR*; SAS198, *251TR*; SAS199.

B) Colonies from the fluctuation tests were analysed by colony PCR. Primers 69 and 80 (as listed in Materials and Methods) were used for the PCR reaction and 5% DMSO was added to facilitate the melting of the GC-rich template DNA (Hentges et al., 2005; Jensen et al., 2010). The PCR products were separated by agarose gel electrophoresis. Colonies used for analysis were taken from selective (S) and non-selective (N) plates. Controls (C) with or without *nat1*$^+$ are indicated with + and -, respectively. Marker sizes are shown on the left in kb and the expected fragment lengths are listed in the box on the right. As expected, after TR deletion (S) all strains yielded a fragment of 1213bp corresponding to C+, a functional *nat1*$^+$.

3.4 TR deletion events are independent of homologous recombination, postreplication repair and mismatch repair

In *E. coli*, chromosomal repeats of up to 787bp were shown to be rearranged mainly in a RecA-independent manner (Lovett et al., 1993; Goldfless et al., 2006). TR rearrangements on plasmids were RecA-dependent if they exceeded 300bp in length (Bi and Liu, 1994). Lovett et al. (1993) have proposed a model for postreplicative gap-filling in which cross-fork template switching occurs as part of a recombinational repair mechanism to account for the RecA-independent TR rearrangements (Figure 3.1B).

I analysed spontaneous deletions in the *nat1 101TR* assay and found that deletion of *rhp51*$^+$, which encodes Rad51, the homologue of RecA, did not significantly decrease the deletion rate (Figure 3.4A), whilst two clones of *rad22*Δ (*rad22*$^+$ encodes Rad52), *rad22*Δ 1 and *rad22*Δ 2, showed an increase in the deletion rate of about 8-fold compared to wild-type. *rad22*Δ cells are prone to suppressor mutations in the *fbh1*$^+$ gene encoding an F-box helicase (Doe et al., 2004; Osman et al., 2005), and Fbh1 was shown to prevent Rad51-dependent recombination in the absence of Rad52 (Doe et al., 2004). The suppressor mutation is ineffective in the *rad22*Δ *rhp51*Δ double mutant. I tested the TR deletion rate in *rad22*Δ *rhp51*Δ and found this to be similar to that in *rad22*Δ. These results suggest that TR deletions are not dependent on HR. The increase in rearrangements observed in *rad22*Δ and *rad22*Δ *rhp51*Δ cells could be due to either more initiation events because of secondary lesions or suppression of a silent repair pathway and channelling into error-prone repair. These possibilities were previously suggested to explain an increase in direct repeat rearrangements in HR mutant backgrounds in *S. cerevisiae* (Liefshitz et al., 1995).

Plasmid assays in *E. coli* have shown that deletions of homeologous but not homologous repeats are prevented by MMR (Bzymek et al., 1999). I found that the deletion rate in *nat1 101TR* in a MMR deficient background (*msh2*Δ) was similar to wild-type levels, suggesting that MMR does not suppress TR deletions (Figure 3.4A).

To test whether TR deletions are dependent on PRR, I used mutants abolishing PRR by preventing the ubiquitylation of PCNA on lysine 164 (*pcn1-K164R*) and specifically the polyubiquitylation-dependent error-free pathway (*rad8*Δ and *ubc13*Δ). Rad8 and Ubc13-Mms2 catalyse the polyubiquitylation of PCNA in *S. pombe* (Frampton et al., 2006). TR deletions were slightly increased in the *K164R* mutant (2-3 fold) and deletion of *rad8*$^+$ or *ubc13*$^+$ showed no effect (Figure 3.4B). *ubc13*Δ cells were analysed with all three TR constructs, *nat1 101TR, 41TR* and *251TR,* but no significant difference was found. Sws1, the homologue of *S. cerevisiae* Shu2, has been previously identified as a regulatory protein involved in HR-dependent error-free repair (Shor et al., 2005; Martín et al., 2006). The *S. cerevisiae* protein Shu2 was suggested to play a role in recruit-

ment of HR proteins to facilitate template switching in error-free PRR (Ball et al., 2009). *sws1*Δ cells did not affect the TR deletion rate of *nat1 101TR*, which is in agreement with the observations for *rhp51*Δ and PRR mutants (Figure 3.4A and B).

A) **TR deletion rate**

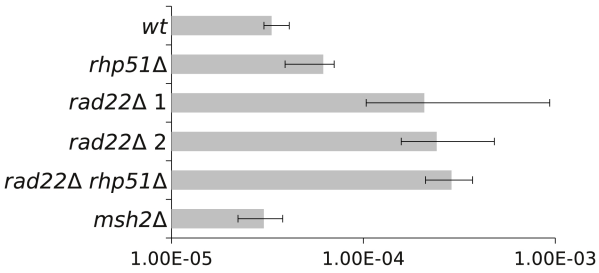

genotype	n	deletion rate x 10^{-5} (95% ci)	p
wt	44	3.3 (3.0-4.1)	
*rhp51*Δ	33	6.2 (3.9-7.0)	0.0013
*rad22*Δ 1	10	20.8 (10.4-93.5)	<0.0001
*rad22*Δ 2	11	24.1 (15.8-48.2)	<0.0001
*rad22*Δ *rhp51*Δ	21	28.8 (21.1-37.1)	<0.0001
*msh2*Δ	43	3.0 (2.2-3.8)	0.091

B) **TR deletion rate**

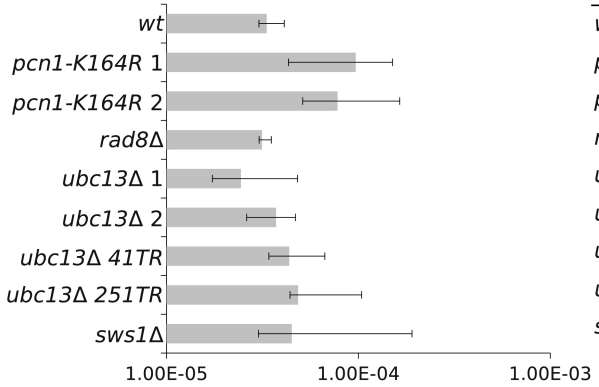

genotype	n	deletion rate x 10^{-5} (95% ci)	p
wt	44	3.3 (3.0-4.1)	
pcn1-K164R 1	11	9.7 (4.3-10.5)	0.0007
pcn1-K164R 2	10	7.8 (5.1-16.4)	0.0121
*rad8*Δ	33	3.1 (3.0-3.5)	0.9601
*ubc13*Δ 1	11	2.4 (1.7-4.8)	0.0424
*ubc13*Δ 2	11	3.7 (2.6-4.7)	0.8729
*ubc13*Δ *41TR*	11	4.4 (3.4-6.7)	0.0751
*ubc13*Δ *251TR*	11	4.9 (4.4-10.4)	0.0036
*sws1*Δ	11	4.5 (3.0-19)	0.0688

Figure 3.4: TR deletions are not dependent on homologous recombination or postreplication repair and not suppressed by mismatch repair
A) Analysis of HR mutants and **B)** analysis of PRR mutants. Fluctuation tests were carried out as described in Figure 3.3A. Deletion rates are presented in the bar chart and error bars represent 95% confidence intervals (ci). Numeric values of the deletion rates and the amount of colonies assayed (n) are shown in the table on the right. The p-value was determined for the deletion rates in comparison to wild-type (wt) 101TR. The strains used in this analysis all carry the *nat1 101TR* allele unless indicated otherwise. Strain genotypes are listed in Materials and Methods. Strains used: wt; SAS197, *rhp51*Δ; SAS315, *rad22*Δ-1; SAS271, *rad22*Δ-2; SAS272, *rad22*Δ *rhp51*Δ; SAS433, *msh2*Δ; SAS413, *pcn1-K164R*-1; SAS229, *pcn1-K164R*-2; SAS239, *rad8*Δ; SAS323, *ubc13*Δ-1; SAS344, *ubc13*Δ-2; SAS345, *sws1*Δ; SAS410, *ubc13*Δ *41TR*; SAS382, *ubc13*Δ *251TR*; SAS384.

3.5 DNA damage induced by ultraviolet (UV) radiation and methyl methanesulfonate (MMS) do not increase TR deletion rates

The previous experiments described in this chapter analysed TR deletions in the absence of exogenous DNA damage. Endogenous DNA damage occurs frequently in cells and can perturb DNA replication without the application of external DNA damaging agents (De Bont and van Larebeke, 2004). The TR deletion assay could reflect a process at the replication fork that is induced by endogenous obstacles that interfere with replication. Therefore the application of DNA damaging agents might also elevate TR deletion rates by inducing DNA lesions that could act as possible initiation sites for TR rearrangements. Inducing DNA lesions might activate different pathways for repair and DNA damage tolerance, like PRR.

The alkylating agent MMS was used to determine whether *nat1 101TR* deletion rates could be increased in a damage-dependent manner and if so, whether this increase is dependent on error-free PRR. Several different experimental conditions were tested in order to give a broad overview of the effect of MMS-induced DNA damage on TR deletions. Figure 3.5A (a) shows the survival of wild-type, *rad8*Δ and *ubc13*Δ cells grown in media containing different concentrations of MMS for 3 hours. For the TR deletion analysis, the cells were grown in 0.001% MMS which should only slightly affect viability according to the survival assay in Figure 3.5A (a). The cells were grown for 11 hours in MMS-containing media in order to allow for multiple rounds of replication. MMS treatment did not inhibit culture growth as the cell numbers in treated and untreated cultures were similar (data not shown). The TR deletion frequency was determined and the fold increase of treated versus non-treated cells is shown in Figure 3.5A (b). MMS treatment resulted in a slight PRR-independent increase in TR deletions (1.5-2 fold). In an alternative approach the cells were treated more acutely with MMS: four single colonies of wild-type and *rad8*Δ cells were grown in 0.01% MMS for 2 hours, washed and grown in non-selective media for 4.5 hours for recovery and analysed by fluctuation analysis. TR deletion events were again increased by 1.5-2 fold in wild-type cells after MMS treatment, independently of PRR (Figure 3.5A (c)).

The effect of chronic treatment with MMS on wild-type and *rad8*Δ cells was tested by spot test as shown in Figure 3.5B (a). *rad8*Δ cells showed sensitivity to chronic treatment with 0.004% MMS. For fluctuation analysis a concentration-range of MMS that does not affect viability of *rad8*Δ mutants was chosen. 11 colonies were excised from plates containing MMS and TR deletion rates of wild-type and *rad8*Δ cells were determined (Figure 3.5B (c)). The deletion rates slightly increased after MMS treatment, however *rad8*Δ and wild-type cells showed similar results.

PRR pathways are best described in the response to UV lesions, that block replication fork

progression. If UV irradiation stimulates TR deletions, this might be dependent on PRR. Exponentially growing wild-type cells were irradiated with 254nm UV light using a Stratalinker (Stratagene) at 0, 50, 100, and 200 J/m^2 and either directly plated onto selective and non-selective plates or incubated overnight at 30°C before plating (Figure 3.5C). Cell viability was only slightly affected up to 100 J/m^2, whereas irradiation with 200 J/m^2 reduced viability by about 90%. The deletion frequency of *nat1 101TR* was overall higher in cells which were plated directly after irradiation compared to cells left to recover in liquid culture overnight. However, UV irradiation did not appear to increase TR deletions at the doses tested (Figure 3.5C). One explanation for this would be that the introduction of UV damage into DNA is sequence specific for the formation of pyrimidine dimers and the lack of increase in TR deletions could be due to a lack of pyrimidines in the *nat1 101TR* construct.

Taken together, DNA damage introduced by MMS and UV radiation did not lead to a significant increase in TR deletion events. In the case of MMS treatment, a slight increase could be observed, however this was not dependent on PRR.

Figure 3.5 *(following page)*: Treatment with DNA damaging agents does not increase PRR-dependent deletion events

A) Acute treatment with the alkylating agent MMS did not increase PRR-dependent TR deletion events. Survival of MMS treated wild-type and *rad8*Δ cells containing *nat1 101TR* was tested by growing cells at 30°C for 3 hours in media containing MMS. Cells were diluted and plated onto three plates for each dose (a). In (b) single colonies were grown in preculture over night, diluted and incubated in 0.001% MMS for 11 hours, washed and plated onto YEA and YEA+NAT plates (three plates each). The graph shows the average fold increase in the deletion frequency of four cultures from two experiments. (c) Four colonies were excised from YEA plates, resuspended in 1ml of YE, grown for 2 hours at 30°C, 0.01% MMS was added and incubated for 1 hour. Cells were washed and let to recover at 30°C for 4.5 hours. Then they were diluted and plated onto YEA or YEA+NAT plates immediately (3 plates each). The graph shows the median deletion rates and the error bars indicate the highest and lowest deletion rate.

B) Chronic treatment with MMS did not affect deletion rates in either wild-type or *rad8*Δ cells containing the *nat1 101TR* allele. Cells were grown in non-selective media over night, serially diluted and spotted onto YEA plates containing MMS (a). The wild-type strain 972 was used as a control without the *nat1 101TR* allele (wt). Cells were plated in 10-fold serial dilutions starting with 10^5 cells on the left. (b) 11 colonies were excised from plates containing MMS and used for fluctuation analysis as described in Figure 3.2A. Strain genotypes are listed in Materials and Methods. Strains used: wild-type *101TR*; SAS197, *rad8*Δ *101TR*; SAS323.

C) UV irradiation did not increase TR deletion rates. *nat1 101TR* cells were grown in non-selective media over night, diluted and exponentially growing cells were irradiated with 254nm of UV light using a Stratalinker (Stratagene) at the indicated doses. Cultures were diluted and plated onto YEA and YEA+NAT plates (three plates each) immediately (blue) or incubated over night at 30°C for recovery and plated the next day (red). The graphs show the survival (left) and the deletion frequency (right).

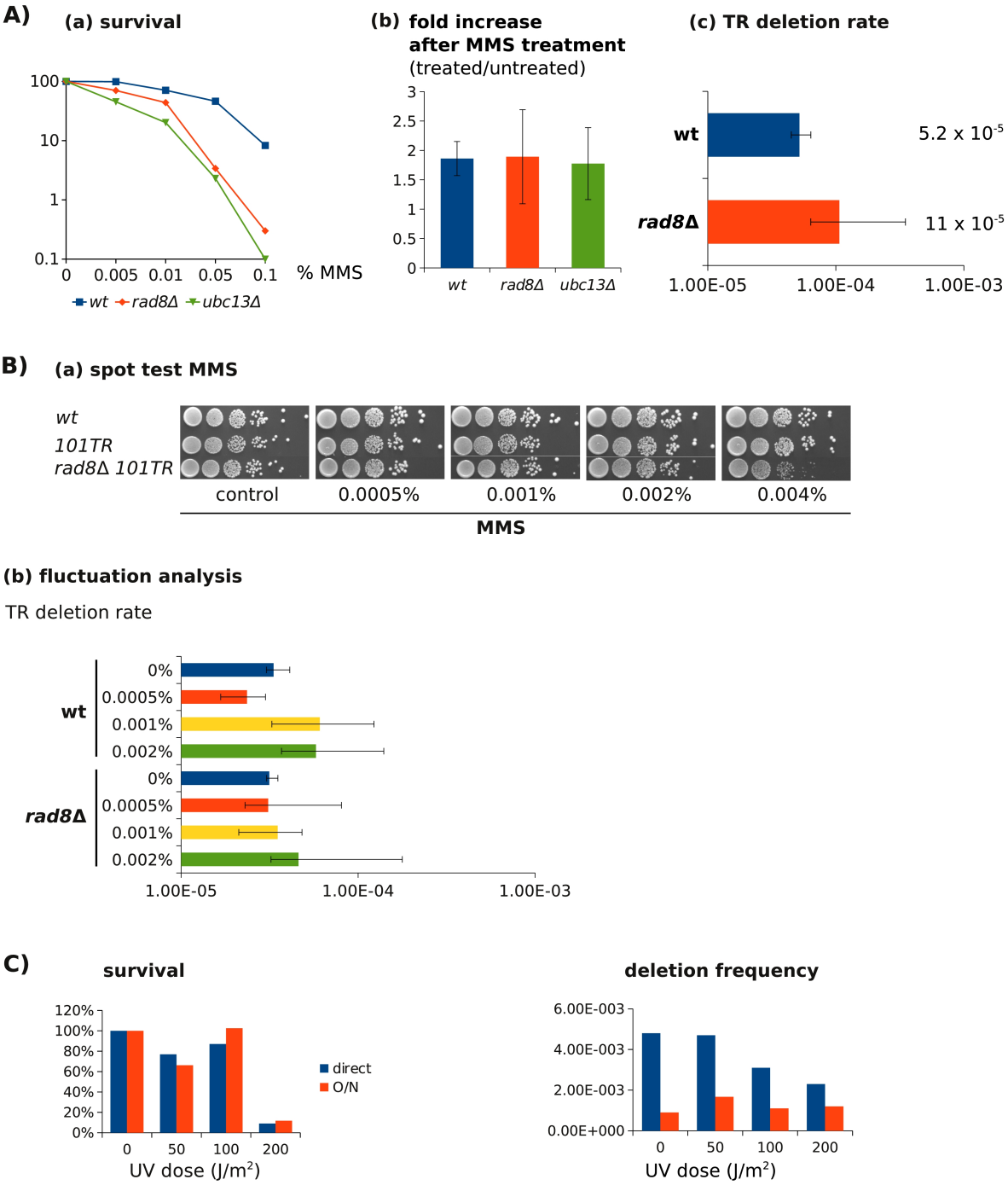
A)
(a) survival
100
10
1
0.1
0
0.005
0.01
0.05
0.1
% MMS
wt
rad8Δ
ubc13Δ
(b) fold increase
after MMS treatment
(treated/untreated)
3
2.5
2
1.5
1
0.5
0
wt
rad8Δ
ubc13Δ
(c) TR deletion rate
wt
5.2 x 10-5
rad8Δ
11 x 10-5
1.00E-05
1.00E-04
1.00E-03
B)
(a) spot test MMS
wt
101TR
rad8Δ 101TR
control
0.0005%
0.001%
0.002%
0.004%
MMS
(b) fluctuation analysis
TR deletion rate
wt
0%
0.0005%
0.001%
0.002%
rad8Δ
0%
0.0005%
0.001%
0.002%
1.00E-05
1.00E-04
1.00E-03
C)
survival
120%
100%
80%
60%
40%
20%
0%
0
50
100
200
UV dose (J/m2)
direct
O/N
deletion frequency
6.00E-003
4.00E-003
2.00E-003
0.00E+000
0
50
100
200
UV dose (J/m2)

3.6 Mutations compromising the replisome and the replication checkpoint increase TR deletion rates

It has been reported that *E. coli* plasmid and chromosomal TR deletion levels are affected by aberrant replication (Saveson and Lovett, 1997). Izumi Miyabe in our lab cloned and characterised the *cdc6-L591M* mutant allele of Pol δ (Miyabe et al., 2011). *cdc6*$^{+}$ encodes the catalytic subunit of Pol δ. This mutant was used in the *nat1 101TR* assay for fluctuation analysis by I. Miyabe and the deletion rate increased about 70-fold in the *cdc6-L591M* background (I. Miyabe, personal communication). In order to test whether this increase is dependent on PRR, I combined the *cdc6-L591M* allele with PRR mutant backgrounds *rhp18*Δ and *ubc13*Δ. Rhp6 and Rhp18 catalyse the monoubiquitylation of PCNA in *S. pombe* (Frampton et al., 2006). Because of the high deletion rates spot tests were performed with cultures grown from single colonies to saturation. Deletion events in *nat1 101TR* increased 50-100 fold in the *cdc6-L591M* background compared to wild-type (Figure 3.6A). These results agree with the fluctuation analysis carried out by I. Miyabe. However, assaying the *cdc6-L591M* allele combined with PRR mutant backgrounds suggest that the observed elevated deletion events in *cdc6-L591M* cells were not dependent on PRR (Figure 3.6A).

Swi1 and Swi3 form the replication fork protection complex (FPC) and are important for checkpoint activation during replication stress (Noguchi et al., 2004). Mrc1 (mediator of the replication checkpoint) is part of the replication machinery and is also required for the activation of the replication checkpoint (Alcasabas et al., 2001; Katou et al., 2003; Osborn and Elledge, 2003). Mrc1 travels with the fork and was shown to be important for replication fork progression in the absence of exogenous DNA damage in *S. cerevisiae* (Szyjka et al., 2005; Gambus et al., 2006). To test whether replication fork progression and the replication checkpoint affect TR instability of *nat1 101TR*, I assayed TR deletions in *mrc1*Δ and *swi1*Δ cells. The deletion rate was significantly increased in both backgrounds, by 8- (*mrc1*Δ) and 17-fold (*swi1*Δ) (Figure 3.6B). Mrc1 is thought to be involved in replication and checkpoint functions and two phosphorylation sites (T645 and T653) in *sp*Mrc1 were shown to be important for Cds1 activation in response to HU (Xu et al., 2006). In *S. cerevisiae*, mutations of phosphorylation sites suppressing the activation of the checkpoint kinase Rad53 (*sp*Cds1), resulted in a separation of function allele of *mrc1*$^{+}$ (Osborn and Elledge, 2003). However, whether only the checkpoint function of *mrc1*$^{+}$ in *S. pombe* cells carrying the *mrc1-T645,653A* allele is affected, remains to be shown. The deletion rate in *mrc1-T645,653A* cells was increased 11-fold compared to wild-type (Figure 3.6B). Taken together, the effects of *swi1*Δ, *mrc1*Δ, and *mrc1-T645,653A* on the TR deletion rate suggest an important role of replication fork stabilisation in the suppression of TR deletions.

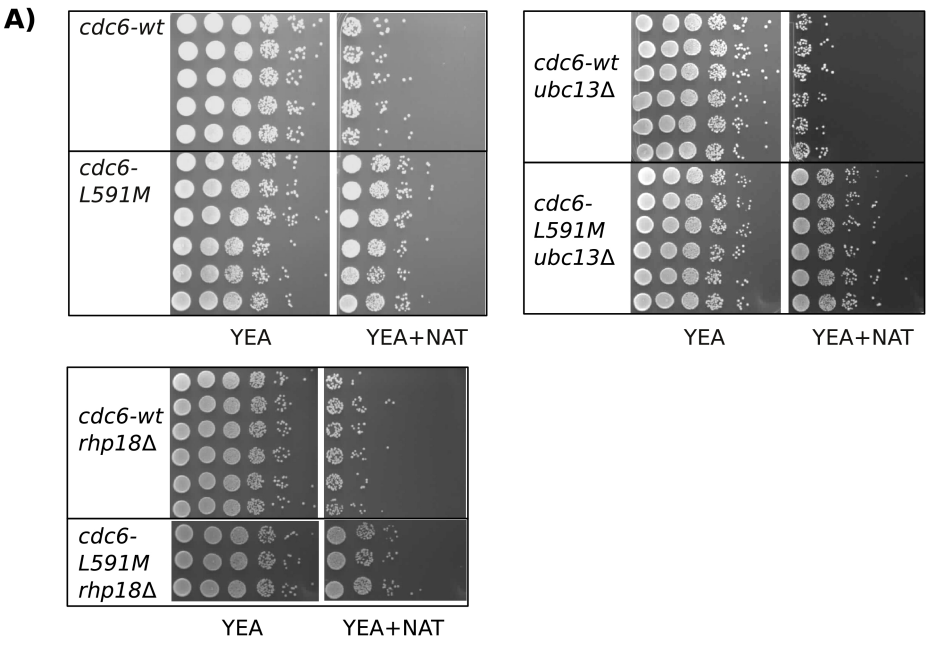

B) **TR deletion rate**

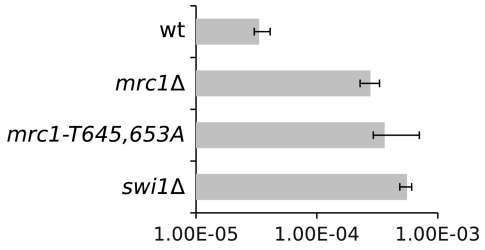

genotype	n	deletion rate x 10^{-5} (95% ci)	p
wt	44	3.3 (3.0-4.1)	
mrc1Δ	33	27.8 (22.8-33.0)	<0.0001
mrc1-T645,653A	21	36.3 (29.3-70.5)	<0.0001
swi1Δ	33	55.6 (48.5-60.8)	<0.0001

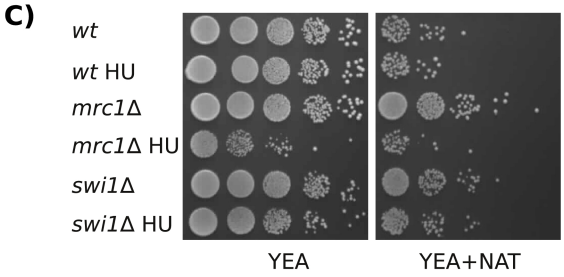

Figure 3.6: Replication mutants increase TR deletion events, independently of PRR
A) The increase of TR deletion rates in cells carrying the *cdc6-L591M* allele was not dependent on PRR. Single colonies were grown to saturation in non-selective media, serially diluted and spotted onto YEA and YEA+NAT plates. The genotypes of the strains used in this experiment are listed in Materials and Methods. Strains used: *cdc6-wt*; A460 and *cdc6-L591M*; A462 were constructed by Izumi Miyabe. *ubc13*Δ; SAS345, *rhp18*Δ; KAF1177, *cdc6-wt ubc13*Δ; SAS711, *cdc6-L591M ubc13*Δ; SAS714, *cdc6-wt rhp18*Δ; SAS718, *cdc6-L591M ubc13*Δ; SAS719.
B) Fluctuation analysis of mutants defective in the replication checkpoint was carried out as described in Figure 3.3A. The p-value was determined for the deletion rates in comparison to wild-type (wt). The genotypes of the strains used in this experiment are listed in Materials and Methods. Strains used: wt; SAS197, *mrc1*Δ; SAS509, *mrc1-T645,653A*; SAS1000, *swi1*Δ; SAS510.
C) HU treatment did not affect the TR deletion rate in wild-type, *swi1*Δ or *mrc1* Δ cells. Cultures of exponentially growing cells were split and grown in the absence or presence of 10mM HU for 4 hours at 30°C. Cells were washed, counted, serially diluted and spotted onto YEA and YEA + NAT (100 μg/ml) plates. Cells were plated in 10-fold serial dilutions starting with 10^5 cells on the left.

Hydroxyurea (HU) depletes the dNTP pool and causes replication forks to stall (Reichard, 1988; Lopes et al., 2001). *swi1*$^+$ and *mrc1*$^+$ have been shown to be important for replication fork stability in the response to HU treatment (Alcasabas et al., 2001; Noguchi et al., 2003). I tested if HU treatment increases TR deletion events and whether this is elevated in *swi1*Δ and *mrc1*Δ cells. Due to the high levels of deletions in these mutants I decided to compare the deletion events in wild-type, *swi1*Δ and *mrc1*Δ cells grown in the presence and absence of HU by spot tests (Figure 3.6C). In the absence of HU, *swi1*Δ and *mrc1*Δ cells showed an increase in deletions compared to wild-type, as observed by fluctuation analysis (Figure 3.6B and C). HU did not increase TR deletion events in either wild-type or mutant cells. The apparent decrease in deletion events in *mrc1*Δ cells is likely due to viability loss.

3.7 *nat1 101TR* contains a putative G4-motif

Mrc1 and Tof1 (*sp*Swi1) have been previously reported to prevent instability of trinucleotide repeats, prone to form secondary structures, in *S. cerevisiae* (Razidlo and Lahue, 2008). Voineagu et al. (2009b) showed an increase of replication fork stalling at CGG repeats in *mrc1*Δ and *tof1*Δ mutant cells, which was independent of the checkpoint function of *MRC1*. The *nat1 101TR* construct is neither a trinucleotide repeat nor does it contain inverted homology to give rise to hairpin structures or palindromes. However, the *nat1*$^+$ gene is very GC-rich. G-rich sequences are prone to form secondary structures, one of which is characterised as G4, also termed G-quadruplex or tetraplex, and contains repeats of Guanines (Gellert et al., 1962; Duquette et al., 2004). I used the online tool QGRS (Quadruplex forming G-Rich Sequences) (Kikin et al., 2006) to map putative G4-motifs in the *nat1*$^+$ sequence. With stringent settings searching for at least four repeats of G-triplets, QGRS found one putative G4-motif in *nat1*$^+$ which is situated in the 101bp repeat sequence (Figure 3.7A). G4-motifs have been implicated in mutagenesis (Cahoon and Seifert, 2009). A sequence which is intrinsically difficult to replicate would agree with the observations of elevated levels of deletion rates in cells mutated in replisome components. Moreover, a sequence-specific effect could possibly interfere with the introduction of DNA lesions by MMS and UV and explain why TR deletions were not significantly increased under such conditions.

Circular dichroism (CD) was used to measure secondary structure formation of the putative G4-motif in *nat1*$^+$. The measurements were performed using oligonucleotides containing the characteristic sequences (Figure 3.7B). A recently published G4-sequence from *Neisseria gonorrhoeae* (G4) was used as a positive control (Cahoon and Seifert, 2009). Negative controls consisted of a point mutant, abolishing the G4-structure (G4m) and part of the *ura4*$^+$ sequence (ura). These oligonucleotides were compared to the putative *nat1*$^+$ G4-motif (nat1) as well as a mutated version

containing G to A substitutions in two G-triplets (nat1m). Potassium (K^+) was used to stabilise G4-structures, which has been shown before (Oliver and Kneale, 1999). The oligonucleotides were resuspended at 10μM in phosphate buffer in the absence or presence of K^+, melted and annealed by heating to 90-95°C followed by slowly cooling down to room temperature and stabilised at 4°C for 24 hours. The CD spectra for G4 showed peaks at 210nm and 260nm characteristic for monomer G4-structures (Dapić et al., 2003) when annealed in buffer containing K^+, which were reduced in G4m (Figure 3.7C (a)). This result corresponds to the spectra published previously and therefore confirms the methodology used (Cahoon and Seifert, 2009). The CD spectra of nat1 showed a clear difference when annealing in the presence of K^+ compared to H_2O indicating a secondary structure (Figure 3.7C (b)). However, it showed smaller and broader peaks at 210nm and 260-300nm, compared to G4. This difference in peak intensity is likely due to the variation in loop sizes and compositions as demonstrated previously (Guédin et al., 2008, 2009, 2010). It is known that CD spectra of G-quadruplexes can vary in peak position and intensity (Dapić et al., 2003). The nat1m oligonucleotide showed a similar spectra as *nat1*, although the effect of K^+ was lost, suggesting that the mutated Gs are important for secondary structure formation. ura contains no obvious G arrays and showed neither a distinct peak as seen for G4 oligonucleotides nor a difference in the absence or presence of K^+. An overlay of the spectra is shown in Figure 3.7C (c). This analysis strongly suggests the presence of structured DNA, possibly a G4-motif, in *nat1*$^+$.

Figure 3.7 *(following page)*: The *nat1 TR* sequence contains a putative G4 motif
A) The Quadruplex forming G-Rich Sequences (QGRS) Mapper (Kikin et al., 2006) was used to analyse the *nat1*$^+$ sequence for putative G4-motifs. One motif was found in the open reading frame (ORF) and the sequence coincides with the 101bp used for the TR assay. Bases 20-101 of one repeat in *nat1 101TR* are shown in the box and the runs of Gs in the G4-motif are indicated in red.
B) Oligonucleotides used for Circular Dichroism (CD) spectroscopy. G4 has been shown to form a G4-structure (G4), which can be mutated (G4m) (Cahoon and Seifert, 2009). The sequence of the ura oligonucleotide was taken from the *ura4*$^+$ ORF, nat1 contains the putative G4-motif detected in *nat1*$^+$, which was mutated in nat1m. Point mutations (G to A) are shown in red.
C) CD spectroscopy reveals a secondary structure formed by nat1 in the presence of K^+. Oligonucleotides were resuspended to 1mM in H_2O and diluted to a final concentration of 10μM in 100mM phosphate buffer pH 7.4 in the presence (red, K^+) or absence (blue, H_2O) of 100mM KCl. The oligonucleotide solutions were heated to 95°C-100°C in a waterbath, cooled down slowly and stabilised at 4°C for 24 hours. CD measurements were taken with a JASCO J-715 CD spectropolarimeter. The graphs show the average of three measurements which were corrected for concentration differences and are shown in molar ellipticity $[\theta]$ (deg$\times$M$^{-1}\times$m^{-1}).

A)

Sequence View

Search Parameters: QGRS Max Length: 30 | Min G-Group Size: 3 | Loop size: from 0 to 36 | Loop search string:

Gene Information	
Gene ID:	**Number of Products:** 1
Gene Symbol:	**Number of poly A Signals:**
Gene Size: 573 nt.	**QGRS found:** 1
	QGRS found (including overlaps): 6

```
000001 ATGGGTACCA CTCTTGACGA CACGGCTTAC CGGTACCGCA CCAGTGTCCC GGGGGACGCC GAGGCCATCG AGGCACTGGA TGGGTCCTTC ACCACCGACA
000101 CCGTCTTCCG CGTCACCGCC ACCGGGGACG GCTTCACCCT GCGGGAGGTG CCGGTGGACC CGCCCCTGAC CAAGGTGTTC CCCGACGACG AATCGGACGA
000201 CGAATCGGAC GACGGGGAGG ACGGCGACCC GGACTCCCGG ACGTTCGTCG CGTACGGGGA CGACGGCGAC CTGGCGGGCT TCGTGGTCGT CTCGTACTCC
000301 GGCTGGAACC GCCGGCTGAC CGTCGAGGAC ATCGAGGTCG CCCCGGAGCA CCGGGGCAC GGGGTCGGGC GCGCGTTGAT GGGGCTCGCG ACGGAGTTCG
000401 CCCGCGAGCG GGGCGCCGGG CACCTCTGGC TGGAGGTCAC CAACGTCAAC GCACCGGCGA TCCACGCGTA CCGGCGGATG GGGTTCACCC TCTGCGGCCT
000501 GGACACCGCC CTGTACGACG GCACCGCCTC GGACGGCGAG CAGGCGCTCT ACATGAGCAT GCCCTGCCCC TAA
```

Total time: 10.9679698944 ms

Bases 20-101 of the nat1 101bp repeat sequence

5'-gtcgccccggagcaccg**gggg**cac**gggg**tc**ggg**cgcgcgttgat**gggg**ctcgcgacggagttcgcccgcgagcggggcgcc

B)

oligo	sequence
G4	GGGTGGGTTGGGTGGG
G4m	GGGTGGGTTGAGTGGG
G4rev	CCCACCCAACCCACCC
ura	ATACAGTGCCAGGCGAGGG
nat1	GGGGCACGGGGTCGGGCGCGCGTTGATGGG
nat1m	GGGGCACGAGGTCGAGCGCGCGTTGATGGG

C)

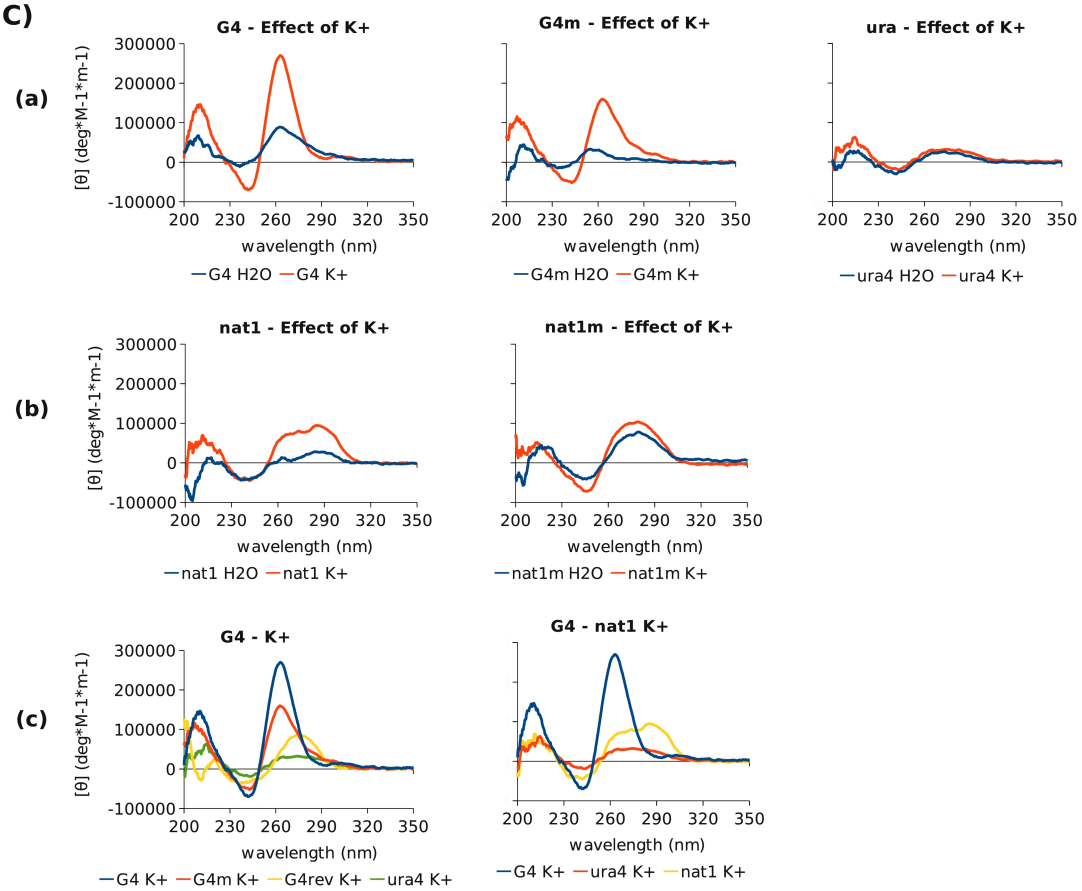

3.8 Conclusion and discussion

Lesions in the DNA can interfere with replication and stall replication forks. Damage avoidance pathways are important to ensure the progress of replication, leaving the damaged template behind to be repaired after replication. PRR employs different mechanisms to achieve this (Figure 3.1A) (Lawrence, 1994). One such mechanism is the error-free pathway involving Rad8 (*sc*Rad5) and Ubc13-Mms2 (Hofmann and Pickart, 1999; Hoege et al., 2002; Frampton et al., 2006). This pathway is thought to involve a template switch mechanism, which could be demonstrated by introducing plasmids carrying synthetic lesions into *S. cerevisiae* and analysing the products of replication (Zhang and Lawrence, 2005). Template switching has also been suggested to occur during HR-dependent replication fork restart in *S. pombe* (Lambert et al., 2005; Mizuno et al., 2009). Goldfless et al. (2006) have identified a chaperone (*Dna*K) in *E. coli* that plays an important role in TR deletions. Genetic and molecular analysis of such TR assays in *E. coli* have suggested that they occur during a repair process at the replication fork involving template switching (Lovett et al., 1993; Goldfless et al., 2006) (Figure 3.1B). *Dna*K was suggested to facilitate the remodelling of the replication fork to allow bypass, which could be similar to error-free PRR in eukaryotes (Goldfless et al., 2006).

In this chapter I describe the development of a TR assay in *S. pombe*, using the marker gene *nat1*$^{+}$. Deletion events can be selected for by resistance to nourseothricine and TR deletion rates can be measured by fluctuation analysis. Initial characterisation of three different lengths of TRs (41bp, 101bp, 251bp) yielded similar spontaneous mutation rates 4.25 x 10^{-5}, 3.3 x 10^{-5} and 3.21 x 10^{-5} respectively (Figure 3.3A). Analysis of spontaneous deletion rates showed that they occur in the absence of HR, MMR and PRR (Figure 3.4A and B). Treatment with MMS and UV irradiation did not significantly elevate deletion events (Figure 3.5), whereas aberrant replication in a *pol* δ mutant background (*cdc6-L591M*) increased the deletion rate by 70-fold (I. Miyabe, personal communication and Figure 3.6A). It was reported previously that TR deletions in *E. coli* are elevated in replication mutants (Saveson and Lovett, 1997). Neither the observed minor increase after MMS treatment (1.5-2 fold) nor the substantial increase in *cdc6-L591M* cells were dependent on PRR (Figure 3.5 and Figure 3.6A).

Genetic analysis suggested that the stability of the replisome plays an important role in the suppression of TR deletions in *nat1 101TR*. Mrc1 and Swi1 are involved in replication fork stabilisation and checkpoint activation (Alcasabas et al., 2001; Noguchi et al., 2003; Szyjka et al., 2005). TR deletion rates were significantly increased in *mrc1*Δ and *swi1*Δ as well as in *mrc1-T645,653A* cells, in which Cds1 activation by Mrc1 is abolished (Xu et al., 2006) (Figure 3.6B). It would be interesting to know whether the replication checkpoint is required for TR stability. Fur-

ther experiments should include mutants of the ATR orthologue *rad3*$^+$, the replication checkpoint kinase *cds1*$^+$ and the DNA damage checkpoint kinase *chk1*$^+$ in order to distinguish between the S-phase and G2/M checkpoint signalling, respectively. Checkpoint proteins have been previously implicated in the stability of repetitive sequences (Voineagu et al., 2009a). The 101bp repeat in *nat1*$^+$ is a direct repeat and is therefore not prone to form secondary structures. However, the sequence is very G-rich and a putative G4-motif was found by the prediction tool QGRS (Kikin et al., 2006) in the repeat sequence and its potential to form a secondary structure was confirmed by CD (Figure 3.7A, B and C). TR deletion events in the *nat1*$^+$ gene might be affected by the formation of a G4-structure. This could have implications for replication and repair responses at this locus.

It has been reported previously that *sc*Rad5 promotes the alteration of repeat length of poly(GT) tracts (Johnson et al., 1994). In contrast, TR deletions in *nat1 101TR* were unaffected in *rad8*Δ (*scRAD5*) cells (Figure 3.4B). This could either be due to a different mechanism, such as simple slippage versus cross-fork template switching (see Figure 3.1) and/or a secondary structure-related pathway. The possibility that structured DNA temporarily stalls the replication fork and requires checkpoint signalling for efficient replication could explain the Mrc1- and Swi1-dependent suppression of TR deletions in *nat1 101TR*. It might also explain why replication fork stalling by HU treatment did not further elevate TR deletions (Figure 3.6C). It would be interesting to compare the deletion rates in *nat1 101TR* and *nat1 41TR* in mutant backgrounds because the G4-motif is duplicated in the 101TR construct, while there is only a single motif in *nat1 41TR*. As the spontaneous deletion rates in these constructs were similar, if not slightly elevated in *nat1 41TR*, one G4-motif might be sufficient to interfere with replication and cause mutagenesis, as previously shown in *Neisseria gonorrhoeae* (Cahoon and Seifert, 2009).

It has been shown in *E. coli* that direct repeat deletions are elevated by the introduction of a secondary structure (inverted repeat) in between them, which stimulates SSA (Bzymek and Lovett, 2001). Stimulation was found to be due to processing by the nuclease SbcCD and by perturbation of lagging strand replication, as ssDNA allows for secondary structure formation (Bzymek and Lovett, 2001). In this context, it is interesting that the endonuclease Mre11 was reported to bind and cleave G4-structures *in vitro* (Ghosal and Muniyappa, 2005). Endonucleolytic processing of structured DNA in the *nat1 TR* constructs might influence TR deletion rates. Although I have not tested the effect of Mre11 on TR deletions, SSA in *S. pombe* is dependent on Rad52 (Raji and Hartsuiker, 2006; Watson et al., 2011) and I showed an increase of TR deletions in a *rad22*Δ background (Figure 3.4A). Work in *S. cerevisiae* has shown that the minimum homology require-

ment for SSA is between 63 and 89bp (Sugawara and Haber, 1992). This requirement would not be met in the *nat1 41TR* allele and the positioning of the G4-motif in the *nat1 101TR* allele leaves a homology of less than 20bp upstream of the G4-motif. Furthermore, the G4-structure formation is strand-specific, which argues against a simultaneous cleavage to create a DSB. The complementary region of the G4 sequence is C-rich and is likely to form an i-motif (Brooks et al., 2010). The processing of i-motifs by nucleases is currently unknown. In *E. coli*, secondary structure formation of palindromes was increased on the lagging strand and SSA was stimulated if replication was perturbed (Bzymek and Lovett, 2001). The deletion rate in the *nat1 101TR* allele was elevated when lagging strand synthesis was compromised (Figure 3.6A). However, the G4-motif is situated on the leading strand in the *nat1 TR* assays.

Taken together, the results show that *nat1 TR* assays are not suitable as a tool to study template switching during PRR. Interestingly, recently Ede et al. (2011) have published the development of a very similar TR assay in *S. cerevisiae*. By duplicating a 266bp fragment in the kanMX4 marker cassette, they were able to select for deletions by resistance to Geneticin. The spontaneous deletion rates in a wild-type background were about $9x10^{-6}$ in their assay (Ede et al., 2011), which is 3-4 fold lower as compared to *nat1 101TR*. Deletion events could be induced by DNA damage 4-Nitroquinoline 1-oxide (4-NQO) and spontaneous as well as damage-induced deletions were dependent on Rad52 (Ede et al., 2011). While the majority of damage-induced deletions were dependent on Rad51, spontaneous deletions were actually increased in *rad51*Δ cells (Ede et al., 2011). The authors suggest that in the absence of Rad51, spontaneous events could be repaired by SSA due to DSB formation and that most damage-induced deletions require strand invasion. Furthermore, the helicase Mph1 was required for damage-induced deletion formation (Ede et al., 2011). Mph1 has been previously suggested to function in an error-free bypass of replication blocks in a HR-dependent, but PRR-independent manner (Schürer et al., 2004). I expect the different observations in the ”kankanMX4“ assay by Ede et al. (2011) and the *nat1 101TR* assay to be due to either the sequence length of the repeats or the sequence content. 101bp of homologous sequence (and probably less, depending on where blockage occurs) might not be sufficient for HR-dependent strand invasion. And considering that the spontaneous deletion rate in *nat1 101TR* is 3-4 fold higher than in the ”kankanMX4“ assay, a damage-induced effect might be masked by an intrinsic effect on replication, which leads to rearrangements.

My results suggest that the *nat1 TR* assays can be used to study the effect of structured DNA on genome stability. It would be interesting to measure the effect on TR deletions when proteins known to play a role in G4-metabolism are absent. Such factors have been characterised in vari-

ous organisms and include the helicase Pif1 (Ribeyre et al., 2009), the nucleases Mre11 (Ghosal and Muniyappa, 2005), Kem1 (Liu and Gilbert, 1994) and also Dna2 (Masuda-Sasa et al., 2008). Furthermore, G4-stabilising chemicals, such as Phen-DC compounds could be used to elevate the effect of G4-DNA on genome stability (Piazza et al., 2010).

Because of the results presented here I have decided to investigate the effect of secondary structures on TR deletions in more detail. Therefore, I developed TR assays which enabled me to measure TR deletions in the presence or absence of a defined G4-structure (G4 in Figure 3.7C and (Cahoon and Seifert, 2009)) on either the leading or the lagging strand. The results of these experiments are shown in Chapter 5. I also combined a site-specific system for replication fork collapse and HR-dependent restart, which introduces genomic instability after fork restart (as described in Chapter 4) with the new TR assay. This allowed me to measure the fidelity of a restarted fork replicating TR sequences in the presence or absence of G4-DNA (see Chapter 5).

Chapter 4

Genomic instability after replication fork collapse and restart

4.1 Introduction

Inhibition of replication is a threat to the cell because it prevents the completion of genome duplication, which is important for subsequent cell division. Replication forks can arrest at lesions, secondary structures in the DNA, by encountering DNA metabolism (such as transcription), from depletion of dNTPs or due to protein-DNA barriers (Lambert and Carr, 2005). The responses to arrested replication forks is dependent on several factors, such as the cause of the blockage and its context (Labib and Hodgson, 2007; Carr et al., 2011). In bacteria, replication of the circular chromosome is initiated from a single origin and replication forks frequently encounter DNA damage and need to be restarted in order to complete replication (Sandler and Marians, 2000). Arrested replication forks are restarted very efficiently by pathways involving replication proteins, such as the helicase and primase PriA, which can reload the replisome, and recombination proteins, such as RecA (Sandler and Marians, 2000; Michel et al., 2004). In eukaryotes however, multiple origins are fired for genome replication. Arrested replication forks could therefore presumably be rescued by a converging fork and there is evidence that dormant origins fire to complete replication (Ge and Blow, 2010; Blow et al., 2011; Kawabata et al., 2011). However, the arrest of two converging forks (where there is no opportunity to fire a new fork in the intervening sequence) or of a replication fork in a locus where replication is unidirectional (such as the rDNA), requires different mechanisms to ensure complete replication (Murray and Carr, 2008).

Sarah Lambert in our lab has developed a system to study site-specific replication fork arrest and its consequences using RTS1 in *S. pombe* (Lambert et al., 2005). RTS1 is a polar replication fork barrier (RFB) found in the *S. pombe* mating type locus on chromosome 2 (Dalgaard and

Klar, 2001). Lambert et al. (2005) integrated two copies of the polar RTS1 barrier on either side of *ura4*$^+$ (RuraR) on chromosome 3, such that the activity of RTS1 blocks replication of *ura4*$^+$ from both directions (Figure 4.1A). The main direction of replication of this locus is from the centromere to the telomere. RTS1 activity can be induced by the removal of thiamine which activates expression of *rtf1*$^+$ (*Pnmt41-rtf1*$^+$) which is required for RFB activity. Replication fork arrest at RuraR induced genomic rearrangements between the RTS1 sequences at the *ura4* locus, resulting in an orientation switch of *ura4*$^+$ and less frequently in translocations between the RTS1 copies on chromosomes 3 and 2 (Lambert et al., 2005). The *ura4*$^+$ orientation switch was dependent on RTS1 homology at the *ura4* locus and could not be observed in the absence of either of the flanking RTS1 sites (Rura and uraR). Therefore, it was suggested that this event corresponds to homology-directed recombination dependent on replication fork arrest. Whereas a functional checkpoint was dispensable, recombination proteins were essential for viability under these conditions and Rad52 (encoded by *rad22*$^+$) was shown to localise to RTS1 (Lambert et al., 2005). This suggests that the replisome is not stabilised and disassembles, resulting in replication fork collapse.

Ken'Ichi Mizuno used the RTS1 barrier system to investigate replication fork collapse in a palindrome (Mizuno et al., 2009). The RuiuR system consists of an inverted repeat of RTS1 and *ura4*$^+$ separated by a 14bp spacer (Figure 4.1A). This arrangement of RTS1 and *ura4*$^+$ forms a palindrome of 5.2kb in size. Replication fork collapse in RuiuR, resulted in the formation of acentric (no centromere) and dicentric (two centromeres) chromosomes at very high levels accompanied by a loss in viability (Mizuno et al., 2009). This observation was dependent on HR, but did not involve a DSB. Mizuno et al. (2009) suggested a replication template exchange mechanism to account for the rearrangements, in which the 3'-end of the nascent strand at RTS1 invades the wrong copy of RTS1 to reinitiate replication. Subsequently, the formation of palindromic chromosomes at a low frequency ($\sim$1-2% per generation) was also observed in RuraR and was dependent on the inverted repeats of RTS1 (Lambert et al., 2010). Taken together, these results suggested that replication fork collapse at RTS1 can result in genomic rearrangements by invasion of ectopic sequences during HR-dependent replication fork restart (Lambert et al., 2005; Mizuno et al., 2009; Lambert et al., 2010).

Curiously, several observations suggested that multiple mechanisms might be activated in response to replication fork collapse at RTS1. The relative amounts of acentric and dicentric chromosomes generated after RTS1 activation were equal in RuraR, but not in RuiuR (K. Mizuno, personal communication). The uncoupling of the formation of acentric and dicentric chromosomes in RuiuR was furthermore supported by the analysis of a different construct. In this construct (RuiuhR, Figure 4.1A) part of one *ura4*$^+$ sequence in RuiuR was replaced by *his3*$^+$ sequence

which allowed the determination of the sequence content of the central part in palindromic chromosomes. Dicentric chromosomes were found to either contain two copies of the *his3*$^+$ sequence or only one (K. Mizuno, personal communication). These observations suggested that, while chromosomal rearrangements are likely to arise due to the restart mechanism, they could also be formed after replication restart, likely due to the replication fidelity of the restarted fork.

4.2 Aim of the project and summary

Our lab was therefore interested to know whether homology to the site of fork collapse (RTS1) is required for genomic instability due to HR-dependent restart and if these rearrangements are unique in the context of inverted sequences.

I decided to investigate these questions collaboratively with K. Mizuno by using constructs generated by K. Mizuno for this specific purpose (as described below). These constructs allowed me to dissect mutagenesis in direct and inverted repeats after HR-dependent restart irrespective of an erroneous template switch between RTS1 sites. The results suggested that repeated sequences show an increase in instability when replicated by a restarted fork and that this occurs in direct repeats as well as in inverted repeats. Furthermore, erroneous replication is elevated between inverted repeats as compared to direct repeats, possibly due to secondary structure formation.

Figure 4.1 *(following page)*: Schematics of RTS1 and rDNA RFB constructs at the *ura4* locus
A) RuraR and RuiuR, are integrated at the *ura4* locus on chromosome 3. The main direction of replication is from the centromere side (Lambert et al., 2005; Mizuno et al., 2009). The red boxes represent ARS sequences as in Segurado et al. (2003). RuraR consists of two RTS1 flanking *ura4*$^+$. RTS1, prevents replication of *ura4*$^+$ by arresting replication forks approaching from the centromere and from the telomere and is controlled by *rtf1*$^+$ expression. *Pnmt41-rtf1*$^+$ can be switched on by removal of thiamine from the media. RuiuR contains two inverted copies of RTS1 and *ura4*$^+$ separated by a 14bp spacer. In RuiuhR, part of one *ura4*$^+$ sequence in RuiuR was replaced by *his3*$^+$ (grey). Dicentric chromosomes formed after replication fork collapse in this construct were found to either contain two copies of the *his3*$^+$ sequence or only one, as indicated by the black arrows (K. Mizuno, personal communication). Cells carrying RuraR, RuiuR and RuiuhR are ura+. The grey arrows denote repeated sequences. The arrow shape of the *ura4*$^+$ sequence indicates direction of transcription. The centromere is indicated as a black circle.
B) In ruraR, the telomere-proximal RTS1 sequence was replaced by three repeats of the polar rDNA RFB (Ter2/3). The rDNA RFB is constitutively ON and pauses replication forks approaching from the telomere. Activity of RTS1 is controlled by *Pnmt41-rtf1*$^+$. *ura4*$^+$ was divided into three parts; 'a' (693bp), 'b' (516bp) and 'c' (553bp). The construct rura(dir)R contains a tandem repeat of 'b' (c-b-b-a) and rura(inv)R an inverted repeat of 'b' flanking 'c' (b-c-b-a). Both constructs are *ura4-*.
C) Rearrangements between the repeated sequences in the parental constructs, a deletion for rura(dir)R and an inversion for rura(inv)R, can result in the restoration of *ura4*$^+$ (rearranged). In rura(inv)R the inverted repeat remains intact after rearrangements resulting in *ura4*$^+$. The arrows in both directions (rura(inv)R) indicate that, if cells are grown in non-selective media (+uracil), orientation switch of 'c' is reversible.

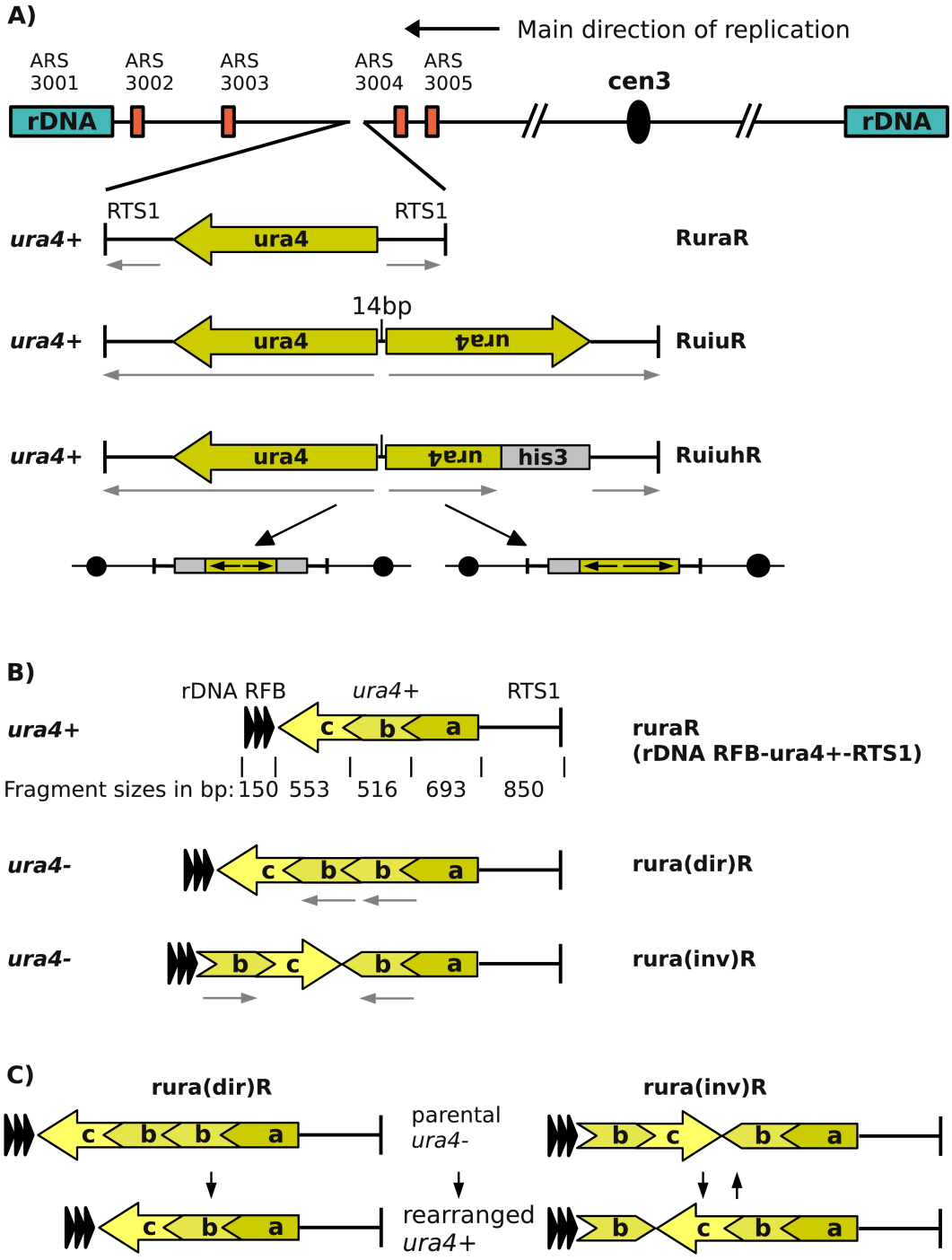
A)
Main direction of replication
ARS 3001
ARS 3002
ARS 3003
ARS 3004
ARS 3005
cen3
rDNA
rDNA
RTS1
RTS1
ura4+
ura4
RuraR
14bp
ura4+
ura4
ura4
RuiuR
ura4+
ura4
ura4
his3
RuiuhR
B)
rDNA RFB
ura4+
RTS1
ura4+
c
b
a
ruraR
(rDNA RFB-ura4+-RTS1)
Fragment sizes in bp: 150 553 516 693 850
ura4-
c
b
b
a
rura(dir)R
ura4-
b
c
b
a
rura(inv)R
C)
rura(dir)R
rura(inv)R
parental
ura4-
rearranged
ura4+

4.3 Constructs, rura(dir)R and rura(inv)R, for analysis of error-prone replication after restart

In order to measure the requirement of the inverted RTS1 sequence for the formation of acentric and dicentric chromosomes, K. Mizuno modified the RuraR system. Figure 4.1B shows an overview of these modified constructs. The telomeric RTS1 sequence was replaced by three repeats of consensus sequence of the RFB derived from the rDNA locus (rDNA RFB, Ter2/3). The rDNA RFB is constitutively ON, whereas activity of RTS1 is controlled by *rtf1*$^+$ expression (*Pnmt41-rtf1*$^+$). As the main direction of replication in this locus is from the centromere to the telomere (Figure 4.1A), the majority of forks will collapse at RTS1 when *Pnmt41-rtf1*$^+$ is expressed. Unlike RuraR and RuiuR, these systems have only one RTS1 sequence at the *ura4* locus. Furthermore, *ura4*$^+$ was divided into three parts, labelled a, b and c. Part 'a' consists of 693bp (*Bpl*I-*Ava*II), 'b' of 516bp (*Ava*II-*Eco*RV), and 'c' of 553bp (*Eco*RV-*Afl*II). These parts were rearranged in different ways, creating a direct repeat (a-b-b-c), called rura(dir)R and an inverted repeat (a-b-c-b), called rura(inv)R (Figure 4.1B). Both constructs are lacking an inverted repeat of RTS1. The inverted repeat in rura(inv)R is located telomere-proximal of RTS1 and is separated by 'a' (693bp) from RTS1. In rura(dir)R there is no inverted repeat sequence at the *ura4* locus. Cells carrying these constructs are initially ura-, but rearrangements of *ura4*, by either direct repeat recombination (rura(dir)R) or inverted repeat recombination and orientation switch (rura(inv)R) would result in the restoration of *ura4*$^+$ (Figure 4.1C). The orientation change of 'c' in rura(inv)R is possible in both directions, because the inverted repeat sequence is retained. Therefore *ura4*$^+$ can rearrange to *ura4-* if no selection for ura+ cells is applied. Whereas in rura(dir)R, selection for *ura4*$^+$ results in the deletion of one direct repeat sequence and the loss of the substrate for recombination.

4.4 Replication fork collapse at RTS1 in rura(dir)R and rura(inv)R induces rearrangements restoring *ura4*$^+$

Rearrangements after replication fork collapse at RTS1 in rura(dir)R (deletion) and rura(inv)R (inversion) were analysed by spot tests. Experiments were carried out with cells in which expression of *rtf1*$^+$ is either controlled by the *nmt41*$^+$ promoter (*Pnmt41-rtf1*$^+$) or completely abolished by deletion of *rtf1*$^+$ (*rtf1*Δ). Replication fork collapse at RTS1 is induced by the removal of thiamine from the media in *Pnmt41-rtf1*$^+$ cells, whereas in *rtf1*Δ cells RTS1 activity is always OFF. As controls, the previously characterised palindrome strain RuiuR (Mizuno et al., 2009) and ruraR were used (Figure 4.1A).

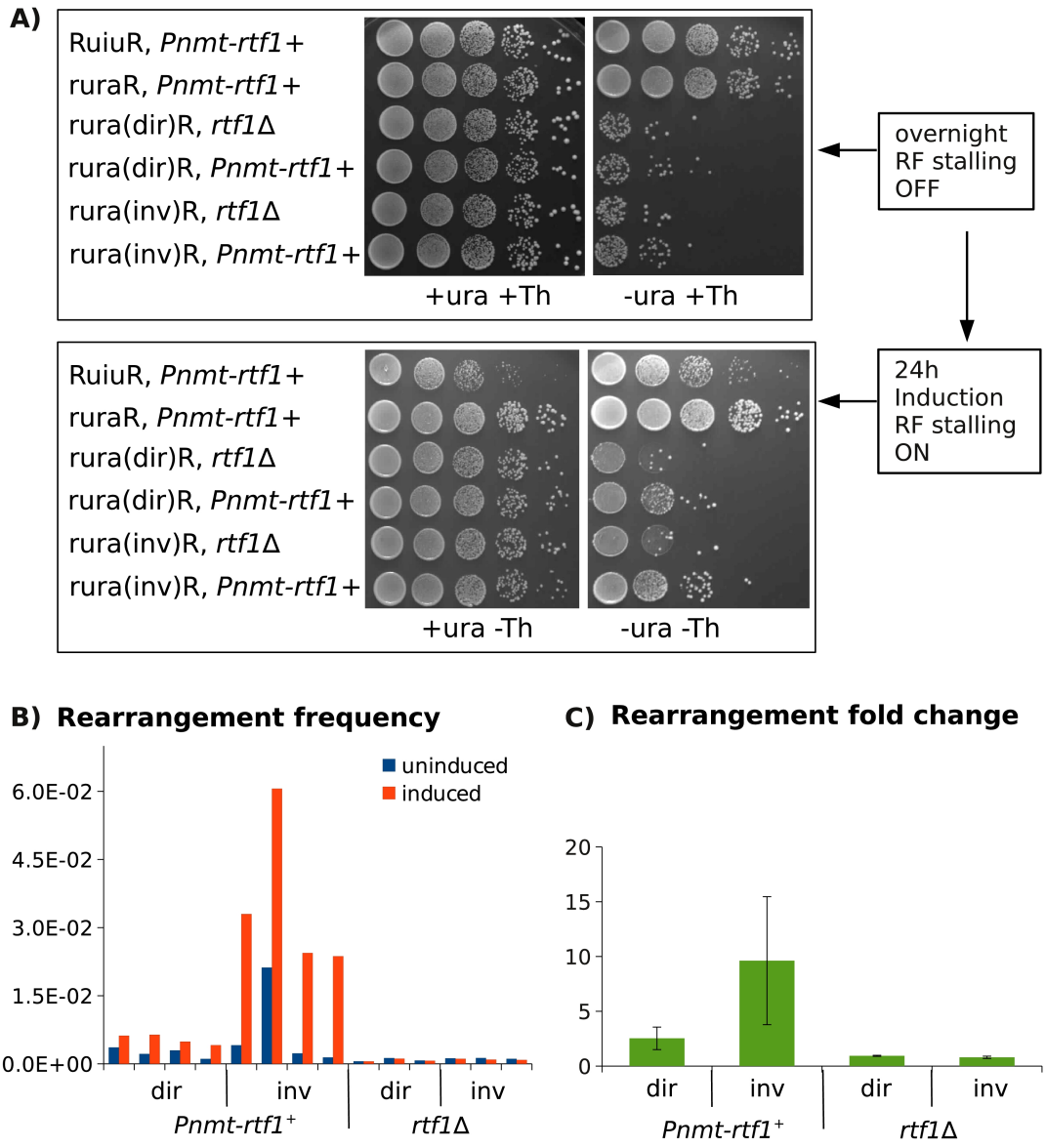

Figure 4.2: Replication fork collapse at RTS1 induces rearrangements in rura(dir)R and rura(inv)R which restore *ura4*$^+$

A) Cells were inoculated from a plate containing 5-FOA and grown in rich media containing thiamine (RTS1 OFF) over night, washed, inoculated in media lacking thiamine (RTS1 ON) and grown for 24 hours. Cultures were counted, serially diluted and spotted onto agar plates, starting with 10^5 cells on the left, before and after 24 hours. In the *Pnmt-rtf1*$^+$ background, *rtf1*$^+$ expression is induced after the removal of thiamine (-Th). In *rtf1*Δ cells, RTS1 is always OFF. Rearrangements resulting in *ura4*$^+$ cells were selected for on plates lacking uracil (-ura). The agar plates contained (+Th) or lacked thiamine (-Th) as indicated at the bottom. The RuiuR strain was previously shown to lose viability after replication fork collapse (Mizuno et al., 2009) whereas ruraR shows no loss of viability. After 24 hours of induction of *Pnmt-rtf1*$^+$, rura(dir)R and rura(inv)R show an increase in ura+ colonies when compared to the cultures before induction or to *rtf1*Δ strains. The spot tests shown are representative data from at least three experiments. Strain genotypes are listed in Materials and Methods. Strains used: RuiuR *Pnmt-rtf1*$^+$; SAS461/YKM041, ruraR *Pnmt-rtf1*$^+$; SAS456/YKM044, rura(dir)R *Pnmt-rtf1*$^+$; SAS462/YKM613, rura(dir)R *rtf1*Δ; SAS488, rura(inv)R *Pnmt-rtf1*$^+$; SAS465/YKM616, rura(inv)R *rtf1*Δ; SAS492.

B) The frequency of rearrangements resulting in a change from ura- to ura+ cells was calculated. Cells from the over night culture in rich media (RTS1 OFF, +ura) in **A** and cells from the cultures after induction for 24 hours were plated onto media plus or minus uracil (ura) and plus or minus thiamine (Th). The bars illustrate the rearrangement frequency in conditions where *Pnmt-rtf1*$^+$ is repressed (blue) or induced (orange). The graph in **C)** shows the average fold change with standard deviation of the rearrangement frequency shown in **B**.

Cells growing in non-selective media (containing uracil, +ura) containing thiamine were washed, diluted and grown in non-selective media without thiamine for 24 hours (~8 generations) to induce replication fork collapse at RTS1. Viability and *ura4*$^+$ rearrangements were analysed by spot tests (Figure 4.2A). The non-selective plates allow for visualisation of a loss of viability and ura- plates select for rearrangements resulting in *ura4*$^+$ (Figure 4.1C). The palindrome strain RuiuR showed a loss of viability after replication fork collapse, as previously published (Mizuno et al., 2009). The viability of ruraR, rura(dir)R and rura(inv)R was not affected in this assay. The RuiuR and ruraR strains contain a functional *ura4*$^+$ and there is no detectable loss of *ura4*$^+$ after replication fork collapse. rura(dir)R and rura(inv)R cells are *ura-* and therefore unable to grow on plates lacking uracil (-ura). Rearrangements in the *ura4* locus of rura(dir)R and rura(inv)R (Figure 4.1C) can restore *ura4*$^+$, which can be measured by growth on -ura plates.

Basal levels of rearrangements can be detected without RTS1 activity (+Th or *rtf1*Δ), which demonstrates an intrinsic level of instability of the repeated sequences. This level of instability could also result from leaking expression of *Pnmt41-rtf1*$^+$ in cells carrying this allele. Activation of RTS1 (-Th, *Pnmt41-rtf1*$^+$) increased the levels of rearrangements. This shows that replication fork collapse at RTS1 results in an increase of rearrangements at repeated sequences. Furthermore, rearrangements are induced at a higher level in rura(inv)R than in rura(dir)R, which suggests that inverted repeats are more prone to instability after replication fork collapse than direct repeats. In order to calculate the frequency of the rearrangements, cells from the cultures used for the spot tests (at least 3 experiments) were plated on selective and non-selective media. The level of rearrangements resulting in *ura4*$^+$ is very low in cells where RTS1 is OFF (*rtf1*Δ) (about 1x10^{-3}), compared to cells where RTS1 is ON (*Pnmt41-rtf1*$^+$, -Th) (Figure 4.2B). Replication fork collapse and restart at RTS1 increases the level of rearrangements in rura(dir)R and rura(inv)R by 3-fold and 10-fold, respectively (Figure 4.2C). These numbers correlate with the observation in the spot test experiment, where rura(inv)R showed a higher increase in rearrangements than rura(dir)R.

4.5 PCR analysis of the rearrangements restoring *ura4*$^+$

Polymerase chain reaction (PCR) analysis was used in order to characterise the physical nature of the rearrangements restoring *ura4*$^+$ in rura(dir)R and rura(inv)R after replication fork collapse at RTS1. Six *ura4*$^+$ clones of each construct were isolated from selective plates (-uracil), after activation of RTS1 in *Pnmt41-rtf1*$^+$ cells (Figure 4.2B). These clones were cultured under selection for uracil and repressive conditions for *Pnmt41-rtf1*$^+$ (+Th). As a control, parental (p) genomic DNA was extracted from rura(dir)R and rura(inv)R cells isolated from plates containing 5-FOA, which provides selection against ura+ cells, and cultured in non-selective media (+ura)

under repressive conditions (+Th) for *Pnmt41-rtf1*$^{+}$. Genomic DNA was extracted, quantified and the same amount of DNA was used for all reactions of the PCR analysis. In Figure 4.3A, the

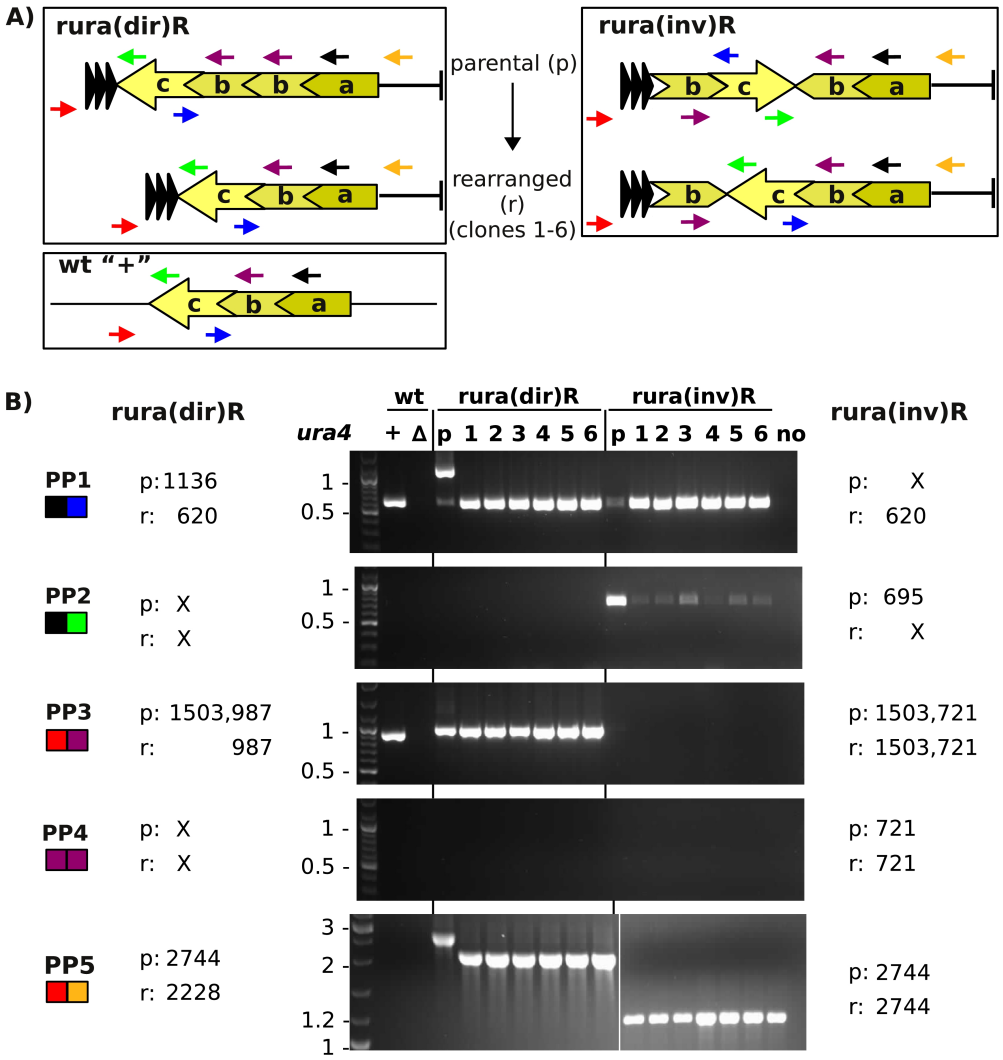

Figure 4.3: PCR analysis confirms the expected rearrangements in rura(dir)R and rura(inv)R to restore *ura4*$^{+}$

A) shows the parental (p) and expected rearranged (r) *ura4* loci of rura(dir)R and rura(inv)R as well as wild-type *ura4*$^{+}$ (wt '+'). Coloured arrows indicate the orientation and binding sites of primers used in the PCR analysis. The arrow shape of the *ura4* sequence indicates direction of transcription of the wild-type.
B) *Pnmt-rtf1*$^{+}$ was induced in rura(dir)R and rura(inv)R cells by removal of thiamine for 24 hours. Cells were plated onto -ura plates and six ura+ colonies were selected for each construct and cultured for DNA extraction. The parental (p) template DNA was extracted from uninduced cells isolated from plates selective for ura- cells (containing 5-FOA). Genomic DNA was extracted and quantified. Equal amounts were used as template DNA for the PCR reactions. The reactions were analysed by agarose gel electrophoresis. The colours of the boxes on the left correspond to the primers used in each reaction. PP stands for primer pair. Expected fragment sizes (in bp) for parental (p) and rearranged (r) *ura4* loci are listed for rura(dir)R (left) and rura(inv)R (right). The wild-type (wt) '+' contains the *ura4* locus without the RFBs. 'Δ' indicates the *ura4-D18* allele, where *ura4*$^{+}$ is deleted. 'no' is a negative control reaction lacking template DNA. The sizes of the marker DNA are indicated in kb. The sequences of the primers used are listed in Materials and Methods. Primers: black; P292, blue; P293, green; P294, red; P81, purple; P25, orange; P323.

orientation and binding sites of the primers used are indicated for each construct. Schematics for rura(dir)R and rura(inv)R parental (p) and rearranged (r, clones 1-6) constructs are shown. As controls, genomic DNA from cells containing the wild-type *ura4*$^+$ (wt '+') or a deletion of *ura4*$^+$ (wt 'Δ') was used. No PCR products with any primer pair are expected when using the wt 'Δ' template DNA. The wt '+' DNA is lacking the RFBs and therefore also the binding site of the orange primer used in primer pair 5 (PP5).

All the primer pairs used (PP1-PP5) showed the expected products for wild-type controls ('+' and 'Δ') and for rura(dir)R (Figure 4.3B). For PP1, the parental DNA sample of rura(dir)R shows the expected product of 1136bp as well as a band (620bp) of less intensity. The smaller fragment corresponds to the size expected for the rearranged samples (as seen for clones 1-6), indicating an intrinsic instability of the direct repeat in rura(dir)R. This confirms the previous results (Figure 4.2), which showed a basal level of rearrangements without replication fork collapse at RTS1, detected by spot tests. The decrease in size of the products for clones 1-6 compared to the parental DNA, indicates the loss of one 'b' repeat ('c-b-b-a' to 'c-b-a'), as expected.

The analysis by PCR of the samples for rura(inv)R is shown on the right in Figure 4.3B. Reactions using PP1 yielded the expected products for clones 1-6. The parental construct is not expected to show a product in this reaction due to the orientation of the primers of PP1. However, similarly as seen for rura(dir)R, a faint band can be detected at the size of the rearranged *ura4* locus (620bp), reflecting the intrinsic instability of the inverted repeats in rura(inv)R. In contrast to rura(dir)R, the repeated sequences in rura(inv)R are maintained after the rearrangement. This means that the repeated sequences can still recombine with each other (Figure 4.1C). For this reason, PP2 shows the expected product of 695bp for the parental DNA of rura(inv)R as well as a faint band of the same size for clones 1-6. Although the rearranged clones 1-6 were grown under selective conditions (-ura), which should ensure one orientation of 'c' (*ura4*$^+$), a basal instability still remains. PP3 and PP4 did not yield any product for the samples of rura(inv)R. This could be due to the binding of one primer (purple) to the inverted repeat sequence. The possibility of secondary structure formation of an inverted repeat might interfere with the PCR reaction. In order to confirm that the overall size of the rura(inv)R construct before and after rearrangements remains the same, PP5 was used. The binding sites of this primer pair are located outside the inverted repeat. However, these reactions resulted in a fragment of about 1250bp rather than the expected 2744bp. This is not likely to be due to inefficiency of the reactions because of the fragment size, as for the parental sample of rura(dir)R the fragment of 2744bp could be amplified using the same primers (PP5). Because rura(inv)R contains an inverted repeat sequence the template DNA might be more difficult to amplify due to secondary structures, even if the binding sites are not located within the

repeat, as it is the case when using PP3 and PP4. The short fragment of 1250bp amplified by PP5 was analysed further to determine its sequence content as shown in Appendix B (Figure B.1). This fragment is considered to be an artefact, as it shows the same band intensity before (p) and after (r) replication fork collapse in Figure 4.3B (PP5).

The PCR analysis of the rearrangements in rura(dir)R and rura(inv)R confirmed the expected products as shown in Figure 4.1C. However, this technique seems to be limited by inverted repeats and might not be suitable to fully characterise the physical nature of these constructs. Therefore restriction fragment length analysis (RFLA) was used for further analysis of the rearrangements.

4.6 Restriction fragment length analysis (RFLA) of ura+ cells after replication fork collapse

The genomic DNA used for analysis by PCR (Figure 4.3) was subjected to RFLA. The same amount of DNA of each sample was cut with *Ase*I, which for rura(dir)R and rura(inv)R results in a 5kb fragment containing the *ura4* locus (Figure 4.4A). The digested DNA was separated by agarose gel electrophoresis, transferred to a membrane and fragments were detected by radioactively labelled probes which hybridise either centromere-proximal 'cen' or telomere-proximal 'tel' to *ura4*$^+$. In this analysis, both probes yielded the same results (Figure 4.4B). The rura(dir)R locus showed a reduction in size when comparing the parental locus (p) to the rearranged clones 1-6. This confirms the previous observation by PCR analysis (Figure 4.3B). Rearrangements in the rura(inv)R locus did not affect the size of the locus, which is consistent with an orientation switch of 'c' (Figure 4.1C), retaining the inverted repeat 'b-c-b', as expected.

For further analysis, the genomic DNA was cut with *Sca*I in addition to *Ase*I. 'c' in *ura4*$^+$ contains a *Sca*I site, which can be used to visualise size changes within *ura4*$^+$ in rura(dir)R and rura(inv)R (Figure 4.5A). As expected, the fragments of rura(dir)R showed a reduction in size when using the 'cen' probe but remained the same when probing with 'tel' (Figure 4.5B). The fragments of rura(inv)R showed either a reduction in size or an increase in size when using 'cen' or 'tel', respectively.

These results strongly support the rearrangements predicted in Figure 4.1C, a deletion of 'b' in rura(dir)R and an inversion of 'c' in rura(inv)R, restoring *ura4*$^+$.

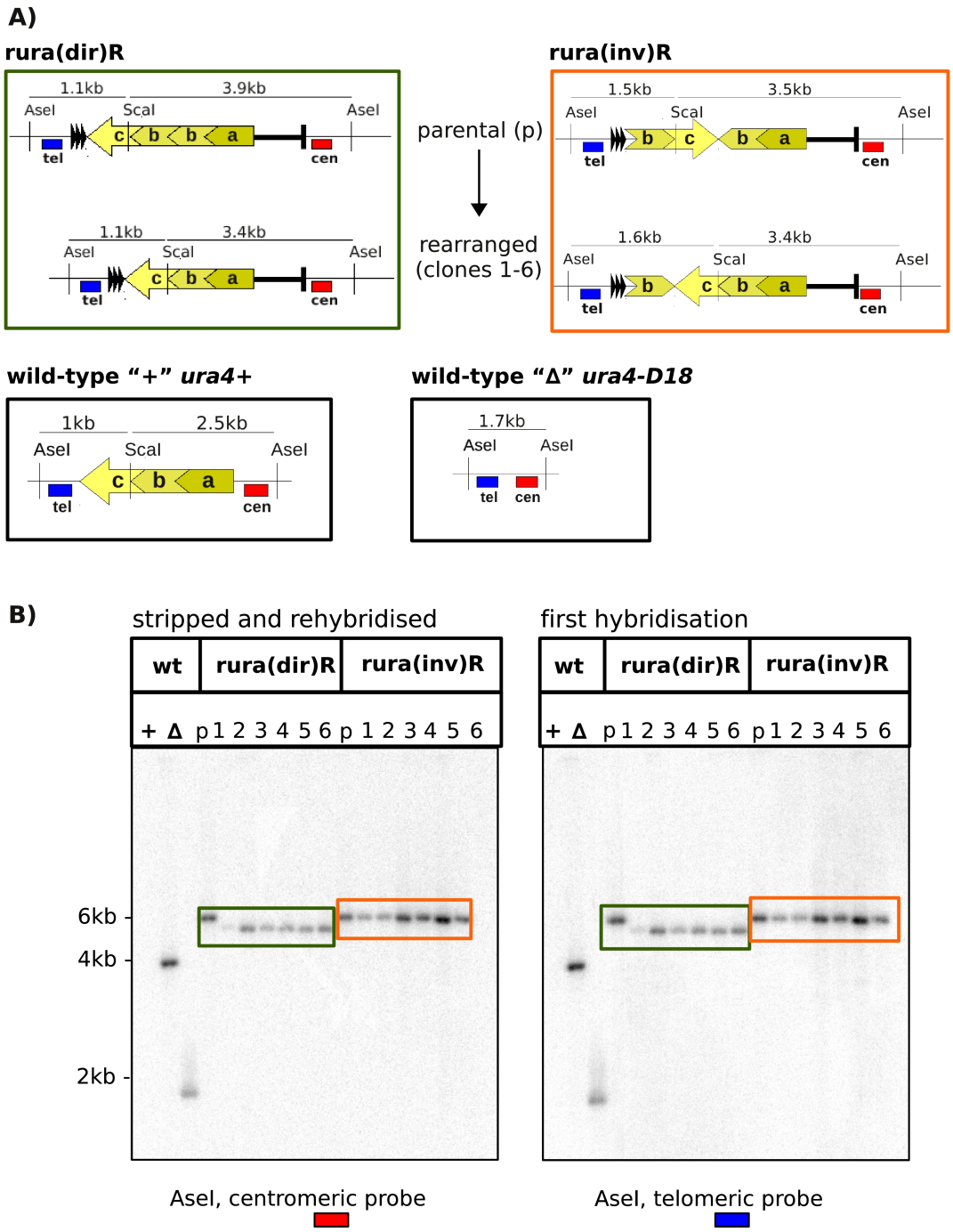

Figure 4.4: Confirmation of *ura4* rearrangements by Restriction Fragment Length Analysis (RFLA) using *Ase*I

A) Map of restriction sites in the parental (p) and rearranged rura(dir)R (clones 1-6) (green box) and rura(inv)R (orange box) loci. The telomere-proximal 'tel' and centromere-proximal 'cen' probes used for detection are shown in blue and red boxes, respectively. Control strains carrying the *ura4*$^{+}$ allele ('+') and *ura4-D18* ('Δ') are shown below. The arrow shape of the *ura4* sequence indicates direction of transcription of the wild-type.

B) The DNA used for RFLA corresponds to the template DNA of the PCR analysis in Figure 4.3B. The DNA was cut with *Ase*I, separated by agarose gel electrophoresis, transferred to a membrane and detected with radioactively labelled probes 'tel' and 'cen'. The green and orange boxes indicate detected fragments for rura(dir)R and rura(inv)R, respectively. The same membrane was used for detection by both probes, stripping off the probe after hybridisation.

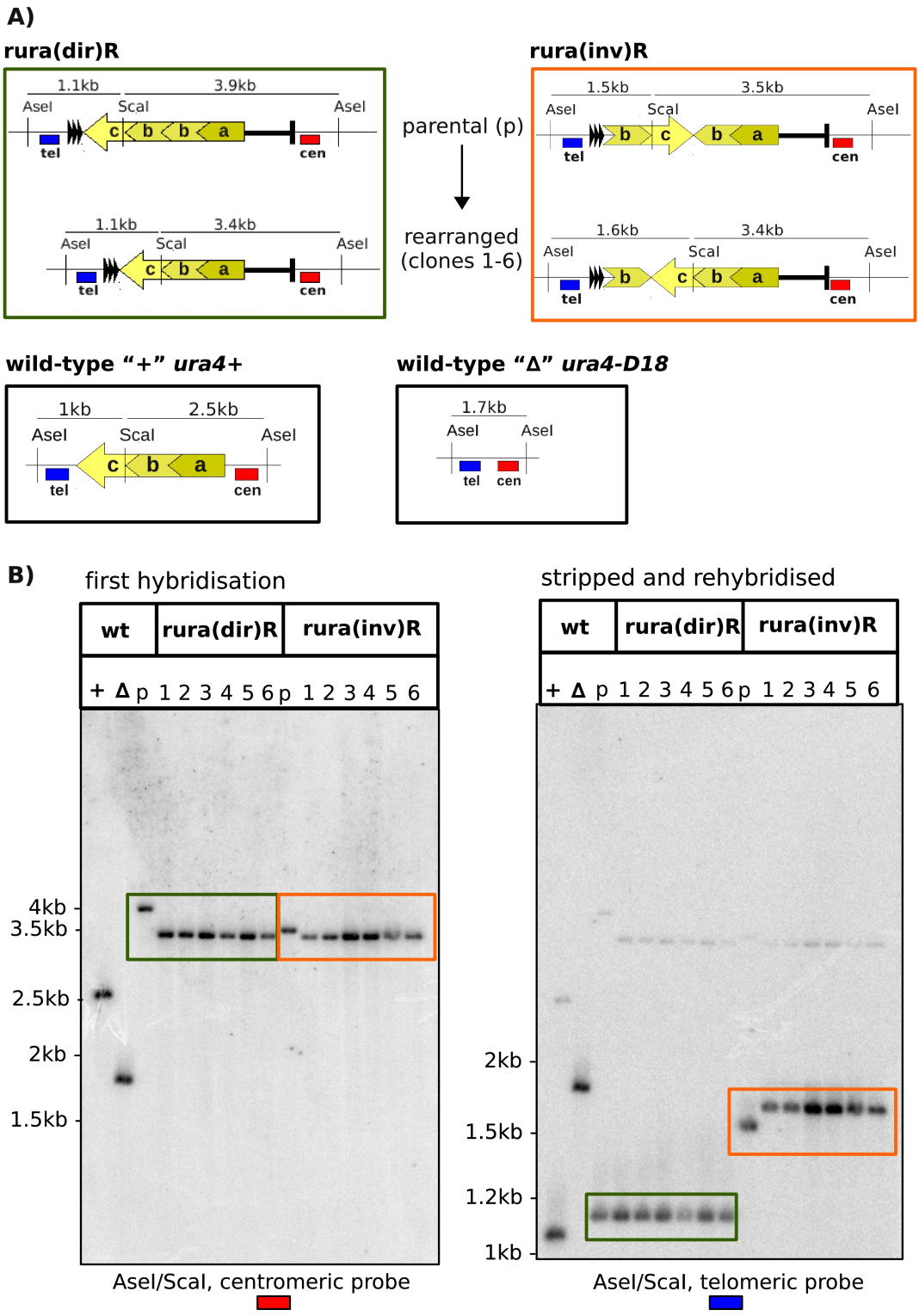

Figure 4.5: Confirmation of orientation switch in rura(inv)R by RFLA using *Ase*I and *Sca*I
A) as described in Figure 4.4A.
B) The experiment was carried out as described in Figure 4.4B, but in addition to *Ase*I, *Sca*I was used for the restriction digest. *Sca*I cuts in 'c' and facilitates the detection of an orientation switch. Probe 'cen' confirms the decrease in size resulting from the rearrangement in rura(dir)R, as seen in Figure 4.4B. Because the telomeric probe only detects DNA telomere-proximal of the *ura* 'b' fragments, there is no size change in this assay for rura(dir)R. Probes 'cen' and 'tel' confirm the expected decrease and increase in fragment size in rura(inv)R, respectively.

4.7 Detection of dicentric and acentric chromosomes after replication fork collapse in rura(inv)R by RFLA of bulk DNA

Induction of replication fork collapse at RTS1 can lead to the formation of palindromic chromosomes if an inverted repeat is nearby. This has been shown by Mizuno et al. (2009) using an inverted repeat of *ura4*$^+$ flanked by inverted RTS1 sequences (RuiuR, see Figure 4.1A) and also by Lambert et al. (2010) using *ura4*$^+$ flanked by inverted RTS1 sequences (RuraR, see Figure 4.1A). Both of these systems contain an inverted repeat of the site of fork collapse (RTS1). I used rura(dir)R and rura(inv)R to test the sequence (repeat) requirements for the formation of palindromic chromosomes in the context of fork collapse at RTS1.

Bulk DNA after induction of RTS1 activity was analysed to detect rearrangements irrespective of the functionality of *ura4*$^+$. Cells were grown in non-selective media (+uracil), inducing *Pnmt41-rtf1*$^+$ (-thiamine) for 24 hours. Under these conditions there is no selection for a specific rearrangement. The non-selective growth and direct analysis of an induced culture should give an insight of the proportion of rearrangements and the possible formation of palindromic chromosomes as seen before for RuiuR (Mizuno et al., 2009). The DNA was subjected to RFLA using *Ase*I and probes 'cen', 'tel' and 'c' for fragment detection (Figure 4.6). Probe 'c' detects five distinct bands in RuiuR which correspond to a parental fragment (p), dicentric (d) and acentric (a) chromosomes and two smaller fragments which are indicative of half sizes of these palindromic chromosomes (as detected previously by K. Mizuno, personal communication). Probes 'cen' and 'tel' specifically detect the dicentric and acentric fragments, respectively, in addition to the parental fragment.

Surprisingly, palindromic chromosomes could be detected in rura(inv)R, but at a lower intensity as compared to RuiuR. This shows that homology to the site of fork collapse (RTS1) is not required for the formation of palindromic chromosomes. The relative intensity of each band compared to the total, which is the sum of all quantified bands, is shown in Figure 4.6C. The quantification of the fragments representing the broken arms of the palindromic chromosomes (a/2 and d/2) showed a relatively high percentage compared to previous experiments done by K. Mizuno (personal communication). This could be due to the method used for DNA extraction. In rura(dir)R a faint band below the parental fragment of 5kb is detected by all three probes after replication fork collapse (+). The decrease by about 500bp is consistent with the deletion of 'b', which was previously shown by PCR (Figure 4.3B) and RFLA (Figure 4.4B and Figure 4.5B). However, this rearrangement was only detected in about 1% of the cells (Figure 4.6C). The quantification of the detected bands is depicted in Figure 4.6C. The intensity of palindromic chromosomes is significant in rura(inv)R compared to RuiuR and the acentric signal is slightly higher than the dicentric

signal. Taking into account that this is a single experiment, it would have to be repeated in order to compare these relative amounts.

Taken together these results suggest that homology to the site of fork collapse (RTS1) is dispensable for the formation of palindromic chromosomes. A template-exchange mechanism between repeats could account for the formation of palindromic chromosomes in rura(inv)R and the deletion of one repeat in rura(dir)R. Homology as small as 500bp is sufficient for induced rearrangements in proximity of RTS1 and these rearrangements are not fully dependent on possible secondary structures formed by inverted repeats.

For a more detailed analysis of the rearrangements the same samples were used for RFLA with *Ase*I and *Sca*I (Figure 4.7). Probing with 'c' revealed a distinct faint band indicating the orientation switch of 'c' in rura(inv)R ('s' in Figure 4.7B). However, the signal was quite faint and too close to the parental fragment, which made it difficult to quantify. In order to minimise possible artefacts due to the method of DNA preparation and to get a more clear result for quantification of the orientation switch, the genomic DNA was analysed in agarose plugs (as in previous experiments by K. Mizuno) and different restriction enzymes were used.

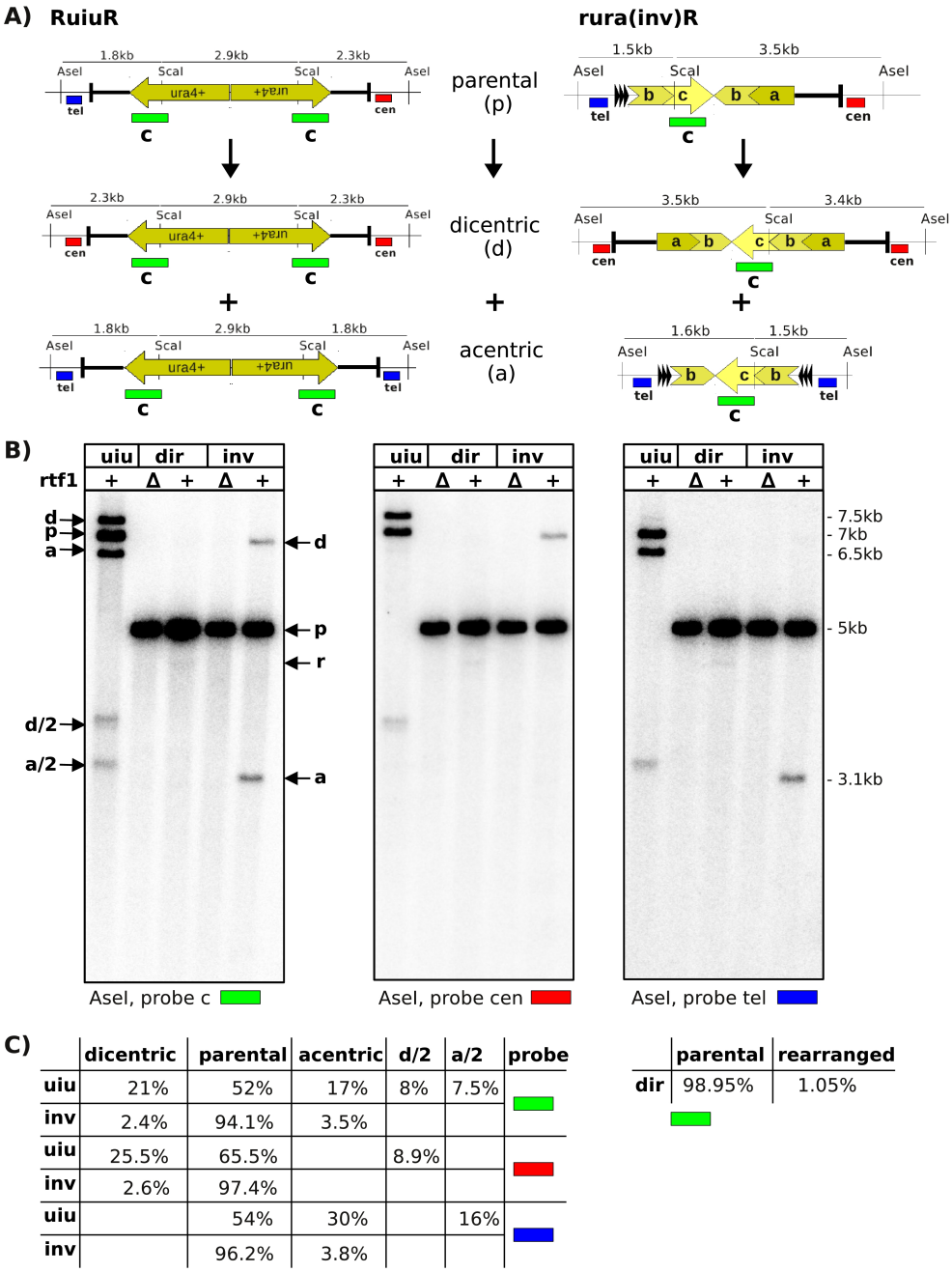

Figure 4.6: RFLA of bulk DNA reveals the formation of palindromic chromosomes in RuiuR and rura(inv)R

A) Map of restriction sites in the RuiuR and rura(inv)R loci showing the parental (p), dicentric (d) and acentric (a) fragments. Probes 'cen' (red), 'tel' (blue) and 'c' (green) are indicated in coloured boxes. The arrow shape of the *ura4* sequence indicates direction of transcription of the wild-type.

B) Cells containing *Pnmt-rtf1*$^{+}$ (+) or *rtf1*Δ (Δ) were grown in non-selective media (containing uracil), but lacking thiamine (RTS1 ON in *Pnmt-rtf1*$^{+}$) for 24 hours. DNA was extracted and analysed by RFLA using *Ase*I. 'uiu': RuiuR, 'dir': rura(dir)R and 'inv': rura(inv)R. Arrows indicate parental (p), dicentric (d), acentric (a) and half size fragments (d/2 and a/2) for RuiuR and rura(inv)R when carrying *Pnmt41-rtf1*$^{+}$. 'r' indicates the rearranged fragment resulting from a deletion of one 'b' in rura(dir)R *Pnmt41-rtf1*$^{+}$ (Figure 4.5A). Sizes of fragments are indicated on the right. The same membrane was used for all three probes, stripping off the probes after each hybridisation. The formation of palindromic chromosomes can be detected in RuiuR and rura(inv)R.

C) Quantification of the relative amounts of parental, dicentric and acentric signals. The sum of all indicated fragments is considered as the total signal. The number of hybridisation sites per fragment of each probe was taken into consideration.

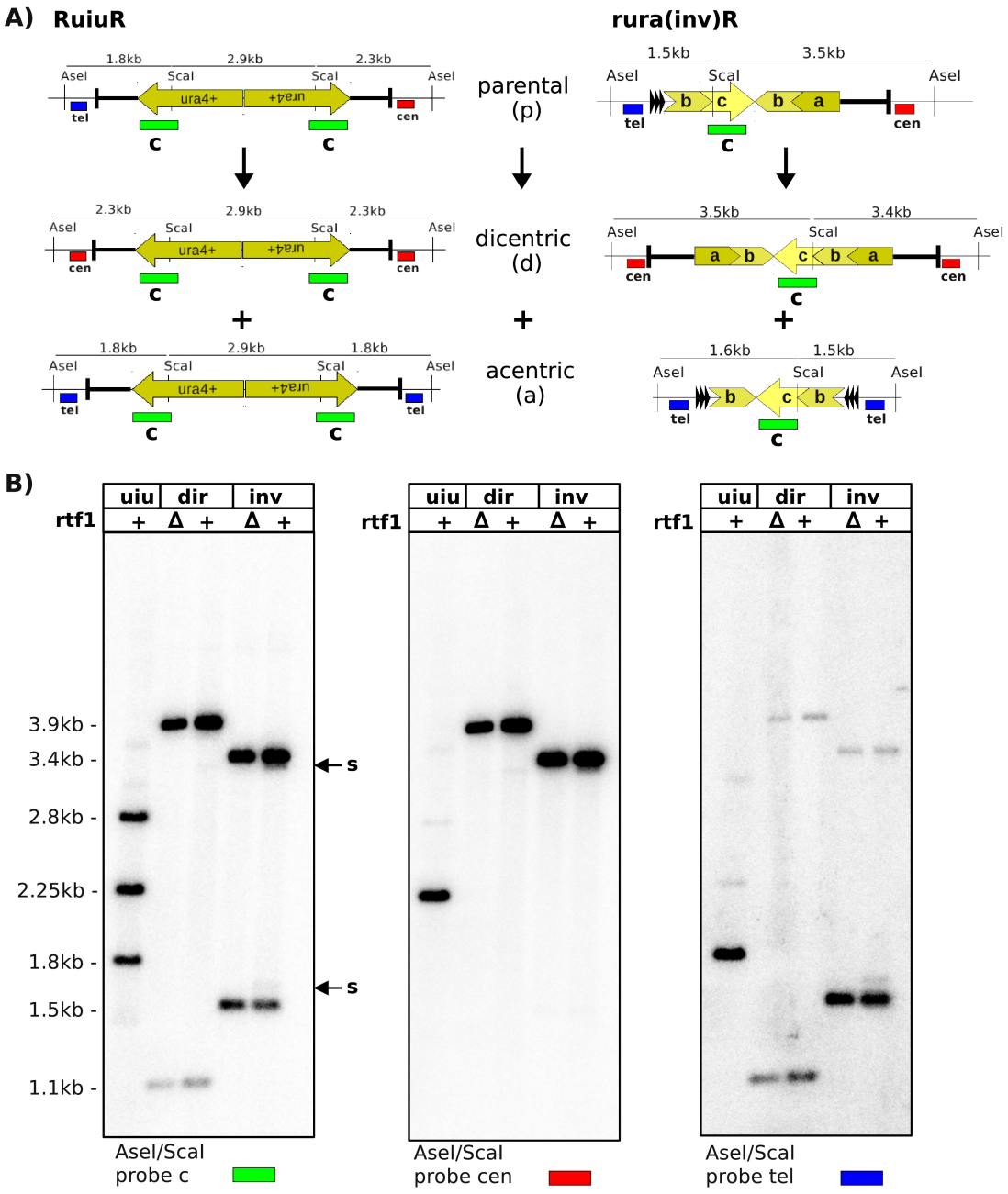

Figure 4.7: RFLA of bulk DNA detects an orientation switch rura(inv)R
A) As described in Figure 4.6A.
B) DNA was extracted from cells grown in non-selective media with RTS1 ON (+, *Pnmt41-rtf1*$^{+}$) or OFF (Δ, *rtf1*Δ). The experiment was carried out as described in Figure 4.6 using *Ase*I and *Sca*I for RFLA. 's' indicates the orientation switch in 'c'. The same membrane was used for all three probes, stripping off the probes after each hybridisation. On the membrane on the right (probe tel) some residual signal from the previous probe (cen) is visible due to incomplete stripping of the membrane.

4.8 Analysis of bulk DNA after replication fork collapse by a different method of DNA preparation

In this analysis, the cells were embedded in agarose gel plugs. Restriction digest was carried out in the plugs and they were subsequently inserted in an agarose gel. RFLA using *Ase*I (Figure 4.8A and B; the lanes marked with X are irrelevant for this experiment) showed that the palindromic chromosomes still represent about 50% of the fragments in RuiuR, with a relatively higher percentage of dicentric compared to acentric as seen before (Figure 4.6C). The intensities of the fragments 'd/2' and 'a/2' were substantially decreased, which suggests that the method of DNA preparation does play a role in the generation of these fragments. The percentage of dicentric chromosomes in rura(inv)R increased from 2.4% (Figure 4.6C) to 6% when using probe 'a'. However, probe 'a' only detects dicentric and parental fragments, whereas probe 'c', used in Figure 4.6C, detects also acentric fragments. Therefore the relative amounts detected by the two different probes can not be compared directly. Comparing the relative amounts of dicentric and acentric chromosomes with probes 'cen' and 'tel', respectively, shows a higher percentage of the dicentric fragment. This contrasts the previous analysis in Figure 4.6C, but correlates with the relative amounts detected for RuiuR (K. Mizuno, personal communication).

In order to analyse the orientation change in rura(inv)R in more detail, *Hind*III was used in RFLA (Figure 4.9A) which results in a clear band indicating the orientation switch ('s') of 'c'. Quantification of 's', using probe 'a' yielded a relative amount of 8.5%. The percentage of dicentric chromosomes of this sample was 6% using the same probe ('a') (Figure 4.8C). Whether the orientation switch of 'c' is coupled to the formation of palindromic chromosomes or the percentage of palindromic chromosomes containing a switched 'c' cannot be analysed using this assay.

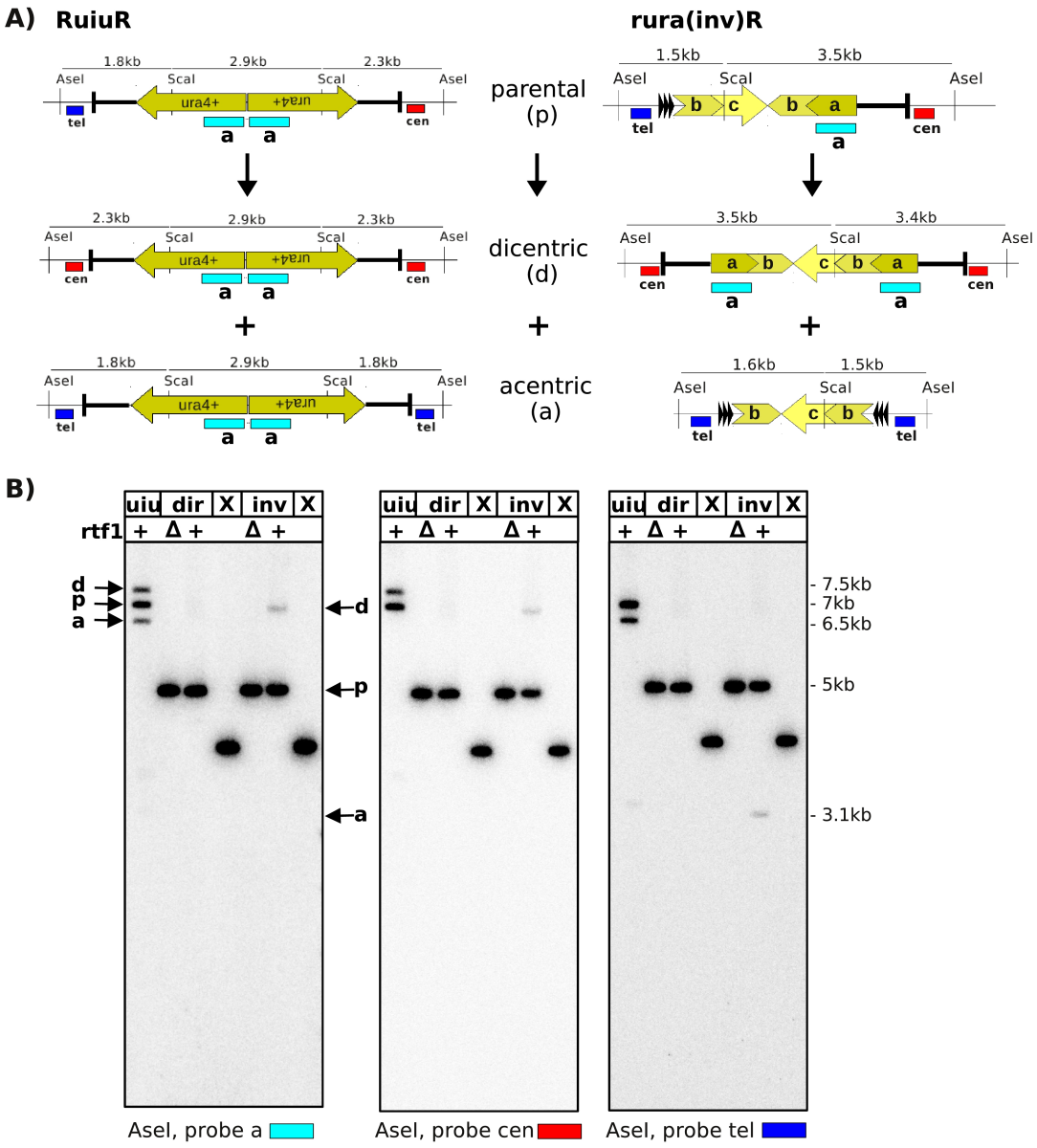

C)

	dicentric	parental	acentric	d/2	a/2	probe
uiu	25.1%	52.1%	18.8%	2.7%	1.4%	
inv	6%	94%				
uiu	31.4%	66.3%		2.3%		
inv	3.4%	96.6%				
uiu		70.2%	27.9%		1.9%	
inv		97.8%	2.2%			

Figure 4.8: RFLA of bulk DNA using DNA plugs instead of phenol extracted genomic DNA reduced the amounts of half fragments 'a/2' and 'd/2' in RuiuR

A) As described in Figure 4.6A. Probe 'a' (cyan box) was used instead of 'c'.

B) Cells were grown as described in Figure 4.6B, collected and embedded in agarose plugs. Cell lysis and restriction digests were performed in the plugs, which were subsequently integrated into an agarose gel. The DNA was separated by gel electrophoresis, transferred onto a membrane and fragments were detected using radioactively labelled probes. Lanes marked with X are samples of no relevance for this experiment. Labelling of fragments and samples are as described in Figure 4.6B. The signal for the rearrangement in rura(dir)R was too low for detection under these conditions.

C) Quantification of detected fragments as described in Figure 4.6C.

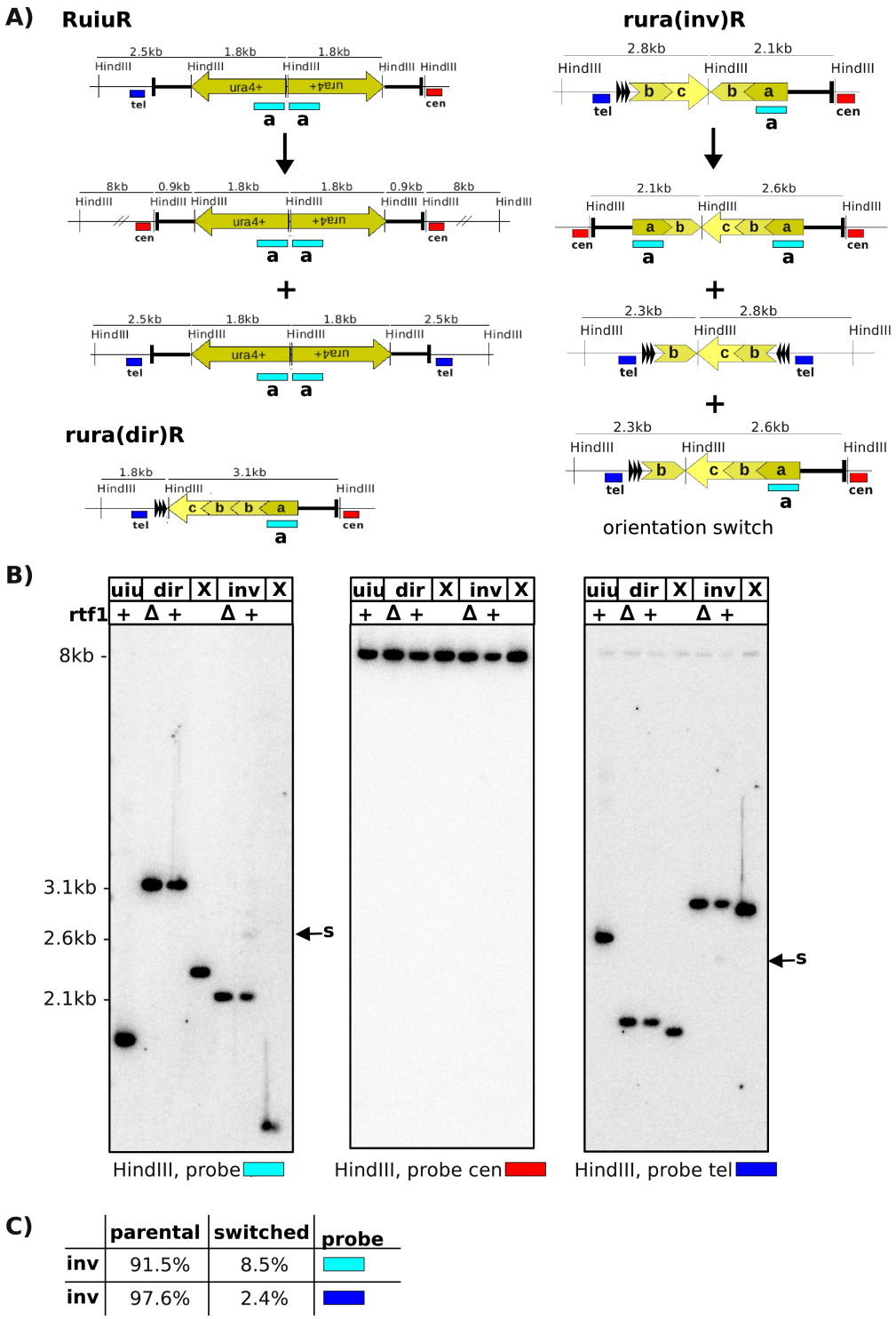

Figure 4.9: RFLA of bulk DNA using DNA plugs and *Hind*III to visualise the orientation switch in 'c'
A) Map of restriction sites of parental and rearranged sequences as described in Figure 4.8A. In addition a restriction map of rura(dir)R is shown. The orientation switch of 'c' in rura(inv)R is indicated on the right. The orientation of 'c' specifically in the dicentric and acentric chromosomes is not known.
B) As described in Figure 4.8A, *Hind*III was used for RFLA. Probes 'a' and 'tel' visualise the orientation switch of 'c' (s: switched). Probe 'cen' hybridises upstream of *Hind*III and shows an 8kb fragment which can be used as a loading control.
C) Quantification of the relative amounts of fragments 'p' and 's' detected in rura(inv)R. As described in Figure 4.6C.

4.9 Microscopy of rura(dir)R and rura(inv)R cells before and after replication fork collapse

Replication fork collapse at RTS1 in RuiuR results in the formation of palindromic chromosomes, which can lead to catastrophic mitosis (Mizuno et al., 2009). The results described in this chapter so far show that RTS1 activity in rura(inv)R produces palindromic chromosomes as in RuiuR, if to a lower extent. Microscopy was used in order to test if cells undergo catastrophic mitosis in this background. Figure 4.10A shows representative pictures of cells from the previously described experiments, after induction of replication fork collapse at RTS1 (*Pnmt41-rtf1*$^{+}$), as well as of cells where RTS1 is not active (*rtf1*Δ). Cell elongation (15-20% in RuiuR cultures and 3-5% in rura(inv)R cultures) and catastrophic mitosis were detected in RuiuR and rura(inv)R after replication fork collapse at RTS1. Neither rura(inv)R cells in the absence of replication fork collapse (*rtf1*Δ), nor rura(dir)R cells after activation of RTS1 show cell elongation or catastrophic mitosis (Figure 4.10A and B).

4.10 Conclusion and discussion

Previously published work has shown that replication fork collapse and HR-dependent restart at RTS1 in RuraR and RuiuR results in GCRs, including orientation switch (RuraR) and the formation of palindromic chromosomes (Lambert et al., 2005; Mizuno et al., 2009). RuraR and RuiuR contain inverted RTS1 sequences. Therefore, a possible explanation for the observed rearrangements is template switching between the two RTS1 sequences during the restart process. Comparing the relative amounts of dicentric and acentric chromosomes produced in RuraR (similar) and RuiuR (more dicentric than acentric), indicates different or additional mechanisms of rearrangements in RuiuR (K. Mizuno, personal communication). Furthermore, a construct in which part of the *ura4*$^{+}$ sequence in RuiuR was replaced by *his3*$^{+}$, also generated palindromic chromosomes upon replication fork collapse. However, the distribution of the *his3*$^{+}$ and *ura4*$^{+}$ in the dicentric and acentric chromosomes suggests that there are multiple mechanisms resulting in rearrangements (K. Mizuno, personal communication and see Figure 4.1A).

The two constructs I analysed in this chapter, rura(dir)R and rura(inv)R, contain only one RTS1 sequence. RTS1 is located centromere-proximal of *ura4*$^{+}$ and blocks the replication forks approaching from the main replication direction, which is from the centromere. In order to avoid replication of *ura4*$^{+}$ from the telomere, three rDNA RFBs were integrated telomere-proximal of *ura4*$^{+}$. Therefore, by activating RTS1 the majority of forks will collapse at RTS1 and restart for completion of replication. Using an equivalent ruraR setup, I. Miyabe in the lab has estimated by

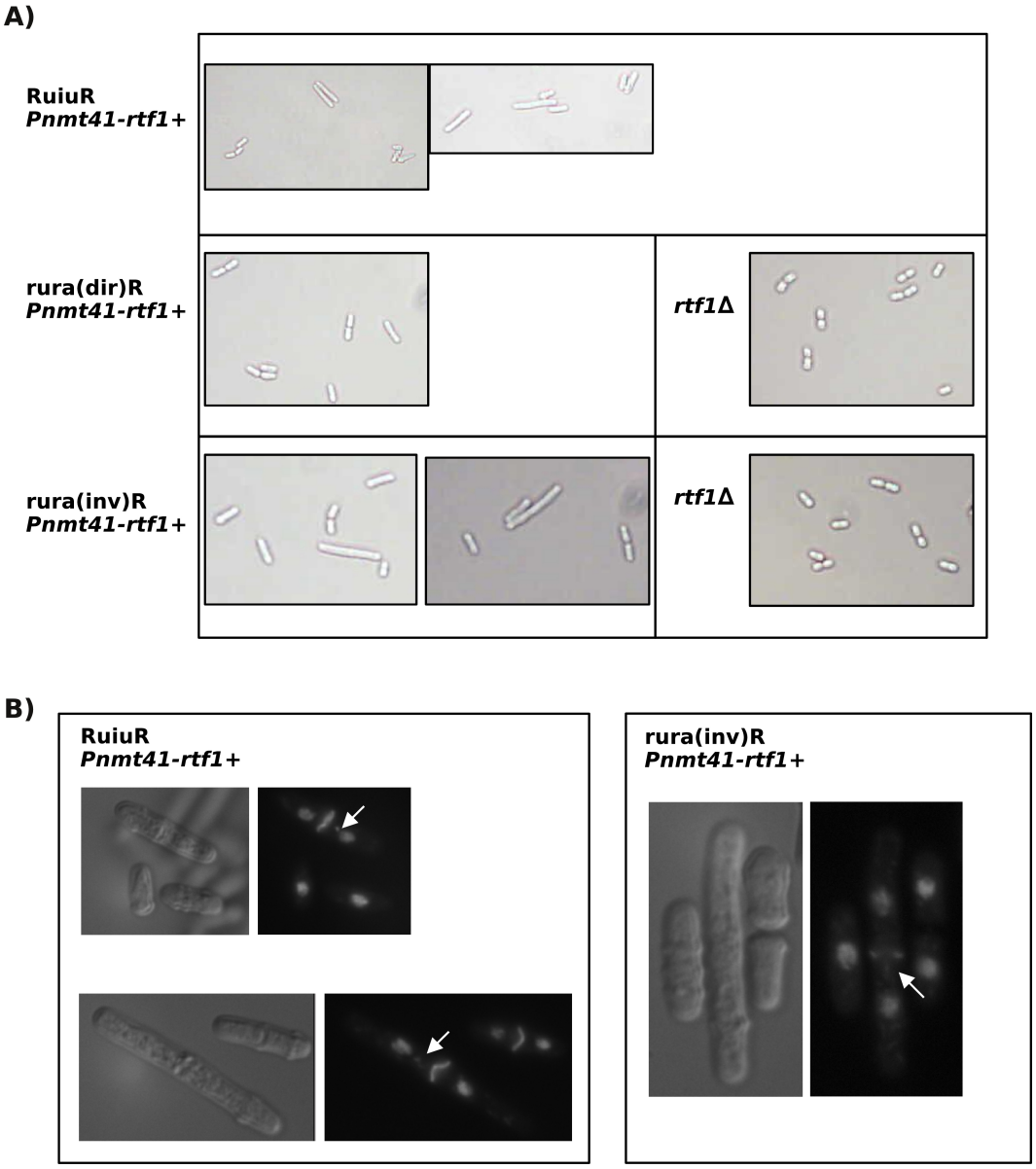

Figure 4.10: Aberrant mitosis in cells containing an inverted repeat nearby an active RTS1
A) Representative images taken on the light microscope of cells after induction of replication fork collapse at RTS1.
B) DNA and septum were visualised with DAPI and calcufluor, respectively. RuiuR was shown previously to undergo aberrant mitosis (white arrows) after replication fork collapse at RTS1 (Mizuno et al., 2009). Also elongated cells of rura(inv)R showed aberrant mitosis at a low frequency. Pictures were taken with a DeltaVision microscope.

2D-gel analysis that about 50% of replication through this locus is a result of a restarted fork (personal communication). The template switch between inverted RTS1 sequences is not possible in this system and any repeat recombination event is not due to homology to the actual site of fork collapse. This creates a system to specifically study genomic instability after replication fork collapse and restart at RTS1 uncoupled from recombination events between homologous RTS1 sequences at this locus. Analysis of rura(dir)R and rura(inv)R by spot tests, PCR and RFLA showed that rearrangements in both constructs were induced by replication fork collapse and restart at RTS1 (see Figure 4.2, Figure 4.3, Figure 4.4 and Figure 4.5). Direct repeat recombination (rura(dir)R) occurred at a lower frequency compared to inverted repeat recombination (rura(inv)R). In contrast to RuiuR, a loss of viability could not be detected by spot test in rura(inv)R after replication fork collapse at RTS1 (Figure 4.2A). However, analysis of bulk DNA after replication fork collapse showed that rura(inv)R but not rura(dir)R has the potential to form palindromic chromosomes (Figure 4.6B). When using the same method for DNA preparation as K. Mizuno, preliminary results indicate that slightly more dicentric chromosomes are present compared to acentric. However, the total amount of palindromic chromosomes is greatly reduced in rura(inv)R compared to RuiuR. This could explain why there is no detectable loss of viability in rura(inv)R after replication fork collapse, although cell elongation and aberrant mitosis can be detected in a subset of rura(inv)R cells (Figure 4.10), which is consistent with the formation of palindromic chromosomes at a low frequency.

These results show that the formation of palindromic chromosomes could result from a template switch between inverted repeats, but not between direct repeats. Furthermore, the homology to the site of fork collapse (RTS1) is not necessary to induce genome instability by HR-dependent restart. This suggests that a template switch mechanism might not only occur at RTS1 as a consequence of the replication fork restart process, but possibly as a consequence of the restarted fork. Erroneous replication after replication fork restart by BIR has been suggested in *S. cerevisiae* (Deem et al., 2011). Importantly, replication fork collapse and restart at RTS1 does not involve a DSB, suggesting strand invasion of the nascent 3'-end exposed by disassembly of the replisome (Lambert et al., 2005; Mizuno et al., 2009).

Mutations affecting the fidelity of polymerases result in mutator phenotypes (Arana and Kunkel, 2010). This could also be a consequence if the stability of the replisome is affected (see Chapter 3). Therefore, one explanation of the restart-induced mutagenesis could be the nature of the restarted replication fork. If either the replication process itself or replisome components are altered as compared to a 'normal' fork, this could lead to instability and erroneous replication.

The restart process at RTS1 was shown to be dependent on HR (Lambert et al., 2005) and

homology-directed repeat rearrangements are likely to require HR. In the present system, it is impossible to distinguish the requirement of HR for the restart and the recombination event between the repeated sequences. The repeat sizes analysed here are around 500bp. It would be interesting to know whether deletions of shorter repeats, more likely to form in a HR-independent manner (see Chapter 3) are elevated when replicated by an error-prone restarted fork. Furthermore, sequences intrinsically difficult to replicate might elevate such defects. I have therefore decided to combine TR assays containing short TRs and G4-DNA with the RTS1-rDNA RFB system. Positioning the G4-DNA on either the leading or the lagging strand allows for the analysis of strand-specific mutagenesis induced by G4-DNA and furthermore how this is affected when the sequence is replicated by a restarted replication fork. This work is described in Chapter 5.

Chapter 5

TR instability induced by G4-DNA and erroneous replication after fork restart

5.1 Introduction

The experiments in Chapter 3 show that TR sequences (*nat1 101TR*) are unstable and rearrange at a rate of 3.3 x 10^{-5} deletions per cell per generation. This spontaneous instability is independent of PRR, MMR and HR. Treatment with genotoxic agents (MMS and UV) as well as depletion of dNTPs by HU did not significantly increase the TR deletion rate. However, mutant backgrounds affecting replication and checkpoint activation, such as *cdc6-L591M*, *swi1*Δ and *mrc1*Δ resulted in an increase in TR deletions. *nat1*$^{+}$ is very G-rich and contains a putative G4-motif. It has been previously shown that G4-DNA can induce genomic instability if they are stabilised (Piazza et al., 2010) or in cells that are deficient in factors implicated in G4-DNA processing during replication (Johnson et al., 2008; Ribeyre et al., 2009; Sarkies et al., 2010). It has been demonstrated that telomeric G4-DNA can introduce mutagenicity in human cells (Damerla et al., 2010) and G-rich sequences and G4-DNA interfere with DNA synthesis (d'Ambrosio and Furano, 1987; Kamath-Loeb et al., 2001). Analysis of G4-DNA in leading and lagging strand replication has suggested that these structures might interfere to a greater extent with leading strand DNA synthesis as compared to lagging strand DNA synthesis (Damerla et al., 2010; Sarkies et al., 2010). This raises the question if the presence of G4-DNA increases TR instability and if the *nat1 101TR* characteristics are specific for G-rich sequences.

In Chapter 4, I characterised a system, which suggests error-prone replication after HR-dependent replication fork restart at RTS1 in agreement with previous work from our lab (Lambert et al., 2005; Mizuno et al., 2009), K. Mizuno, personal communication). Rearrangements of repeated sequences downstream of RTS1 are increased when RTS1 is active. This suggests that,

the replication of these sequences is error-prone and that mutagenesis induced by replication fork collapse and restart can be due to the fidelity of the restarted fork as well as the restart process.

5.2 Aim of the project and summary

In this chapter, I describe the development and analysis of a system to address the strand-specific mutagenicity of G4-DNA on TRs. I am using this system to measure the effect of G4-DNA on mutagenic replication after replication fork collapse and restart at RTS1. Surprisingly, although deletions of short TRs are increased when replicated by a restarted fork, the presence of G4-DNA does not enhance this mutagenicity. Furthermore, the results suggest that G4-DNA does not show a strand-specific mutagenic effect on TRs, in the strain backgrounds tested and can therefore not be used to address questions about leading and lagging strand synthesis in the context of HR-dependent restart at RTS1. However, I am suggesting a genetic analysis of a restarted replication fork using the developed TR assay and show some preliminary results.

5.3 Overview of *arg3 82TR* constructs

In order to compare TR deletion rates in the presence and absence of G4-DNA, *arg3*$^+$ was used as a marker gene in this assay. *arg3*$^+$ is not as G-rich as *nat1*$^+$ and does not contain any putative G4-DNA motifs. The 82bp upstream of the *Nru*I restriction site in *arg3*$^+$ were duplicated, including the first three nucleotides of the *Nru*I site. Oligonucleotides containing these sequences were designed for both strands, annealed and ligated into *Nru*I-cut *arg3*$^+$ on the plasmid paR3 (Waddell and Jenkins, 1995). The oligonucleotides contained either only the 82bp repeat sequence or additional G4-DNA Figure 5.1A. The G4-DNA, as well as the mutated G4-DNA sequence was described previously by Cahoon and Seifert (2009) and has also been analysed by CD in Chapter 3 (Figure 3.7). The point mutation in the mutated G4-DNA (see Figure 5.1A in grey) significantly compromises the capacity of G4-structure formation (Figure 3.7). The oligonucleotides were designed, such that the G4-DNA sequence was contained on either the leading or the lagging strand (Figure 5.1A). These *arg3 82TR* constructs were introduced into the *ura4* locus on chromosome 3 in *S. pombe* as described below and in Materials and Methods.

Replication of the *ura4*$^+$ locus on chromosome 3 has been well characterised in our lab and it was established that the main direction of replication is from the centromere to the telomere (Lambert et al., 2005; Miyabe et al., 2011). As described in Chapter 4, the rDNA-*ura4*$^+$-RTS1 system is designed such that RTS1, if activated, arrests the replication forks centromere-proximal to *ura4*$^+$ and the rDNA RFB arrests replication forks telomere-proximal to *ura4*$^+$. In order to integrate the *arg3 82TR* constructs, I deleted the *ura4*$^+$ locus in a wild-type strain by inserting a kanMX6 marker cassette flanked by loxP and loxM3 sites (*ura4* base strain, see Materials and Methods). The deleted sequence was cloned into the pAW8 plasmid that contains loxP and loxM3 sites (Watson et al., 2008). The RTS1 and rDNA RFB elements were then introduced such that they had the same orientations as in the previously described rDNA-*ura4*$^+$-RTS1 system (Chapter 4). I inserted the different *arg3 82TR* constructs into a *Not*I site which is located in between *ura4*$^+$ and RTS1 on the plasmid and used the resulting plasmids for integration by RMCE (Figure 5.1B). Before integration, the *arg3-D4* allele was crossed into the background of the *ura4* base strain to generate arg- cells and to avoid any homology to the *arg3-TR* constructs (Waddell and Jenkins, 1995). Furthermore, in the *ura4* base strain, the endogenous copy of *rtf1*$^+$, which regulates the activity of the RTS1 barrier, is deleted (*rtf1*Δ). Therefore, RTS1 is always OFF and the rDNA RFB is constitutively active, which results in $>$95% of replication forks approaching from the centromere as measured by 2-D gel electrophoresis (I. Miyabe, personal communication).

In the following paragraphs I will use the following abbreviations for the different *arg3 82TR* constructs: the 82bp TR (*arg3 82TR*), the G4-DNA sequence flanked by the 82bp repeat (*G4 TR*)

and the mutated G4-DNA sequence flanked by the 82bp repeat (*G4m TR*). Figure 5.1 shows an overview of these constructs and their orientation in the genome in the context of replication.

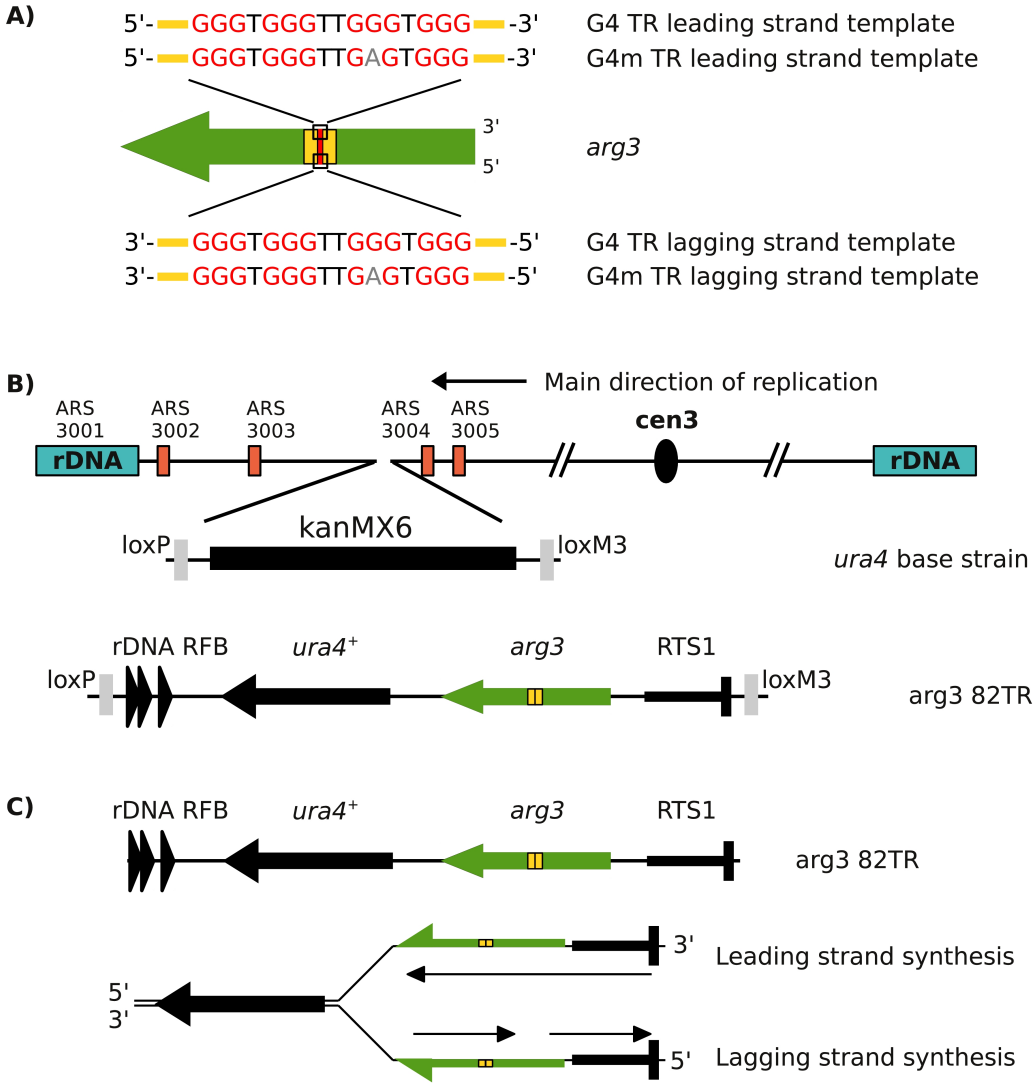

Figure 5.1: Overview of the *arg 82TR* constructs in the rDNA RFB-*ura4*$^+$-RTS1 locus
A) The G4-DNA (*G4 TR*) was introduced into *arg3 82TR* (*arg3*: green arrow, 82TR: yellow boxes). In addition a point mutation in the G4 sequence (*G4m TR*, grey), destabilising the G4-structure was used as a control (Cahoon and Seifert, 2009). Integration of these sequences on either strand, resulted in the G4 constructs being contained on the leading or the lagging strand template (see **C**).
B) Overview of the *ura4* locus on chromosome 3. *arg3*$^+$ containing a tandem repeat (TR) of 82bp (*arg3 82TR*) was introduced upstream of *ura4*$^+$ and downstream of the polar RFB RTS1 by RMCE. For this integration a *ura4* base strain was constructed in which *ura4*$^+$ was replaced by kanMX6 flanked by loxP and loxM3 sites, as shown (SAS732). The *arg3 82TR* constructs together with the rDNA barrier, RTS1 and *ura4*$^+$ were cloned into pAW8, which was used for cassette exchange (RMCE) to replace kanMX6, as explained in Materials and Methods. RTS1 is oriented in such a way, that activation of RTS1 results in arrest of replication forks approaching from the centromere. Three copies of the rDNA RFB downstream of *ura4*$^+$ arrests replication from the telomere. The arrow shape of *ura4*$^+$ and *arg3* indicates the direction of transcription. Red boxes represent ARS sequences as in Segurado et al. (2003).
C) The main direction of replication is from the centromere to the telomere. The direction of replication defines leading and lagging strand.

5.4 Effect of HR, MMR, PRR and *mrc1*$^+$ on TR deletions in the absence of G4-DNA

The analysis of *nat1 101TR* in Chapter 3 showed that the deletion of this 101bp TR is not dependent on either HR, MMR or PRR. In order to examine whether this was due to the G-rich nature of this TR or if it is a common feature of repeats of that size, I analysed the TR deletion rate of *arg3 82TR* in different mutant backgrounds. *arg3*$^+$ lacks any putative G4-motifs and is more AT-rich compared to *nat1*$^+$. The results of the fluctuation analysis are shown in Figure 5.2A. Dependencies on HR were examined by using *rad22*Δ and *rad22*Δ *rhp51*Δ mutant strains and the effect of MMR and PRR was measured using *msh2*Δ and *pcn1-K164R* cells, respectively. While the deletion rate in *arg3 82TR* is slightly increased in the *pcn1-K164R* background and is similar to wild-type in *msh2*Δ cells, HR defective strains show an increase in TR deletion rates. These effects are similar as to what was observed for the *nat1 101TR* assay (Figure 3.4). However, the rate of spontaneous TR deletions in *arg3 82TR* is significantly lower as compared to *nat1 101TR*, 0.68 x 10^{-5} and 3.3 x 10^{-5}, respectively. This is a 5-fold difference between the two assays, which mainly differ in the G-content of the sequence. Deletion rates in *arg3 82TR* were elevated about 3-fold in the absence of *mrc1*$^+$. This 3-fold increase is less than the 8-fold increase previously observed in the *nat1 101TR* assay (Figure 3.6B). It is interesting to note that Mrc1 is important for replication fork progression through G-rich sequences (CGG repeats) (Voineagu et al., 2009b) and also for replication progression and replication fork stability in perturbed and unperturbed replication (Tanaka, 2010).

That the deletion of one repeat results in the restoration of the *arg3*$^+$ ORF, was confirmed by PCR analysis (Figure 5.2B). Colonies isolated from arg- plates (arg+ cells) showed a band corresponding in size to the PCR fragment expected from the wild-type allele (*arg3*$^+$), whereas colonies isolated from arg+ plates (arg- cells) showed a larger fragment corresponding to the additional repeat sequence.

A)

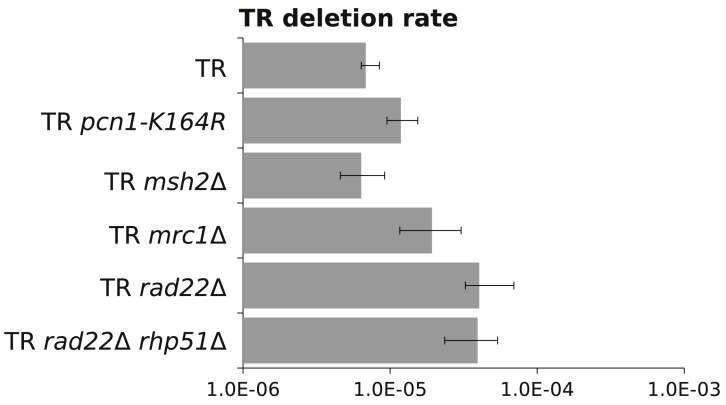

genotype	n	deletion rate x 10^{-5} (95% ci)	p
TR	33	0.68 (0.64-0.85)	
TR pcn1-K164R	33	1.2 (0.95-1.5)	0.0002
TR *msh2*Δ	21	0.64 (0.46-0.92)	0.1835
TR *mrc1*Δ	21	1.9 (1.2-3.0)	<0.0001
TR *rad22*Δ	17	4.0 (3.3-6.9)	<0.0001
TR *rad22*Δ *rhp51*Δ	15	3.9 (2.4-5.4)	<0.0001

B)

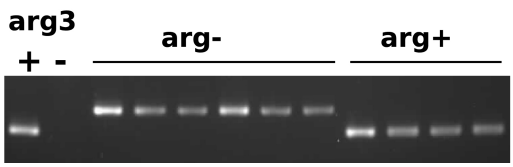

Figure 5.2: Genetic dependency of TR deletions in the *arg3 TR* assay
A) Cells containing the *arg3 82TR* construct and *rtf1*Δ (RTS1 OFF) were streaked to single colonies on non-selective media. Colonies were excised, resuspended in 200μl of water, serially diluted and plated onto non-selective (EMM2 +arg) and selective (EMM2 -arg) plates. Deletion rates were calculated by the Method of the Median (Lea and Coulson, 1949). The graph on the left shows the median deletion rates on a logarithmic scale. Error bars represent 95% confidence intervals (ci). The table below lists the genotypes, number of colonies analysed (n), deletion rates with 95% ci and the p-value for statistic significance (p). Two-tailed p-values were calculated using the Mann-Whitney Test as described in Materials and Methods. The p-value on the right is always determined for the respective mutant strain in comparison to the wild-type (*TR*). TR; arg3 82TR, G4; G4 sequence, G4m; mutated G4 sequence. Strain genotypes are listed in Materials and Methods. Strains used: TR; SAS756, TR *pcn1-K164R*; SAS873, TR *msh2*Δ; SAS1030, TR *mrc1*Δ; SAS911, TR *rad22*Δ; SAS1141, TR *rad22*Δ *rhp51*Δ; SAS1144.
B) *arg3 82TR* cells were spread on minus and plus arginine plates. Single colonies were used for colony PCR with primers flanking the 82bp TR in *arg3 82TR*. PCR products were analysed by agarose gel electrophoresis. Cells isolated from -arg plates (arg+ cells) show a band corresponding to the wild-type *arg3*$^+$ control fragment (+), which corresponds to a deletion of one repeat. Cells isolated from +arg plates (arg- cells) show a fragment of bigger size, corresponding to the presence of the TR. As a positive control an *arg3*$^+$ wild-type strain (+), and as negative control strain AMC358 containing the *arg3-D4* allele (-) were used.

5.5 The effect of G4-DNA on TR deletions

Next, I examined the effect of G4-DNA on TR deletions. Cells carrying the *G4 TR* or *G4m TR* constructs on either the leading or the lagging strand template (as illustrated in Figure 5.1A and C) were streaked to single colonies on non-selective media (containing arginine, +arg). Three colonies were used to inoculate individual cultures, which were grown to saturation without selection and serial dilutions were plated onto +arg and -arg plates (Figure 5.3A). The difference in the amount of arg+ colonies growing for *G4 TR* or *G4m TR* strains showed clearly that more arg+ colonies were formed in the presence of G4-DNA (*G4 TR*), and so TR deletion occurred more frequently in the strains containing the *G4 TR* allele as compared to the *G4m TR* allele. It was less clear whether the position of the G4-DNA on the leading or lagging strand affected the amount of deletion events differently. To analyse the deletion rates in these constructs in more detail and to quantitatively compare the effect of G4-DNA on either DNA strand, fluctuation analysis was carried out for the *arg3 82TR*, *G4 TR* and *G4m TR* constructs. The results of this analysis are depicted in Figure 5.3B. As already observed in the spot test analysis in Figure 5.3A, the presence of G4-DNA results in an increase of the TR deletion rate (about 10-fold). The spontaneous deletion rate in *arg3 82TR* cells was similar to *G4m TR*, confirming that the increased deletion rate in *G4 TR* is dependent on the capacity for secondary structure formation. Whether the G4-DNA was present on the leading or the lagging strand template did not affect the deletion rate.

The *arg3*$^{+}$ ORF is oriented such that transcription has the same direction as replication. In order to examine if the direction of transcription had an effect on the TR deletion rate, the *arg3 82TR* and *G4 TR* constructs were analysed in strains, in which the direction of the ORF was inverted (Figure 5.4A). The deletion rates were determined by fluctuation analysis and the results are shown in Figure 5.4B. The dark grey bars represent the constructs with the initial orientation of *arg3*, in which transcription and replication proceed in the same direction. The light grey bars represent the inverted orientation of *arg3*, resulting in transcription and replication proceeding in opposite directions. The *arg3 82TR* constructs placed in either orientation show similar deletion rates. Analysis of the *G4 TR* strains suggests that, if transcription does not occur in the same direction as replication, TR deletion rates are decreased. Although this decrease is statistically significant, TR deletion rates were still increased in the presence of G4-DNA, independently of the direction of transcription.

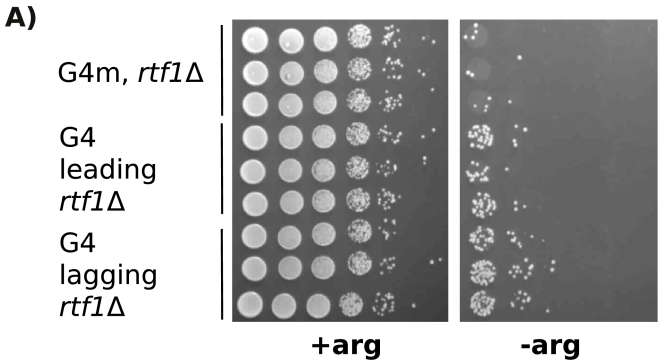

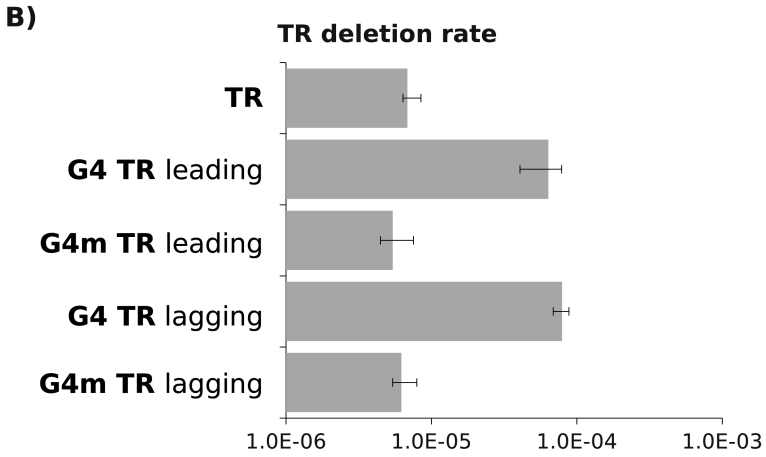

genotype	n	deletion rate x 10^{-5} (95% ci)	p
TR	33	0.68 (0.64-0.85)	
G4 TR leading	33	6.4 (4.1-7.9)	<0.0001
G4m TR leading	32	0.54 (0.45-0.75)	
G4 TR lagging	33	7.9 (6.8-8.8)	<0.0001
G4m TR lagging	33	0.62 (0.54-0.79)	

Figure 5.3: The intrinsic instability of TRs is higher in the presence of a G4 motif
A) Single colonies of *arg3 82TR*, *G4 TR* or *G4m TR* were grown to saturation in non-selective media, serially diluted and spotted onto plates plus (+arg) or minus (-arg) arginine. RTS1 is OFF (*rtf1*Δ). Constructs and their position on leading or lagging strands are indicated on the left.
B) Fluctuation analysis was carried out as described in Figure 5.2A. The position of the G4-DNA on the leading or the lagging strand template is indicated. Two-tailed p-values are comparisons between the indicated *G4 TR* strain and *TR*. Strain genotypes are listed in Materials and Methods. Strains used: *TR*; SAS756, *G4 TR* leading; SAS762, *G4m TR* leading; SAS753, *G4 TR* lagging; SAS749, *G4m TR* lagging; SAS910.

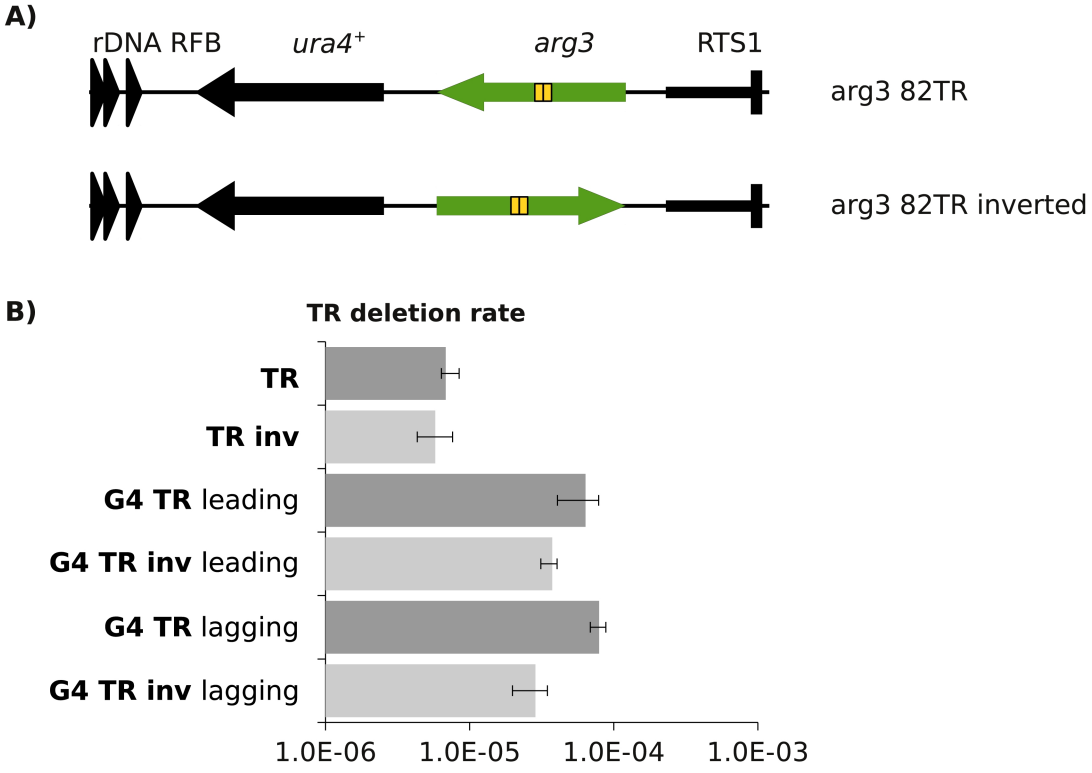

genotype	n	deletion rate x 10^{-5} (95% ci)	p
TR	33	0.68 (0.64-0.85)	
TR inv	18	0.58 (0.43-0.76)	
G4 TR leading	33	6.37 (4.06-7.85)	
G4 TR inv leading	25	3.74 (3.12-4.04)	0.0001
G4 TR lagging	33	7.90 (6.87-8.82)	
G4 TR inv lagging	25	2.86 (1.98-3.46)	<0.0001

Figure 5.4: Effect of transcription direction on TR deletions
A) Overview of the rDNA-*ura4*$^{+}$-RTS1 locus including the *arg3 82TR* construct (as described in Figure 5.1A). The arrow of the genes indicates the direction of transcription.
B) Fluctuation analysis was carried out as described in Figure 5.2A. Bars in dark grey represent constructs with the original direction of transcription (as described in Figure 5.1A). Bars in light grey indicate constructs with inverted direction of transcription as indicated in **A**. Two-tailed p-values are comparisons between the direction of transcription of *arg3* in strains containing *G4 TR* on the same strand (either leading or lagging). Strain genotypes are listed in Materials and Methods. Strains used: *TR*; SAS756, *TR inv*; SAS758, *G4 TR* leading; SAS762, *G4 TR inv* leading; SAS751, *G4 TR* lagging; SAS749, *G4 TR inv* lagging; SAS760.

5.6 The effect of *rev1*$^{+}$ on *G4 TR* stability on the leading and the lagging strand

Using a plasmid-based replication assay, Sarkies et al. (2010) have shown that in chicken DT40 cells REV1 is required for efficient replication of G4-DNA on the leading strand. The authors suggested that in *rev1*$^{-}$ cells a gap is formed at the G4-DNA, which leads to a loss of epigenetic marks during the gap-filling (Sarkies et al., 2010). I tested by fluctuation analysis whether the absence of *rev1*$^{+}$ has an effect on TR stability in the presence of G4-DNA and whether this differs on the leading or the lagging strand (Figure 5.5). In strains which carry the G4-DNA on the leading strand template, the TR deletion rate in *rev1*Δ cells was similar as in wild-type cells. If the G4-DNA is placed on the lagging strand template, the TR deletion rate was increased about 1.5-fold in *rev1*Δ cells compared to wild-type cells. These results suggest, that a possible perturbation of replication of G4-DNA due to the absence of *rev1*$^{+}$ does not have a major effect on TR deletion formation.

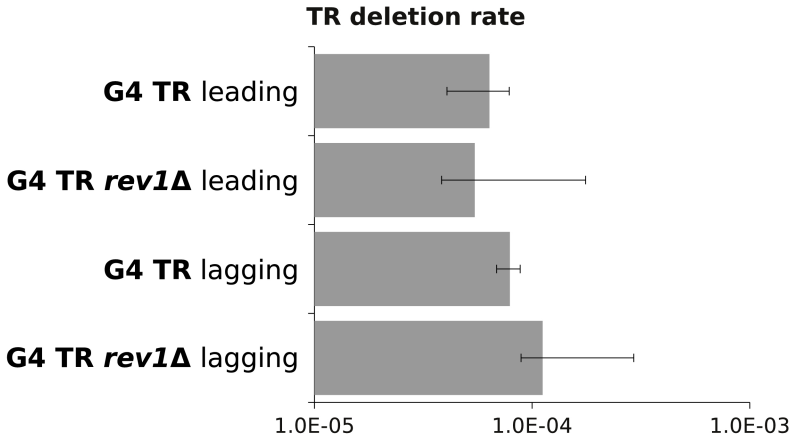

genotype	n	deletion rate x 10^{-5} (95% ci)	p
G4 TR leading	33	6.37 (4.06-7.85)	0.9601
G4 TR *rev1*Δ leading	11	5.45 (3.84-17.6)	
G4 TR lagging	33	7.9 (6.87-8.82)	0.0017
G4 TR *rev1*Δ lagging	11	11.2 (8.9-29.3)	

Figure 5.5: G4 TR deletions in *rev1*Δ cells
Fluctuation analysis was carried out as described in Figure 5.2A. Two-tailed p-values are comparisons between the absence or presence of the *rev1*$^{+}$ allele in strains containing *G4 TR* on the same strand (either leading or lagging). Strain genotypes are listed in Materials and Methods. Strains used: *G4 TR* leading; SAS762, *G4 TR rev1*Δ leading; SAS919, *G4 TR* lagging; SAS749, *G4 TR rev1*Δ lagging; SAS929.

5.7 TR instability and HR-dependent replication fork restart

In Chapter 4 I showed that the genomic instability induced by replication fork collapse and restart at RTS1 does not require homology to RTS1. Therefore, template switching downstream of RTS1 could be a consequence of the restarted replication fork itself, rather than the HR-dependent restart mechanism. With the *arg3 82TR* systems, described here, I could ask the following questions: is the TR instability observed in the construct rura(dir)R analysed in Chapter 4 dependent on the long homology of 500bp ("b" in Figure 4.1B) or does replication fork restart in this system also induce instability in shorter repeats (82bp), which rearrange independently of HR? And if replication fork restart does induce instability in these short repeats, is this effect elevated in the presence of G4-DNA?

In order to investigate these questions I analysed the *arg3 82TR*, *G4 TR* and *G4m TR* constructs in the presence (RTS1 ON) or absence (RTS1 OFF) of *rtf1*$^{+}$. The *Pnmt41-rtf1*$^{+}$ allele was used to induce replication fork collapse at RTS1 in the absence of thiamine (Th-). Cells were grown to exponential phase in the presence of thiamine (Th+), washed and used to inoculate Th+ and Th- cultures. The cultures were grown for 24 hours (approximately 7-8 generations), serially diluted and spotted onto arg- and arg+ plates (Figure 5.6A). The results of this spot test suggest that induction of replication fork collapse at RTS1 induces TR deletions only in the absence of G4-DNA.

In order to investigate this result in more detail, fluctuation analysis was carried out with the *arg3 82TR*, *G4 TR* and *G4m TR* strains. For this analysis the endogenous copy of *rtf1*$^{+}$ was used to induce constitutive replication fork collapse at RTS1. This background is suitable for these experiments, since absolute numbers of mutation rates can be determined by fluctuation analysis. However, the *Pnmt41-rtf1*$^{+}$ allele leads to *rtf1*$^{+}$ overexpression and could be more stringent in the arrest. The effect of replication fork collapse at RTS1 on the deletion rates is depicted in Figure 5.6B. Activation of RTS1 increases the deletion rate in *arg3 82TR* about 16-fold. Therefore, induced TR instability does not require a homology of 500bp, but can also be observed in TRs of only 82bp. Similar results can be observed for the *G4m TR* constructs on either the leading or the lagging strand. Surprisingly, the deletion rates in the *G4 TR* constructs, on leading or lagging strand, were not increased after replication fork collapse at RTS1. This suggests that although the presence of G4-DNA induces repeat instability and replication of TRs by a restarted replication fork is error-prone, these two factors combined, do not further elevate TR instability. The measured deletion rates correspond to the observation by spot test analysis (Figure 5.6A), as the amount of TR deletion events in *arg3 82TR* after activation of RTS1 are similar as the amount of TR deletion events in the presence of G4-DNA.

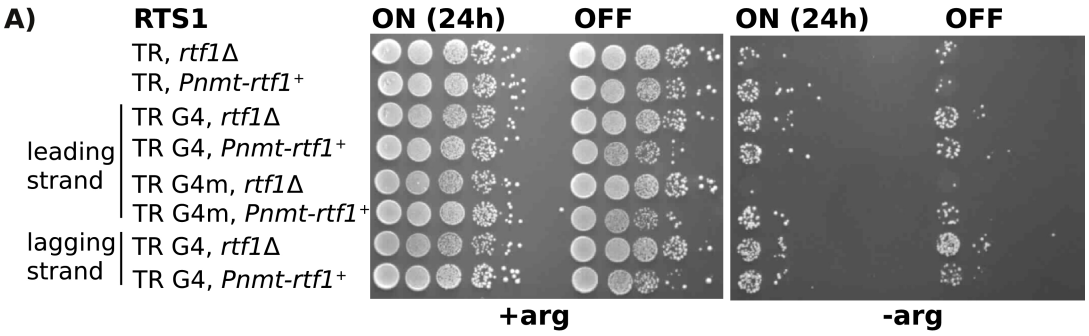

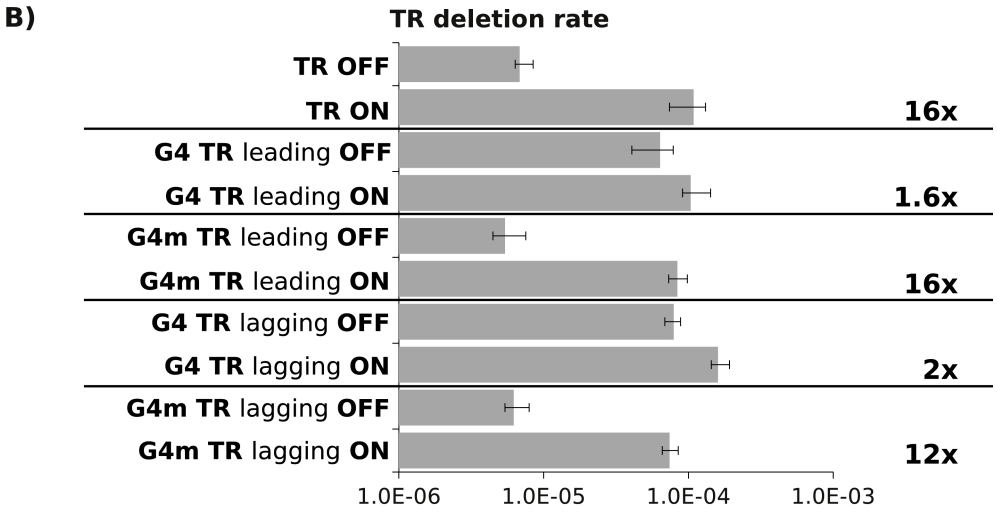

genotype	n	deletion rate x 10^{-5} (95% ci)	p
TR OFF	33	0.68 (0.64-0.85)	<0.0001
TR ON	43	10.9 (7.4-13.1)	
G4 leading OFF	33	6.4 (4.1-7.9)	<0.0001
G4 leading ON	32	10.4 (9.1-14.2)	
G4m leading OFF	32	0.54 (0.45-0.75)	<0.0001
G4m leading ON	32	8.4 (7.3-9.8)	
G4 lagging OFF	33	7.9 (6.9-8.8)	<0.0001
G4 lagging ON	32	16 (14.4-19.2)	
G4m lagging OFF	33	0.62 (0.54-0.79)	<0.0001
G4m lagging ON	33	7.4 (6.6-8.5)	

Figure 5.6: TR instability induced by replication fork collapse and restart
A) Cells containing the *arg3 82TR*, *G4 TR* and *G4m TR* constructs and either the *Pnmt-rtf1*$^+$ or *rtf1*Δ alleles were used for this experiment. In cells containing *Pnmt-rtf1*$^+$, RTS1 is activated in the absence of thiamine (ON) and inactive in the presence of thiamine (OFF). In *rtf1*Δ cells RTS1 is always OFF. Cells were grown over night in non-selective media, cultures were washed, diluted and cells were grown for 24 hours in the presence of arginine, plus (OFF) or minus thiamine (ON). Cells were serially diluted and spotted on plates plus (+arg) or minus arginine (-arg), lacking thiamine. The position of the G4-motif on the leading or lagging strand is indicated on the left. Cells were spotted in 10-fold dilutions from left to right, starting with 10^5 cells.
B) Fluctuation analysis was carried out as described in Figure 5.2A. The presence of the *rtf1*Δ allele (RTS1 OFF) or the *rtf1*$^+$ allele (RTS1 ON) and the position of the G4-motif on the leading or lagging strand is indicated on the left. Fold increase is shown on the right for each pair (separated by lines). Two-tailed p-values are comparisons between ON and OFF of each construct. Strain genotypes are listed in Materials and Methods. Strains used: *TR* OFF; SAS756, *TR* ON; SAS1009/1010, *G4 TR* leading OFF; SAS762, *G4 TR* leading ON; SAS1056, *G4m TR* leading OFF; SAS753, *G4m TR* leading ON; SAS1050, *G4 TR* lagging OFF; SAS749, *G4 TR* lagging ON; SAS1052, *G4m TR* lagging OFF; SAS910, *G4m TR* lagging ON; SAS1054.

5.8 Genetic analysis of a restarted replication fork

As already suggested in Chapter 4, error-prone replication after collapse and restart at RTS1 could be due to a lower fidelity of the restarted replication fork. This might be the consequence of replication by an alternative replisome, lacking components which are important for its integrity (immature replisome) or an alternative mechanism/uncoupling of replication. Interestingly, using a palindrome assay flanked by the rDNA RFB and RTS1, K. Mizuno has recently established that rearrangements after replication fork collapse at RTS1 decrease with increasing distance from RTS1 (personal communication). This observation suggests that the restarted replication fork matures and gains in fidelity over distance. To address the question of which components of the replisome might be compromised after restarting at RTS1, I decided to trial an epistasis analysis of replication factors in the *arg3 82TR* system in the presence and absence of *rtf1*$^+$. The assumption behind this analysis is illustrated in Figure 5.7A. A unperturbed replication fork arrests at RTS1, collapses and subsequently restarts in a HR-dependent mechanism to resume replication. The restarted fork however is error-prone, possibly due to an altered replisome.

For this analysis I chose four candidate components of the replisome and assayed TR deletion rates in mutant backgrounds with RTS1 OFF or ON (Figure 5.7B). The candidates included *mrc1*$^+$, which is important for the replication checkpoint (Alcasabas et al., 2001; Xu et al., 2006), *mcl1*$^+$, the homolog of *scCTF4*, which has been suggested to couple Pol α and MCM (Gambus et al., 2009) and *cdc27-D1* and *swi7-H4*, mutant alleles affecting Pol δ and Pol α, respectively. *cdc27-D1* contains a C-terminal truncation which abolishes the interaction with PCNA resulting in low processivity of *pol*δ (Bermudez et al., 2002). *swi7-H4* affects the catalytic subunit of Pol α (Murakami and Okayama, 1995). *CTF4* and *mcl1*$^+$ have also been implicated in sister chromatid cohesion (Hanna et al., 2001; Williams and McIntosh, 2002). In the TR analysis shown in Figure 5.2A and Figure 5.7B, TR deletions are increased in *mrc1*Δ cells and this is further elevated when RTS1 is ON. A similar result was observed for *cdc27-D1*. This suggests to be an additive effect of replication fork restart on the deletion rate in these mutants. In *mcl1-101* cells and in *swi7-H4* cells the activation of RTS1 (RTS1 ON) does not further increase the deletion rates measured when RTS1 is OFF. RTS1 activation and the mutant background seem to be epistatic. This epistasis analysis suggests that functions related to Pol α or its accessory factor Mcl1 might not be required for or are absent during replication downstream of RTS1 after replication fork restart. As mentioned previously, Pol α and Mcl1 are associated with lagging strand DNA synthesis and Mcl1 was implicated in sister-chromatid cohesion. This could suggest that replication downstream of RTS1 might be uncoupled. However, epistasis was not observed in the Pol δ mutant *cdc27-D1*.

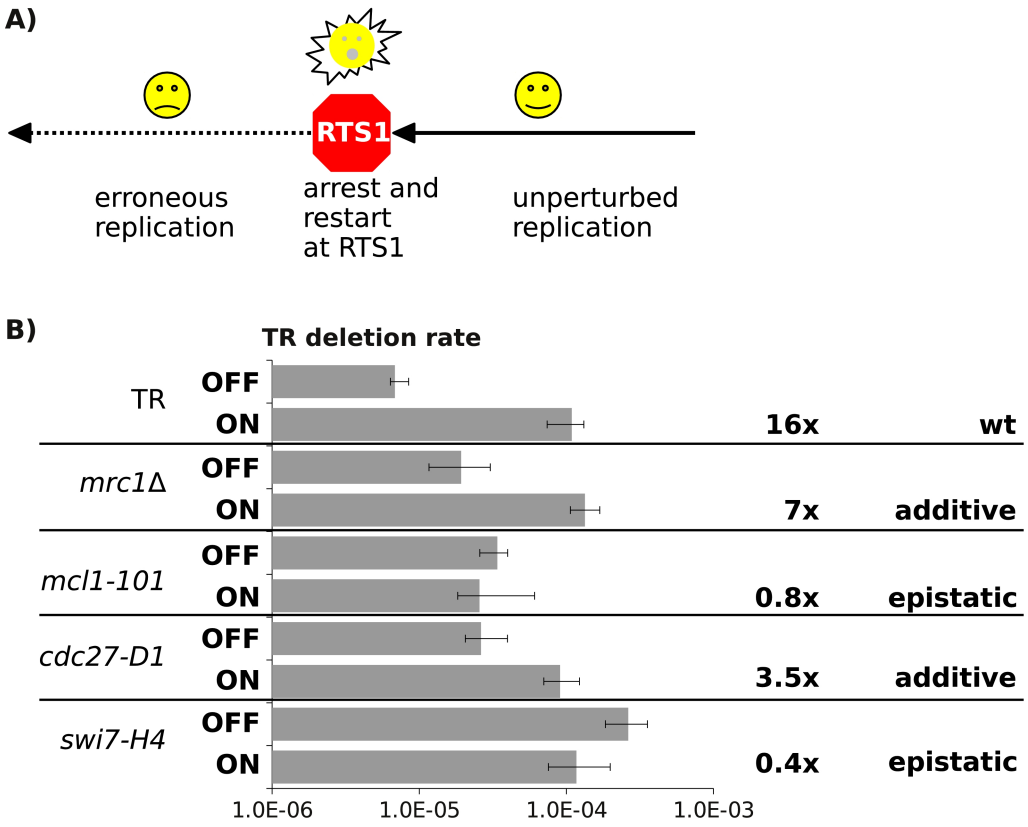

genotype	n	deletion rate x 10^{-5} (95% ci)	p
TR OFF	33	0.68 (0.64-0.85)	<0.0001
TR ON	43	10.9 (7.4-13.1)	
*mrc1*Δ OFF	21	1.9 (1.2-3.0)	0.0004
*mrc1*Δ ON	10	13.4 (10.6-16.9)	
mcl1-101 OFF	22	3.4 (2.6-4.0)	0.5823
mcl1-101 ON	11	2.6 (1.8-6.1)	
cdc27-D1 OFF	28	2.6 (2.1-4.0)	<0.0001
cdc27-D1 ON	21	9.1 (7.0-12.3)	
swi7-H4 OFF	22	26.3 (18.4-35.6)	0.0006
swi7-H4 ON	11	11.7 (7.6-19.8)	

Figure 5.7: Genetic analysis of a restarted replication fork
A) Schematic overview of the model of replication at an active RTS1. A "normal" replication fork approaches RTS1, arrests, collapses and restarts. The replication/replisome is altered downstream of RTS1, maybe due to components missing in the replisome or alternative components present. The arrows indicate the direction of replication.
B) Fluctuation analysis was carried out as described in Figure 5.2A. The presence of the *rtf1*Δ allele (RTS1 OFF) or the *rtf1*$^{+}$ allele (RTS1 ON) and the mutant allele are indicated on the left. On the right, the fold increase between ON and OFF in each background (pairs are separated by lines) and the observed effect are indicated. Two-tailed p-values are comparisons between OFF and ON of each construct. Strain genotypes are listed in Materials and Methods. Strains used: *TR* OFF; SAS756, *TR* ON; SAS1009/1010, *mrc1*Δ OFF; SAS911, *mrc1*Δ ON; SAS914, *mcl1-101* OFF; SAS1006, *mcl1-101* ON; SAS1007, *cdc27-D1* OFF; SAS881, *cdc27-D1* ON; SAS1176, *swi7-H4* OFF; SAS1125, *swi7-H4* ON; SAS1122.

I am aware of the possibility that mutations affecting the replisome could also affect fork arrest and collapse at RTS1 or the potential to restart. These possibilities could be accounted for by performing 2D-gel electrophoresis and measuring viability loss in the RuraR system, respectively. A more thorough analysis of the effects of these mutants on fork collapse and restart at RTS1 is required before conclusions can be made. I. Miyabe is currently investigating the requirement for different polymerases after replication restart at RTS1 using a well characterised mutational analysis (Miyabe et al., 2011, personal communication).

5.9 Conclusion and discussion

The results in this chapter demonstrate that the deletion of repeats of 82bp in *arg3 82TR* does not require HR, MMR or PRR and that the sequence (G-content) of repeated sequences does have an impact on their stability. The differences in the increase of the TR deletion rates in *mrc1*Δ cells in the G-rich *nat1 101TR* assay (Figure 3.6B) and the AT-rich *arg3 82TR* assay (Figure 5.2B) suggests that *mrc1*$^+$ is more important for the progression of replication in G-rich DNA. This is in agreement with an observation by Voineagu et al. (2009b) that replication fork stalling in CGG repeats is induced in the absence of *scMRC1* (Voineagu et al., 2009b). It would be interesting to know whether the checkpoint function of *mrc1*$^+$ is required or not. I have analysed TR deletions in *nat1 101TR* in the *mrc1-T645A/T653A* mutant, which abolishes the activation of the Cds1 checkpoint kinase (Xu et al., 2006). However, the replication phenotype of this mutant is not characterised. Checkpoint mutants, such as *cds1*Δ, could be used to measure the effect of the replication checkpoint on TR deletions or alternatively, *mrc1-T645A/T653A* should be tested for separation of checkpoint and replication functions of *mrc1*$^+$. A direct comparison between the *G4m TR* and *G4 TR* constructs in *mrc1*Δ cells could be used to confirm the requirement for *mrc1*$^+$ in the replication of G4-DNA. The role of *mrc1*$^+$ in the replication of G4-DNA on either leading or lagging strand could be addressed using the corresponding assays (*G4 TR* in *mrc1*Δ cells). This would be interesting as *scMRC1* has been shown to interact with Pol ε (Lou et al., 2008).

The presence of G4-DNA in repeated sequences does induce TR instability (TR deletions). Interestingly, the spontaneous deletion rates of the *G4 TR* constructs are similar to the deletion rates of the *nat1 101TR* assay, and both are about 5-10-fold higher than *arg3 82TR,* lacking a G-rich sequence or than *G4m TR*. Leading and lagging strand DNA synthesis does not show a different effect on this instability (Figure 5.3B) and also the deoxycytidyl transferase Rev1, does not seem to be required for TR stability (Figure 5.5A). Whether Rev1 is required for efficient replication of G4 can not be directly addressed with these assays, as replication perturbations in *rev1*Δ cells might not result in TR deletions. It is important to note that in chicken DT40 cells, Rev1 is re-

quired for efficient replication of damaged DNA, independently of PCNA ubiquitylation, which is more important for postreplicative gap-filling (Edmunds et al., 2008). In yeast however, Rev1 belongs to the Rad6 epistasis group (Kunz et al., 2000) and is highly expressed in G2/M suggesting a role in postreplicative gap-filling (Waters and Walker, 2006). Therefore the requirement of Rev1 in replication might be different in DT40 cells and *S. pombe*.

As shown previously, replication fork collapse at RTS1 and HR-dependent restart induces repeat rearrangements (Lambert et al., 2005; Mizuno et al., 2009; Lambert et al., 2010). In Chapter 4 I could demonstrate that genomic instability was not abolished by the removal of homology to RTS1. TR instability in the absence of homology to the site of fork collapse (RTS1) strongly suggests a separation of error-prone replication from an error-prone restart mechanism involving template switching between RTS1 sites. Replication fork restart in this assay induces deletions in direct TRs of a homology of only 82bp (Figure 5.6B). This increase can be observed after RTS1 activation by over-expression of *rtf1*$^+$ (*Pnmt41-rtf1*$^+$) or if *rtf1*$^+$ is expressed at endogenous levels. The overall efficiency of fork arrest at RTS1 might differ in the two backgrounds. 2D-gel analysis, performed by I. Miyabe in the lab, has shown that 95% of replication forks at the rDNA-*ura4*$^+$-RTS1 locus approach from the centromere-proximal side (personal communication). Activation of RTS1 by expression of the endogenous copy of *rtf1*$^+$, changes the replication of this locus to 50% of forks approaching from each side (I. Miyabe, personal communication). So far there was no report of genomic instability induced by the rDNA RFB, but whether the observed effects on genomic instability are due to a change in the balance of replication direction or replication fork collapse and restart at RTS1 can not be fully determined in the current assay. S. Lambert has shown that in a system which only contains the centromere-proximal RTS1 site upstream of *ura4*$^+$ (uraR) replication fork collapse leads to error-prone replication of *ura4*$^+$ (personal communication). This supports the model that the mutagenic effects observed in the *arg3 82TR* and rura(dir)R systems described here (and in Chapter 4) are likely due to error-prone replication following replication fork restart.

If replication of a restarted replication fork is compromised and in some way more unstable or error-prone, G4-DNA might lead to further genomic instability. It has been shown previously that special enzymatic activities are needed for genome maintenance in the context of G4-DNA (Ribeyre et al., 2009; Sarkies et al., 2010, ML Bochman, personal communication). Surprisingly, TR deletion rates in *G4 TR* were not increased when replicated by a restarted replication fork. It seems that the way the rDNA-*ura4*$^+$-RTS1 locus is replicated after replication fork collapse at RTS1 is not sensitive for secondary structures, such as G4-DNA. Whether this is due to different enzymatic activities at the restarted fork, that are more capable in replicating G4-DNA, or a dif-

ferent coordination of replication, is not yet clear.

The TR assays used here are limited to the detection of deletion events. Therefore, different assays to detect a broader spectrum of genomic instability should be used to confirm the missing effect of G4-DNA on replication by a fork restarted at RTS1. I am currently developing a construct in which the ORF of *ura4*$^{+}$ is modified to contain a G4-motif. By only applying slight changes in the amino acid sequence the functionality of *ura4*$^{+}$ is maintained. With this construct, genomic instability resulting in the loss of *ura4*$^{+}$ functionality - due to base mutations, deletions or expansions - can be selected for with 5-FOA.

Chapter 6

In vivo analysis of the *S. pombe* Mus81 winged helix domain

The heterodimer Mus81-Eme1 is a structure-specific endonuclease, which was shown to be important in mitotic and meiotic recombination and to be involved in replication and the tolerance of replication perturbations (Osman and Whitby, 2007). *In vitro* studies established the preferred substrate for Mus81 complexes as nicked HJs, D-loops, 3'-flaps and replication fork-like structures (Whitby et al., 2003; Gaillard et al., 2003; Osman et al., 2003; Ciccia et al., 2003; Fricke et al., 2005). Fadden et al. (submitted) have identified a novel domain in human MUS81, determined its structure and analysed its properties *in vitro*. In collaboration we have characterised the conserved *S. pombe* domain *in vivo*. In this first section I will give a detailed introduction about the structural and functional properties of the Mus81-Eme1/Mms4 complexes reported in the literature.

6.1 Introduction and background

MUS81 (MMS and UV sensitive clone 81) was first identified by Interthal and Heyer (2000) as an interaction partner of the HR mediator *RAD54* in *S. cerevisiae* (Interthal and Heyer, 2000). *S. pombe* Mus81 was found to interact with the forkhead-associated-1 (FHA1) domain of the replication checkpoint kinase Cds1 in *S. pombe* (Boddy et al., 2000). *S. cerevisiae* and *S. pombe mus81*Δ cells are not sensitive to ionizing radiation, but show a profound sensitivity to replication perturbations induced by MMS, HU and CPT (Interthal and Heyer, 2000; Boddy et al., 2000; Doe et al., 2004). Sequence alignments and homology searches led to the subsequent identification of MUS81 in human and mouse cells (Chen et al., 2001). These initial studies in yeast and mammals, suggested Mus81 to belong to the XPF family of endonucleases and that it was involved in the processing of HR-intermediates arising during replication and meiosis. I will first discuss

the structural properties of Mus81 complexes and their *in vitro* substrate specificity and then the phenotypes of *mus81*Δ cells.

6.1.1 Structural characterisation of Mus81-Eme1/Eme2/Mms4

Sequence alignments and structural work have shown similarities between Mus81, XPF and Hef nucleases (Boddy et al., 2000; Interthal and Heyer, 2000; Nishino et al., 2003; Chang et al., 2008). Eukaryotic members of the XPF/Mus81 family function as heterodimers that consist of a catalytic and a non-catalytic subunit (Ciccia et al., 2008). Characteristic for all members of the XPF/Mus81 family is the catalytic ERCC4 domain, which is highly conserved in the catalytic subunits, but more diverged in the non-catalytic subunits (Figure 6.1A) (Ciccia et al., 2008). Tandem helix-hairpin-helix $(HhH)_2$ domains are a second characteristic feature and are thought to be important for dimer formation and sequence-independent DNA-binding (Doherty et al., 1996; Ciccia et al., 2008; Chang et al., 2008).

The ERCC4 nuclease domain in Mus81 contains the conserved motif GDX_nERKX_3D, which is required for metal-dependent endonuclease activity (Enzlin and Schärer, 2002; Nishino et al., 2003). Mutation of two aspartic residues to alanine in this motif (VERKXXDD) of Mus81 resulted in a nuclease-dead protein (Chen et al., 2001; Gaillard et al., 2003). In Mus81, the $(HhH)_2$ are split between the N- and the C-terminus (Figure 6.1A). Additionally there is a pseudo-HhH motif, which contains an additional small insertion, at the C-terminus. The functionality of which is not known (Ciccia et al., 2008). Because the $(HhH)_2$ motif is important for DNA-binding, it was suggested that the N- and C-terminal motifs are in close proximity in the protein complex (Ciccia et al., 2008).

The non-catalytic subunit of the Mus81 complex was identified as Mms4 in *S. cerevisiae* (Kaliraman et al., 2001; Mullen et al., 2001), Eme1 in *S. pombe* (Boddy et al., 2001) and EME1 or EME2 in human cells (Ciccia et al., 2003). The ERCC4 domains in EME1, EME2, Eme1 and Mms4 are catalytically inactive and these proteins, like Mus81, contain a HhH and a pseudo-HhH at their C-termini (Figure 6.1A) (Ciccia et al., 2008). Similar to XPF and ERCC1, Mus81 and Mms4 interact with their C-terminal domains to form a heterodimer and dimer formation is necessary for endonucleolytic activity (de Laat et al., 1998; Fu and Xiao, 2003). Fu and Xiao (2003) showed that the G173R mutation in the N-terminus of Mms4 prevents binding to Mus81, which suggests more complex interactions (Fu and Xiao, 2003). The two subunits are epistatic in response to DNA damage and also share similar meiotic phenotypes (Boddy et al., 2001; de los Santos et al., 2001; Oğrünç and Sancar, 2003) . Mus81 and Mms4 were shown to localize to the nucleus independently and for this a nuclear localization signal in Mms4 (244-263) and the

N-terminal half of Mus81 were required (Fu and Xiao, 2003).

A chimeric Mus81-Eme1 complex consisting of zebrafish Mus18ΔN and human EME1ΔN, lacking the N-terminal domains, has been crystallised and Chang et al. (2008) showed that both, the C-terminal $(HhH)_2$ motif and the ERCC4 motifs of Mus81 and Eme1 are important for complex formation. The $(HhH)_2$ and a linker in the Eme1 ERCC4 domain contribute to DNA binding (Chang et al., 2008). In addition, this study suggests that the N-termini of Mus81 and Eme1 are not crucial for endonuclease activity and complex formation (Chang et al., 2008). Interestingly, it was shown that in the heterodimer XPF-ERCC1, the DNA-binding activity solely resides in the HhH motif in ERCC1 and not in the $(HhH)_2$ motif of the catalytic subunit XPF (Ciccia et al., 2008). In particular, the second HhH motif in ERCC1, which contains a classical Gly-hydrophobic residue-Gly (GhG) hairpin, is thought to be involved in DNA binding, whereas the HhH motifs in XPF are lacking GhG hairpins and are unable to bind DNA (Ciccia et al., 2008). Interestingly, only the N-terminal HhH and the pseudo HhH motif in the C-terminus of Mus81 seem to contain a classical GhG motif. The contribution of individual domains of Mus81 and Eme1/Mms4 to substrate recognition and their effect on the protein function has to be further clarified *in vitro* and *in vivo*.

The activity of Mus81-Eme1 *in vivo* might also depend on modifications and interactions with other proteins, which influence localisation and conformation of the complex. Several studies indicate such regulatory mechanisms, as for example Cds1-dependent phosphorylation of Mus81 after HU treatment in *S. pombe* (Kai et al., 2005) and different phosphorylation states of Mms4 before and after exposure to DNA damaging agents were observed in *S. cerevisiae* (Ehmsen and Heyer, 2008).

6.1.2 *In vitro* substrate specificity of Mus81-Eme1/Mms4

The mitotic and meiotic phenotypes of *mus81*Δ, *eme1*Δ and *mms4*Δ cells suggested that Mus81-Eme1/Mms4 are important for the processing of recombination and replication intermediates (Boddy et al., 2000; de los Santos et al., 2001; Interthal and Heyer, 2000; Doe et al., 2002). The meiotic defects of these mutants and the synthetic lethality with RecQ helicases - which prevent the accumulation of HJs - indicated HJs as a possible substrate (Doe et al., 2000; Mullen et al., 2001). The suppression of mitotic and meiotic phenotypes of *mus81* mutants by overexpression of the bacterial HJ resolvase RusA supported this idea (Boddy et al., 2001; Doe et al., 2002; Odagiri et al., 2003; Bastin-Shanower et al., 2003). Therefore, the activity of Mus81-Eme1/Mms4 complexes on substrates resembling replication forks and recombination intermediates (including HJs) were characterised. Figure 6.1B shows an overview of substrates used in these assays.

Experiments using *S. pombe* TEV-eluates of Mus81-Eme1 determined nicked HJs as a much

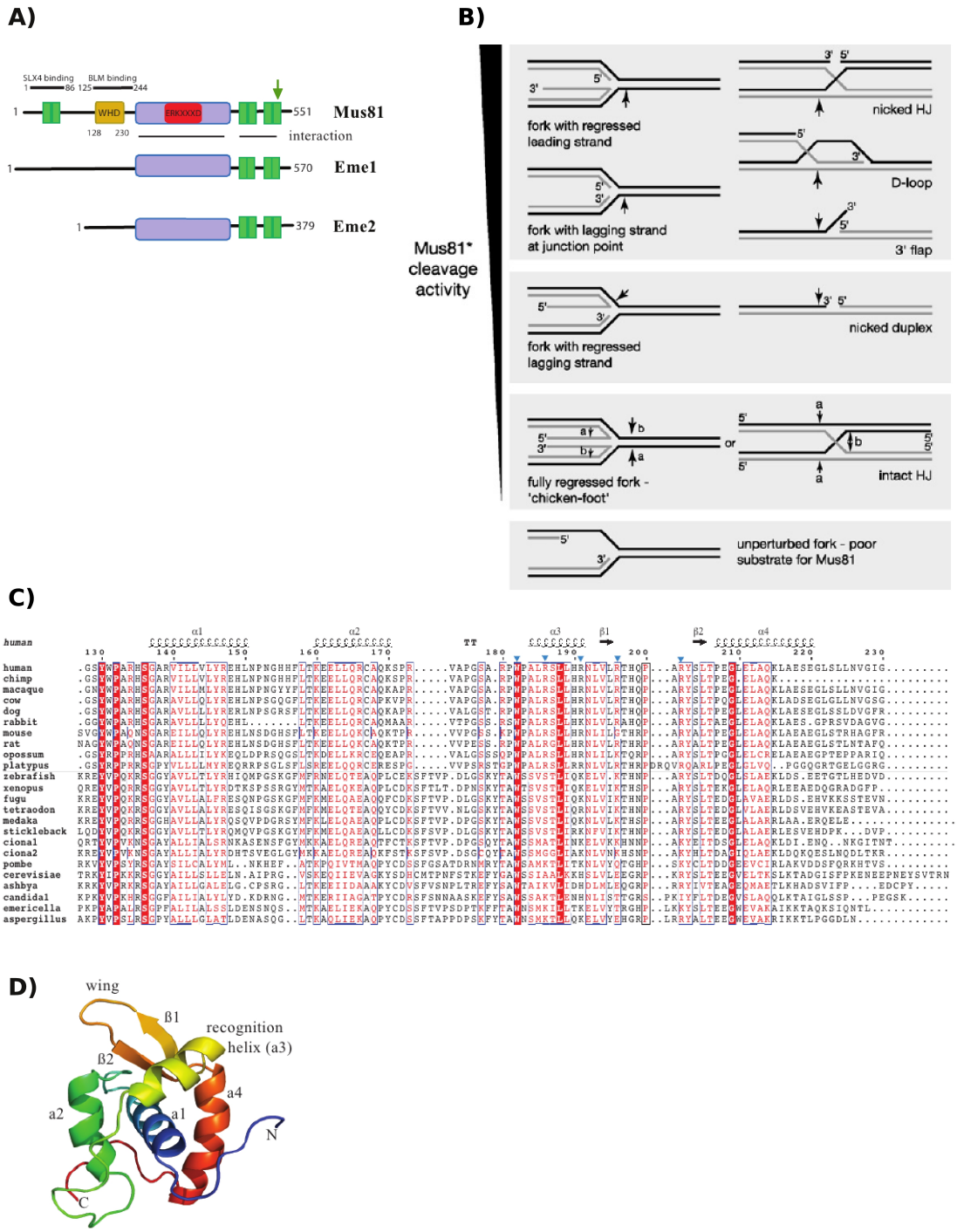

Figure 6.1: Identification of a winged helix (WH) domain in the N-terminus of human MUS81
A) Domain structure of human MUS81, EME1 and EME2. WHD; winged helix domain, the red box shows the nuclease motif in the catalytic domain (purple). Helix turn helix (HhH) motifs are shown in green. The pseudo-HhH motif is indicated by the green arrow. The previously published interaction sites of hMUS81 with SLX4 and BLM are indicated (Zhang et al., 2005; Fekairi et al., 2009). This figure was adapted and modified from Fadden et al., submitted.
B) *in vitro* substrate specificity of Mus81-Eme1/Mms4 (Mus81*). The substrate specificity decreases from top to bottom. Parental DNA strands are shown in black and nascent strands in grey. 5'- and 3'-ends and the observed cleavage sites for Mus81 complexes (arrows) are indicated. This figure was adapted from Osman and Whitby (2007).
C) Sequence alignment of the N-terminal WH domain of Mus81. The secondary structures above the alignment represent the NMR data. Conserved residues are highlighted in red and blue triangles indicate mutations. This figure was adapted from Fadden et al., submitted.
D) Representative domain structure of the WH domain. The wing motif and the recognition helix a3 are indicated. This figure was adapted from Fadden et al., submitted.

preferred substrate of endogenous Mus81-Eme1, as well as 3'-flaps and replication fork-like structures, but there was almost no activity on intact HJs (Doe et al., 2002; Gaillard et al., 2003). A previous study compared the cleavage of fixed HJs to migratable HJs and found activity on both substrates with a more homogeneous cleavage pattern on migratable HJs (Boddy et al., 2001). However, the products of a classical HJ resolvase would be expected to create ligatable ends and this was not the case for Mus81-Eme1 (Boddy et al., 2001). Similar results were obtained in experiments with Mus81-Mms4 in *S. cerevisiae*, although endogenous preparations of the endonuclease showed no activity on intact HJs, but readily cut nicked HJs, 3'-flaps and replication fork-like structures (Kaliraman et al., 2001; Bastin-Shanower et al., 2003; Fricke et al., 2005; Ehmsen and Heyer, 2008). A side-by-side comparison of recombinant *S. pombe* Mus81-Eme1 and *S. cerevisiae* Mus81-Mms4 complexes showed that both behaved very similarly, with poor activity on HJs and normal replication fork-like structures, but cleavage of replication fork-like structures resembling arrested or regressed replication forks with ssDNA overhangs (Whitby et al., 2003).

Mus81 immunoprecipitates from HeLa cells were shown to cleave migratable and fixed HJs, partial HJs and splayed arms (Y-structures) (Chen et al., 2001). However, fractions from HeLa cell extracts enriched for Mus81 and also recombinant human MUS81-EME1 proteins, expressed in *E. coli*, showed preferential cleavage of 3'-flaps and replication fork-like structures and activity on migratable HJs but not on fixed HJs (Constantinou et al., 2002; Ciccia et al., 2003). To clarify the different observations, Taylor and McGowan (2008) tested in parallel a minimal recombinant Mus81-Eme1 complex expressed in *E. coli*, full-length endogenous Mus81-Eme1 from HeLa cells and full-length recombinant Mus81-Eme1 expressed in insect cells and showed that all of these preparations cut nicked HJs and 3'-flaps as their preferred substrate compared to intact HJ.

These studies led to the conclusion that apart from minor differences, possibly originating from different preparation methods or source and assay conditions, Mus81-Eme1/Mms4/EME1 preferentially cleave 3'-flaps and replication fork-like structures, but HJs to a lesser extent. The activity of the enzyme seen on nicked HJs was interpreted as an ability to act through a nick and counter-nick mechanism, where the first cut, transforming an intact HJ into a nicked HJ, is the rate-limiting step (Boddy et al., 2001; Gaillard et al., 2003). Therefore the activity of some preparations on intact HJ could be due to a contamination or post-translational modification, which would catalyse the first cut. However, in *S. cerevisiae*, even phosphorylated Mus81-Mms4 purified after MMS- or HU-treatment, showed no activity on HJs (Ehmsen and Heyer, 2008). It was suggested that there is no need for an activating factor to stimulate HJ cleavage by Mus81-Eme1/Mms4, but that a dimer of heterodimers might be necessary for cleavage of an intact HJ, while one heterodimer could be sufficient to cleave a nicked HJ (Gaskell et al., 2007). If an intact HJ is not the preferred

substrate during HR, Mus81-Eme1/Mms4 might cleave a D-loop that forms by strand invasion preceding double HJ formation. This was demonstrated by Osman et al. (2003) using recombinant Mus81-Eme1/Mms4.

Suitable substrates for this enzyme, such as 3'-flaps, replication fork-like structures, D-loops and nicked HJs, are likely to arise during replication perturbation and HR in meiosis or mitosis and support a role of Mus81-Eme1/Mms4 in these processes.

6.1.3 Roles of Mus81-Eme1/Mms4 in HR, at broken forks and its regulation by Cds1

HR in *S. pombe* and *S. cerevisiae* is well conserved and Rad52 (encoded by *rad22*$^+$ in *S. pombe*) plays a major role in both Rad51-dependent and -independent pathways (encoded by *rhp51*$^+$ in *S. pombe*) (Symington, 2002; Doe et al., 2004). In *S. cerevisiae*, Mus81-Mms4 was found to function in the *RAD52* pathway in response to MMS and in the *RAD54* subpathway in response to UV damage (Interthal and Heyer, 2000; Odagiri et al., 2003). In *S. pombe*, initially *mus81*$^+$ was shown to be epistatic with *rhp51*$^+$ in response to UV damage (Boddy et al., 2000). A more detailed analysis revealed that Mus81 functions mainly in a *rad22*$^+$-dependent *rhp51*$^+$-independent pathway in response to DNA damage and that *rhp51*$^+$ has a deleterious effect in *mus81*Δ *rad22*Δ cells (Doe et al., 2004). Using a direct repeat assay, it was shown that *mus81*$^+$ acts in a *rad22*$^+$-dependent pathway in deletion formation (Doe et al., 2004).

It was further noticed that CPT treatment mainly induced deletions in this direct repeat assay (Doe et al., 2004). CPT immobilizes topoisomerase 1 on the DNA and can cause replication-related DSBs (Pommier et al., 2003). One possibility for this observation is that replication fork breakage can give rise to deletions by strand invasion into the wrong repeat template during fork repair (Bierne et al., 1997; Doe et al., 2004). Doe et al. (2004) demonstrated *in vitro* that Rad52 could generate D-loops by catalysing strand invasion of a 3'-overhang into dsDNA, which can subsequently be cleaved by Mus81-Eme1. This would suggest that fork breakage is predominantly repaired by a Rad52-dependent mechanism promoting strand invasion to repair the one-ended DSB.

Consistent with this model is a recent report that *mus81*$^+$ and the *rad22*$^+$ epistasis group are essential for sister-chromatid recombination at a broken replication fork (polar DSB) (Roseaulin et al., 2008). In support of this, Mus81 is thought to be important for crossover formation during meiosis (Osman et al., 2003). In this model, Mus81 cleaves D-loops, thereby preveting the generation of double HJs and also processes the downstream substrate generated after second-end capture (Osman et al., 2003).

Treatment with HU leads to replication fork stalling by depleting the dNTP pool, which might give rise to lesions after chronic exposure (Reichard, 1988; Lopes et al., 2001; Lisby et al., 2004). In response to acute HU treatment, but not to CPT, Mus81 is phosphorylated in a manner dependent on the replication checkpoint kinase Cds1 and dissociates from the chromatin (Kai et al., 2005). The observation that *mus81*Δ cells are sensitive to chronic but not to acute HU treatment (Kai et al., 2005), might reflect that different types of lesions can arise after prolonged exposure to HU (Lisby et al., 2004; Kai et al., 2005). Kai et al. (2005) mapped the interaction site between the two proteins and showed that mutation of a possibly phosphorylated threonine residue (T239A) in the T-X-X-D motif of Mus81 is sufficient to prevent Cds1-dependent phosphorylation. The impairment of this regulation was shown to enhance direct repeat recombination in response to HU (Kai et al., 2005). This suggests that Mus81 is removed from stalled replication forks in order to prevent genomic instability. In support of this, Froget et al. (2008) demonstrated that Cds1 prevents Mus81-dependent chromosome degradation after acute HU treatment, however no degradation could be detected in *mus81-T239A* cells. Cds1 regulates multiple proteins, such as Rad60 (Boddy et al., 2003) and Dna2 (Hu et al, submitted). Therefore exclusion of Mus81 from the chromatin is just one component in the regulation of fork stability.

The *pol*α mutant *swi7-H4* shows a mutator phenotype due to base deletions that are greatly reduced in *rhp51*Δ, *eme1*Δ and *mus81*Δ cells (Kai and Wang, 2003; Kai et al., 2005). The phosphorylation site mutant *mus81-T239A*, which remains chromatin-associated, was shown to elevate the mutator phenotype of *swi7-H4* (Kai et al., 2005). This suggests that structures arising due to replication perturbations in a *pol*α mutant background are processed by Mus81-Eme1 at the expense of genomic stability. Cells lacking *mus81*$^+$ or *eme1*$^+$ also show increased mutation rates, although the mutation spectra differs from *swi7-H4* cells (Kai et al., 2005).

Ehmsen and Heyer (2009) observed different phosphorylation states of Mms4 before and after exposure to DNA damaging agents. Recent studies suggest that Eme1 is phosphorylated by Rad3 in a cell cycle regulated manner and abolishing this phosphorylation leads to GCRs in *rqh1*Δ cells (S. Coulon, personal communication). This suggests multiple pathways of regulation of Mus81-Eme1/Mms4 activity by post-translational modification.

6.1.4 Implications of Mus81-Eme1/Mms4 in HR in the context of replication

The nature of the rDNA makes it a suitable locus to study replication fork arrest and recovery (Tsang and Carr, 2008; Murray and Carr, 2008). Zou and Rothstein (1997) observed that HJs occur in the rDNA during S-phase in *S. cerevisiae*, and that replication mutants involved in lagging strand synthesis accumulate HJs in a Rad52-dependent mechanism. This suggests that recombi-

national repair is active during or after replication and elevated if replication is perturbed. Ii et al. (2007) showed that the RecQ helicase *SGS1* and *MUS81* are important to maintain genomic stability of the rDNA. In both mutants, fork arrest at the rDNA RFB was increased and in *mus81*Δ cells X-shaped structures accumulated and the rDNA was expanded (Ii et al., 2007). *sgs1*Δ cells maintained the same number of rDNA repeats and did not accumulate X-shaped molecules, however an instability of the rDNA repeat structure was detected (Ii et al., 2007). Increased recombination rates at the rDNA have been observed for *sgs1*Δ but not for *mus81*Δ cells, which might reflect different recombination outcomes for the two mutants (Gangloff et al., 1994; Ii et al., 2011). Although HJs are not the preferred substrate of Mus81-Eme1/Mms4 *in vitro*, the enzyme might be required to process recombination intermediates and replication structures, enabling repair and replication fork restart. Fabre et al. (2002) suggested that *SGS1* and *MUS81* are involved in the recombinational repair of ssDNA gaps, formed during replication. Recent evidence has led to a model in which the Sgs1-Top3-Rmi1 complex is mainly responsible for the repair of recombination intermediates containing HJs, although Mus81-Mms4 provides an alternative mechanism for their resolution (Fabre et al., 2002; Ashton et al., 2011).

The model of RecQ helicases and Mus81 nucleases as components of alternative mechanisms in recombinational repair during replication or in response to replication perturbations is supported by the synthetic lethality of the double mutants in *S. cerevisiae* (Kaliraman et al., 2001), *S. pombe* (Boddy et al., 2000), *D. melanogaster* (Trowbridge et al., 2007) and *Arabidopsis thaliana* (Hartung et al., 2006). In *S. cerevisiae* and *D. melanogaster*, this phenotype can be largely suppressed in the absence of *RAD51* or its homolog SPN-A, respectively (Fabre et al., 2002; Trowbridge et al., 2007). In *S. pombe*, the synthetic lethality is dependent on the HR-mediator *swi5*$^+$ and can be suppressed by overexpression of the bacterial HJ resolvase RusA (Doe et al., 2002; Akamatsu et al., 2007; Hope et al., 2007). Interestingly, overexpression of RusA can suppress the sensitivity of *mus81*Δ and *rqh1*Δ cells to HU, but it only suppresses the sensitivity to CPT in *mus81*Δ cells and not in *rqh1*Δ cells, suggesting overlapping and separate functions of these proteins (Doe et al., 2000, 2002).

Differences in functions of RecQ helicases and Mus81-Eme1 are also reflected by the requirement for *mus81*$^+$ in sister-chromatid recombination at a broken fork, whereas *rqh1*$^+$ is dispensable (Roseaulin et al., 2008). Both factors show negative genetic interactions with replication mutants. For example, deletion of *mus81*$^+$ lowered the restrictive temperature of a temperature-sensitive allele of *pol*α (Boddy et al., 2000), and *mus81*Δ *pol*α *(pol1-1)* mutant cells exhibit a synthetic slow growth phenotype and accumulate recombination intermediates in the rDNA (Gaillard et al., 2003). Furthermore, *mus81*Δ is synthetically lethal or sick with components of the replication

fork protection complex (FPC), *swi1*$^+$ and *swi3*$^+$ in *S. pombe* and it was proposed that replication abnormalities, like ssDNA gaps, arise in *swi1*Δ and *swi3*Δ mutants that lead to HJ formation without fork breakage (Noguchi et al., 2003, 2004). Deletion of *rad22*$^+$ suppressed the synthetic lethality of *mus81*Δ *swi1*Δ cells as well as the accumulation of X-shaped molecules in the rDNA (Noguchi et al., 2004). Similar genetic interactions were observed for *rqh1*$^+$ (Noguchi et al., 2003; Ansbach et al., 2008).

The essential Smc5/6 complex is a suppressor of rDNA instability (Murray and Carr, 2008) and it was proposed to stabilise arrested forks and facilitate replication fork restart by HR (Irmisch et al., 2009). *mus81*Δ and *rqh1*Δ show negative genetic interactions with components of the Smc5/6 complex (Morikawa et al., 2004; Pebernard et al., 2006).

The 5'-flap endonuclease FEN1 - encoded by *rad2*$^+$ in *S. pombe* and *RAD27* in *S. cerevisiae* is synthetically lethal with *mus81*Δ or *rqh1*Δ/*sgs1*Δ (Murray et al., 1997; Osman and Whitby, 2007; Tong et al., 2001; Liu et al., 1999). HR is essential in the absence of *sprad2*$^+$ and *scRAD27* suggesting that it is required for lagging strand DNA synthesis or processing of intermediates arising in the absence of *RAD27/rad2*$^+$ (Muris et al., 1996; Symington, 1998). The essential helicase and exo-/endonuclease Dna2 functions with Rad27 during lagging strand synthesis and is important for Okazaki fragment maturation (Budd and Campbell, 1997). In *S. cerevisiae*, Rad27 physically interacts with Mus81 and stimulates its activity (Kang et al., 2010). Overexpression of Mus81-Mms4 can rescue the lethality of *dna2-K1080E* (Kang et al., 2010). Similarly, the human RecQ helicases BLM and WRN were shown to physically interact with and stimulate FEN1 (Brosh et al., 2001, 2002; Sharma et al., 2008) and BLM was suggested to interact with MUS81 and stimulate its activity (Zhang et al., 2005).

RNAse H2 plays a non-essential role in Okazaki fragment maturation and *rnh202*Δ cells exhibit a slow-growth phenotype in combination with *sgs1*Δ or *mus81*Δ (Qiu et al., 1999; Ii and Brill, 2005). A possible role of dynamic flap-processing by Fen1 (5'-flaps) and Mus81 (3'-flaps) could explain the observed phenotypes. It has been reported that whereas Rad27 prefers dually flapped substrates, Mus81-Mms4 does not and the cleavage products cannot be religated (Kao et al., 2002; Ehmsen and Heyer, 2009). A dynamic interplay between nucleases and helicases in lagging strand synthesis would be possible to ensure completion of DNA replication. It has been suggested that RecQ helicases might play such a role in certain loci, where repetitive sequences can lead to secondary structures in Okazaki fragments and inhibit their processing by FEN1 (Bachrati and Hickson, 2008). The helicase *SRS2* exhibits negative genetic interactions with *MUS81*, *SGS1* and *RAD27*, which can be suppressed by eliminating HR (Klein, 2001; Fabre et al., 2002). It was suggested that these genes play important roles in the repair of ssDNA gaps arising due to replica-

tion fork stalling, possibly involving synthesis-dependent strand-annealing (SDSA) (Fabre et al., 2002). ssDNA gaps could also arise behind the replication fork as a result from defective Okazaki fragment processing.

It is not always clear whether a factor is required due to its enzymatic activity or because of physical interactions. For example, the CPT sensitivity of *sgs1*Δ could be suppressed by overexpression of a *sgs1* helicase-dead mutant, which was proficient in the interaction with the topoisomerase Top3, suggesting a role in protein stimulation or recruitment rather than enzymatic activity for *SGS1* (Mankouri and Morgan, 2001).

6.1.5 Mus81-Eme1/Mms4 in meiosis and the role of *scYEN1*

Mus81 and Eme1 were shown to be essential proteins for meiosis in *S. pombe* (Boddy et al., 2000). Further investigation of the phenotype in *S. pombe* revealed that Mus81 function was required after the initiation of DSBs and, in contrast to *rhp51*Δ, which also exhibits a low spore viability, *mus81*Δ cells failed to segregate DNA equally between the spores (Boddy et al., 2001). This phenotype could be substantially rescued by overexpression of the HJ resolvase RusA (Boddy et al., 2001). These results suggested that Mus81-Eme1 is essential for the resolution of HR intermediates, like HJs, arising during meiosis.

Using *in vivo* and *in vitro* assays, Osman et al. (2003) found that Mus81 could process HR intermediates (D-loops) which can arise prior to double HJ formation in meiosis. The *in vitro* cleavage analysis of D-loops by Mus81-Eme1 suggests that in this pathway crossovers would be more likely generated than noncrossovers and *in vivo* assays comparing crossover and noncrossover formation in *S. pombe* support this suggestion (Osman et al., 2003).

In *S. cerevisiae*, spore viability of *mus81*Δ cells is reduced by only about 50% compared to wild-type (Interthal and Heyer, 2000). This is due to the alternative HJ resolvase Yen1, because almost no sporulation could be detected in a *yen1*Δ *mus81*Δ double mutant (Ip et al., 2008; Agmon et al., 2011). Matos et al. (2011) have demonstrated that in *S. cerevisiae* meiosis, Mus81-Mms4 and Yen1 are regulated by phosphorylation, so that Mus81-Mms4 is activated in meiosis I and Yen1 in meiosis II. Yen1 was discovered in parallel with its human ortholog GEN1 (Ip et al., 2008). They are members of the Rad2 family of endonucleases, which are known to specifically cleave 5'-flaps (Ip et al., 2008). An ortholog in *S. pombe* has not been identified which corresponds to the much more severe meiotic phenotype in *mus81*Δ cells (Boddy et al., 2000).

In *S. cerevisiae yen1*Δ further increased the sensitivity of *mus81*Δ cells to DNA damaging agents and overexpression of *YEN1* partially rescued the DNA damage sensitivity of *mus81*Δ cells, but not *sgs1*Δ cells (Blanco et al., 2010). Other members of the Rad2 family in *S. cere-*

visiae, *RAD27*, *EXO1* and *RAD2*, failed to rescue a *mus81*Δ phenotype (Blanco et al., 2010). *yen1*Δ *mus81*Δ cells show a higher sensitivity to DNA damaging agents affecting DNA replication (HU, MMS, CPT, UV, phleomycin, 4-NQO, nitrogen mustard, cisplatin) than the *mus81*Δ single mutant and *yen1*Δ cells behave like wild-type (Blanco et al., 2010). Neither the single nor the double mutants show sensitivity to ionizing radiation (Blanco et al., 2010; Tay and Wu, 2010). Mus81 and Yen1 seem to have redundant functions in DNA damage responses and meiosis. The epistatic relationship with *RAD52* and the fact that *rad52*Δ alleviates the sensitivity of *yen1*Δ *mus81*Δ cells to MMS and 4-NQO suggests that toxic recombination intermediates accumulate in *yen1*Δ *mus81*Δ cells (Blanco et al., 2010). Furthermore, *yen1*Δ *sgs1*Δ cells are viable and show a similar sensitivity to MMS, HU and 4-NQO as *sgs1*Δ cells (Blanco et al., 2010).

Because overexpression of *YEN1* can suppress the lethality of *sgs1*Δ *mus81*Δ and produce sick but viable cells, Blanco et al. (2010) suggested that *YEN1* is not epistatic with *SGS1* and provides an alternative pathway for repair in the absence of Sgs1 and Mus81. Using a plasmid-based assay to measure HJ resolution, Tay and Wu (2010) showed that *yen1*Δ and *mus81*Δ have redundant functions in HJ resolution as seen in the response to genotoxins (Blanco et al., 2010). However, the remaining resolution of 50% of HJ-substrate in *yen1*Δ *mus81*Δ cells, suggests the presence of additional resolvases, although based on this assay, Rad1 and Slx1 can be ruled out (Tay and Wu, 2010). Overexpression of GEN1 can complement the *mus81*Δ phenotypes in *S. pombe*, which is consistent with the functional overlap of Mus81 and Yen1 in *S. cerevisiae* (Lorenz et al., 2010).

6.1.6 Mus81-Eme1 in higher organisms

Human and mouse cells deficient in MUS81 show proliferation defects and chromosomal rearrangements (Abraham et al., 2003; Dendouga et al., 2005; Hiyama et al., 2006). Cells heteroallelic for MUS81 also show genome instability (McPherson et al., 2004). Two labs generated Mus81 deficient mice. Both mouse models were viable and fertile and *MUS81*$^{-/-}$ mice and cells were sensitive to cross-linking agents (McPherson et al., 2004; Dendouga et al., 2005). Whereas McPherson et al. (2004) reported a predisposition to cancer in *MUS81*$^{-/-}$ mice, this was not observed by Dendouga et al. (2005).

Gao et al. (2003) showed that MUS81 co-localises with the RecQ helicases BLM and WRN in the nucleolus, which contains the rDNA, during S-phase in human cells. MUS81$^{-/-}$ and EME1$^{-/-}$ cells are sensitive to cross-linking agents, but not to HU, UV, CPT or IR suggesting their main role in the removal of DNA crosslinks (Abraham et al., 2003; McPherson et al., 2004; Dendouga et al., 2005; Hiyama et al., 2006).

6.2 Background and aim of the project

A. Fadden identified a novel domain in the N-terminus of human MUS81 which is well conserved in yeast, but is absent in *C. elegans* and *D. melanogaster* (Figure 6.1C) (Fadden et al., submitted). The domain forms a winged helix (WH). These domains are found in DNA-binding proteins, but are also thought to be involved in protein-protein interactions (Gajiwala and Burley, 2000). The WH domain in Mus81 overlaps with the previously reported interaction site with the BLM helicase (Zhang et al., 2005). However, Fadden et al. could not reproduce this result (Fadden et al., submitted). They determined the structure of the WH domain by NMR (Figure 6.1D) and purified protein was used for *in vitro* DNA-binding assays.

This analysis revealed that the WH domain binds to dsDNA and ssDNA and that the recognition helix a3 and the N-terminus of the domain are important for DNA-binding (Fadden et al., submitted). Human MUS81 was purified with and without the WH domain and used for *in vitro* cleavage assays with both non-catalytic subunits, *h*Eme1 and *h*Eme2. While the activity of Mus81-Eme1 has been analysed *in vitro* previously, Mus81-Eme2 complexes in particular are not well characterised, partially due to weak complex formation (Chen et al., 2001; Ciccia et al., 2003). Fadden et al. (submitted) analysed splayed arms, 3'-flaps and a fork-like structure as substrates. Although Mus81-Eme1 showed no activity on splayed arms, it cleaved 3'-flaps and the fork-like structure and the presence of the WH domain had no effect on cleaving efficiency. Mus81-Eme2 showed activity on all the substrates and deletion of the WH domain reduced the activity on the splayed arm structure and moved the incision site on the 3'-flaps and the fork closer to the branch point. These results suggest that the WH of Mus81 might be important for DNA-binding and positioning of the substrate particularly in Mus81-Eme2 complexes (Fadden et al., submitted).

In *S. pombe* Mus81 forms a complex only with Eme1 and no ortholog for Eme2 has been identified so far. The WH domain in the N-terminus though is well conserved (Figure 6.1D, Fadden et al., submitted). In order to complement the *in vitro* studies of Fadden et al. (submitted) on the human MUS81 WH domain and give further insight into the biological significance of this domain, I carried out mutational analysis of the Mus81 WH domain in *S. pombe* in collaboration with two project students.

6.3 Mutations of the winged helix domain of Mus81 in *S. pombe*

For the investigation of the *in vivo* function of the Mus81 WH domain in *S. pombe*, a *mus81* base strain was constructed which is compatible for recombination-mediated cassette exchange (RMCE) (Watson et al., 2008). *mus81* variants were integrated into the *mus81*$^+$ locus and expressed under the native *mus81*$^+$ promoter. A WH domain deletion mutant, *mus81-WH*Δ, was constructed by fusion PCR, combining residues 1-116 and 215-608, and therefore eliminating residues 117-214. Figure 6.2A shows an overview of the Mus81 protein sequence in *S. pombe*. The WH domain is shown in grey and includes residues 117 to 214. Point mutations in the N-terminal part and in the vicinity of the recognition helix a3 are indicated. These parts of the domain in the human protein were shown to affect DNA binding (Fadden et al., submitted). The plasmid carrying the wild-type copy of *mus81*$^+$, pAW8-*mus81*$^+$, was used as a template for site-directed mutagenesis and all the mutations were confirmed by sequencing before and after integration.

All mutants were tested for DNA damage sensitivity. Mus81 was previously reported to be sensitive to DNA damaging agents that affect replication (Boddy et al., 2000; Doe et al., 2004). We tested sensitivity to HU, CPT, MMS and 4-NQO. As controls, the *mus81* base strain (*mus81*Δ), wild-type *mus81*$^+$ integrated in the base strain and the previously published catalytic mutant *mus81-DD* (D395,396A) abolishing nuclease activity (Boddy et al., 2001), were used. Figure 6.2B shows the results of the DNA damage sensitivity assay of the *mus81* strains in response to chronic treatment with HU, CPT, MMS and 4-NQO. Encircled in grey are the control strains and the *mus81-WH*Δ. *mus81*Δ cells are sensitive to all of these DNA damaging agents, as reported previously (Boddy et al., 2000; Doe et al., 2004). The catalytic mutant *mus81-DD* shares this phenotype, as expected (Boddy et al., 2001). Interestingly, the sensitivity of *mus81-WH*Δ is comparable to *mus81*Δ and *mus81-DD*. This result is unexpected, because *in vitro* analysis of the human WH domain has revealed that it is dispensable for nuclease activity of the MUS81-EME1 complex (Fadden et al., submitted).

Point mutations in the helix a3 and the N-terminal part of the WH were analysed. These parts of the WH domain were shown to be important for DNA binding in the *in vitro* analysis of the human protein (Fadden et al., submitted). Mutation of the tetrabasic motif *R113A/K114A/-R115A/K116A* preceding the WH domain did not sensitise the cells to DNA damage, however the double mutant *Y122A/R123A* showed increased sensitivity to all DNA damaging agents, similar to *mus81-WH*Δ. Mutations *R165,168A* and *H189A/K192A* in the vicinity of the recognition helix a3 had no effect on the DNA damage sensitivity. In the human MUS81 WH domain, mutations *R186,191A* in the recognition helix a3 reduced the DNA binding capacity by about 10-fold (Fadden et al., submitted). The corresponding mutations in *S. pombe* (*K176,181A*) had no effect on the

DNA damage sensitivity. In order to aggravate the effect of the mutations, the residues K176 and K181 were substituted with glutamate (*K176,181E*), which should not only disadvantage DNA binding, but counteract by positive charge. These mutants were also combined with the previously tested mutant *R165,168A* (*R165,168A/K176,181A* and *R165,168A/K176,181E*) in order to elevate the effect. Interestingly, *K176,181E* and *R165,168A/K176,181A* result in a relatively higher sensitivity, especially to HU and 4-NQO, but not in response to MMS and CPT. At the concentrations tested, the sensitivity to HU and 4-NQO is intermediate compared to *mus81*Δ and *mus81*$^+$. Combination of *K176,181E* with *R165,168A* resulted in a phenotype comparable to *mus81-WH*Δ.

These results demonstrate that the WH domain in *S. pombe* is essential for the *in vivo* function of Mus81. This effect could be due to several reasons, as the mutations could affect the protein folding and/or the endonucleolytic activity, protein-protein interactions, DNA-binding and regulation of the protein. I focused on three mutants; *mus81-WH*Δ (*WH*Δ), *K176,181E* (*mus81-KE*) and *R165,168A/K176,181E* (*mus81-KER*) in order to address some of these possibilities.

I would like to acknowledge two project students who worked with me on this part of the project; Ms Sarah Curry constructed the *mus81-DD* and *mus81-R165,168A* mutants and helped to set up the site-directed mutagenesis. Ms Rebecca Haigh constructed the mutant *mus81-Y122A/R123A*.

Figure 6.2 *(following page)*: DNA damage sensitivity of conserved residues in the *S. pombe* Mus81 WH domain

A) Cartoon of *S. pombe* Mus81. Indicated in grey are the residues corresponding to the hMUS81 WH domain (117-214). The box below shows a close-up of the WH domain and lists an overview of the point mutations analysed. A; alanine, E; glutamate. Whether these mutations affect the N-terminus or the recognition helix a3 is indicated. Abbreviations, *KE* for *mus81-K176,181E* and *KER* for *mus81-R165,168A/K176,181E*, are indicated. The four helices (a1-a4) and the two β-strands are shown in grey rounded squares and arrows, respectively.

B) DNA damage sensitivity analysis of WH mutants as indicated in **A**. Cells were grown overnight, diluted and spotted onto YEA plates containing DNA damaging agents as indicated, CPT; camptothecin (dissolved in DMSO), MMS; methyl methanesulfonate, HU; Hydroxyurea, 4-NQO; 4-nitroquinoline 1-oxide. The control with DMSO contains the same concentration corresponding the one in 2μM CPT. Control strains (501; wild-type, *mus81*$^+$; *mus81*$^+$ integrated in the base strain, *mus81*Δ; *mus81* base strain, *mus81-DD*; nuclease-dead D395,396A (Boddy et al., 2001) and *mus81-WH*Δ; WH domain delete are encircled in grey. All the point mutants are integrated in the *mus81* base strain and a3 and N indicate the position of the mutation in the recognition helix a3 or the N-terminal part of the domain, respectively. Cells were spotted in 10-fold dilutions from left to right, starting with 10^5 cells. The genotypes of the strains are listed in Materials and Methods. Strains used: *mus81*Δ; SAS48, *mus81-DD* (D395,396A); SAS240, *mus81*$^+$; SAS70; *mus81-WH*Δ; SAS72, R165,168A; SAS243, K176,181A; SAS74, R165,168A K176,181A; SAS260, K176,181E; SAS293, R165,168A K176,181E; SAS337, H189A K192A; SAS296, Y122A R123A; SAS340, R113A K114A R115A K116A; SAS396.

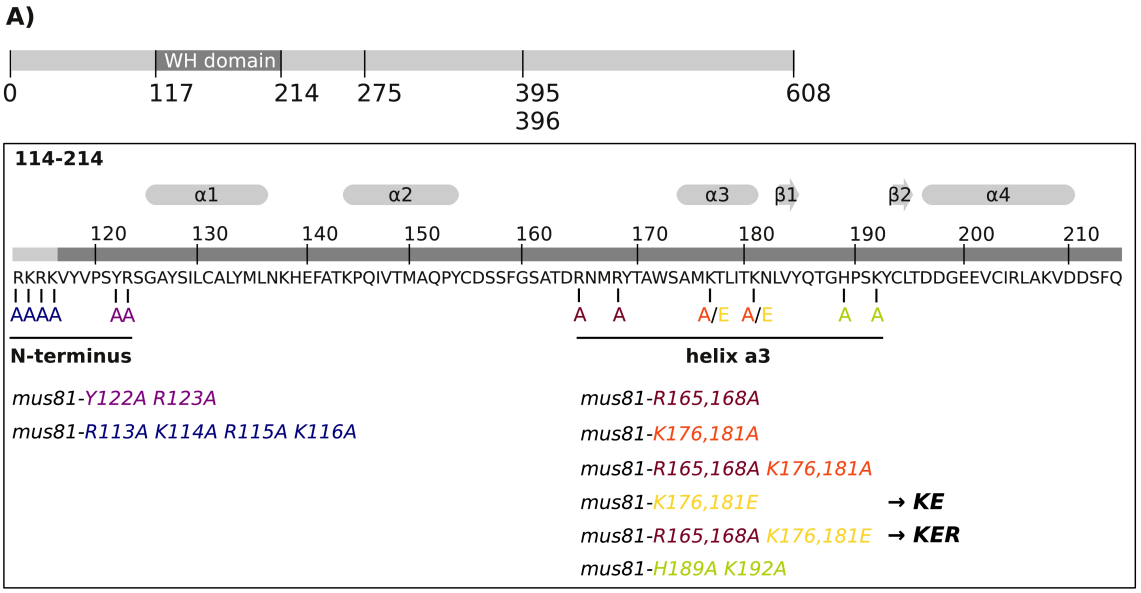
A)
WH domain
0
117
214
275
395
396
608
114-214
α1
α2
α3
β1
β2
α4
120
130
140
150
160
170
180
190
200
210
RKRKVYVPSYRSGAYSILCALYMLNKHEFATKPQIVTMAQPYCDSSFGSATDRNMRYTAWSAMKTLITKNLVYQTGHPSKYCLTDDGEEVCIRLAKVDDSFQ
AAAA
AA
A
A
A/E
A/E
A
A
N-terminus
helix a3
mus81-Y122A R123A
mus81-R113A K114A R115A K116A
mus81-R165,168A
mus81-K176,181A
mus81-R165,168A K176,181A
mus81-K176,181E → KE
mus81-R165,168A K176,181E → KER
mus81-H189A K192A

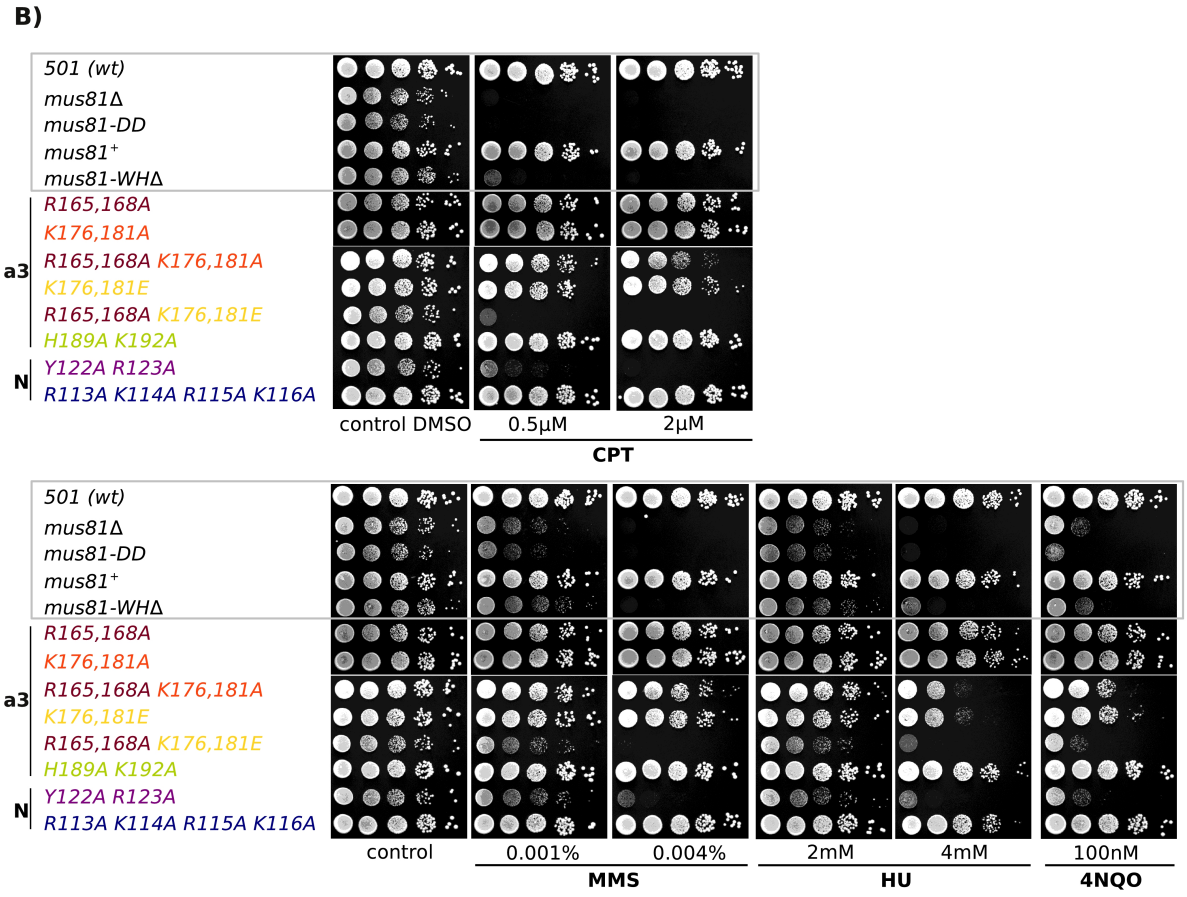
B)
501 (wt)
mus81Δ
mus81-DD
mus81+
mus81-WHΔ
a3
R165,168A
K176,181A
R165,168A K176,181A
K176,181E
R165,168A K176,181E
H189A K192A
N
Y122A R123A
R113A K114A R115A K116A
control DMSO
0.5μM
2μM
CPT
control
0.001%
0.004%
2mM
4mM
100nM
MMS
HU
4NQO

6.4 Effects of WH mutations on protein localisation

Mus81-Eme1 is a nuclear protein and its correct localisation is vital for its function as an endonuclease (Chen et al., 2001). A functional analysis in *S. cerevisiae* has shown that the N-terminus of Mus81 is essential for nuclear localisation (Fu and Xiao, 2003). I assayed localisation of *mus81-WH*Δ mutants by microscopy and chromatin fractionation.

For the chromatin fractionation assay, a C-terminal TAP tag was fused to the endogenous copy of the *mus81* mutants. Expression of TAP-tagged wild-type, *mus81-WH*Δ, *mus81-KE* and *mus81-KER* strains was tested by western blot (Figure 6.3A). All proteins were expressed at their expected sizes and at similar levels. The TAP-tagged strains were analysed by spot tests for interference of the TAP-tag with their *in vivo* function. The TAP-tagged and untagged *mus81*$^+$ showed no sensitivity at the concentrations used (Figure 6.3B). The *mus81-WH*Δ-TAP strain showed no additional sensitivity as compared to *mus81*Δ. As for the *mus81-KE* and *mus81-KER* mutants, the TAP tag shows no effect on *mus81-KER*, whereas there is a slight additional sensitivity to MMS of the *mus81-KE*-TAP mutant. Overall the TAP-tagged strains had a slightly increased generation time compared to the untagged strains, but the tag did not have a major impact on the *in vivo* function of the protein.

For the chromatin fractionation, exponentially growing cells were harvested and the cell wall digested. They were lysed and protein extracts were split into three equal aliquots for the fractionations: whole extract (W), soluble (S) and chromatin fraction (C). The chromatin fraction was separated using a sucrose cushion. The fractions of wild-type and mutant C-terminally TAP-tagged strains were analysed by western blot (Figure 6.3C). An equal amount of sample was loaded for W and S, whereas 5-times more was used for C, because of possible protein loss in the sucrose centrifugation step. In order to control for the fractionation, α-tubulin and histone H3 were analysed on the same membrane. α-tubulin was detected in S and H3 in C, showing that the separation of the fractions was successful (Figure 6.3C). The TAP-tagged Mus81, *Mus81-WH*Δ and *Mus81-KER* proteins accumulated in the chromatin fraction. The level of *Mus81-WH*Δ was reduced in the chromatin fraction compared to Mus81 and *Mus81-KER*, but it is unlikely that this would cause the observed phenotype since the *Mus81-KER* mutant with a similar phenotype shows levels comparable to wild-type Mus81 in the chromatin fraction.

Localisation by immunofluorescence microscopy of the TAP-tagged Mus81 variants was unsuccessful, possibly because of low abundance of Mus81. Fu and Xiao (2003) have analysed Mus81 and Mms4 localisation by overexpression of GFP-tagged proteins. I therefore cloned Mus81 wild-type, *mus81-WH*Δ and *mus81-KER* into a plasmid which allows overexpression under the *nmt41*$^+$ promoter and visualisation by fusion to a N-terminal EGFP fluorophore. Ex-

pression was induced for 18 hours, the cells were fixed with methanol and analysed with a Delta Vision microscope (Figure 6.3D). The dispersed green staining of the whole cell observed for the vector only control could be due to autofluorescence or expression of the EGFP molecule (Figure 6.3D). In comparison, the cells expressing the EGFP-tagged wild-type and mutant Mus81 proteins showed a distinct accumulation of green signal, which colocalises with DAPI staining and can therefore be interpreted as nuclear localisation.

In summary, the chromatin fractionation and overexpression experiments demonstrate that the phenotypes of the *mus81-WH*Δ mutants shown in Figure 6.2B are not due to mislocalisation of the proteins.

Figure 6.3 *(following page)*: Localisation of Mus81 WH mutant proteins
A) C-terminally TAP-tagged Mus81 wild-type and mutant cells were grown to exponential phase and proteins were extracted. Whole cell extracts were separated by SDS-PAGE and transferred to a nitrocellulose membrane. Proteins transferred were stained with Ponceau. TAP-tagged proteins were detected with peroxidase anti-peroxidase (PAP). The first lane contains extract from an untagged control strain (501). Expected molecular weights are indicated in the box on the right. The molecular weight marker is indicated on the left. The genotypes of the strains are listed in Materials and Methods. Strains used: Mus81-TAP; SAS973, *Mus81-WH*Δ-TAP; SAS975, *Mus81-KE*-TAP; SAS977, *Mus81-KER*-TAP; SAS979.
B) Spot test of TAP-tagged WH mutants. As described in Figure 6.2B. The presence of the TAP tag is indicated on the left and the DNA damaging agents below the pictures.
C) Chromatin fractionation of TAP-tagged *mus81*$^+$, *mus81-WH*Δ and *mus81-KER*. Exponentially growing cells were digested, lysed and chromatin was isolated using a sucrose cushion (see Materials and Methods). W; whole extract, S; soluble fraction/supernatant, C; chromatin fraction. Samples were separated by SDS-PAGE whereby 5x more was loaded of fraction C. The first 3 lanes are from an untagged wid-type strain (no tag). The purity of fractions was analysed with anti-α-tubulin and anti-histone H3. The Mus81-TAP constructs were probed with peroxidase anti-peroxidase (PAP). The arrows on the right indicate the TAP-tagged proteins.
D) Representative pictures of cells overexpressing EGFP-tagged Mus81 WH mutant proteins. The wild-type and mutant proteins were expressed under the control of the *nmt41*$^+$ promoter from a vector containing an N-terminal fusion of the EGFP fluorophore (vector 469, plasmid collection Carr lab). Cells were grown in selective media (-leucine) and expression was induced by removal of thiamine for 18 hours. Cells were fixed with methanol and analysed for EGFP and DAPI staining with a DeltaVision microscope. Samples are indicated on the right and detection for EGFP or EGFP and DAPI at the top.

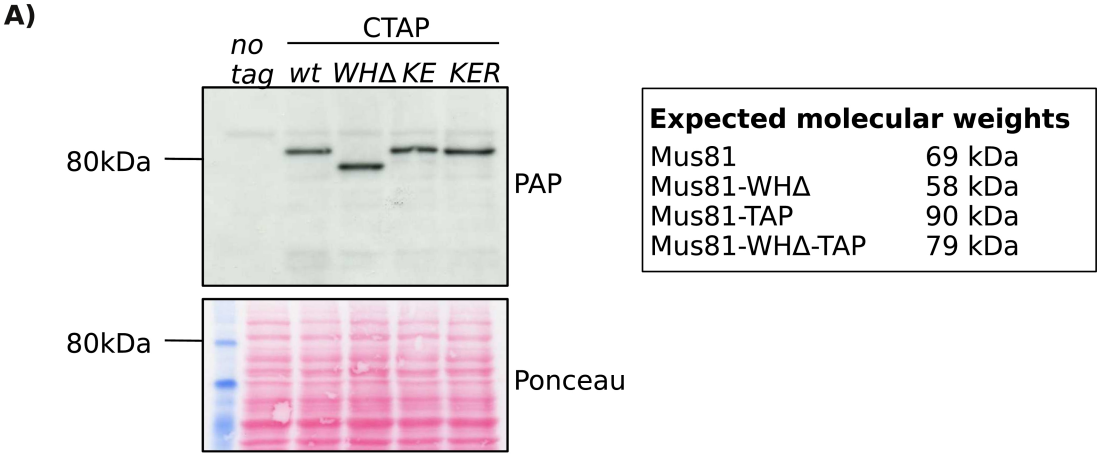
A)
CTAP
no tag
wt
WHΔ
KE
KER
80kDa
PAP
80kDa
Ponceau
Expected molecular weights
Mus81 69 kDa
Mus81-WHΔ 58 kDa
Mus81-TAP 90 kDa
Mus81-WHΔ-TAP 79 kDa

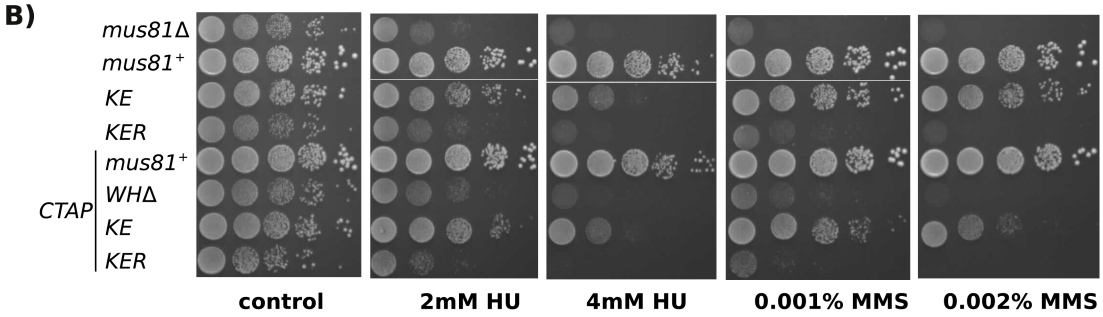
B)
mus81Δ
mus81+
KE
KER
CTAP
mus81+
WHΔ
KE
KER
control
2mM HU
4mM HU
0.001% MMS
0.002% MMS

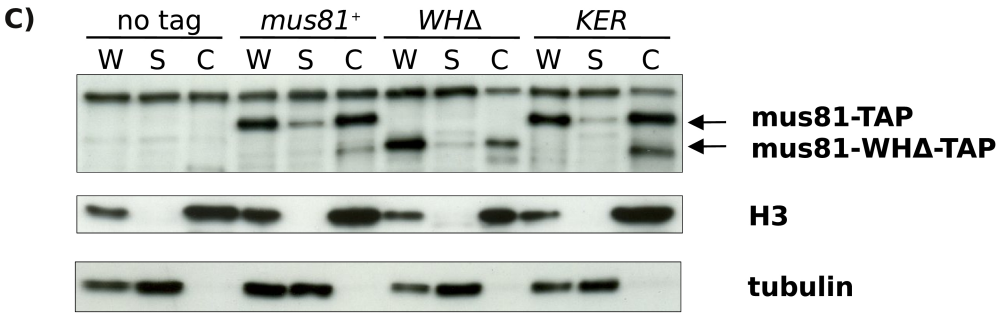
C)
no tag
mus81+
WHΔ
KER
W S C W S C W S C W S C
mus81-TAP
mus81-WHΔ-TAP
H3
tubulin

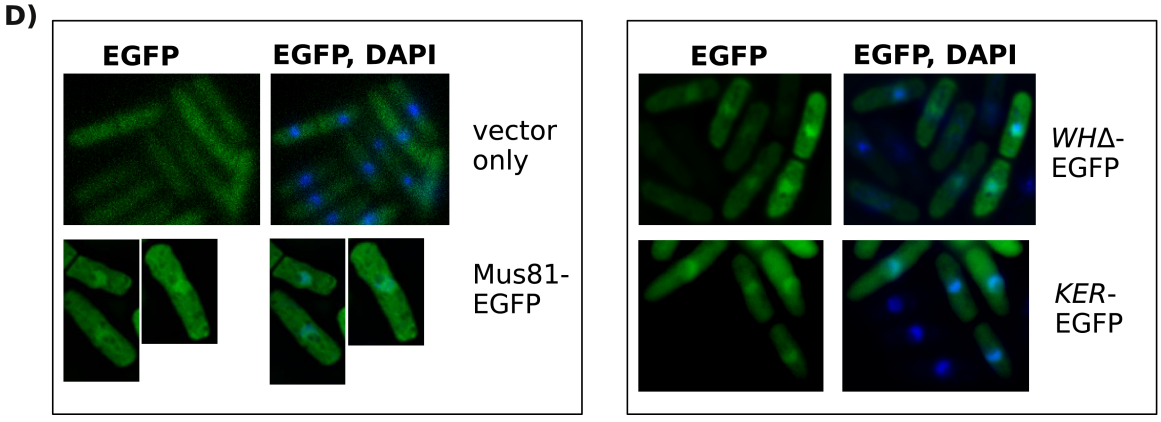
D)
EGFP
EGFP, DAPI
vector only
Mus81-EGFP
EGFP
EGFP, DAPI
WHΔ-EGFP
KER-EGFP

6.5 The *mus81-KE* mutant: a separation of function?

One of the first phenotypes characterised for *mus81*Δ cells, was the requirement for *mus81*$^+$ in meiosis in *S. pombe*. Boddy et al. (2001) reported a spore viability of 0.1% of *mus81*Δ cells due to a defect after meiotic DSB formation, which resulted in an inability to equally segregate the DNA between the four spores. I tested the spore viability of *mus81-KE* and wild-type cells (Figure 6.4A). Both strains showed very similar spore viability and tetrad dissection resulted mainly in viable spores. Therefore, *mus81-KE* seems to be proficient in the meiotic role of Mus81. Osman et al. (2003) suggested that the role of Mus81 in meiosis might be the processing of D-loops that form prior to a double HJ.

An assay, in which Mus81 was also suggested to resolve a D-loop, following a one-ended DSB, was developed by Roseaulin et al. (2008). I decided to analyse the proficiency of *mus81-KE* in the repair of a polar DSB with this assay. Taking advantage of the well characterised mating type locus and switching mechanism in *S. pombe*, Roseaulin et al. (2008) used two particular strain backgrounds to generate a one-ended or polar DSB (Figure 6.4B). Strain 1 is proficient for an imprint (single-strand break, SSB) at the mating-type locus (*mat1*), which will be converted to a DSB during the next round of replication, but lacks the homologous sequences (*mat2,3*Δ), which are normally used for the repair of the DSB. Strain 2 is deficient for the imprint (-SSB), but proficient for the homologous *mat2,3* regions and contains the mutant background to analyse (*mus81*Δ, *mus81-KE*).

The two strains were crossed and the progeny were used to analyse the ability of *mus81* mutants to repair a polar DSB using the sister-chromatid template. In this assay, *mus81*$^+$ has been previously shown to be essential for sister-chromatid recombination (Roseaulin et al., 2008). I used the assay with *mus81*Δ and *mus81-KE* (Figure 6.4C). As expected, cells proficient for the SSB (+SSB) were dead or very sick in combination with the *mus81*Δ allele (Roseaulin et al., 2008). However, *mus81-KE* cells were viable, which suggests that *mus81-KE* is proficient in its function in sister-chromatid recombination. Damage induced by CPT can lead to DSBs during replication. The relatively mild sensitivity of *mus81-KE* to CPT, compared to *mus81*Δ, is in agreement with its proficiency in sister-chromatid recombination (Figure 6.4C).

*mus81*Δ is synthetically lethal with *rqh1*Δ (Boddy et al., 2000). This suggests that *mus81*$^+$ and *rqh1*$^+$ have essential overlapping functions or in the absence of one protein, toxic substrates are formed which require the processing by the other protein. There is evidence that the lethality of these double mutants can be suppressed by eliminating the HR-mediator *swi5*$^+$ which suggests that in the absence of *mus81*$^+$ and *rqh1*$^+$, toxic recombination intermediates are formed (Akamatsu et al., 2007; Hope et al., 2007). Roseaulin et al. (2008) found that *rqh1*$^+$ was not required

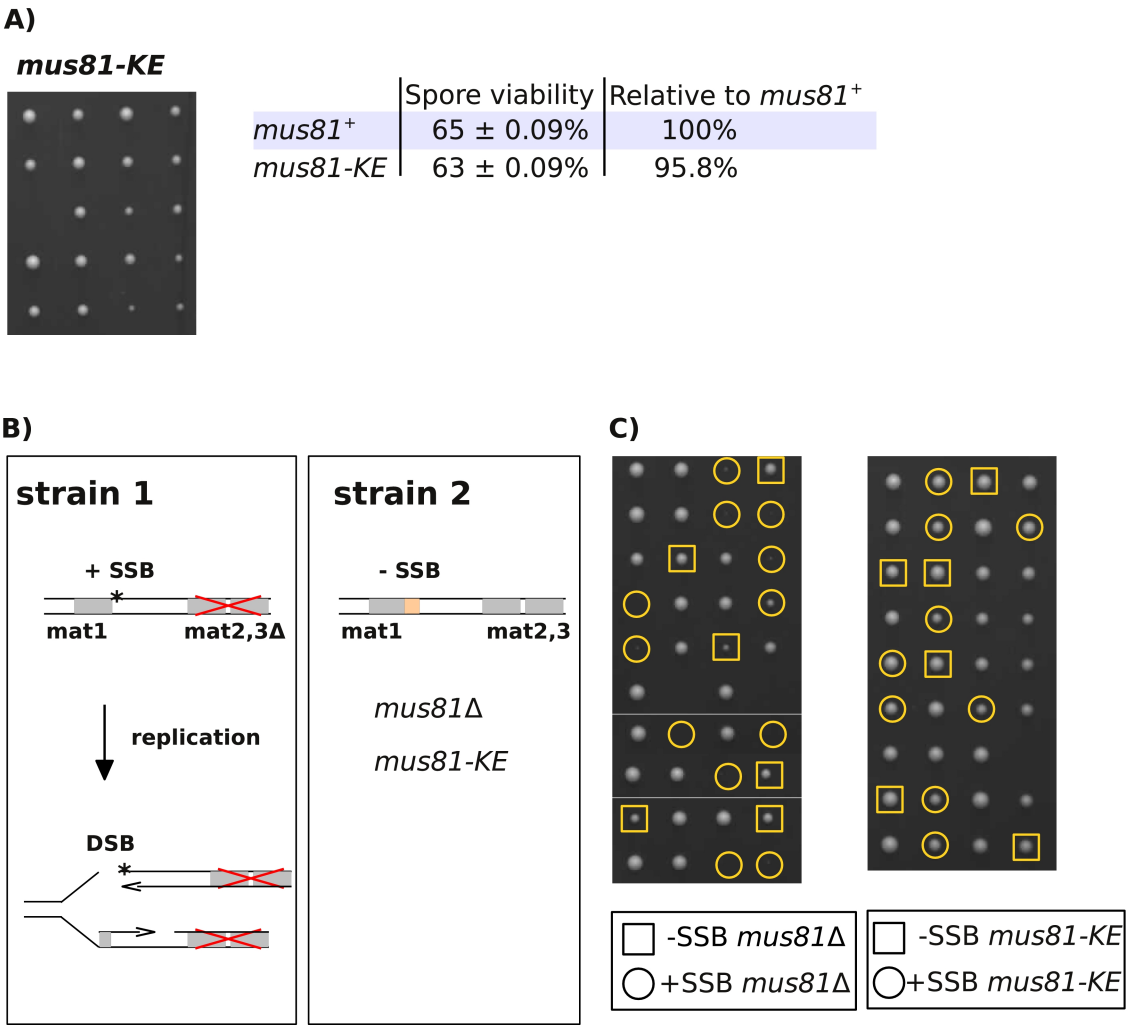

Figure 6.4: *Mus81-KE* is proficient in meiosis and sister-chromatid recombination
A) Tetrad dissection of *mus81-KE* cells. SAS293 (*mus81-KE*, h^-) was mated with SAS573 (*mus81-KE*, h^+) on low nitrogen (ELN) plates for 2 days at 25°C and tetrads were dissected on YEA plates and incubated at 30°C for 3-4 days (see Materials and Methods). The spore viability of wild-type and *mus81-KE* mutants are shown in the table on the right. Two independent matings of SAS293/SAS573 (*mus81-KE*) or SAS70/SAS567 (*mus81*$^+$) were incubated on low nitrogen (ELN) plates for 2 days at 25C. Three independent digests with snail enzyme from these two matings were set up for spore viability analysis. Spores were counted and 500 spores were plated on YEA plates (3 each). The average number and standard deviation are shown.
B) Cartoon of the sister-chromatid recombination assay developed by Roseaulin et al. (2008). Indicated is the mating type locus with *mat1* and the homologous regions *mat2,3* (grey boxes). The asterisk shows the position of the imprint if proficient (+SSB; single-strand break) and deficiency in SSB formation (-SSB) is shown as an orange box . The mutant *mus81* strain backgrounds are shown for strain 2.
C) Tetrad analysis of tester strains in *mus81* mutant backgrounds. Strains SAS564 (*mus81*Δ; -SSB) and SAS573 (*KE*; -SSB) were mated with SAS558 (+SSB; *mat2,3*Δ; *mus81*$^+$) and tetrads were dissected on YEA plates (as described in **A**). *mus81* mutants deficient for the imprint (-SSB) are marked with boxes and *mus81* mutants proficient for the imprint (+SSB) are encircled. The *mus81*Δ and *mus81-KE* alleles were identified by colony PCR (primers 299/300 for *mus81-KE* and 291/299 for *mus81*Δ) and the mating type by mating to tester strains.

for sister-chromatid recombination at the mating-type locus, which is in agreement with its anti-recombinogenic function, but might be due to other helicases substituting for *rqh1*$^+$ (Roseaulin et al., 2008). In order to investigate the genetic interaction between *mus81-KE* and *rqh1*$^+$ I tested the viability of the double mutant. Figure 6.5A shows the tetrad analysis of crosses between *mus81-KE* and *rqh1*Δ cells. The double mutants are clearly inviable. Therefore I can conclude that the function of *mus81*$^+$ that is important to ensure viability in the absence of *rqh1*$^+$, is compromised in the *mus81-KE* mutant. It was shown in human cells that the RecQ helicase BLM co-localises and interacts with MUS81 *in vivo* and also stimulates the activity of Mus81 (Zhang et al., 2005). Because the mapped interaction domain overlaps with the WH domain in Mus81, Fadden et al. (submitted) tested this interaction with purified proteins, but could not reproduce this result. Whether Mus81 and Rqh1 in *S. pombe* physically interact, is currently unknown.

The human FEN1 5'-flap endonuclease interacts with the RecQ helicases BLM and WRN and this interaction has been suggested to stimulate the endonuclease activity of FEN1 (Brosh et al., 2001, 2002; Sharma et al., 2008). The FEN1 homologue Rad27 in *S. cerevisiae* was shown to interact with Mus81 and increase its activity (Kang et al., 2010). Interestingly, *RAD27* is synthetically lethal with *MUS81* (Tong et al., 2001) and this genetic interaction is conserved in *S. pombe* between the FEN1 homologue *rad2*$^+$ and *mus81*$^+$ (Osman and Whitby, 2007). Additionally, *rad2*Δ/*rad27*Δ is also synthetically lethal with the RecQ helicases *rqh1*Δ/*sgs1*Δ in *S. pombe* and *S. cerevisiae*, respectively (Liu et al., 1999; Tong et al., 2001). I therefore tested the viability of *rad2*Δ *mus81-KE* cells in *S. pombe* by tetrad dissection. As shown in Figure 6.5B, the double mutant *rad2*Δ *mus81-KE* is viable, suggesting that *mus81-KE* is proficient in the function which is required in the absence of *rad2*$^+$.

The essential Smc5/6 complex has important functions in replication and recombination and *mus81*$^+$ was shown to be essential if the Smc5/6 complex is compromised (Morikawa et al., 2004; Torres-Rosell et al., 2005). Like *mus81*Δ, *mus81-KE* is lethal in combination with *rad62-1* (*nse4-1*) and *smc6-X*, but viable with *smc6-74* (Figure 6.5C) (Morikawa et al., 2004; Sheedy et al., 2005, J. Murray, personal communication). *mus81-KE* is therefore deficient in ensuring viability if the Smc5/6 complex is impaired. Interestingly, while both, *smc6-X* and *smc6-74* are reported to be defective in their role in HR after replication fork collapse, *smc6-74* in addition is defective in keeping HU-stalled forks in a recombination-competent state (Irmisch et al., 2009).

Mus81 was shown to be regulated by the checkpoint kinase Cds1 in *S. pombe* (Kai et al., 2005). Cds1-dependent phosphorylation of Mus81 after acute HU treatment, resulted in the dissociation of Mus81 from the chromatin (Kai et al., 2005). I combined the allele *mus81-KE* with a mutation which abolishes the interaction with Cds1 and therefore Cds1-dependent regulation (*mus81-*

T275A). Throughout the literature the *mus81-T275A* mutation is annotated as *mus81-T239A*, which resulted from a difference in residue numbering in the original publication (Boddy et al., 2000). Both annotations concern the same Threonine residue of the T-X-X-D motif in Mus81 (Kai et al., 2005). Abolishing Cds1-dependent regulation of Mus81 had no effect on the sensitivity to DNA damaging agents of *mus81-KE* (Figure 6.5D). However, this regulation was shown after acute treatment with HU, and I have only checked chronic treatment so far. Further experiments under different conditions would be needed to allow conclusions about the exact phenotype of *mus81-KE/T275A*.

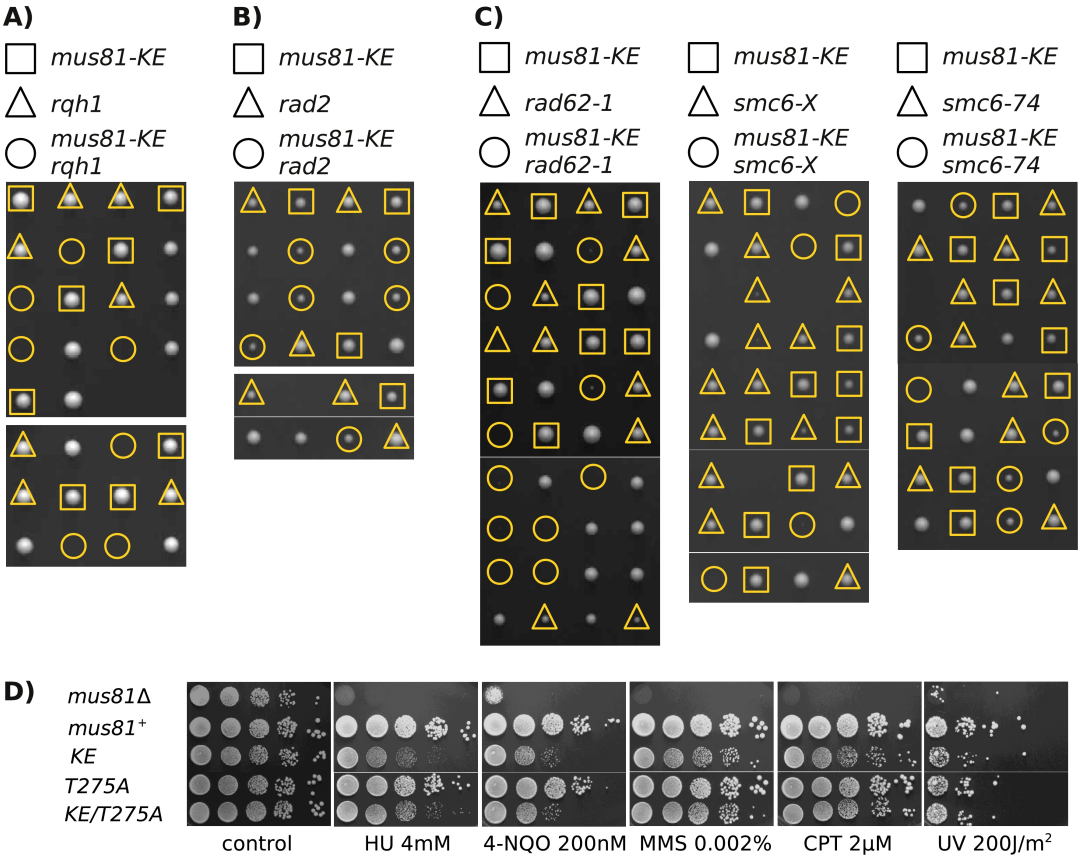

Figure 6.5: Genetic interactions of *mus81-KE* with *rad2*Δ, *rqh1*Δ and mutant alleles of the Smc5/6 complex

A)-C) Strains were mated and tetrads were dissected on YEA plates as described in Figure 6.4A. *mus81-KE* mutants are shown in boxes. *rqh1*Δ, *rad2*Δ, *rad62-1*, *smc6-x* and *smc6-74* mutants are shown in triangles and the corresponding double mutants are encircled. The strains used in **A** are SAS293/573 (*mus81-KE*) and SAS1058/1059 (*rqh1*Δ). The strains used in **B** are SAS293/778 (*mus81-KE*) and AMC168 (*rad2*Δ). The strains used in **C** are SAS293 and SAS501/502 (*rad62-1*), SAS507 (*smc6-X*), SAS512 (*smc6-74*). The presence of the mutant alleles was tested for by replica plating onto plates containing G-418 disulphite (*rqh1::kanMX6*), or lacking uracil (*rad2::ura4*), or by colony PCR with primers 299/300 (*mus81-KE*), 163/303 (*rad62-1*), 313/315 (*smc6-X*) and 317/318 (*smc6-74*).

D) DNA damage sensitivity of *mus81-KE* combined with *mus81-T275A*. Cells were grown and spotted as described in Figure 6.2B. DNA damaging agents are indicated below the pictures. The genotypes of the strains are listed in Materials and Methods. Strains used: *mus81*Δ; SAS48, *mus81*$^{+}$; SAS70, T275A; SAS469, KE; SAS293, T275A/KE; SAS471.

6.6 Conclusion and discussion

Fadden et al. (submitted) identified a novel conserved domain in the N-terminus of human MUS81. The structure was determined by NMR which showed that it folds into a winged helix (WH) domain. The N-terminus of MUS81 is not well characterised as previous crystal structures were N-terminal truncations (Chang et al., 2008). However, it has been reported that the N-terminus of *MUS81* is important for nuclear localisation in *S. cerevisiae* (Fu and Xiao, 2003) and interacts with BLM and SLX4 in human cells (Zhang et al., 2005; Fekairi et al., 2009). WH domains are thought to be important for DNA-binding and protein-protein interactions (Gajiwala and Burley, 2000). The interaction site of MUS81 with BLM overlaps with the newly identified WH domain, however Fadden et al. (submitted) could not reproduce the interaction between these proteins. The WH domain was shown to bind ssDNA and dsDNA *in vitro* and to affect the cleavage activity of MUS81-EME2, but not MUS81-EME1 complexes (Fadden et al., submitted).

In *S. pombe*, Mus81 forms a complex with Eme1, which is the only identified homolog of the human EME1 and EME2 proteins. A mutational analysis of the WH domain was carried out in order to establish its significance *in vivo*. Strikingly, the deletion of the WH (*WH*Δ) domain resulted in a complete loss of function when tested for DNA damage sensitivity. *mus81-WH*Δ showed a similar phenotype as *mus81*Δ or the nuclease-dead protein *mus81-DD*. This suggests that either the WH domain has an essential function in the Mus81-Eme1 complex in the response to DNA damage or its deletion impaired other essential parts of the complex.

In vitro experiments with the human WH domain demonstrated that the recognition helix a3 and the N-terminal part of the domain are important for DNA-binding and a double mutation in the helix a3 (*R186,191A*) resulted in a 10-fold decrease in DNA-binding (Fadden et al., submitted). Although the *in vivo* analysis in *S. pombe* on corresponding residues found combinations of mutations which resulted in a *WH*Δ phenotype, there were discrepancies to the *in vitro* data of the human MUS81 WH domain (Figure 6.2B). The mutations *K176,181A* in *S. pombe* which correspond to *R186,191A* in the human protein, had no effect on DNA damage sensitivity. Mutation of these residues to glutamate (*K176,181E* or *mus81-KE*) or combination with two other mutations (*R165,168A/K176,181A*) resulted in an intermediate sensitivity to 4-NQO and HU, whereas the tested concentrations of CPT and MMS were tolerated well. Further enhancement of these mutations by combining *mus81-KE* with *R165,168A*, abolished the residual function of Mus81-Eme1 and showed a phenotype similar to *mus81-WH*Δ.

The gradual increase in severity of the phenotype could result from an increase in deformation of the structure, dependent on the number of mutated residues or their change in charge. Chang et al. (2008) demonstrated that the folding of the nuclease and $(HhH)_2$ domains of the N-terminally

truncated zebrafish Mus81ΔN, its complex formation with *h*EME1ΔN and its nuclease activity were intact. However a distortion of the WH domain could still interfere with the overall structure of the complex. It was unexpected to find a phenotype which is relatively more severe in response to HU and 4-NQO as compared to CPT and MMS.

*mus81*Δ cells elongate without exposure to DNA damage, grow relatively slowly compared to wild-type cells and activate the checkpoint delay of mitosis (Boddy et al., 2000). Also spontaneous diploidisation has been observed in *mus81*Δ cells (K. Tomita, personal communication and own observations). Consistent with the intermediate phenotype in the response to DNA damage, *mus81-KE* cells have a rather mild morphological phenotype and only a comparably small fraction of cells elongate. The observation of intermediate phenotypes suggests that the severe loss of function in *mus81-WH*Δ is most likely not due to impaired localisation of the protein in the cell. In agreement with this assumption *Mus81-WH*Δ-TAP and *Mus81-KER*-TAP localise to the nucleus like the Mus81-TAP protein (Figure 6.3C and D).

Functional analysis of *mus81-KE* showed that, in contrast to *mus81*Δ, it is proficient in meiosis and sister-chromatid recombination (Figure 6.4C). In agreement with this, *mus81-KE* cells are not sensitive to replication-associated DSBs arising after treatment with CPT.

*mus81*Δ cells are synthetically lethal with proteins that function in replication and repair (Osman and Whitby, 2007). In order to investigate genetic similarities and discrepancies of *mus81-KE* and *mus81*Δ cells, I analysed genetic interactions of *mus81-KE* with mutants that are already known to cause lethality in combination with *mus81*Δ. Interestingly, *mus81-KE* was synthetically lethal with mutant alleles of the Smc5/6 complex (*smc6-X* and *nse4-1*) as well as the RecQ helicase *rqh1*Δ. Although *mus81-KE* was viable in combination with the *smc6-74* mutation, this is in agreement with the viability of *mus81*Δ in this background (Sheedy et al., 2005).

These results were rather surprising because of the relatively mild phenotype of *mus81-KE* cells overall. The synthetic lethality of *mus81*Δ *rqh1*Δ (Boddy et al., 2000) suggests that Mus81 and Rqh1 could resolve the same structure and would therefore be expected to be redundant, or in the absence of one protein, aberrant structures could arise that absolutely require the processing by the other protein. It has been reported that *mus81*$^+$ and *rqh1*$^+$, or *SGS1* in *S. cerevisiae*, function in both overlapping and separate pathways (Doe et al., 2002; Fabre et al., 2002). *mus81*$^+$, but not *rqh1*$^+$, is required for the repair of a polar DSB at the *mat1* locus by sister-chromatid recombination (Roseaulin et al., 2008). This might reflect a function of *mus81*$^+$ that is non-redundant with *rqh1*$^+$. Processing of a D-loop after strand invasion could reset the fork, while branch migration of the single HJ by Rqh1 would regenerate a polar break. That *mus81-KE* was proficient in this

assay, but lethal with *rqh1*Δ thus suggests that *mus81-KE* is defective in a function redundant with *rqh1*$^+$. In order to fully address the question of the interplay between *mus81*$^+$ and *rqh1*$^+$ in general and in respect of the Mus81-WH domain, clarification of the physical interaction of these proteins is required. Also it needs to be shown that the *S. pombe* WH domain acts as a DNA-binding domain and whether it affects the cleavage activity of Mus81-Eme1 complexes. Since the DNA-binding and substrate positioning was shown to be dependent on the nuclease and $(HhH)_2$ domains in the C-terminus (Chang et al., 2008), the role of the WH domain might be in accurate positioning on the substrate, as suggested by Fadden et al. (submitted) and/or in interactions or modifications that regulate the function of Mus81.

mus81-KE cells were found to be viable in the absence of the 5'-flap endonuclease FEN1 homologue *rad2*$^+$ (Figure 6.5B) in contrast to the inviability of *mus81*Δ *rad2*Δ cells (Osman and Whitby, 2007). *rad2*$^+$ is involved in Okazaki fragment processing and a defect in this process could result in ssDNA gaps, leading to DSBs during the next S-phase. Therefore, the viability of *mus81-KE rad2*Δ cells would be in agreement with the proficiency of *mus81-KE* to repair polar DSBs (Figure 6.4C).

Combination of *mus81-KE* with *mus81-T275A* did not enhance its DNA damage sensitivity. However it was shown that despite the Cds1-dependent regulation of Mus81 in response to HU, *mus81*Δ is sensitive to chronic, but not to acute HU treatment ((Kai et al., 2005), and own observations). It has not yet been shown whether *mus81-T275A* is sensitive to acute HU treatment, this needs to be established and repeated in combination with the *mus81-KE* mutations in order to be conclusive. The sensitivity of *mus81*Δ cells in response to chronic HU might be due to fork physiology, as forks could collapse after stalling for a long time. And as mentioned above, there might be alternative mechanisms of Mus81 complex regulation. For example it has been reported that Mms4 and Eme1 undergo phosphorylation and that this might affect Mus81-Eme1/Mms4 activity (Ehmsen and Heyer, 2008; Matos et al., 2011, S. Coulon, personal communication).

In summary, *mus81-KE* cells could have a defect in processing collapsed replication forks or structures associated with them, whereas they are proficient in the repair of broken forks (polar DSB). To gain further insights in the defect of *mus81-KE* cells, *in vitro* experiments are required to establish substrate specificities and it would also be interesting to test whether post-translational modifications or protein-protein interactions are impaired in this mutant.

Chapter 7

Final discussion and conclusions

7.1 The importance of studying DNA replication and genome rearrangements

Replication errors can lead to mutagenesis and disease. The fidelity of replication is controlled on several levels to counteract mutation rates, examples of fidelity include nucleotide selectivity, proofreading and MMR, (Arana and Kunkel, 2010). In addition to point mutations and deletions, also genome rearrangements have been found to be caused by aberrant replication. Lee et al. (2007b) sequenced genomic DNA from patients suffering from PMD (Pelizaeus-Merzbacher Disease) and identified rearrangements linked by microhomology, which could be explained by a model in which replication forks arrest and restart on the wrong template. Complex rearrangements resulting in copy number change of MECP2 have been proposed to occur by replication fork arrest and template switching due to repeat elements in its vicinity (Carvalho et al., 2009). Furthermore, to explain the sequence rearrangements found in human inverted triplication syndromes, Brewer et al. (2011) proposed a model of replication-dependent amplification and integration of a sequence containing an origin and inverted repeats. Importantly, these replication-based models for genome rearrangements differ from the widely accepted models for GCRs resulting from HR in that they do not absolutely require a DSB to initiate the homology-directed rearrangement.

The replication of the genome is of fundamental importance to all forms of live. In order to understand this process several levels of complexity have to be considered. The replisome is a multi-protein complex containing enzymatic activities to unwind and synthesise the DNA at high fidelity and needs to disassemble and reassemble chromatin (Hübscher, 2009). Eukaryotic DNA is not a clean "naked" molecule, but it is organised in higher order structures of chromatin. Chromatin consists of nucleosomes, DNA wrapped around histones, which carry epigenetic markers important for genome regulation (Quina et al., 2006). Chromatin needs to be disassembled to al-

low for DNA synthesis and reassembled in a controlled manner to ensure faithful propagation of epigenetic markers (Sarkies et al., 2010). Proteins other than histones interact with DNA for regulatory purposes or to promote DNA metabolism, such as transcription and replication. Topological stress occurring from unwinding of the DNA has to be released by topoisomerases (Schvartzman and Stasiak, 2004). DNA sequences can have different properties and form secondary structures like hairpins/palindromes, Z-DNA, H-DNA or G4-DNA. The DNA is also altered by lesions which are constantly formed in cells because of endogenous or exogenous sources and these can interfere with DNA metabolism (Friedberg et al., 2004). The interplay of mechanisms ensuring faithful DNA replication and its completion is hence required at the replication fork. Perturbation of replication by encountering these obstacles can inhibit replisome progression and activate checkpoint responses. Checkpoint responses ensure not only the coordination of replication with the cell cycle and repair, but also promote the stabilisation of the replisome (Segurado and Tercero, 2009). This involves, amongst other things, the regulation of enzymatic activities, such as the structure-specific endonuclease Mus81-Eme1 (Kai et al., 2005).

To coordinate specific processes of DNA metabolism, i.e. rDNA transcription and replication, programmed replication fork barriers regulate the direction of replication, as is seen at the heavily transcribed rDNA (Dalgaard et al., 2009). This phenomenon can also be observed in the context of imprinting in *S. pombe* at the mating type locus, which relies on leading and lagging strand specificity (Dalgaard and Klar, 2001). The RFB RTS1 at the mating type locus in *S. pombe* and the rDNA barriers of different organisms function by specific sequence elements and interacting proteins. It is still unclear how these barriers enable the replisome to progress from one direction, but not from the other (Dalgaard et al., 2009).

In eukaryotes, replication is initiated at many sites in the genome and arrested forks can be rescued by forks approaching from the other direction. However, if two converging forks arrest and there is no possibility to fire an origin in between them, continued or restarted DNA replication of at least one of the replication forks is required to ensure the completion of genome duplication. In order to study this process, DNA damaging agents or dNTP depletion could be used. However, site-specifc systems enable us to monitor replication progression and genome instability at specific sites of fork arrest and restart.

During my PhD I have focussed my studies on the stability of short (41-251bp) TRs in the context of G4-DNA, replication and DNA repair. At the same time I have investigated homology requirements for DNA rearrangements after site-specific replication fork collapse and HR-dependent restart. This has enabled me to show that the formation of GCRs does not require homology to the site of fork collapse and can therefore arise from error-prone replication by a restarted fork in

addition to template switching during the restart mechanism. By combining the TR assays and the site-specific fork collapse and restart system I have studied the effect of G4-DNA on TRs when they are replicated by a restarted replication fork.

The structure-specific endonuclease Mus81-Eme1 is regulated in response to replication fork stalling (Kai et al., 2005), but has been shown to be required to ensure replication fork restart at a polar DSB (Roseaulin et al., 2008). In collaboration with Neil McDonald and Andrew Fadden from the London Research Institute, who have identified and characterised a novel DNA-binding domain in *h*MUS81 (Fadden et al., submitted), I have characterised the *in vivo* role of this domain in *S. pombe*.

In order to gain insights into the biochemistry of replication fork collapse and restart I have tried to develop a system for proximity-dependent protein purification. This system could be used to tag proteins like Rtf1, which is responsible for replication fork arrest at RTS1 and would allow us to get a snapshot of the proteins present a this site during replication. This work is added as an appendix. I have already discussed my results in the corresponding chapters, but I would like to give further attention to some key points of my thesis in the next few paragraphs.

7.2 TR deletions in the context of their sequence content

In Chapter 3 of this thesis I investigated the genetic dependencies of TR rearrangements in particular of a 101bp repeat. In this analysis I could not identify a factor responsible for the spontaneous rearrangements, however, the results suggest that the integrity of the replisome or of replisome components is important for the suppression of TR deletions. These experiments were designed to detect deletion events, rather than expansion events or other random rearrangements involving micro-homology directed template switching. This could be a limitation in certain mutants, which might be more prone to result in expansion than deletions (Tishkoff et al., 1997). Strikingly, the TR deletion rates in this assay were significantly increased by mutations in Pol δ as well as deletion of either *swi1*$^+$ or *mrc1*$^+$ (Figure 3.5). As *swi1*$^+$ (*scTOF1*) and *mrc1*$^+$ have been implicated in replication fork stability and checkpoint activation (Alcasabas et al., 2001; Noguchi et al., 2003), their impairment might lower the fidelity of replication and result in a higher mutation rate. A mutant allele of *mrc1*$^+$ that was shown to abolish Cds1 activation, also results in an increase in TR deletions. This is interesting as it implies that the replication checkpoint could be important to maintain repeat stability. However, the separation between the checkpoint function and effect on replication progression of *mrc1*$^+$ in this mutant needs to be clarified.

The fact that the *nat1 101TR* contains a putative G4-motif raised the question of whether possible replication fork arrest at this motif could lead to instability, requiring the checkpoint function

in order to ensure faithful progression of replication and processing of this structure. Checkpoints have been implicated in genome stability at sites containing alternative DNA structures or fragile sites (Voineagu et al., 2009a) and increased replication fork arrest at CGG repeats has been observed in *tof1*Δ and *mrc1*Δ cells in *S. cerevisiae*, although in this assay, the checkpoint function of *mrc1*$^+$ was not required to prevent fork arrest (Voineagu et al., 2009b). My own observation that TR deletions in *mrc1*Δ cells are increased to a different extent in the *nat1 101TR* and the *arg 82TR* assays suggests that *mrc1*$^+$ is more important for replication fidelity in G-rich sequences prone to form secondary structures (Figure 3.6B and Figure 5.2A). These two assays differ mainly in their sequence content as *nat1*$^+$ is GC-rich and *arg3*$^+$ is comparatively more AT-rich.

The development of assays where the direct repeats in *arg3 TR* are bisected by a defined G4 structure on either the leading strand or the lagging strand, as described in Chapter 5, allows detailed analysis of the checkpoint requirements for genome stability in this context. In addition it would be interesting to compare the deletion rate in *nat1 101TR* and *nat1 41TR* in *mrc1*Δ, *swi1*Δ and *cdc6-L591M* cells, because the putative G4-motif is contained in both repeats in *nat1 101TR* whereas only once in *nat1 41TR*. In a wild-type background the deletion rate in both repeats was similar, but analysis in mutant strains would address whether the position of such a G4-motif relative to the repeat makes a difference or if two G4-motifs are worse than one. Ideally one would use repeat sizes of the same length in this analysis. Further work would include the assessment of specific enzymatic requirements in the replication of G4-DNA, such as Rev1 and Pif1 (Ribeyre et al., 2009; Sarkies et al., 2010). I have analysed TR rearrangements in *rev1*Δ cells using the *arg3 82TR* assays, which contain G4-DNA (*G4 TR*) on either the leading or the lagging strand and could not detect a major effect on TR deletions. Candidates that show an effect on TR deletions could then be further tested in the *arg3 82TR* assays with the mutated G4-DNA (*G4m TR*) that reduce the secondary structure or drugs that enhance G4 stability (Piazza et al., 2010, and see Chapter 5) to confirm structure-specificity.

I would like to use these assays to address the requirement for checkpoint, replisome components and other enzymatic activities, such as helicases and polymerases, for the faithful replication of G4-DNA. One limitation of my assays is that only deletion events are detected. In the *arg3 G4* assays a *ura4*$^+$ is placed downstream of *arg3* and can be used to select for random mutations leading to *ura4*$^+$-loss, following replication fork restart and replication of G4-DNA, by resistance to 5-FOA. I am currently developing a separate assay, in which I have altered the sequence of *ura4*$^+$ to contain a G4-motif, keeping functionality of the gene intact. Selection for *ura4*$^+$-loss will allow selection for random mutations induced by the G4-sequence. A mutated G4 in *ura4*$^+$ serves as a control. These assay systems will first have to be verified for their potential to form secondary

structures, but once established, they will allow for a less biased selection of rearrangements and errors.

7.3 Why is replication restarted at RTS1 error-prone?

As described in detail in the introduction (Chapter 1) and in Chapter 5, previous work from our lab and others has characterised replication fork collapse, restart and recombination at RTS1 (Lambert et al., 2005; Ahn et al., 2005; Mizuno et al., 2009; Lambert et al., 2010) (RuraR and RuiuR, Figure 7.1A). In particular, HR-dependent replication fork restart after collapse at an inverted repeat of RTS1 sites results in genome rearrangements (Lambert et al., 2005; Mizuno et al., 2009). The presence of a large palindromic sequence (RuiuR) leads to the formation of acentric and dicentric chromosomes in a high percentage of cells and thus viability loss (Mizuno et al., 2009). Further observations made by K. Mizuno suggest that multiple mechanisms lead to rearrangements as a result of RTS1 activity (K. Mizuno, personal communication). RuiuhR was modified from RuiuR and carries a unique sequence (grey in Figure 7.1B) in the centromere-proximal copy of *ura4*$^{+}$. Analysis of dicentric chromosomes formed after replication fork collapse at RTS1 showed that they contained either one or two copies of this sequence. This suggests that more than one mechanism accounts for the formation of dicentric chromosomes and that strand-invasion could occur at or downstream of the site of fork collapse (K. Mizuno, personal communication). Rearrangements occurring downstream of RTS1 raise the possibility that the restarted replication is error-prone and therefore HR-dependent restart at RTS1 could result in low-fidelity replication. Figure 7.1A shows an overview of the constructs using RTS1 as sites of fork collapse and repeated sequences as a substrate for genome rearrangements. Sites of homology where template switching could occur are indicated with coloured arrows (RTS1: red arrows, repeats downstream of RTS1: blue arrows).

I was interested in the possibility that error-prone replication occurs after replication fork restart. In order to investigate this further and to use this site-specific system of error-prone replication in combination with my TR assays, I took advantage of a modified RTS1 assay constructed by K. Mizuno. In the rura(dir/inv)R systems (see Chapter 4) the homology to the RTS1 site is lost and direct and inverted repeats of the same length and sequence are placed downstream of RTS1 (Figure 7.1A). Using these constructs I demonstrated that homology to RTS1 is not absolutely required for genome rearrangements to occur after fork collapse at RTS1. Also the presence of an inverted repeat downstream of RTS1 (rura(inv)R, Figure 7.1A) resulted in the formation of palindromic chromosomes and orientation switching of the intervening sequence, although at a lower frequency than in RuiuR. In the original RuraR and RuiuR systems an exposed 3'-end at RTS1

has the choice of two closely placed homologous sequences (RTS1) for strand-invasion, but in ruraR, genomic rearrangements are likely to result from a restart event only after the re-invasion of the same copy of RTS1. Repeat rearrangements were not only observed in inverted repeats (rura(inv)R), but also in direct repeats (rura(dir)R) (see Figure 7.1A), although less frequently. These results support the idea that replication following HR-dependent restart at RTS1 is error-prone and that rearrangements occur independently of inverted sequences.

I subsequently combined this system with my TR assays and observed that TR deletions in the 82bp TR in *arg3* 82*TR* (rarg(dir)R, Figure 7.1A) was increased upon RTS1 activation by *Pnmt41-rtf1*$^{+}$ expression. Comparing this result with *arg3 82TR* that contain G4-DNA (*G4 TR*) (rargG4(dir)R, Figure 7.1A) showed that although the presence of G4-DNA increases TR deletions to about the same extent as RTS1 activity, combination of these effects do not result in an increased deletion frequency. I have confirmed these experiments by fluctuation analysis, using endogenous expression of *rtf1*$^{+}$. One could argue that overexpression of Rtf1 leads to a more robust arrest at RTS1 and therefore to a greater requirement of HR factors and processing. However, 2D-gel analysis of ruraR with Rtf1 at endogenous levels has confirmed efficient replication fork arrest at RTS1 and also association of Rad22 (I. Miyabe, personal communication).

Another explanation for the induced TR rearrangements when RTS1 is active would be the change in the direction of replication. While ruraR is replicated mainly from the centromere when RTS1 is OFF, 50% of the replication forks approach this locus from the telomere (through the rDNA barrier) when RTS1 is ON. The possibility that replication from the telomere is responsible for the mutagenic effect is unlikely as rDNA RFBs are not known to induce genomic rearrangements (Calzada et al., 2005, and I. Miyabe, personal communication). Therefore I conclude that the increased instability in large (500bp) and small (82bp) direct repeats induced by RTS1 activity are a result of replication of this locus by a restarted fork. The observation that G4-DNA did not increase the deletion rate in this assay is surprising, because structured DNA is expected to have a mutagenic effect on replication. One explanation for this is that the DNA downstream of RTS1 is replicated by an altered replisome and that a polymerase and/or helicase that is error-free in the replication of G4-structures is part of this alternative complex.

A detailed characterisation of the developed TR assays (described in Chapter 5) could help to establish the genetic requirements not only for G4-DNA replication but also for replication restarted at RTS1. *S. pombe pfh1*$^{+}$ (*scPIF1*), encoding a helicase, would be a good candidate, as it has been implicated in the suppression of genomic instability at protein-DNA barriers (Sofueva et al., 2011). *scPIF1* has been shown to suppress genome instability in the context of G4-DNA and promote its replication (Ribeyre et al., 2009; Paeschke et al., 2011). This model would be

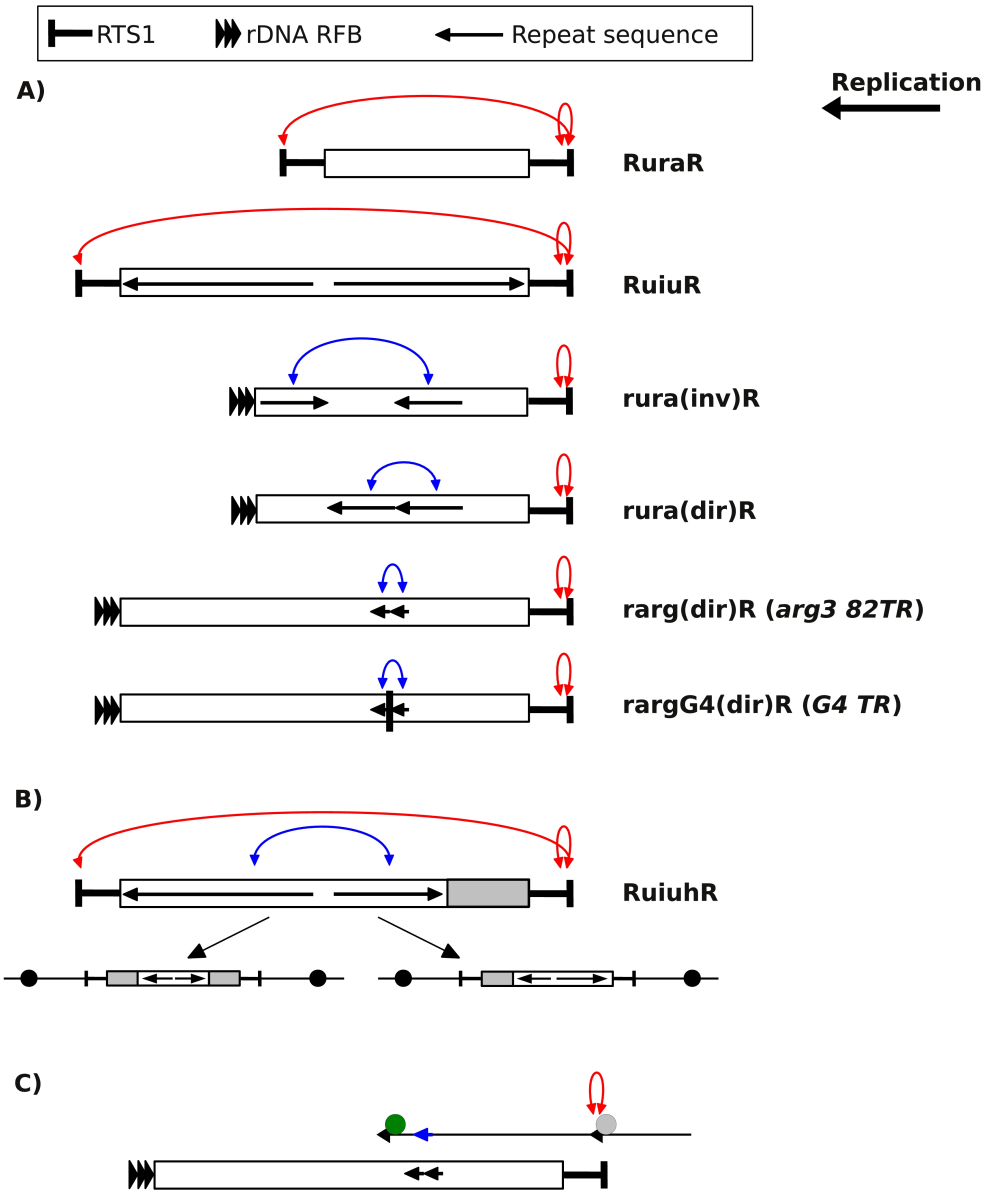

Figure 7.1: Overview of RTS1 constructs and the replication restart model
Top box: Symbols used for RTS1, the rDNA replication fork barrier (rDNA RFB) and repeated sequences. Repeated sequences are indicated by black arrows. Red arrows show homologies to RTS1 as a possible substrate for template switching and blue arrows indicate homologies downstream of RTS1.
A) The majority of replication forks are approaching from the centromere and the direction of replication relative to the constructs is indicated. Schematics of the different RTS1 constructs are shown. rarg(dir)R corresponds to the *arg3 82TR* construct and rargG4(dir)R to the same construct containing G4-DNA (*G4 TR*). The G4-DNA is shown as a black rectangle. In the presence of two RTS1 at the *ura4* locus, the nascent 3'-end can either invade the centromere-proximal or the telomere-proximal copy of RTS1. Replacement of the telomere-proximal RTS1 by the rDNA RFB abolishes the homology to the site of fork collapse and leaves a single RTS1 copy as a template for strand-invasion at the *ura4* locus.
B) RuiuhR represents a construct based on RuiuR. In this construct the 3'-region of the centromere-proximal *ura4*$^+$ was replaced by *his3*$^+$ (grey). K. Mizuno has shown that dicentric chromosomes formed after induction of replication fork collapse at RTS1 contained either one or two copies of the *his3*$^+$ sequence (personal communication). The centromere is indicated as a black cirlce.
C) Model for replication fork restart at RTS1. As an example rarg(dir)R is shown. The replication fork (simplified as black arrow) approaches RTS1 and the replisome (grey circle) arrests and disassembles (fork collpase). Invasion of RTS1 after fork collapse restarts replication. The replisome of the restarted fork contains alternative components (green circle) and can therefore proceed through RTS1 at the cost of genome stability measured as TR deletions (blue arrow).

attractive for an additional reason. Strand invasion and replication fork restart at either copy of RTS1 in RuraR, RuiuR or the constructs using rDNA RFB and RTS1 as barriers does not explain how the replication fork can progress through the barrier. The mechanisms of replication fork collapse and restart are not yet understood in detail. However, if specific fork components such as the MCM helicase were required for efficient arrest, an alternative helicase at the restarted fork would not necessarily be stopped at RTS1. Therefore enzymatic activities during strand invasion or as part of an alternative replisome could allow for replication through RTS1. Figure 7.1C illustrates a possible scenario in which, after replication fork collapse at RTS1, replication restart by re-invasion at the same site continues replication with alternative replisome components.

I have used the *arg3 82TR* assay in order to test for the genetic requirements at a restarted replication fork (Figure 5.7). However this approach needs to be completed by measuring the efficiency of replication fork arrest by 2D-gels and the requirements for the restart mechanism itself by viability loss in RuraR in the mutant backgrounds. A change in or absence of replisome components after restart at RTS1 could also be caused by an alternative mode of replication, such as uncoupling of leading and lagging strand.

K. Mizuno has developed an assay in which an inverted repeat of *ura4* sequences is flanked by an rDNA RFB and RTS1, similar to the rura(dir/inv)R systems. By examining palindromic chromosome formation after replication fork collapse at RTS1 in constructs varying the distance from RTS1, he has recently shown that rearrangements decrease with increasing distance from RTS1 (K. Mizuno, personal communication). This suggests that replication downstream of RTS1 is initially error-prone, but gains in fidelity over time and distance. This supports a model in which the restarted replication fork matures or replisome components are exchanged gradually after the restart (K. Mizuno, personal communication). Furthermore, I. Miyabe is currently investigating the question which polymerase is responsible for DNA synthesis downstream of RTS1. These and future studies which will use ChIP and other methods to identify replisome factors will answer specific questions about the composition of a restarted replisome.

7.4 Which function of Mus81-Eme1 is defective in the *Mus81-KE* mutant?

In the context of replication fork arrest and restart, the structure-specific endonuclease Mus81 is of particular interest. As discussed in the introduction and in Chapter 6, Mus81 has been implicated in the response to replication perturbations and restart of replication forks (Osman and Whitby, 2007). I have analysed the *in vivo* function of a novel domain of Mus81 in *S. pombe*. This domain

(WH domain) has been identified in *h*MUS81 and characterised *in vitro* by Fadden et al. (submitted). The WH domain has no effect on the cleavage efficiency of *h*MUS81-EME1, but reduced the activity of *h*MUS81-EME2 on the splayed arm structure and moved the incision site on the 3'-flaps and the fork structure closer to the branch point. Surprisingly, as compared to these minor effects in *in vitro* assays of *h*MUS81 complexes, deletion of this domain in *S. pombe* seems to abolish *mus81*$^{+}$ function in the response to DNA damage and replication stress (Figure 6.2B). A point mutant (*K176,181E*, *mus81-KE*) in the recognition helix of this domain showed an intermediate phenotype in comparison to *mus81*Δ cells. *mus81-KE* showed a relatively greater sensitivity to HU and 4-NQO as compared to CPT and MMS (Figure 6.2B). Adding more mutations close to these lysine residues increased the phenotype so that it was similar to *mus81-WH*Δ or *mus81*Δ cells. These results suggest a hypomorphic mutant and that the activity is gradually decreased by further deformation of the WH domain.

However, the increased sensitivity to HU and 4-NQO was curious. I decided to investigate *mus81-KE* further by testing known *mus81*Δ phenotypes. Using different assays I found that *mus81-KE* cells are, like *mus81*Δ, lethal in combination with *smc6-X* and *rqh1*Δ and viable with *smc6-74* (Boddy et al., 2000; Sheedy et al., 2005, J. Murray, personal communication and Figure 6.5A and C). However, contrary to *mus81*Δ cells, *mus81-KE* was viable in a *rad2*Δ background and proficient in the repair of a polar DSB (Osman and Whitby, 2007; Roseaulin et al., 2008, Figure 6.5B and Figure 6.4C).

To try and put the *mus81-KE* phenotypes into context and give a possible explanation, I would like to stress the different physiologies of replication forks as explained in the introduction. I defined a "stalled fork" as a structure where the replisome stays associated with the DNA and the ends of the nascent strands are protected, whereas a "collapsed" fork describes the disassembly of the replisome and the exposure of the nascent ends (Lambert et al., 2007; Carr et al., 2011). A "broken" fork is formed either as a result of replication of ssDNA gaps (replisome "run-off") or enzymatic cleavage of a replication fork (Figure 1.2 and Figure 7.2).

The observed phenotypes of *mus81-KE* could be explained by a model in which *mus81-KE* cells are proficient in the downstream processing of a broken fork, but deficient at breaking a fork, i.e. cleavage of a collapsed fork. One could imagine that polar DSBs are formed in cells that replicate DNA with unprocessed Okazaki fragments (gaps) from the previous round of replication in the absence of *rad2*$^{+}$ (Figure 7.2). The viability of *mus81-KE rad2*Δ cells would therefore suggest that *mus81-KE* cells can process downstream intermediates following a polar DSB, which is in agreement with the viability of *mus81-KE* cells in the presence of a polar DSB in the mating type locus (Figure 6.4C and Figure 6.5B). This assumption is further supported by the relatively

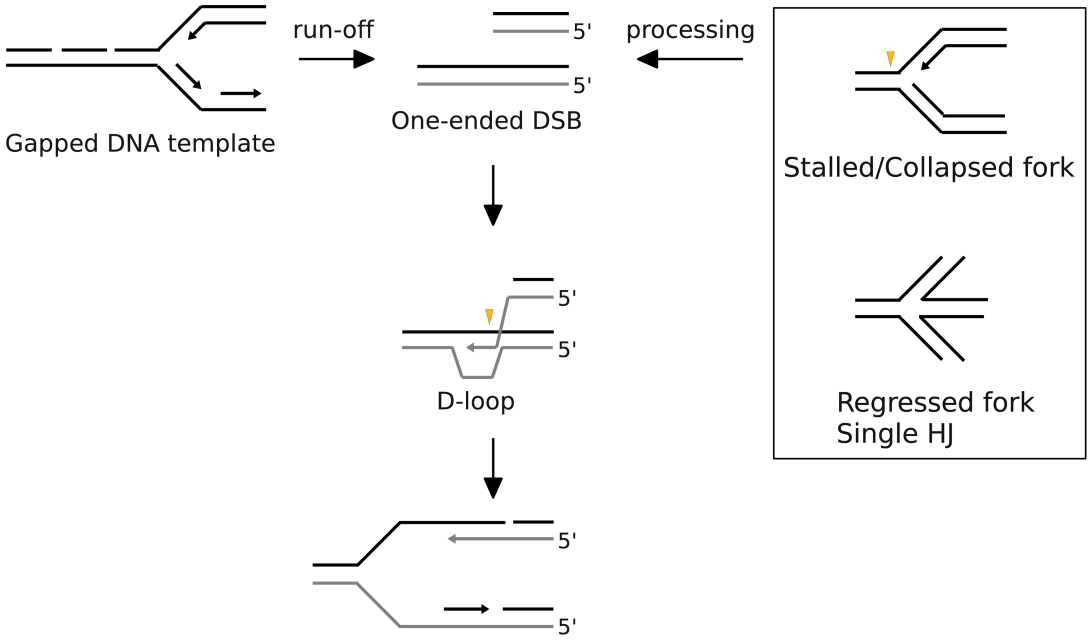

Figure 7.2: Role of Mus81 in the processing of collapsed and broken replication forks and defects in *mus81-KE* cells
Impairment of Okazaki fragment processing could lead to a gapped DNA template, which would result in polar DSBs by polymerase "run-off" in the next round of replication. Similarly, a polar DSB is formed at the mating-type locus in *S. pombe* and can be used as an assay to measure sister-chromatid replication (Roseaulin et al., 2008). Strand-invasion of the resected 3'-end of the DSB into the sister duplex leads to D-loop formation. This intermediate can be processed by Mus81-Eme1 (yellow triangle) resulting in resolution and resetting of the replication fork. Loss of replisome components at stalled replication forks results in fork collapse and can lead to fork regression (single HJ). Processing of such structures by Mus81-Eme1 might be required for replication fork repair.

---

mild sensitivity of *mus81-KE* cells to CPT and the proficiency in processing of HR-intermediates is supported by the lack of a meiotic phenotype in *mus81-KE* cells.

The *S. cerevisiae* RecQ helicase Sgs1 has been shown to stabilise the association of Pol ε and Pol α at stalled replication forks (Cobb, 2003). If RecQ helicases are important for replisome stabilisation, the absence of *rqh1*$^+$ could potentially lead to fork collapse and fork regression (Figure 7.2, box on the right). Assuming that in the absence of *rqh1*$^+$ replication forks collapse, cleavage of these structures by Mus81-Eme1 might be required to restart replication. The inviability of *mus81-KE rqh1*Δ cells could therefore be due to a deficiency in processing of collapsed or regressed forks. The lethality of *mus81-KE smc6-X* cells might be due to a similar reason, as stalled replication forks in *smc6-X* cells are less stable and prone to collapse (Irmisch et al., 2009). It would be interesting to test the synthetic interactions of *mus81-KE* and *swi1*$^+$ and *swi3*$^+$, which are components of the fork protection complex and have been shown to be synthetically sick or lethal with *mus81*Δ (Noguchi et al., 2004).

Although the proposed defect of *mus81-KE* mainly agrees with the observations I made, there

are some caveats. The structures of replication forks and their fate in the mutant backgrounds mentioned above are largely unknown, which makes it difficult to separate collapsed from broken forks. In order to have more insight in the endonucleolytic efficiency of *Mus81-KE*-Eme1, *in vitro* assays with purified proteins could be informative. As key substrates I would test replication fork-like structures, splayed arms, D-loops, HJs and 3'-flaps. However, the deficiency in processing a certain structure might not be directly related to the catalytic efficiency of the protein. Mutations in the WH domain could also impair protein modification, protein-protein interactions and its regulation. As described in Chapters 1 and 6, evidence is accumulating that enzymatic activities stimulate each other through direct interaction and Mus81-Eme1 is regulated by post-translational modifications. An analysis of Mus81, *Mus81-KE* and *Mus81-WH*Δ protein-protein interactions in the response to different damaging agents, as well as post-translation modifications in this context would help to understand a regulatory role of this domain. Residues in the WH-domain might be important for protein modifications.

The observation that the combination of mutations in this domain led from an intermediate (*mus81-KE*) to a severe (*mus81-KER*) phenotype could be due to the gradual impairment of one or several factors. Either the overall structure, or the DNA-binding function is partially or fully affected. Alternatively, a regulatory function might be affected by one mutation and be combined with a deformation of the domain or protein due to another mutation. Keeping in mind that WH domains have been shown to act as protein interaction domains, domain impairment might change the accessibility for interaction partners. Further work is required to understand the function of the Mus81-WH domain and the phenotype of *mus81-KE* cells.

7.5 A biochemical assay for proximity-dependent protein modification

Questions about components important for collapse and restart at RTS1 and Mus81 interaction partners could be answered by pulldown assays of proteins and identification of interaction partners by mass spectrometry. Very often these assays are limited by the strength of the interactions, so that transient interactions or proteins in close proximity are hard to detect. As outlined in Appendix A, I have started to set up a purification assay which would allow the proximity-dependent identification of proteins (Figure 7.3). This assay needs to be further developed and enzymatic activities of the mutated BirA biotin ligase in different constructs should be tested *in vitro*. Once biotinylation of a partner peptide, as for example the Flag tag in Flag-gBirA-R118G, is established, *in vivo* conditions for this assay can be optimised. The introduction of different sized linkers, ei-

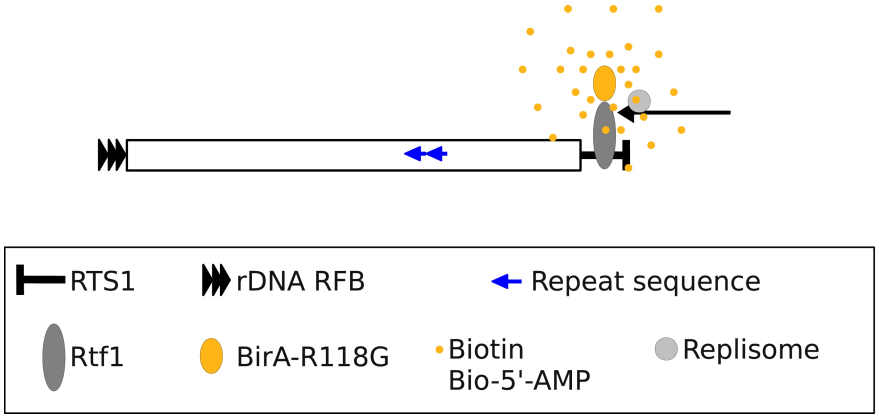

Figure 7.3: Overview of RTS1 constructs and the replication restart model
Proximity-dependent protein biotinylation as a method to gain insight into factor recruitment and interactions. As an example, a replication fork approaching RTS1 is shown. Rtf1 is required for fork arrest and binds to RTS1. Tagging of Rtf1 with the mutated biotin ligase *BirA-R118G* would lead to the release of the intermediate bio-5'-AMP at RTS1. Lysine residues in close proximity could then be biotinylated when reacting with this intermediate. Biotinylated proteins can be purified by streptavidin-coupled magnetic beads and identified by mass spectrometry. The replication fork approaching RTS1 is indicated by an arrow.

---

ther flexible or dynamic, between the ligase and the Flag tag might help to establish the reach of passive biotinylation.

One major drawback of this technique *in vivo* is the high background of endogenous biotinylation. A chromatin fractionation assay as shown in Figure 6.3C might help to lower this background and allow for more efficient purification.

Bibliography

Abraham, J., Lemmers, B., Hande, M. P., Moynahan, M. E., Chahwan, C., Ciccia, A., Essers, J., Hanada, K., Chahwan, R., Khaw, A. K., McPherson, P., Shehabeldin, A., Laister, R., Arrowsmith, C., Kanaar, R., West, S. C., Jasin, M., and Hakem, R. (2003). Eme1 is involved in DNA damage processing and maintenance of genomic stability in mammalian cells. *The EMBO Journal*, 22(22):6137–6147. PMID: 14609959. 141

Acharya, S., Wilson, T., Gradia, S., Kane, M. F., Guerrette, S., Marsischky, G. T., Kolodner, R., and Fishel, R. (1996). hMSH2 forms specific mispair-binding complexes with hMSH3 and hMSH6. *Proceedings of the National Academy of Sciences of the United States of America*, 93(24):13629–13634. PMID: 8942985. 18

Adams, K. E., Medhurst, A. L., Dart, D. A., and Lakin, N. D. (2006). Recruitment of ATR to sites of ionising radiation-induced DNA damage requires ATM and components of the MRN protein complex. *Oncogene*, 25(28):3894–3904. PMID: 16474843. 14

Agmon, N., Yovel, M., Harari, Y., Liefshitz, B., and Kupiec, M. (2011). The role of holliday junction resolvases in the repair of spontaneous and induced DNA damage. *Nucleic Acids Research*. PMID: 21609961. 140

Ahn, J. S., Osman, F., and Whitby, M. C. (2005). Replication fork blockage by RTS1 at an ectopic site promotes recombination in fission yeast. *The EMBO Journal*, 24(11):2011–2023. PMID: 15889146 PMCID: 1142605. 27, 39, 40, 160

Ahnesorg, P., Smith, P., and Jackson, S. P. (2006). XLF interacts with the XRCC4-DNA ligase IV complex to promote DNA nonhomologous end-joining. *Cell*, 124(2):301–313. PMID: 16439205. 21

Akamatsu, Y., Tsutsui, Y., Morishita, T., Siddique, M. S. P., Kurokawa, Y., Ikeguchi, M., Yamao, F., Arcangioli, B., and Iwasaki, H. (2007). Fission yeast Swi5/Sfr1 and Rhp55/Rhp57 differentially regulate rhp51-dependent recombination outcomes. *The EMBO Journal*, 26(5):1352–1362. PMID: 17304215. 138, 149

Albertini, A. M., Hofer, M., Calos, M. P., and Miller, J. H. (1982). On the formation of spontaneous deletions: the importance of short sequence homologies in the generation of large deletions. *Cell*, 29(2):319–28. PMID: 6288254. 69

Alberts, B., Johnson, A., Lewis, J., Raff, M., Roberts, K., and Walter, P. (2002). *Molecular Biology of the Cell [Book and CD-ROM]*. Garland Science, 4 edition. 3, 7, 19, 26, 30

Alcasabas, A. A., Osborn, A. J., Bachant, J., Hu, F., Werler, P. J., Bousset, K., Furuya, K., Diffley, J. F., Carr, A. M., and Elledge, S. J. (2001). Mrc1 transduces signals of DNA replication stress to activate rad53. *Nature Cell Biology*, 3(11):958–965. PMID: 11715016. 9, 12, 15, 82, 84, 87, 126, 158

Allen, C., Ashley, A. K., Hromas, R., and Nickoloff, J. A. (2011). More forks on the road to replication stress recovery. *Journal of Molecular Cell Biology*, 3(1):4 –12. 26, 27

Ansbach, A. B., Noguchi, C., Klansek, I. W., Heidlebaugh, M., Nakamura, T. M., and Noguchi, E. (2008). RFCCtf18 and the Swi1-Swi3 complex function in separate and redundant pathways required for the stabilization of replication forks to facilitate sister chromatid cohesion in schizosaccharomyces pombe. *Molecular Biology of the Cell*, 19(2):595–607. PMID: 18045993 PMCID: 2230603. 139

Araki, H. (2011). Initiation of chromosomal DNA replication in eukaryotic cells; contribution of yeast genetics to the elucidation. *Genes & Genetic Systems*, 86(3):141–149. 4

Arana, M. E. and Kunkel, T. A. (2010). Mutator phenotypes due to DNA replication infidelity. *Seminars in Cancer Biology*, 20(5):304–311. PMID: 20934516. 18, 112, 156

Araújo, S. J., Tirode, F., Coin, F., Pospiech, H., Syväoja, J. E., Stucki, M., Hübscher, U., Egly, J. M., and Wood, R. D. (2000). Nucleotide excision repair of DNA with recombinant human proteins: definition of the minimal set of factors, active forms of TFIIH, and modulation by CAK. *Genes & Development*, 14(3):349–359. PMID: 10673506. 20

Arcangioli, B. and Klar, A. J. (1991). A novel switch-activating site (SAS1) and its cognate binding factor (SAP1) required for efficient mat1 switching in schizosaccharomyces pombe. *The EMBO Journal*, 10(10):3025–3032. PMID: 1915277. 37

Ashton, T. M., Mankouri, H. W., Heidenblut, A., McHugh, P. J., and Hickson, I. D. (2011). Pathways for holliday junction processing during homologous recombination in saccharomyces cerevisiae. *Mol. Cell. Biol.*, 31(9):1921–1933. 24, 138

Aves, S. J. (2009). DNA replication initiation. *Methods in Molecular Biology (Clifton, N.J.)*, 521:3–17. PMID: 19563098. 3, 4, 6

Aylon, Y., Liefshitz, B., and Kupiec, M. (2004). The CDK regulates repair of double-strand breaks by homologous recombination during the cell cycle. *The EMBO Journal*, 23(24):4868–4875. PMID: 15549137. 23

Bachrati, C. Z. and Hickson, I. D. (2008). RecQ helicases: guardian angels of the DNA replication fork. *Chromosoma*, 117(3):219–233. PMID: 18188578. 139

Bae, K., Kim, H., Bae, S., Kang, H., Brill, S., and Seo, Y. (2003). Bimodal interaction between replication-protein a and dna2 is critical for dna2 function both in vivo and in vitro. *Nucleic Acids Research*, 31(12):3006–3015. PMID: 12799426. 8

Bae, S. H., Bae, K. H., Kim, J. A., and Seo, Y. S. (2001). RPA governs endonuclease switching during processing of okazaki fragments in eukaryotes. *Nature*, 412(6845):456–461. PMID: 11473323. 8

Ball, L. G., Zhang, K., Cobb, J. A., Boone, C., and Xiao, W. (2009). The yeast shu complex couples error-free post-replication repair to homologous recombination. *Molecular Microbiology*, 73(1):89–102. PMID: 19496932. 78

Bastin-Shanower, S. A., Fricke, W. M., Mullen, J. R., and Brill, S. J. (2003). The mechanism of Mus81-Mms4 cleavage site selection distinguishes it from the homologous endonuclease Rad1-Rad10. *Molecular and Cellular Biology*, 23(10):3487–3496. PMID: 12724407. 133, 135

Beach, D., Nurse, P., and Egel, R. (1982). Molecular rearrangement of mating-type genes in fission yeast. *Nature*, 296(5858):682–683. 37

Beattie, T. R. and Bell, S. D. (2011). The role of the DNA sliding clamp in okazaki fragment maturation in archaea and eukaryotes. *Biochemical Society Transactions*, 39(1):70–76. PMID: 21265749. 8, 9

Bell, S. P. and Stillman, B. (1992). ATP-dependent recognition of eukaryotic origins of DNA replication by a multiprotein complex. *Nature*, 357(6374):128–134. 4

Bermejo, R., Branzei, D., and Foiani, M. (2008). Cohesion by topology: sister chromatids interlocked by DNA. *Genes & Development*, 22(17):2297 –2301. 6

Bermudez, V. P., Lindsey-Boltz, L. A., Cesare, A. J., Maniwa, Y., Griffith, J. D., Hurwitz, J., and Sancar, A. (2003). Loading of the human 9-1-1 checkpoint complex onto DNA by the check-

point clamp loader hRad17-replication factor c complex in vitro. *Proceedings of the National Academy of Sciences of the United States of America*, 100(4):1633–1638. PMID: 12578958. 14

Bermudez, V. P., MacNeill, S. A., Tappin, I., and Hurwitz, J. (2002). The influence of the cdc27 subunit on the properties of the schizosaccharomyces pombe DNA polymerase delta. *The Journal of Biological Chemistry*, 277(39):36853–36862. PMID: 12124382. 126

Beucher, A., Birraux, J., Tchouandong, L., Barton, O., Shibata, A., Conrad, S., Goodarzi, A. A., Krempler, A., Jeggo, P. A., and Löbrich, M. (2009). ATM and artemis promote homologous recombination of radiation-induced DNA double-strand breaks in g2. *The EMBO Journal*, 28(21):3413–3427. PMID: 19779458. 20

Bi, X. and Liu, L. F. (1994). recA-independent and recA-dependent intramolecular plasmid recombination. differential homology requirement and distance effect. *Journal of molecular biology*, 235(2):414–23. PMID: 8289271. 77

Bienko, M., Green, C. M., Crosetto, N., Rudolf, F., Zapart, G., Coull, B., Kannouche, P., Wider, G., Peter, M., Lehmann, A. R., Hofmann, K., and Dikic, I. (2005). Ubiquitin-Binding domains in Y-Family polymerases regulate translesion synthesis. *Science*, 310(5755):1821 –1824. 29

Bierne, H., Ehrlich, S. D., and Michel, B. (1997). Deletions at stalled replication forks occur by two different pathways. *The EMBO Journal*, 16(11):3332–3340. PMID: 9214648. 136

Blanco, M. G., Matos, J., Rass, U., Ip, S. C. Y., and West, S. C. (2010). Functional overlap between the structure-specific nucleases yen1 and Mus81-Mms4 for DNA-damage repair in s. cerevisiae. *DNA Repair*, 9(4):394–402. PMID: 20106725. 140, 141

Blastyák, A., Pintér, L., Unk, I., Prakash, L., Prakash, S., and Haracska, L. (2007). Yeast rad5 protein required for postreplication repair has a DNA helicase activity specific for replication fork regression. *Molecular Cell*, 28(1):167–175. PMID: 17936713. 70

Blow, J. J., Ge, X. Q., and Jackson, D. A. (2011). How dormant origins promote complete genome replication. *Trends in Biochemical Sciences*, 36(8):405–414. 27, 91

Boddy, M. N., Gaillard, P. H., McDonald, W. H., Shanahan, P., 3rd Yates, J. R., and Russell, P. (2001). Mus81-Eme1 are essential components of a holliday junction resolvase. *Cell*, 107(4):537–548. PMID: 11719193. 132, 133, 135, 140, 143, 144, 149

Boddy, M. N., Lopez-Girona, A., Shanahan, P., Interthal, H., Heyer, W., and Russell, P. (2000). Damage tolerance protein mus81 associates with the FHA1 domain of checkpoint kinase cds1.

Molecular and Cellular Biology, 20(23):8758–8766. PMID: 11073977 PMCID: 86503. 24, 131, 132, 133, 136, 138, 140, 143, 149, 152, 154, 164

Boddy, M. N., Shanahan, P., McDonald, W. H., Lopez-Girona, A., Noguchi, E., Yates III, J. R., and Russell, P. (2003). Replication checkpoint kinase cds1 regulates recombinational repair protein rad60. *Molecular and Cellular Biology*, 23(16):5939–5946. PMID: 12897162. 17, 137, 219

Bonilla, C. Y., Melo, J. A., and Toczyski, D. P. (2008). Colocalization of sensors is sufficient to activate the DNA damage checkpoint in the absence of damage. *Molecular Cell*, 30(3):267–276. PMID: 18471973. 14

Boye, E., Skjølberg, H. C., and Grallert, B. (2009). Checkpoint regulation of DNA replication. *Methods in Molecular Biology (Clifton, N.J.)*, 521:55–70. PMID: 19563101. 12, 14

Boyer, L. A., Langer, M. R., Crowley, K. A., Tan, S., Denu, J. M., and Peterson, C. L. (2002). Essential role for the SANT domain in the functioning of multiple chromatin remodeling enzymes. *Molecular Cell*, 10(4):935–942. PMID: 12419236. 38

Branzei, D. and Foiani, M. (2008). Regulation of DNA repair throughout the cell cycle. *Nature Reviews. Molecular Cell Biology*, 9(4):297–308. PMID: 18285803. 2, 13, 14, 18, 20

Brewer, B. J. and Fangman, W. L. (1988). A replication fork barrier at the 3 end of yeast ribosomal RNA genes. *Cell*, 55(4):637–643. 35

Brewer, B. J., Lockshon, D., and Fangman, W. L. (1992). The arrest of replication forks in the rDNA of yeast occurs independently of transcription. *Cell*, 71(2):267–276. PMID: 1423594. 39

Brewer, B. J., Payen, C., Raghuraman, M. K., and Dunham, M. J. (2011). Origin-Dependent Inverted-Repeat amplification: A Replication-Based model for generating palindromic amplicons. *PLoS Genet*, 7(3):e1002016. 156

Brooks, T. A., Kendrick, S., and Hurley, L. (2010). Making sense of g-quadruplex and i-motif functions in oncogene promoters. *The FEBS Journal*, 277(17):3459–3469. PMID: 20670278. 89

Brosh, R. M. J., Driscoll, H. C., Dianov, G. L., and Sommers, J. A. (2002). Biochemical characterization of the WRN-FEN-1 functional interaction. *Biochemistry*, 41(40):12204–12216. PMID: 12356323. 139, 151

Brosh, R. M. J., von Kobbe, C., Sommers, J. A., Karmakar, P., Opresko, P. L., Piotrowski, J., Dianova, I., Dianov, G. L., and Bohr, V. A. (2001). Werner syndrome protein interacts with human flap endonuclease 1 and stimulates its cleavage activity. *The EMBO Journal*, 20(20):5791–5801. PMID: 11598021. 139, 151

Brown, M., Zhu, Y., Hemmingsen, S. M., and Xiao, W. (2002). Structural and functional conservation of error-free DNA postreplication repair in schizosaccharomyces pombe. *DNA Repair*, 1(11):869–880. PMID: 12531016. 70

Budd, M. E. and Campbell, J. L. (1997). A yeast replicative helicase, dna2 helicase, interacts with yeast FEN-1 nuclease in carrying out its essential function. *Molecular and Cellular Biology*, 17(4):2136–2142. PMID: 9121462 PMCID: 232061. 139

Burge, S., Parkinson, G. N., Hazel, P., Todd, A. K., and Neidle, S. (2006). Quadruplex DNA: sequence, topology and structure. *Nucleic Acids Research*, 34(19):5402–5415. PMID: 17012276. 30

Burgers, P. M. J. (2009). Polymerase dynamics at the eukaryotic DNA replication fork. *The Journal of Biological Chemistry*, 284(7):4041–4045. PMID: 18835809. 8

Byun, T. S., Pacek, M., ching Yee, M., Walter, J. C., and Cimprich, K. A. (2005). Functional uncoupling of MCM helicase and DNA polymerase activities activates the ATR-dependent checkpoint. *Genes & Development*, 19(9):1040–1052. PMID: 15833913 PMCID: 1091739. 12

Bzymek, M. and Lovett, S. T. (2001). Evidence for two mechanisms of palindrome-stimulated deletion in escherichia coli: single-strand annealing and replication slipped mispairing. *Genetics*, 158(2):527–540. PMID: 11404319 PMCID: 1461685. 88, 89

Bzymek, M., Saveson, C. J., Feschenko, V. V., and Lovett, S. T. (1999). Slipped misalignment mechanisms of deletion formation: in vivo susceptibility to nucleases. *Journal of bacteriology*, 181(2):477–82. PMID: 9882661. 77

Cahoon, L. A. and Seifert, H. S. (2009). An alternative DNA structure is necessary for pilin antigenic variation in neisseria gonorrhoeae. *Science (New York, N.Y.)*, 325(5941):764–767. PMID: 19661435 PMCID: 2803317. 33, 34, 84, 85, 88, 90, 116, 117

Caldecott, K. W. (2008). Single-strand break repair and genetic disease. *Nat Rev Genet*, 9(8):619–631. 19

Caldecott, K. W., McKeown, C. K., Tucker, J. D., Ljungquist, S., and Thompson, L. H. (1994). An interaction between the mammalian DNA repair protein XRCC1 and DNA ligase III. *Molecular and Cellular Biology*, 14(1):68–76. PMID: 8264637. 19

Callegari, A. J. and Kelly, T. J. (2007). Shedding light on the DNA damage checkpoint. *Cell Cycle (Georgetown, Tex.)*, 6(6):660–666. PMID: 17387276. 11

Calzada, A., Hodgson, B., Kanemaki, M., Bueno, A., and Labib, K. (2005). Molecular anatomy and regulation of a stable replisome at a paused eukaryotic DNA replication fork. *Genes & Development*, 19(16):1905–1919. PMID: 16103218. 16, 27, 39, 40, 161

Capra, J. A., Paeschke, K., Singh, M., and Zakian, V. A. (2010). G-quadruplex DNA sequences are evolutionarily conserved and associated with distinct genomic features in saccharomyces cerevisiae. *PLoS Computational Biology*, 6(7):e1000861. PMID: 20676380. 31

Carr, A. M. (2002). DNA structure dependent checkpoints as regulators of DNA repair. *DNA Repair*, 1(12):983–994. 12, 13, 15, 16

Carr, A. M., Paek, A. L., and Weinert, T. (2011). DNA replication: Failures and inverted fusions. *Seminars in Cell & Developmental Biology*. PMID: 22020070. 72, 91, 164

Carvalho, C. M. B., Zhang, F., Liu, P., Patel, A., Sahoo, T., Bacino, C. A., Shaw, C., Peacock, S., Pursley, A., Tavyev, Y. J., Ramocki, M. B., Nawara, M., Obersztyn, E., Vianna-Morgante, A. M., Stankiewicz, P., Zoghbi, H. Y., Cheung, S. W., and Lupski, J. R. (2009). Complex rearrangements in patients with duplications of MECP2 can occur by fork stalling and template switching. *Human Molecular Genetics*, 18(12):2188–2203. PMID: 19324899. 156

Caspari, T. and Carr, A. M. (1999). DNA structure checkpoint pathways in schizosaccharomyces pombe. *Biochimie*, 81(1-2):173–181. 12

Caspari, T., Dahlen, M., Kanter-Smoler, G., Lindsay, H. D., Hofmann, K., Papadimitriou, K., Sunnerhagen, P., and Carr, A. M. (2000). Characterization of schizosaccharomyces pombe hus1: a PCNA-related protein that associates with rad1 and rad9. *Molecular and Cellular Biology*, 20(4):1254–1262. PMID: 10648611. 14

Cejka, P., Plank, J. L., Bachrati, C. Z., Hickson, I. D., and Kowalczykowski, S. C. (2010). Rmi1 stimulates decatenation of double holliday junctions during dissolution by Sgs1-Top3. *Nature Structural & Molecular Biology*, 17(11):1377–1382. PMID: 20935631. 24

Chang, J. H., Kim, J. J., Choi, J. M., Lee, J. H., and Cho, Y. (2008). Crystal structure of the Mus81-Eme1 complex. *Genes & Development*, 22(8):1093–1106. PMID: 18413719. 132, 133, 153, 155

Chapman-Smith, A. and Cronan, J. E. J. (1999). The enzymatic biotinylation of proteins: a post-translational modification of exceptional specificity. *Trends in Biochemical Sciences*, 24(9):359–363. PMID: 10470036. 217

Chen, X. B., Melchionna, R., Denis, C. M., Gaillard, P. H., Blasina, A., Van de Weyer, I., Boddy, M. N., Russell, P., Vialard, J., and McGowan, C. H. (2001). Human mus81-associated endonuclease cleaves holliday junctions in vitro. *Molecular Cell*, 8(5):1117–1127. PMID: 11741546. 131, 132, 135, 142, 146

Choi-Rhee, E., Schulman, H., and Cronan, J. E. (2004). Promiscuous protein biotinylation by escherichia coli biotin protein ligase. *Protein science : a publication of the Protein Society*, 13(11):3043–50. PMID: 15459338. 217, 218, 220, 223

Chou, D. M. and Elledge, S. J. (2006). Tipin and timeless form a mutually protective complex required for genotoxic stress resistance and checkpoint function. *Proceedings of the National Academy of Sciences*, 103(48):18143 –18147. 16

Ciccia, A., Constantinou, A., and West, S. C. (2003). Identification and characterization of the human mus81-eme1 endonuclease. *The Journal of Biological Chemistry*, 278(27):25172–25178. PMID: 12721304. 24, 131, 132, 135, 142

Ciccia, A., McDonald, N., and West, S. C. (2008). Structural and functional relationships of the XPF/MUS81 family of proteins. *Annual Review of Biochemistry*, 77:259–287. PMID: 18518821. 132, 133

Cimprich, K. A. and Cortez, D. (2008). ATR: an essential regulator of genome integrity. *Nature Reviews. Molecular Cell Biology*, 9(8):616–627. PMID: 18594563. 12, 13, 14, 16

Clyne, R. K. and Kelly, T. J. (1995). Genetic analysis of an ARS element from the fission yeast schizosaccharomyces pombe. *The EMBO Journal*, 14(24):6348–6357. PMID: 8557055 PMCID: 394760. 4

Cobb, J. A. (2003). DNA polymerase stabilization at stalled replication forks requires mec1 and the RecQ helicase sgs1. *The EMBO Journal*, 22:4325–4336. 165

Codlin, S. and Dalgaard, J. Z. (2003). Complex mechanism of site-specific DNA replication termination in fission yeast. *The EMBO Journal*, 22(13):3431–3440. PMID: 12840005. 37, 38

Constantinou, A., Chen, X., McGowan, C. H., and West, S. C. (2002). Holliday junction resolution in human cells: two junction endonucleases with distinct substrate specificities. *The EMBO Journal*, 21(20):5577–5585. PMID: 12374758. 135

Cortez, D., Guntuku, S., Qin, J., and Elledge, S. J. (2001). ATR and ATRIP: partners in checkpoint signaling. *Science (New York, N.Y.)*, 294(5547):1713–1716. PMID: 11721054. 14

Cronan, J. E. (2005). Targeted and proximity-dependent promiscuous protein biotinylation by a mutant escherichia coli biotin protein ligase. *The Journal of nutritional biochemistry*, 16(7):416–8. PMID: 15992681. 217

Cronan, J. E. J. (1990). Biotination of proteins in vivo. a post-translational modification to label, purify, and study proteins. *The Journal of Biological Chemistry*, 265(18):10327–10333. PMID: 2113052. 217

Daigaku, Y., Davies, A. A., and Ulrich, H. D. (2010). Ubiquitin-dependent DNA damage bypass is separable from genome replication. *Nature*, 465(7300):951–955. PMID: 20453836. 29

Dalgaard, J. Z., Eydmann, T., Koulintchenko, M., Sayrac, S., Vengrova, S., and Yamada-Inagawa, T. (2009). Random and site-specific replication termination. *Methods in Molecular Biology (Clifton, N.J.)*, 521:35–53. PMID: 19563100. 35, 37, 157

Dalgaard, J. Z. and Klar, A. J. (1999). Orientation of DNA replication establishes mating-type switching pattern in s. pombe. *Nature*, 400(6740):181–184. PMID: 10408447. 37

Dalgaard, J. Z. and Klar, A. J. (2000). swi1 and swi3 perform imprinting, pausing, and termination of DNA replication in s. pombe. *Cell*, 102(6):745–751. PMID: 11030618. 16, 37, 38

Dalgaard, J. Z. and Klar, A. J. (2001). A DNA replication-arrest site RTS1 regulates imprinting by determining the direction of replication at mat1 in s. pombe. *Genes & Development*, 15(16):2060–2068. PMID: 11511538 PMCID: 312760. 37, 91, 157

d'Ambrosio, E. and Furano, A. V. (1987). DNA synthesis arrest sites at the right terminus of rat long interspersed repeated (LINE or L1Rn) DNA family members. *Nucleic Acids Research*, 15(7):3155–3175. PMID: 2436148 PMCID: 340917. 114

Damerla, R. R., Knickelbein, K. E., Kepchia, D., Jackson, A., Armitage, B. A., Eckert, K. A., and Opresko, P. L. (2010). Telomeric repeat mutagenicity in human somatic cells is modulated by repeat orientation and g-quadruplex stability. *DNA Repair*, 9(11):1119–1129. PMID: 20800555. 34, 114

Dapić, V., Abdomerović, V., Marrington, R., Peberdy, J., Rodger, A., Trent, J. O., and Bates, P. J. (2003). Biophysical and biological properties of quadruplex oligodeoxyribonucleotides. *Nucleic Acids Research*, 31(8):2097–2107. PMID: 12682360. 85

De Bont, R. and van Larebeke, N. (2004). Endogenous DNA damage in humans: a review of quantitative data. *Mutagenesis*, 19(3):169–185. PMID: 15123782. 79

de Laat, W. L., Sijbers, A. M., Odijk, H., Jaspers, N. G., and Hoeijmakers, J. H. (1998). Mapping of interaction domains between human repair proteins ERCC1 and XPF. *Nucleic Acids Research*, 26(18):4146–4152. PMID: 9722633 PMCID: 147836. 132

de los Santos, T., Loidl, J., Larkin, B., and Hollingsworth, N. M. (2001). A role for MMS4 in the processing of recombination intermediates during meiosis in saccharomyces cerevisiae. *Genetics*, 159(4):1511–1525. PMID: 11779793. 132, 133

Deem, A., Keszthelyi, A., Blackgrove, T., Vayl, A., Coffey, B., Mathur, R., Chabes, A., and Malkova, A. (2011). Break-Induced replication is highly inaccurate. *PLoS Biol*, 9(2):e1000594. 112

Delacroix, S., Wagner, J. M., Kobayashi, M., ichi Yamamoto, K., and Karnitz, L. M. (2007). The Rad9-Hus1-Rad1 (9-1-1) clamp activates checkpoint signaling via TopBP1. *Genes & Development*, 21(12):1472–1477. PMID: 17575048. 14

Dendouga, N., Gao, H., Moechars, D., Janicot, M., Vialard, J., and McGowan, C. H. (2005). Disruption of murine mus81 increases genomic instability and DNA damage sensitivity but does not promote tumorigenesis. *Molecular and Cellular Biology*, 25(17):7569–7579. PMID: 16107704. 141

Desany, B. A., Alcasabas, A. A., Bachant, J. B., and Elledge, S. J. (1998). Recovery from DNA replicational stress is the essential function of the s-phase checkpoint pathway. *Genes & Development*, 12(18):2956–2970. PMID: 9744871. 16

di Caprio, L. and Cox, B. S. (1981). DNA synthesis in UV-irradiated yeast. *Mutation research*, 82(1):69–85. PMID: 7022172. 70

Dianov, G. L. and Parsons, J. L. (2007). Co-ordination of DNA single strand break repair. *DNA Repair*, 6(4):454–460. 19

Dianov, G. L., Sleeth, K. M., Dianova, I. I., and Allinson, S. L. (2003). Repair of abasic sites in DNA. *Mutation Research/Fundamental and Molecular Mechanisms of Mutagenesis*, 531(1-2):157–163. 19

Diffley, J. F. X. (2004). Regulation of early events in chromosome replication. *Current Biology: CB*, 14(18):R778–786. PMID: 15380092. 3, 6

Doe, C. L., Ahn, J. S., Dixon, J., and Whitby, M. C. (2002). Mus81-Eme1 and rqh1 involvement in processing stalled and collapsed replication forks. *The Journal of Biological Chemistry*, 277(36):32753–32759. PMID: 12084712. 17, 133, 135, 138, 154

Doe, C. L., Dixon, J., Osman, F., and Whitby, M. C. (2000). Partial suppression of the fission yeast rqh1(-) phenotype by expression of a bacterial holliday junction resolvase. *The EMBO Journal*, 19(11):2751–2762. PMID: 10835372. 133, 138

Doe, C. L., Osman, F., Dixon, J., and Whitby, M. C. (2004). DNA repair by a Rad22–Mus81-dependent pathway that is independent of rhp51. *Nucleic Acids Research*, 32(18):5570–5581. PMID: 15486206 PMCID: 524275. 26, 39, 77, 131, 136, 143

Doherty, A. J., Serpell, L. C., and Ponting, C. P. (1996). The helix-hairpin-helix DNA-binding motif: a structural basis for non-sequence-specific recognition of DNA. *Nucleic Acids Research*, 24(13):2488–2497. PMID: 8692686. 132

Dua, R., Levy, D. L., and Campbell, J. L. (1999). Analysis of the essential functions of the c-terminal protein/protein interaction domain of saccharomyces cerevisiae pol epsilon and its unexpected ability to support growth in the absence of the DNA polymerase domain. *The Journal of Biological Chemistry*, 274(32):22283–22288. PMID: 10428796. 8

Dubiel, W. and Gordon, C. (1999). Ubiquitin pathway: another link in the polyubiquitin chain? *Current Biology: CB*, 9(15):R554–557. PMID: 10469558. 28

Dupaigne, P., Le Breton, C., Fabre, F., Gangloff, S., Le Cam, E., and Veaute, X. (2008). The srs2 helicase activity is stimulated by rad51 filaments on dsDNA: implications for crossover incidence during mitotic recombination. *Molecular Cell*, 29(2):243–254. PMID: 18243118. 25

Duquette, M. L., Handa, P., Vincent, J. A., Taylor, A. F., and Maizels, N. (2004). Intracellular transcription of g-rich DNAs induces formation of g-loops, novel structures containing g4 DNA. *Genes & Development*, 18(13):1618 –1629. 84

Eddy, J. and Maizels, N. (2006). Gene function correlates with potential for g4 DNA formation in the human genome. *Nucleic Acids Research*, 34(14):3887–3896. PMID: 16914419. 31

Eddy, J. and Maizels, N. (2009). Selection for the g4 DNA motif at the 5' end of human genes. *Molecular Carcinogenesis*, 48(4):319–325. PMID: 19306310. 31

Ede, C., Rudolph, C. J., Lehmann, S., Schürer, K. A., and Kramer, W. (2011). Budding yeast mph1 promotes sister chromatid interactions by a mechanism involving strand invasion. *DNA Repair*, 10(1):45–55. PMID: 20951099. 89

Edmunds, C. E., Simpson, L. J., and Sale, J. E. (2008). PCNA ubiquitination and REV1 define temporally distinct mechanisms for controlling translesion synthesis in the avian cell line DT40. *Molecular Cell*, 30(4):519–529. PMID: 18498753. 29, 129

Edwards, R. J., Bentley, N. J., and Carr, A. M. (1999). A Rad3-Rad26 complex responds to DNA damage independently of other checkpoint proteins. *Nature Cell Biology*, 1(7):393–398. PMID: 10559981. 14

Efstratiadis, A., Posakony, J. W., Maniatis, T., Lawn, R. M., O'Connell, C., Spritz, R. A., DeRiel, J. K., Forget, B. G., Weissman, S. M., Slightom, J. L., Blechl, A. E., Smithies, O., Baralle, F. E., Shoulders, C. C., and Proudfoot, N. J. (1980). The structure and evolution of the human beta-globin gene family. *Cell*, 21(3):653–68. PMID: 6985477. 69

Egel, R., Kohli, J., Thuriaux, P., and Wolf, K. (1980). Genetics of the fission yeast schizosaccharomyces pombe. *Annual Review of Genetics*, 14:77–108. PMID: 7011176. 2

Ehmsen, K. T. and Heyer, W. (2008). Saccharomyces cerevisiae Mus81-Mms4 is a catalytic, DNA structure-selective endonuclease. *Nucleic Acids Research*, 36(7):2182–2195. PMID: 18281703 PMCID: 2367710. 133, 135, 155

Ehmsen, K. T. and Heyer, W. (2009). A junction branch point adjacent to a DNA backbone nick directs substrate cleavage by saccharomyces cerevisiae Mus81-Mms4. *Nucleic Acids Research*, 37(6):2026–2036. PMID: 19211663. 137, 139

Ellison, V. and Stillman, B. (2003). Biochemical characterization of DNA damage checkpoint complexes: clamp loader and clamp complexes with specificity for 5' recessed DNA. *PLoS Biology*, 1(2):E33. PMID: 14624239. 14

Emili, A. (1998). MEC1-dependent phosphorylation of rad9p in response to DNA damage. *Molecular Cell*, 2(2):183–189. PMID: 9734355. 15

Enzlin, J. H. and Schärer, O. D. (2002). The active site of the DNA repair endonuclease XPF-ERCC1 forms a highly conserved nuclease motif. *The EMBO Journal*, 21(8):2045–2053. PMID: 11953324. 132

Evrin, C., Clarke, P., Zech, J., Lurz, R., Sun, J., Uhle, S., Li, H., Stillman, B., and Speck, C. (2009). A double-hexameric MCM2-7 complex is loaded onto origin DNA during licensing of eukaryotic DNA replication. 106(48):20240–20245. PMID: 19910535 PMCID: 2787165. 4

Eydmann, T., Sommariva, E., Inagawa, T., Mian, S., Klar, A. J. S., and Dalgaard, J. Z. (2008). Rtf1-mediated eukaryotic site-specific replication termination. *Genetics*, 180(1):27–39. PMID: 18723894. 36, 38

Fabre, F., Chan, A., Heyer, W., and Gangloff, S. (2002). Alternate pathways involving Sgs1/Top3, mus81/ mms4, and srs2 prevent formation of toxic recombination intermediates from single-stranded gaps created by DNA replication. *Proceedings of the National Academy of Sciences of the United States of America*, 99(26):16887–16892. PMID: 12475932. 138, 139, 140, 154

Fanning, E., Klimovich, V., and Nager, A. R. (2006). A dynamic model for replication protein a (RPA) function in DNA processing pathways. *Nucleic Acids Research*, 34(15):4126 –4137. 7

Fekairi, S., Scaglione, S., Chahwan, C., Taylor, E. R., Tissier, A., Coulon, S., Dong, M., Ruse, C., 3rd Yates, J. R., Russell, P., Fuchs, R. P., McGowan, C. H., and Gaillard, P. L. (2009). Human SLX4 is a holliday junction resolvase subunit that binds multiple DNA repair/recombination endonucleases. *Cell*, 138(1):78–89. PMID: 19596236. 134, 153

Feng, W. and D'Urso, G. (2001). Schizosaccharomyces pombe cells lacking the amino-terminal catalytic domains of DNA polymerase epsilon are viable but require the DNA damage checkpoint control. *Molecular and Cellular Biology*, 21(14):4495–4504. PMID: 11416129. 8

Feng, Z., Scott, S. P., Bussen, W., Sharma, G. G., Guo, G., Pandita, T. K., and Powell, S. N. (2011). Rad52 inactivation is synthetically lethal with BRCA2 deficiency. *Proceedings of the National Academy of Sciences*, 108(2):686 –691. 26

Fishman-Lobell, J. and Haber, J. E. (1992). Removal of nonhomologous DNA ends in double-strand break recombination: the role of the yeast ultraviolet repair gene RAD1. *Science (New York, N.Y.)*, 258(5081):480–484. PMID: 1411547. 25

Fishman-Lobell, J., Rudin, N., and Haber, J. E. (1992). Two alternative pathways of double-strand break repair that are kinetically separable and independently modulated. *Molecular and Cellular Biology*, 12(3):1292–1303. PMID: 1545810. 25

Fleck, O. and Nielsen, O. (2004). DNA repair. *Journal of Cell Science*, 117(Pt 4):515–517. PMID: 14730007. 20

Fortin, G. S. and Symington, L. S. (2002). Mutations in yeast rad51 that partially bypass the requirement for rad55 and rad57 in DNA repair by increasing the stability of Rad51-DNA complexes. *The EMBO Journal*, 21(12):3160–3170. PMID: 12065428. 23

Frampton, J., Irmisch, A., Green, C. M., Neiss, A., Trickey, M., Ulrich, H. D., Furuya, K., Watts, F. Z., Carr, A. M., and Lehmann, A. R. (2006). Postreplication repair and PCNA modification in schizosaccharomyces pombe. *Molecular Biology of the Cell*, 17(7):2976–2985. PMID: 16641370. 28, 70, 77, 82, 87, 219

Fricke, W. M., Bastin-Shanower, S. A., and Brill, S. J. (2005). Substrate specificity of the saccharomyces cerevisiae Mus81-Mms4 endonuclease. *DNA Repair*, 4(2):243–251. PMID: 15590332. 24, 131, 135

Friedberg, E. C., McDaniel, L. D., and Schultz, R. A. (2004). The role of endogenous and exogenous DNA damage and mutagenesis. *Current Opinion in Genetics & Development*, 14(1):5–10. PMID: 15108798. 18, 157

Froget, B., Blaisonneau, J., Lambert, S., and Baldacci, G. (2008). Cleavage of stalled forks by fission yeast Mus81/Eme1 in absence of DNA replication checkpoint. *Molecular Biology of the Cell*, 19(2):445–456. PMID: 18032583. 137

Frosina, G., Fortini, P., Rossi, O., Carrozzino, F., Raspaglio, G., Cox, L. S., Lane, D. P., Abbondandolo, A., and Dogliotti, E. (1996). Two pathways for base excision repair in mammalian cells. *The Journal of Biological Chemistry*, 271(16):9573–9578. PMID: 8621631. 19

Fu, Y. and Xiao, W. (2003). Functional domains required for the saccharomyces cerevisiae Mus81-Mms4 endonuclease complex formation and nuclear localization. *DNA Repair*, 2(12):1435–1447. PMID: 14642571. 132, 133, 146, 153

Furuya, K. and Carr, A. M. (2003). DNA checkpoints in fission yeast. *Journal of Cell Science*, 116(Pt 19):3847–3848. PMID: 12953049. 16

Furuya, K., Miyabe, I., Tsutsui, Y., Paderi, F., Kakusho, N., Masai, H., Niki, H., and Carr, A. M. (2010). DDK phosphorylates checkpoint clamp component rad9 and promotes its release from damaged chromatin. *Molecular Cell*, 40(4):606–618. 14

Furuya, K., Poitelea, M., Guo, L., Caspari, T., and Carr, A. M. (2004). Chk1 activation requires rad9 S/TQ-site phosphorylation to promote association with c-terminal BRCT domains of Rad4TOPBP1. *Genes & Development*, 18(10):1154–1164. PMID: 15155581. 14, 219, 222

Gaillard, P. L., Noguchi, E., Shanahan, P., and Russell, P. (2003). The endogenous Mus81-Eme1 complex resolves holliday junctions by a nick and counternick mechanism. *Molecular Cell*, 12(3):747–759. PMID: 14527419. 17, 24, 131, 132, 135, 138

Gajiwala, K. S. and Burley, S. K. (2000). Winged helix proteins. *Current Opinion in Structural Biology*, 10(1):110–116. PMID: 10679470. 142, 153

Gambus, A., Jones, R. C., Sanchez-Diaz, A., Kanemaki, M., van Deursen, F., Edmondson, R. D., and Labib, K. (2006). GINS maintains association of cdc45 with MCM in replisome progression complexes at eukaryotic DNA replication forks. *Nature Cell Biology*, 8(4):358–366. PMID: 16531994. 6, 7, 9, 16, 82

Gambus, A., van Deursen, F., Polychronopoulos, D., Foltman, M., Jones, R. C., Edmondson, R. D., Calzada, A., and Labib, K. (2009). A key role for ctf4 in coupling the MCM2-7 helicase to DNA polymerase alpha within the eukaryotic replisome. *The EMBO Journal*, 28(19):2992–3004. PMID: 19661920. 9, 126

Gangloff, S., McDonald, J. P., Bendixen, C., Arthur, L., and Rothstein, R. (1994). The yeast type i topoisomerase top3 interacts with sgs1, a DNA helicase homolog: a potential eukaryotic reverse gyrase. *Molecular and Cellular Biology*, 14(12):8391–8398. PMID: 7969174 PMCID: 359378. 138

Gao, H., Chen, X., and McGowan, C. H. (2003). Mus81 endonuclease localizes to nucleoli and to regions of DNA damage in human s-phase cells. *Molecular Biology of the Cell*, 14(12):4826–4834. PMID: 14638871. 141

Garcia, V., Furuya, K., and Carr, A. M. (2005). Identification and functional analysis of TopBP1 and its homologs. *DNA Repair*, 4(11):1227–1239. PMID: 15897014. 219

Garg, P., Stith, C. M., Sabouri, N., Johansson, E., and Burgers, P. M. (2004). Idling by DNA polymerase delta maintains a ligatable nick during lagging-strand DNA replication. *Genes & Development*, 18(22):2764–2773. PMID: 15520275. 8

Gaskell, L. J., Osman, F., Gilbert, R. J. C., and Whitby, M. C. (2007). Mus81 cleavage of holliday junctions: a failsafe for processing meiotic recombination intermediates? *The EMBO Journal*, 26(7):1891–1901. PMID: 17363897. 135

Ge, X. Q. and Blow, J. J. (2010). Chk1 inhibits replication factory activation but allows dormant origin firing in existing factories. 191(7):1285–1297. PMID: 21173116 PMCID: 3010067. 6, 91

Gellert, M., Lipsett, M. N., and Davies, D. R. (1962). HELIX FORMATION BY GUANYLIC ACID. *Proceedings of the National Academy of Sciences of the United States of America*, 48(12):2013–2018. PMID: 13947099 PMCID: 221115. 84

Gerber, J. K., Gögel, E., Berger, C., Wallisch, M., Müller, F., Grummt, I., and Grummt, F. (1997). Termination of mammalian rDNA replication: polar arrest of replication fork movement by transcription termination factor TTF-I. *Cell*, 90(3):559–567. PMID: 9267035. 38

Ghazvini, M., Ribes, V., and Arcangioli, B. (1995). The essential DNA-binding protein sap1 of schizosaccharomyces pombe contains two independent oligomerization interfaces that dictate the relative orientation of the DNA-binding domain. *Molecular and Cellular Biology*, 15(9):4939 –4946. 37

Ghosal, G. and Muniyappa, K. (2005). Saccharomyces cerevisiae mre11 is a high-affinity g4 DNA-binding protein and a g-rich DNA-specific endonuclease: implications for replication of telomeric DNA. *Nucleic Acids Research*, 33(15):4692–4703. PMID: 16116037. 32, 88, 90

Goldfless, S. J., Morag, A. S., Belisle, K. A., Sutera, V. A., and Lovett, S. T. (2006). DNA repeat rearrangements mediated by DnaK-dependent replication fork repair. *Molecular cell*, 21(5):595–604. PMID: 16507358. 70, 77, 87

Goldstein, A. L. and McCusker, J. H. (1999). Three new dominant drug resistance cassettes for gene disruption in saccharomyces cerevisiae. *Yeast (Chichester, England)*, 15(14):1541–53. PMID: 10514571. 72

Greenwell, P. W., Kronmal, S. L., Porter, S. E., Gassenhuber, J., Obermaier, B., and Petes, T. D. (1995). TEL1, a gene involved in controlling telomere length in s. cerevisiae, is homologous to the human ataxia telangiectasia gene. *Cell*, 82(5):823–829. PMID: 7671310. 14

Guédin, A., Alberti, P., and Mergny, J. (2009). Stability of intramolecular quadruplexes: sequence effects in the central loop. 37(16):5559–5567. PMID: 19581426 PMCID: 2760802. 85

Guédin, A., De Cian, A., Gros, J., Lacroix, L., and Mergny, J. (2008). Sequence effects in single-base loops for quadruplexes. *Biochimie*, 90(5):686–696. PMID: 18294461. 85

Guédin, A., Gros, J., Alberti, P., and Mergny, J. (2010). How long is too long? effects of loop size on g-quadruplex stability. 38(21):7858–7868. PMID: 20660477 PMCID: 2995061. 85

Guo, C., Tang, T., and Friedberg, E. C. (2010). SnapShot: nucleotide excision repair. *Cell*, 140(5):754–754.e1. PMID: 20211143. 20

Haber, J. E. (1999). DNA recombination: the replication connection. *Trends in Biochemical Sciences*, 24(7):271–275. PMID: 10390616. 26

Haber, J. E. (2000a). Partners and pathways: repairing a double-strand break. *Trends in Genetics*, 16(6):259–264. 26, 28

Haber, J. E. (2000b). Recombination: a frank view of exchanges and vice versa. *Current Opinion in Cell Biology*, 12(3):286–292. PMID: 10801454. 26

Habraken, Y., Sung, P., Prakash, L., and Prakash, S. (1996). Binding of insertion/deletion DNA mismatches by the heterodimer of yeast mismatch repair proteins MSH2 and MSH3. *Current Biology: CB*, 6(9):1185–1187. PMID: 8805366. 18

Hanna, J. S., Kroll, E. S., Lundblad, V., and Spencer, F. A. (2001). Saccharomyces cerevisiae CTF18 and CTF4 are required for sister chromatid cohesion. *Molecular and Cellular Biology*, 21(9):3144–3158. PMID: 11287619. 9, 126

Hartung, F., Suer, S., Bergmann, T., and Puchta, H. (2006). The role of AtMUS81 in DNA repair and its genetic interaction with the helicase AtRecQ4A. *Nucleic Acids Research*, 34(16):4438–4448. PMID: 16945961. 24, 138

Hashimoto, Y., Chaudhuri, A. R., Lopes, M., and Costanzo, V. (2010). Rad51 protects nascent DNA from mre11-dependent degradation and promotes continuous DNA synthesis. *Nature Structural & Molecular Biology*, 17(11):1305–1311. PMID: 20935632. 27

Hefferin, M. L. and Tomkinson, A. E. (2005). Mechanism of DNA double-strand break repair by non-homologous end joining. *DNA Repair*, 4(6):639–648. 20, 21

Helt, C. E., Wang, W., Keng, P. C., and Bambara, R. A. (2005). Evidence that DNA damage detection machinery participates in DNA repair. *Cell Cycle (Georgetown, Tex.)*, 4(4):529–532. PMID: 15876866. 14

Hennessy, K. M., Clark, C. D., and Botstein, D. (1990). Subcellular localization of yeast CDC46 varies with the cell cycle. *Genes & Development*, 4(12B):2252–2263. PMID: 2279699. 7

Hentges, P., Van Driessche, B., Tafforeau, L., Vandenhaute, J., and Carr, A. M. (2005). Three novel antibiotic marker cassettes for gene disruption and marker switching in schizosaccharomyces pombe. *Yeast (Chichester, England)*, 22(13):1013–1019. PMID: 16200533. 72, 76, 229

Hershman, S. G., Chen, Q., Lee, J. Y., Kozak, M. L., Yue, P., Wang, L., and Johnson, F. B. (2008). Genomic distribution and functional analyses of potential g-quadruplex-forming sequences in saccharomyces cerevisiae. *Nucleic Acids Research*, 36(1):144–156. PMID: 17999996. 31, 33

Herskowitz, I. (1988). Life cycle of the budding yeast saccharomyces cerevisiae. *Microbiological Reviews*, 52(4):536–553. PMID: 3070323. 2

Hiyama, T., Katsura, M., Yoshihara, T., Ishida, M., Kinomura, A., Tonda, T., Asahara, T., and Miyagawa, K. (2006). Haploinsufficiency of the Mus81-Eme1 endonuclease activates the intra-S-phase and G2/M checkpoints and promotes rereplication in human cells. *Nucleic Acids Research*, 34(3):880–892. PMID: 16456034. 141

Hodgson, B., Calzada, A., and Labib, K. (2007). Mrc1 and tof1 regulate DNA replication forks in different ways during normal s phase. *Molecular Biology of the Cell*, 18(10):3894–3902. PMID: 17652453. 9

Hoege, C., Pfander, B., Moldovan, G., Pyrowolakis, G., and Jentsch, S. (2002). RAD6-dependent DNA repair is linked to modification of PCNA by ubiquitin and SUMO. *Nature*, 419(6903):135–141. PMID: 12226657. 28, 70, 87, 219

Hoeijmakers, J. H. J. (2001). Genome maintenance mechanisms for preventing cancer. *Nature*, 411(6835):366–374. 18, 19, 20

Hofmann, R. M. and Pickart, C. M. (1999). Noncanonical MMS2-encoded ubiquitin-conjugating enzyme functions in assembly of novel polyubiquitin chains for DNA repair. *Cell*, 96(5):645–53. PMID: 10089880. 70, 87

Hope, J. C., Cruzata, L. D., Duvshani, A., Mitsumoto, J., Maftahi, M., and Freyer, G. A. (2007). Mus81-Eme1-dependent and -independent crossovers form in mitotic cells during double-strand break repair in schizosaccharomyces pombe. *Molecular and Cellular Biology*, 27(10):3828–3838. PMID: 17353272. 138, 149

Huber, M. D., Lee, D. C., and Maizels, N. (2002). G4 DNA unwinding by BLM and sgs1p: substrate specificity and substrate-specific inhibition. *Nucleic Acids Research*, 30(18):3954–3961. PMID: 12235379. 33

Hübscher, U. (2009). DNA replication fork proteins. *Methods in Molecular Biology (Clifton, N.J.)*, 521:19–33. PMID: 19563099. 8, 156

Huertas, P., Cortés-Ledesma, F., Sartori, A. A., Aguilera, A., and Jackson, S. P. (2008). CDK targets sae2 to control DNA-end resection and homologous recombination. *Nature*, 455(7213):689–692. PMID: 18716619. 23

Ii, M. and Brill, S. J. (2005). Roles of SGS1, MUS81, and RAD51 in the repair of lagging-strand replication defects in saccharomyces cerevisiae. *Current Genetics*, 48(4):213–225. PMID: 16193328. 139

Ii, M., Ii, T., and Brill, S. J. (2007). Mus81 functions in the quality control of replication forks at the rDNA and is involved in the maintenance of rDNA repeat number in saccharomyces cerevisiae. *Mutation research*, 625(1-2):1–19. PMID: 17555773 PMCID: 2100401. 138

Ii, M., Ii, T., Mironova, L. I., and Brill, S. J. (2011). Epistasis analysis between homologous recombination genes in saccharomyces cerevisiae identifies multiple repair pathways for sgs1, Mus81-Mms4 and RNase h2. *Mutation Research*. PMID: 21741981. 138

Inagawa, T., Yamada-Inagawa, T., Eydmann, T., Mian, I. S., Wang, T. S., and Dalgaard, J. Z. (2009). Schizosaccharomyces pombe rtf2 mediates site-specific replication termination by inhibiting replication restart. *Proceedings of the National Academy of Sciences of the United States of America*, 106(19):7927–7932. PMID: 19416828. 38

Interthal, H. and Heyer, W. D. (2000). MUS81 encodes a novel helix-hairpin-helix protein involved in the response to UV- and methylation-induced DNA damage in saccharomyces cerevisiae. *Molecular & General Genetics: MGG*, 263(5):812–827. PMID: 10905349. 131, 132, 133, 136, 140

Ip, S. C. Y., Rass, U., Blanco, M. G., Flynn, H. R., Skehel, J. M., and West, S. C. (2008). Identification of holliday junction resolvases from humans and yeast. *Nature*, 456(7220):357–361. PMID: 19020614. 24, 140

Ira, G., Malkova, A., Liberi, G., Foiani, M., and Haber, J. E. (2003). Srs2 and Sgs1-Top3 suppress crossovers during double-strand break repair in yeast. *Cell*, 115(4):401–411. PMID: 14622595. 25

Irmisch, A., Ampatzidou, E., Mizuno, K., O'Connell, M. J., and Murray, J. M. (2009). Smc5/6 maintains stalled replication forks in a recombination-competent conformation. *The EMBO Journal*, 28(2):144–155. PMID: 19158664 PMCID: 2634738. 139, 151, 165

Jazayeri, A., Falck, J., Lukas, C., Bartek, J., Smith, G. C. M., Lukas, J., and Jackson, S. P. (2006). ATM- and cell cycle-dependent regulation of ATR in response to DNA double-strand breaks. *Nature Cell Biology*, 8(1):37–45. PMID: 16327781. 14

Jensen, M. A., Fukushima, M., and Davis, R. W. (2010). DMSO and betaine greatly improve amplification of GC-Rich constructs in de novo synthesis. *PLoS ONE*, 5:e11024. 76, 229

Johnson, J. E., Smith, J. S., Kozak, M. L., and Johnson, F. B. (2008). In vivo veritas: using yeast to probe the biological functions of g-quadruplexes. *Biochimie*, 90(8):1250–1263. PMID: 18331848. 31, 33, 114

Johnson, R. E., Prakash, S., and Prakash, L. (1994). Yeast DNA repair protein RAD5 that promotes instability of simple repetitive sequences is a DNA-dependent ATPase. *The Journal of biological chemistry*, 269(45):28259–62. PMID: 7961763. 88

Johzuka, K. and Horiuchi, T. (2002). Replication fork block protein, fob1, acts as an rDNA region specific recombinator in s. cerevisiae. *Genes to Cells: Devoted to Molecular & Cellular Mechanisms*, 7(2):99–113. PMID: 11895475. 39

Kai, M., Boddy, M. N., Russell, P., and Wang, T. S. (2005). Replication checkpoint kinase cds1 regulates mus81 to preserve genome integrity during replication stress. *Genes & Development*, 19(8):919–932. PMID: 15805465. 17, 133, 137, 151, 152, 155, 157, 158, 219

Kai, M., Furuya, K., Paderi, F., Carr, A. M., and Wang, T. S. F. (2007). Rad3-dependent phosphorylation of the checkpoint clamp regulates repair-pathway choice. *Nature Cell Biology*, 9(6):691–697. PMID: 17515930. 14

Kai, M. and Wang, T. S. (2003). Checkpoint activation regulates mutagenic translesion synthesis. *Genes & Development*, 17(1):64 –76. 137

Kaliraman, V., Mullen, J. R., Fricke, W. M., Bastin-Shanower, S. A., and Brill, S. J. (2001). Functional overlap between Sgs1–Top3 and the Mms4–Mus81 endonuclease. *Genes & Development*, 15(20):2730–2740. PMID: 11641278 PMCID: 312806. 24, 132, 135, 138

Kamath-Loeb, A. S., Loeb, L. A., Johansson, E., Burgers, P. M., and Fry, M. (2001). Interactions between the werner syndrome helicase and DNA polymerase delta specifically facilitate copying of tetraplex and hairpin structures of the d(CGG)n trinucleotide repeat sequence. *The Journal of Biological Chemistry*, 276(19):16439–16446. PMID: 11279038. 114

Kamimura, Y., Masumoto, H., Sugino, A., and Araki, H. (1998). Sld2, which interacts with dpb11 in saccharomyces cerevisiae, is required for chromosomal DNA replication. *Molecular and Cellular Biology*, 18(10):6102–6109. PMID: 9742127. 4

Kamimura, Y., Tak, Y. S., Sugino, A., and Araki, H. (2001). Sld3, which interacts with cdc45 (Sld4), functions for chromosomal DNA replication in saccharomyces cerevisiae. *The EMBO Journal*, 20(8):2097–2107. PMID: 11296242. 4

Kang, M., Lee, C., Kang, Y., Cho, I., Nguyen, T. A., and Seo, Y. (2010). Genetic and functional interactions between Mus81-Mms4 and rad27. *Nucleic Acids Research*, 38(21):7611–7625. PMID: 20660481. 139, 151

Kao, H., Henricksen, L. A., Liu, Y., and Bambara, R. A. (2002). Cleavage specificity of saccharomyces cerevisiae flap endonuclease 1 suggests a double-flap structure as the cellular substrate. *The Journal of Biological Chemistry*, 277(17):14379–14389. PMID: 11825897. 8, 139

Karras, G. I. and Jentsch, S. (2010). The RAD6 DNA damage tolerance pathway operates uncoupled from the replication fork and is functional beyond s phase. *Cell*, 141(2):255–267. PMID: 20403322. 29

Katou, Y., Kanoh, Y., Bando, M., Noguchi, H., Tanaka, H., Ashikari, T., Sugimoto, K., and Shirahige, K. (2003). S-phase checkpoint proteins tof1 and mrc1 form a stable replication-pausing complex. *Nature*, 424(6952):1078–1083. PMID: 12944972. 16, 82

Kawabata, T., Luebben, S. W., Yamaguchi, S., Ilves, I., Matise, I., Buske, T., Botchan, M. R., and Shima, N. (2011). Stalled fork rescue via dormant replication origins in unchallenged s phase promotes proper chromosome segregation and tumor suppression. *Molecular Cell*, 41(5):543–553. PMID: 21362550. 6, 91

Kaykov, A. and Arcangioli, B. (2004). A programmed strand-specific and modified nick in s. pombe constitutes a novel type of chromosomal imprint. *Current Biology: CB*, 14(21):1924–1928. PMID: 15530393. 37

Kearsey, S. E. (1984). Structural requirements for the function of a yeast chromosomal replicator. *Cell*, 37(1):299–307. 3

Kearsey, S. E. and Cotterill, S. (2003). Enigmatic variations: divergent modes of regulating eukaryotic DNA replication. *Molecular Cell*, 12(5):1067–1075. PMID: 14636567. 3, 6

Keil, R. L. and Roeder, G. S. (1984). Cis-acting, recombination-stimulating activity in a fragment of the ribosomal DNA of s. cerevisiae. *Cell*, 39(2 Pt 1):377–386. PMID: 6094015. 35, 39

Kesti, T., Flick, K., Keränen, S., Syväoja, J. E., and Wittenberg, C. (1999). DNA polymerase epsilon catalytic domains are dispensable for DNA replication, DNA repair, and cell viability. *Molecular Cell*, 3(5):679–685. PMID: 10360184. 8

Kikin, O., D'Antonio, L., and Bagga, P. S. (2006). QGRS mapper: a web-based server for predicting g-quadruplexes in nucleotide sequences. *Nucleic Acids Research*, 34(Web Server issue):W676–W682. PMID: 16845096 PMCID: 1538864. 84, 85, 88

Kilkenny, M. L., Doré, A. S., Roe, S. M., Nestoras, K., Ho, J. C. Y., Watts, F. Z., and Pearl, L. H. (2008). Structural and functional analysis of the Crb2-BRCT2 domain reveals distinct roles in checkpoint signaling and DNA damage repair. *Genes & Development*, 22(15):2034–2047. PMID: 18676809. 15

Klar, A. J. and Miglio, L. M. (1986). Initiation of meiotic recombination by double-strand DNA breaks in s. pombe. *Cell*, 46(5):725–731. PMID: 3742597. 48

Klein, H. L. (2001). Mutations in recombinational repair and in checkpoint control genes suppress the lethal combination of srs2Delta with other DNA repair genes in saccharomyces cerevisiae. *Genetics*, 157(2):557–565. PMID: 11156978. 139

Klungland, A. and Lindahl, T. (1997). Second pathway for completion of human DNA base excision-repair: reconstitution with purified proteins and requirement for DNase IV (FEN1). *The EMBO Journal*, 16(11):3341–3348. PMID: 9214649. 19

Kobayashi, T. (2003). The replication fork barrier site forms a unique structure with fob1p and inhibits the replication fork. *Molecular and Cellular Biology*, 23(24):9178–9188. PMID: 14645529. 35

Kobayashi, T., Heck, D. J., Nomura, M., and Horiuchi, T. (1998). Expansion and contraction of ribosomal DNA repeats in saccharomyces cerevisiae: requirement of replication fork blocking (Fob1) protein and the role of RNA polymerase i. *Genes & Development*, 12(24):3821–3830. PMID: 9869636 PMCID: 317266. 39

Kohli, J., Hottinger, H., Munz, P., Strauss, A., and Thuriaux, P. (1977). Genetic mapping in SCHIZOSACCHAROMYCES POMBE by mitotic and meiotic analysis and induced haploidization. *Genetics*, 87(3):471–489. PMID: 17248775 PMCID: 1213754. 2

Komata, M., Bando, M., Araki, H., and Shirahige, K. (2009). The direct binding of mrc1, a checkpoint mediator, to mcm6, a replication helicase, is essential for the replication checkpoint against methyl Methanesulfonate-Induced stress. *Molecular and Cellular Biology*, 29(18):5008–5019. PMID: 19620285 PMCID: 2738294. 9

Kowalczykowski, S. C. (2000). Initiation of genetic recombination and recombination-dependent replication. *Trends in Biochemical Sciences*, 25(4):156–165. PMID: 10754547. 26

Krings, G. and Bastia, D. (2004). swi1- and swi3-dependent and independent replication fork arrest at the ribosomal DNA of schizosaccharomyces pombe. *Proceedings of the National*

Academy of Sciences of the United States of America, 101(39):14085–14090. PMID: 15371597. 35, 37

Krings, G. and Bastia, D. (2005). Sap1p binds to ter1 at the ribosomal DNA of schizosaccharomyces pombe and causes polar replication fork arrest. *The Journal of Biological Chemistry*, 280(47):39135–39142. PMID: 16195226. 37

Krings, G. and Bastia, D. (2006). Molecular architecture of a eukaryotic DNA replication terminus-terminator protein complex. *Molecular and Cellular Biology*, 26(21):8061–8074. PMID: 16940176. 37

Krogh, B. O. and Symington, L. S. (2004). Recombination proteins in yeast. *Annual Review of Genetics*, 38:233–271. PMID: 15568977. 25

Krügel, H., Fiedler, G., Smith, C., and Baumberg, S. (1993). Sequence and transcriptional analysis of the nourseothricin acetyltransferase-encoding gene nat1 from streptomyces noursei. *Gene*, 127(1):127–131. PMID: 8486278. 72

Kubota, Y., Nash, R. A., Klungland, A., Schär, P., Barnes, D. E., and Lindahl, T. (1996). Reconstitution of DNA base excision-repair with purified human proteins: interaction between DNA polymerase beta and the XRCC1 protein. *The EMBO Journal*, 15(23):6662–6670. PMID: 8978692. 19

Kumagai, A. and Dunphy, W. G. (2000). Claspin, a novel protein required for the activation of chk1 during a DNA replication checkpoint response in xenopus egg extracts. *Molecular Cell*, 6(4):839–849. PMID: 11090622. 15, 16

Kumagai, A., Lee, J., Yoo, H. Y., and Dunphy, W. G. (2006). TopBP1 activates the ATR-ATRIP complex. *Cell*, 124(5):943–955. 15

Kumari, S., Bugaut, A., Huppert, J. L., and Balasubramanian, S. (2007). An RNA g-quadruplex in the 5' UTR of the NRAS proto-oncogene modulates translation. *Nature Chemical Biology*, 3(4):218–221. PMID: 17322877. 33

Kunz, B. A., Straffon, A. F., and Vonarx, E. J. (2000). DNA damage-induced mutation: tolerance via translesion synthesis. *Mutation Research/Fundamental and Molecular Mechanisms of Mutagenesis*, 451(1-2):169–185. 29, 129

Kwon, K. and Beckett, D. (2000). Function of a conserved sequence motif in biotin holoenzyme synthetases. *Protein Science: A Publication of the Protein Society*, 9(8):1530–1539. PMID: 10975574. 217

Labib, K. (2010). How do cdc7 and cyclin-dependent kinases trigger the initiation of chromosome replication in eukaryotic cells? *Genes & Development*, 24(12):1208–1219. PMID: 20551170. 4, 6

Labib, K. and Diffley, J. F. (2001). Is the MCM2-7 complex the eukaryotic DNA replication fork helicase? *Current Opinion in Genetics & Development*, 11(1):64–70. PMID: 11163153. 7

Labib, K. and Hodgson, B. (2007). Replication fork barriers: pausing for a break or stalling for time? *EMBO Reports*, 8(4):346–353. PMID: 17401409. 30, 35, 39, 91

Labib, K., Tercero, J. A., and Diffley, J. F. (2000). Uninterrupted MCM2-7 function required for DNA replication fork progression. *Science (New York, N.Y.)*, 288(5471):1643–1647. PMID: 10834843. 7

Lambert, S. and Carr, A. M. (2005). Checkpoint responses to replication fork barriers. *Biochimie*, 87(7):591–602. PMID: 15989976. 6, 30, 39, 91

Lambert, S., Froget, B., and Carr, A. M. (2007). Arrested replication fork processing: interplay between checkpoints and recombination. *DNA Repair*, 6(7):1042–1061. PMID: 17412649. 26, 27, 164

Lambert, S., Mizuno, K., Blaisonneau, J., Martineau, S., Chanet, R., Fréon, K., Murray, J. M., Carr, A. M., and Baldacci, G. (2010). Homologous recombination restarts blocked replication forks at the expense of genome rearrangements by template exchange. *Molecular Cell*, 39(3):346–359. PMID: 20705238. 11, 26, 27, 41, 92, 103, 129, 160

Lambert, S., Watson, A., Sheedy, D. M., Martin, B., and Carr, A. M. (2005). Gross chromosomal rearrangements and elevated recombination at an inducible site-specific replication fork barrier. *Cell*, 121(5):689–702. PMID: 15935756. 11, 26, 27, 39, 40, 41, 42, 72, 87, 91, 92, 93, 110, 112, 114, 116, 129, 160

Lawrence, C. (1994). The RAD6 DNA repair pathway in saccharomyces cerevisiae: what does it do, and how does it do it? *BioEssays: News and Reviews in Molecular, Cellular and Developmental Biology*, 16(4):253–258. PMID: 8031302. 87

Lea, D. and Coulson, C. (1949). The distribution of the numbers of mutants in bacterial populations. *J. Genet.*, 49:264–285. 57, 58, 75, 76, 119

Lee, J., Kumagai, A., and Dunphy, W. G. (2007a). The Rad9-Hus1-Rad1 checkpoint clamp regulates interaction of TopBP1 with ATR. *The Journal of Biological Chemistry*, 282(38):28036–28044. PMID: 17636252. 14

Lee, J. A., Carvalho, C. M. B., and Lupski, J. R. (2007b). A DNA replication mechanism for generating nonrecurrent rearrangements associated with genomic disorders. *Cell*, 131(7):1235–1247. PMID: 18160035. 156

Lee, J. K., Moon, K. Y., Jiang, Y., and Hurwitz, J. (2001). The schizosaccharomyces pombe origin recognition complex interacts with multiple AT-rich regions of the replication origin DNA by means of the AT-hook domains of the spOrc4 protein. *Proceedings of the National Academy of Sciences of the United States of America*, 98(24):13589–13594. PMID: 11717425. 4

Lehmann, A. R. (2003). Replication of damaged DNA. *Cell Cycle (Georgetown, Tex.)*, 2(4):300–302. PMID: 12851478. 11

Lehmann, A. R. and KirkBell, S. (1972). PostReplication repair of DNA in UltravioletIrradiated mammalian cells. *European Journal of Biochemistry*, 31(3):438–445. 28, 70

Lehmann, A. R., Niimi, A., Ogi, T., Brown, S., Sabbioneda, S., Wing, J. F., Kannouche, P. L., and Green, C. M. (2007). Translesion synthesis: Y-family polymerases and the polymerase switch. *DNA Repair*, 6(7):891–899. 29, 70

Lei, M., Kawasaki, Y., Young, M. R., Kihara, M., Sugino, A., and Tye, B. K. (1997). Mcm2 is a target of regulation by Cdc7–Dbf4 during the initiation of DNA synthesis. *Genes & Development*, 11(24):3365–3374. PMID: 9407029 PMCID: 316824. 4

Leman, A. R., Noguchi, C., Lee, C. Y., and Noguchi, E. (2010). Human timeless and tipin stabilize replication forks and facilitate sister-chromatid cohesion. *Journal of Cell Science*, 123(Pt 5):660–670. PMID: 20124417. 16

Leupold, U. (1949). *Die Vererbung von Homothallie und Heterothallie bei Schizosaccharomyces Pombe.* Zurich. 2

Li, G. (2008). Mechanisms and functions of DNA mismatch repair. *Cell Res*, 18(1):85–98. 18

Li, X., Stith, C. M., Burgers, P. M., and Heyer, W. (2009). PCNA is required for initiation of recombination-associated DNA synthesis by DNA polymerase delta. *Molecular Cell*, 36(4):704–713. PMID: 19941829. 23

Lieber, M. R. and Wilson, T. E. (2010). SnapShot: nonhomologous DNA end joining (NHEJ). *Cell*, 142(3):496–496.e1. PMID: 20691907. 21

Liefshitz, B., Parket, A., Maya, R., and Kupiec, M. (1995). The role of DNA repair genes in recombination between repeated sequences in yeast. *Genetics*, 140(4):1199–211. PMID: 7498763. 77

Lim, D. S. and Hasty, P. (1996). A mutation in mouse rad51 results in an early embryonic lethal that is suppressed by a mutation in p53. *Molecular and Cellular Biology*, 16(12):7133–7143. PMID: 8943369. 26

Linskens, M. H. and Huberman, J. A. (1988). Organization of replication of ribosomal DNA in saccharomyces cerevisiae. *Molecular and Cellular Biology*, 8(11):4927–4935. PMID: 3062373. 35

Lipps, H. J. and Rhodes, D. (2009). G-quadruplex structures: in vivo evidence and function. *Trends in Cell Biology*, 19(8):414–422. PMID: 19589679. 30, 31, 32, 33

Lisby, M., Barlow, J. H., Burgess, R. C., and Rothstein, R. (2004). Choreography of the DNA damage response: spatiotemporal relationships among checkpoint and repair proteins. *Cell*, 118(6):699–713. PMID: 15369670. 137

Liu, C., Powell, K. A., Mundt, K., Wu, L., Carr, A. M., and Caspari, T. (2003). Cop9/signalosome subunits and pcu4 regulate ribonucleotide reductase by both checkpoint-dependent and -independent mechanisms. *Genes & Development*, 17(9):1130–1140. PMID: 12695334. 17

Liu, V. F., Bhaumik, D., and Wang, T. S. (1999). Mutator phenotype induced by aberrant replication. *Molecular and Cellular Biology*, 19(2):1126–1135. PMID: 9891047. 139, 151

Liu, Z. and Gilbert, W. (1994). The yeast KEM1 gene encodes a nuclease specific for g4 tetraplex DNA: implication of in vivo functions for this novel DNA structure. *Cell*, 77(7):1083–1092. PMID: 8020096. 90

Llorente, B., Smith, C. E., and Symington, L. S. (2008). Break-induced replication: What is it and what is it for? *Cell Cycle*, 7:859–864. 11, 27, 28

Lopes, M., Cotta-Ramusino, C., Pellicioli, A., Liberi, G., Plevani, P., Muzi-Falconi, M., Newlon, C. S., and Foiani, M. (2001). The DNA replication checkpoint response stabilizes stalled replication forks. *Nature*, 412(6846):557–561. PMID: 11484058. 17, 27, 84, 137

Lopes, M., Foiani, M., and Sogo, J. M. (2006). Multiple mechanisms control chromosome integrity after replication fork uncoupling and restart at irreparable UV lesions. *Molecular Cell*, 21(1):15–27. PMID: 16387650. 28

Lorenz, A., West, S. C., and Whitby, M. C. (2010). The human holliday junction resolvase GEN1 rescues the meiotic phenotype of a schizosaccharomyces pombe mus81 mutant. *Nucleic Acids Research*, 38(6):1866–1873. PMID: 20040574. 141

Lou, H., Komata, M., Katou, Y., Guan, Z., Reis, C. C., Budd, M., Shirahige, K., and Campbell, J. L. (2008). Mrc1 and DNA polymerase epsilon function together in linking DNA replication and the s phase checkpoint. *Molecular Cell*, 32(1):106–117. PMID: 18851837. 9, 128

Lovett, S. T., Drapkin, P. T., Sutera, V. A., and Gluckman-Peskind, T. J. (1993). A sister-strand exchange mechanism for recA-independent deletion of repeated DNA sequences in escherichia coli. *Genetics*, 135(3):631–42. PMID: 8293969. 69, 77, 87

Lovett, S. T. and Feschenko, V. V. (1996). Stabilization of diverged tandem repeats by mismatch repair: evidence for deletion formation via a misaligned replication intermediate. *Proceedings of the National Academy of Sciences of the United States of America*, 93(14):7120–4. PMID: 8692955. 18

Lupardus, P. J., Byun, T., Yee, M., Hekmat-Nejad, M., and Cimprich, K. A. (2002). A requirement for replication in activation of the ATR-dependent DNA damage checkpoint. *Genes & Development*, 16(18):2327–2332. PMID: 12231621. 12

Maga, G. and Hubscher, U. (2003). Proliferating cell nuclear antigen (PCNA): a dancer with many partners. *Journal of cell science*, 116(Pt 15):3051–60. PMID: 12829735. 28

Maga, G., Stucki, M., Spadari, S., and Hübscher, U. (2000). DNA polymerase switching: I. replication factor c displaces DNA polymerase prior to PCNA loading. *Journal of Molecular Biology*, 295(4):791–801. 8

Mahaney, B. L., Meek, K., and Lees-Miller, S. P. (2009). Repair of ionizing radiation-induced DNA double-strand breaks by non-homologous end-joining. *Biochemical Journal*, 417:639. 21

Majka, J., Binz, S. K., Wold, M. S., and Burgers, P. M. J. (2006). Replication protein a directs loading of the DNA damage checkpoint clamp to 5'-DNA junctions. *The Journal of Biological Chemistry*, 281(38):27855–27861. PMID: 16864589. 14

Majka, J. and Burgers, P. M. (2005). Function of Rad17/Mec3/Ddc1 and its partial complexes in the DNA damage checkpoint. *DNA Repair*, 4(10):1189–1194. PMID: 16137930. 14

Manke, I. A., Lowery, D. M., Nguyen, A., and Yaffe, M. B. (2003). BRCT repeats as phosphopeptide-binding modules involved in protein targeting. *Science (New York, N.Y.)*, 302(5645):636–639. PMID: 14576432. 15

Mankouri, H. W. and Morgan, A. (2001). The DNA helicase activity of yeast sgs1p is essential for normal lifespan but not for resistance to topoisomerase inhibitors. *Mechanisms of Ageing and Development*, 122(11):1107–1120. PMID: 11389927. 140

Marchler-Bauer, A., Lu, S., Anderson, J. B., Chitsaz, F., Derbyshire, M. K., DeWeese-Scott, C., Fong, J. H., Geer, L. Y., Geer, R. C., Gonzales, N. R., Gwadz, M., Hurwitz, D. I., Jackson, J. D., Ke, Z., Lanczycki, C. J., Lu, F., Marchler, G. H., Mullokandov, M., Omelchenko, M. V., Robertson, C. L., Song, J. S., Thanki, N., Yamashita, R. A., Zhang, D., Zhang, N., Zheng, C., and Bryant, S. H. (2011). CDD: a conserved domain database for the functional annotation of proteins. *Nucleic Acids Research*, 39(Database issue):D225–229. PMID: 21109532. 38

Martín, V., Chahwan, C., Gao, H., Blais, V., Wohlschlegel, J., 3rd Yates, J. R., McGowan, C. H., and Russell, P. (2006). Sws1 is a conserved regulator of homologous recombination in eukaryotic cells. *The EMBO Journal*, 25(11):2564–2574. PMID: 16710300. 77

Masuda-Sasa, T., Polaczek, P., Peng, X. P., Chen, L., and Campbell, J. L. (2008). Processing of g4 DNA by dna2 Helicase/Nuclease and replication protein a (RPA) provides insights into the mechanism of Dna2/RPA substrate recognition. *The Journal of Biological Chemistry*, 283(36):24359–24373. PMID: 18593712 PMCID: 2528986. 90

Mathews, C. K. (2006). DNA precursor metabolism and genomic stability. *The FASEB Journal: Official Publication of the Federation of American Societies for Experimental Biology*, 20(9):1300–1314. PMID: 16816105. 7, 18

Matos, J., Blanco, M. G., Maslen, S., Skehel, J. M., and West, S. C. (2011). Regulatory control of the resolution of DNA recombination intermediates during meiosis and mitosis. *Cell*, 147(1):158–172. PMID: 21962513. 24, 140, 155

Matsumoto, Y. and Kim, K. (1995). Excision of deoxyribose phosphate residues by DNA polymerase beta during DNA repair. *Science (New York, N.Y.)*, 269(5224):699–702. PMID: 7624801. 19

Maundrell, K., Hutchison, A., and Shall, S. (1988). Sequence analysis of ARS elements in fission yeast. *The EMBO Journal*, 7(7):2203–2209. PMID: 3046932. 4

Mazón, G., Mimitou, E. P., and Symington, L. S. (2010). SnapShot: homologous recombination in DNA double-strand break repair. *Cell*, 142(4):646, 646.e1. PMID: 20723763. 23, 24, 25

McAllister, H. C. and Coon, M. J. (1966). Further studies on the properties of liver propionyl coenzyme a holocarboxylase synthetase and the specificity of holocarboxylase formation. *The Journal of Biological Chemistry*, 241(12):2855–2861. PMID: 4287927. 217

McCulloch, S. D. and Kunkel, T. A. (2008). The fidelity of DNA synthesis by eukaryotic replica-

tive and translesion synthesis polymerases. *Cell Research*, 18(1):148–161. PMID: 18166979. 18

McGlynn, P. and Lloyd, R. G. (2002). Recombinational repair and restart of damaged replication forks. *Nat Rev Mol Cell Biol*, 3(11):859–870. 26

McPherson, J. P., Lemmers, B., Chahwan, R., Pamidi, A., Migon, E., Matysiak-Zablocki, E., Moynahan, M. E., Essers, J., Hanada, K., Poonepalli, A., Sanchez-Sweatman, O., Khokha, R., Kanaar, R., Jasin, M., Hande, M. P., and Hakem, R. (2004). Involvement of mammalian mus81 in genome integrity and tumor suppression. *Science (New York, N.Y.)*, 304(5678):1822–1826. PMID: 15205536. 141

Mejía-Ramírez, E., Sánchez-Gorostiaga, A., Krimer, D. B., Schvartzman, J. B., and Hernández, P. (2005). The mating type switch-activating protein sap1 is required for replication fork arrest at the rRNA genes of fission yeast. *Molecular and Cellular Biology*, 25(19):8755–8761. PMID: 16166653. 35

Michel, B., Grompone, G., Florès, M., and Bidnenko, V. (2004). Multiple pathways process stalled replication forks. *Proceedings of the National Academy of Sciences of the United States of America*, 101(35):12783–8. PMID: 15328417. 91

Mimitou, E. P. and Symington, L. S. (2008). Sae2, exo1 and sgs1 collaborate in DNA double-strand break processing. *Nature*, 455(7214):770–774. PMID: 18806779. 23

Mitchison, J. M. (1957). The growth of single cells. i. schizosaccharomyces pombe. *Experimental Cell Research*, 13(2):244–262. PMID: 13480293. 2

Miyabe, I., Kunkel, T. A., and Carr, A. M. (2011). The major roles of DNA polymerases epsilon and delta at the eukaryotic replication fork are evolutionarily conserved. *PLoS Genetics*, 7(12):e1002407. PMID: 22144917. 7, 8, 82, 116, 128

Mizuno, K., Lambert, S., Baldacci, G., Murray, J. M., and Carr, A. M. (2009). Nearby inverted repeats fuse to generate acentric and dicentric palindromic chromosomes by a replication template exchange mechanism. *Genes & Development*, 23(24):2876–2886. PMID: 20008937. 11, 26, 27, 39, 40, 41, 42, 72, 87, 92, 93, 95, 96, 97, 103, 110, 111, 112, 114, 129, 160

Mochida, S., Esashi, F., Aono, N., Tamai, K., O'Connell, M. J., and Yanagida, M. (2004). Regulation of checkpoint kinases through dynamic interaction with crb2. *The EMBO Journal*, 23(2):418–428. PMID: 14739927. 15

Mohanty, B. K. and Bastia, D. (2004). Binding of the replication terminator protein fob1p to the ter sites of yeast causes polar fork arrest. *The Journal of Biological Chemistry*, 279(3):1932–1941. PMID: 14576157. 35

Mol, C. D., Parikh, S. S., Putnam, C. D., Lo, T. P., and Tainer, J. A. (1999). DNA REPAIR MECHANISMS FOR THE RECOGNITION AND REMOVAL OF DAMAGED DNA BASES. *Annual Review of Biophysics and Biomolecular Structure*, 28:101–128. 19

Moldovan, G., Pfander, B., and Jentsch, S. (2007). PCNA, the maestro of the replication fork. *Cell*, 129(4):665–679. PMID: 17512402. 8

Mordes, D. A., Nam, E. A., and Cortez, D. (2008). Dpb11 activates the Mec1-Ddc2 complex. *Proceedings of the National Academy of Sciences of the United States of America*, 105(48):18730–18734. PMID: 19028869. 15

Morikawa, H., Morishita, T., Kawane, S., Iwasaki, H., Carr, A. M., and Shinagawa, H. (2004). Rad62 protein functionally and physically associates with the smc5/smc6 protein complex and is required for chromosome integrity and recombination repair in fission yeast. *Molecular and Cellular Biology*, 24(21):9401–9413. PMID: 15485909. 139, 151

Moser, J., Kool, H., Giakzidis, I., Caldecott, K., Mullenders, L. H. F., and Fousteri, M. I. (2007). Sealing of chromosomal DNA nicks during nucleotide excision repair requires XRCC1 and DNA ligase III alpha in a cell-cycle-specific manner. *Molecular Cell*, 27(2):311–323. PMID: 17643379. 20

Moser, J., Volker, M., Kool, H., Alekseev, S., Vrieling, H., Yasui, A., van Zeeland, A. A., and Mullenders, L. H. F. (2005). The UV-damaged DNA binding protein mediates efficient targeting of the nucleotide excision repair complex to UV-induced photo lesions. *DNA Repair*, 4(5):571–582. PMID: 15811629. 20

Moyer, S. E., Lewis, P. W., and Botchan, M. R. (2006). Isolation of the Cdc45/Mcm2–7/GINS (CMG) complex, a candidate for the eukaryotic DNA replication fork helicase. *Proceedings of the National Academy of Sciences of the United States of America*, 103(27):10236–10241. PMID: 16798881 PMCID: 1482467. 6, 7

Mullen, J. R., Kaliraman, V., Ibrahim, S. S., and Brill, S. J. (2001). Requirement for three novel protein complexes in the absence of the sgs1 DNA helicase in saccharomyces cerevisiae. *Genetics*, 157(1):103–118. PMID: 11139495. 132, 133

Murakami, H. and Okayama, H. (1995). A kinase from fission yeast responsible for blocking mitosis in s phase. *Nature*, 374(6525):817–819. PMID: 7723827. 16, 126

Muramatsu, S., Hirai, K., Tak, Y., Kamimura, Y., and Araki, H. (2010). CDK-dependent complex formation between replication proteins dpb11, sld2, pol , and GINS in budding yeast. *Genes & Development*, 24(6):602–612. 4

Muris, D. F., Vreeken, K., Carr, A. M., Murray, J. M., Smit, C., Lohman, P. H., and Pastink, A. (1996). Isolation of the schizosaccharomyces pombe RAD54 homologue, rhp54+, a gene involved in the repair of radiation damage and replication fidelity. *Journal of Cell Science*, 109 (Pt 1):73–81. PMID: 8834792. 139

Murray, J. M. and Carr, A. M. (2008). Smc5/6: a link between DNA repair and unidirectional replication? *Nature reviews. Molecular cell biology*, 9(2):177–82. PMID: 18059412. 35, 91, 137, 139

Murray, J. M., Lindsay, H. D., Munday, C. A., and Carr, A. M. (1997). Role of schizosaccharomyces pombe RecQ homolog, recombination, and checkpoint genes in UV damage tolerance. *Molecular and Cellular Biology*, 17(12):6868–6875. PMID: 9372918 PMCID: 232543. 139

Muzi-Falconi, M., Giannattasio, M., Foiani, M., and Plevani, P. (2003). The DNA polymerase alpha-primase complex: multiple functions and interactions. *TheScientificWorldJournal*, 3:21–33. PMID: 12806117. 7

Myers, J. S. and Cortez, D. (2006). Rapid activation of ATR by ionizing radiation requires ATM and mre11. *The Journal of Biological Chemistry*, 281(14):9346–9350. PMID: 16431910. 14

Nasmyth, K. and Nurse, P. (1981). Cell division cycle mutants altered in DNA replication and mitosis in the fission yeast schizosaccharomyces pombe. *Molecular & General Genetics: MGG*, 182(1):119–124. PMID: 6943408. 7

Navadgi-Patil, V. M. and Burgers, P. M. (2008). Yeast DNA replication protein dpb11 activates the Mec1/ATR checkpoint kinase. *The Journal of Biological Chemistry*, 283(51):35853–35859. PMID: 18922789. 15

Nedelcheva, M. N., Roguev, A., Dolapchiev, L. B., Shevchenko, A., Taskov, H. B., Shevchenko, A., Stewart, A. F., and Stoynov, S. S. (2005). Uncoupling of unwinding from DNA synthesis implies regulation of MCM helicase by Tof1/Mrc1/Csm3 checkpoint complex. *Journal of Molecular Biology*, 347(3):509–521. PMID: 15755447. 9

Nick McElhinny, S. A., Gordenin, D. A., Stith, C. M., Burgers, P. M. J., and Kunkel, T. A. (2008). Division of labor at the eukaryotic replication fork. *Molecular Cell*, 30(2):137–144. PMID: 18439893. 7

Niida, H., Shimada, M., Murakami, H., and Nakanishi, M. (2010). Mechanisms of dNTP supply that play an essential role in maintaining genome integrity in eukaryotic cells. *Cancer Science*, 101(12):2505–2509. 16

Nimonkar, A. V., Sica, R. A., and Kowalczykowski, S. C. (2009). Rad52 promotes second-end DNA capture in double-stranded break repair to form complement-stabilized joint molecules. *Proceedings of the National Academy of Sciences of the United States of America*, 106(9):3077–3082. PMID: 19204284. 23

Nishino, T., Komori, K., Ishino, Y., and Morikawa, K. (2003). X-ray and biochemical anatomy of an archaeal XPF/Rad1/Mus81 family nuclease: similarity between its endonuclease domain and restriction enzymes. *Structure (London, England: 1993)*, 11(4):445–457. PMID: 12679022. 132

Noguchi, E., Noguchi, C., Du, L., and Russell, P. (2003). Swi1 prevents replication fork collapse and controls checkpoint kinase cds1. *Molecular and Cellular Biology*, 23(21):7861–7874. PMID: 14560029. 16, 38, 84, 87, 139, 158

Noguchi, E., Noguchi, C., McDonald, W. H., 3rd Yates, J. R., and Russell, P. (2004). Swi1 and swi3 are components of a replication fork protection complex in fission yeast. *Molecular and Cellular Biology*, 24(19):8342–8355. PMID: 15367656. 16, 37, 38, 82, 139, 165

Nurse, P. (1991). The florey lecture, 1990. how is the cell division cycle regulated? *Philosophical Transactions of the Royal Society of London. Series B, Biological Sciences*, 332(1264):271–276. PMID: 1680238. 2, 3

Nurse, P. (1997). Regulation of the eukaryotic cell cycle. *European Journal of Cancer*, 33(7):1002–1004. 2

Nurse, P. M. (2002). Nobel lecture. cyclin dependent kinases and cell cycle control. *Bioscience Reports*, 22(5-6):487–499. PMID: 12635846. 3

Odagiri, N., Seki, M., Onoda, F., Yoshimura, A., Watanabe, S., and Enomoto, T. (2003). Budding yeast mms4 is epistatic with rad52 and the function of mms4 can be replaced by a bacterial holliday junction resolvase. *DNA Repair*, 2(3):347–358. 133, 136

Ogi, T. and Lehmann, A. R. (2006). The y-family DNA polymerase kappa (pol kappa) functions in mammalian nucleotide-excision repair. *Nature Cell Biology*, 8(6):640–642. PMID: 16738703. 20

Ohya, T., Kawasaki, Y., Hiraga, S., Kanbara, S., Nakajo, K., Nakashima, N., Suzuki, A., and Sugino, A. (2002). The DNA polymerase domain of pol(epsilon) is required for rapid, efficient, and highly accurate chromosomal DNA replication, telomere length maintenance, and normal cell senescence in saccharomyces cerevisiae. *The Journal of Biological Chemistry*, 277(31):28099–28108. PMID: 12015307. 8

Okazaki, R., Okazaki, T., Sakabe, K., Sugimoto, K., and Sugino, A. (1968). Mechanism of DNA chain growth. i. possible discontinuity and unusual secondary structure of newly synthesized chains. *Proceedings of the National Academy of Sciences of the United States of America*, 59(2):598–605. PMID: 4967086 PMCID: 224714. 8

Oliver, A. W. and Kneale, G. G. (1999). Structural characterization of DNA and RNA sequences recognized by the gene 5 protein of bacteriophage fd. *Biochemical Journal*, 339(Pt 3):525–531. PMID: 10215589 PMCID: 1220186. 85

Osborn, A. J. and Elledge, S. J. (2003). Mrc1 is a replication fork component whose phosphorylation in response to DNA replication stress activates rad53. *Genes & Development*, 17(14):1755–1767. 15, 82

Osman, F., Dixon, J., Barr, A. R., and Whitby, M. C. (2005). The F-Box DNA helicase fbh1 prevents rhp51-dependent recombination without mediator proteins. *Molecular and Cellular Biology*, 25(18):8084–8096. PMID: 16135800. 25, 77

Osman, F., Dixon, J., Doe, C. L., and Whitby, M. C. (2003). Generating crossovers by resolution of nicked holliday junctions: a role for Mus81-Eme1 in meiosis. *Molecular Cell*, 12(3):761–774. PMID: 14527420. 24, 131, 136, 140, 149

Osman, F. and Whitby, M. C. (2007). Exploring the roles of Mus81-Eme1/Mms4 at perturbed replication forks. *DNA Repair*, 6(7):1004–1017. PMID: 17409028. 24, 131, 134, 139, 151, 154, 155, 163, 164

Oğrünç, M. and Sancar, A. (2003). Identification and characterization of human MUS81-MMS4 structure-specific endonuclease. *The Journal of Biological Chemistry*, 278(24):21715–21720. PMID: 12686547. 132

Paciotti, V., Clerici, M., Scotti, M., Lucchini, G., and Longhese, M. P. (2001). Characterization of mec1 kinase-deficient mutants and of new hypomorphic mec1 alleles impairing subsets of the DNA damage response pathway. *Molecular and Cellular Biology*, 21(12):3913–3925. PMID: 11359899. 17

Paeschke, K., Capra, J. A., and Zakian, V. A. (2011). DNA replication through g-quadruplex motifs is promoted by the saccharomyces cerevisiae pif1 DNA helicase. *Cell*, 145(5):678–691. PMID: 21620135. 161

Paeschke, K., Juranek, S., Simonsson, T., Hempel, A., Rhodes, D., and Lipps, H. J. (2008). Telomerase recruitment by the telomere end binding protein-beta facilitates g-quadruplex DNA unfolding in ciliates. *Nature Structural & Molecular Biology*, 15(6):598–604. PMID: 18488043. 32

Paeschke, K., Simonsson, T., Postberg, J., Rhodes, D., and Lipps, H. J. (2005). Telomere end-binding proteins control the formation of g-quadruplex DNA structures in vivo. *Nature Structural & Molecular Biology*, 12(10):847–854. PMID: 16142245. 32

Painter, R. B. and Young, B. R. (1980). Radiosensitivity in ataxia-telangiectasia: a new explanation. *Proceedings of the National Academy of Sciences of the United States of America*, 77(12):7315–7317. PMID: 6938978. 12

Palecek, J., Vidot, S., Feng, M., Doherty, A. J., and Lehmann, A. R. (2006). The Smc5-Smc6 DNA repair complex. bridging of the Smc5-Smc6 heads by the KLEISIN, nse4, and non-Kleisin subunits. *The Journal of biological chemistry*, 281(48):36952–9. PMID: 17005570. 219

Palombo, F., Iaccarino, I., Nakajima, E., Ikejima, M., Shimada, T., and Jiricny, J. (1996). hMutS-beta, a heterodimer of hMSH2 and hMSH3, binds to insertion/deletion loops in DNA. *Current Biology: CB*, 6(9):1181–1184. PMID: 8805365. 18

Palzkill, T. G. and Newlon, C. S. (1988). A yeast replication origin consists of multiple copies of a small conserved sequence. *Cell*, 53(3):441–450. PMID: 3284655. 3

Papouli, E., Chen, S., Davies, A. A., Huttner, D., Krejci, L., Sung, P., and Ulrich, H. D. (2005). Crosstalk between SUMO and ubiquitin on PCNA is mediated by recruitment of the helicase srs2p. *Molecular Cell*, 19(1):123–133. PMID: 15989970. 29

Parkinson, G. N., Lee, M. P. H., and Neidle, S. (2002). Crystal structure of parallel quadruplexes from human telomeric DNA. *Nature*, 417(6891):876–880. PMID: 12050675. 32

Parrilla-Castellar, E. R., Arlander, S. J. H., and Karnitz, L. (2004). Dial 9-1-1 for DNA damage: the Rad9-Hus1-Rad1 (9-1-1) clamp complex. *DNA Repair*, 3(8-9):1009–1014. PMID: 15279787. 14

Pavlov, Y. I., Frahm, C., Nick McElhinny, S. A., Niimi, A., Suzuki, M., and Kunkel, T. A. (2006). Evidence that errors made by DNA polymerase alpha are corrected by DNA polymerase delta. *Current Biology: CB*, 16(2):202–207. PMID: 16431373. 9

Pebernard, S., Wohlschlegel, J., McDonald, W. H., Yates, J. R., and Boddy, M. N. (2006). The Nse5-Nse6 dimer mediates DNA repair roles of the Smc5-Smc6 complex. *Molecular and Cellular Biology*, 26(5):1617–1630. PMID: 16478984. 139, 219

Petermann, E., Helleday, T., and Caldecott, K. W. (2008). Claspin promotes normal replication fork rates in human cells. *Molecular Biology of the Cell*, 19(6):2373–2378. PMID: 18353973. 16

Petukhova, G., Stratton, S., and Sung, P. (1998). Catalysis of homologous DNA pairing by yeast rad51 and rad54 proteins. *Nature*, 393(6680):91–94. 23

Petukhova, G., Van Komen, S., Vergano, S., Klein, H., and Sung, P. (1999). Yeast rad54 promotes rad51-dependent homologous DNA pairing via ATP hydrolysis-driven change in DNA double helix conformation. *The Journal of Biological Chemistry*, 274(41):29453–29462. PMID: 10506208. 23

Pfander, B., Moldovan, G., Sacher, M., Hoege, C., and Jentsch, S. (2005). SUMO-modified PCNA recruits srs2 to prevent recombination during s phase. *Nature*, 436(7049):428–33. PMID: 15931174. 29

Piazza, A., Boulé, J., Lopes, J., Mingo, K., Largy, E., Teulade-Fichou, M., and Nicolas, A. (2010). Genetic instability triggered by g-quadruplex interacting Phen-DC compounds in saccharomyces cerevisiae. *Nucleic Acids Research*, 38(13):4337–4348. PMID: 20223771. 34, 90, 114, 159

Pickart, C. M. (2000). Ubiquitin in chains. *Trends in Biochemical Sciences*, 25(11):544–548. PMID: 11084366. 28

Pommier, Y., Redon, C., Rao, V. A., Seiler, J. A., Sordet, O., Takemura, H., Antony, S., Meng, L., Liao, Z., Kohlhagen, G., Zhang, H., and Kohn, K. W. (2003). Repair of and checkpoint response to topoisomerase i-mediated DNA damage. *Mutation Research*, 532(1-2):173–203. PMID: 14643436. 136

Prakash, L. (1981). Characterization of postreplication repair in saccharomyces cerevisiae and effects of rad6, rad18, rev3 and rad52 mutations. *Molecular & general genetics : MGG*, 184(3):471–8. PMID: 7038396. 28, 70

Prescott, D. M. (1994). The DNA of ciliated protozoa. *Microbiological Reviews*, 58(2):233–267. PMID: 8078435. 32

Preston, B. D., Albertson, T. M., and Herr, A. J. (2010). DNA replication fidelity and cancer. *Seminars in Cancer Biology*, 20(5):281–293. 18

Prudden, J., Evans, J. S., Hussey, S. P., Deans, B., O'Neill, P., Thacker, J., and Humphrey, T. (2003). Pathway utilization in response to a site-specific DNA double-strand break in fission yeast. *The EMBO Journal*, 22(6):1419–1430. PMID: 12628934. 21

Putnam, C. D., Hayes, T. K., and Kolodner, R. D. (2010). Post-Replication repair suppresses Duplication-Mediated genome instability. *PLoS Genet*, 6(5):e1000933. 58

Qiu, J., Qian, Y., Frank, P., Wintersberger, U., and Shen, B. (1999). Saccharomyces cerevisiae RNase h(35) functions in RNA primer removal during lagging-strand DNA synthesis, most efficiently in cooperation with rad27 nuclease. *Molecular and Cellular Biology*, 19(12):8361–8371. PMID: 10567561. 139

Quina, A. S., Buschbeck, M., and Di Croce, L. (2006). Chromatin structure and epigenetics. *Biochemical Pharmacology*, 72(11):1563–1569. PMID: 16836980. 156

Raji, H. and Hartsuiker, E. (2006). Double-strand break repair and homologous recombination in schizosaccharomyces pombe. *Yeast (Chichester, England)*, 23(13):963–976. PMID: 17072889. 21, 25, 88

Raleigh, J. and O'Connell, M. (2000). The g(2) DNA damage checkpoint targets both wee1 and cdc25. *Journal of Cell Science*, 113(10):1727 –1736. 16

Rawal, P., Kummarasetti, V. B. R., Ravindran, J., Kumar, N., Halder, K., Sharma, R., Mukerji, M., Das, S. K., and Chowdhury, S. (2006). Genome-wide prediction of g4 DNA as regulatory motifs: role in escherichia coli global regulation. *Genome Research*, 16(5):644–655. PMID: 16651665. 31

Razidlo, D. F. and Lahue, R. S. (2008). Mrc1, tof1 and csm3 inhibit CAGÂCTG repeat instability by at least two mechanisms. *DNA Repair*, 7(4):633–640. 84

Reenan, R. A. and Kolodner, R. D. (1992). Characterization of insertion mutations in the saccharomyces cerevisiae MSH1 and MSH2 genes: evidence for separate mitochondrial and nuclear functions. *Genetics*, 132(4):975–85. PMID: 1334021. 58

Reichard, P. (1988). Interactions between deoxyribonucleotide and DNA synthesis. *Annual Review of Biochemistry*, 57:349–374. PMID: 3052277. 84, 137

Remus, D., Beuron, F., Tolun, G., Griffith, J. D., Morris, E. P., and Diffley, J. F. (2009). Concerted loading of mcm2–7 double hexamers around DNA during DNA replication origin licensing. *Cell*, 139(4):719–730. 4

Remus, D. and Diffley, J. F. X. (2009). Eukaryotic DNA replication control: lock and load, then fire. *Current Opinion in Cell Biology*, 21(6):771–777. PMID: 19767190. 6, 7

Ribeyre, C., Lopes, J., Boulé, J., Piazza, A., Guédin, A., Zakian, V. A., Mergny, J., and Nicolas, A. (2009). The yeast pif1 helicase prevents genomic instability caused by G-Quadruplex-Forming CEB1 sequences in vivo. *PLoS Genetics*, 5(5). PMID: 19424434 PMCID: 2673046. 33, 34, 90, 114, 129, 159, 161

Ricke, R. M. and Bielinsky, A. (2004). Mcm10 regulates the stability and chromatin association of DNA polymerase-alpha. *Molecular Cell*, 16(2):173–185. PMID: 15494305. 9

Rijkers, T., Van Den Ouweland, J., Morolli, B., Rolink, A. G., Baarends, W. M., Van Sloun, P. P., Lohman, P. H., and Pastink, A. (1998). Targeted inactivation of mouse RAD52 reduces homologous recombination but not resistance to ionizing radiation. *Molecular and Cellular Biology*, 18(11):6423–6429. PMID: 9774658. 26

Robertson, A. B., Klungland, A., Rognes, T., and Leiros, I. (2009). DNA repair in mammalian cells: Base excision repair: the long and short of it. *Cellular and Molecular Life Sciences: CMLS*, 66(6):981–993. PMID: 19153658. 19

Roseaulin, L., Yamada, Y., Tsutsui, Y., Russell, P., Iwasaki, H., and Arcangioli, B. (2008). Mus81 is essential for sister chromatid recombination at broken replication forks. *The EMBO Journal*, 27(9):1378–1387. PMID: 18388861. 24, 136, 138, 149, 150, 151, 154, 158, 164, 165

Rudin, N. and Haber, J. E. (1988). Efficient repair of HO-induced chromosomal breaks in saccharomyces cerevisiae by recombination between flanking homologous sequences. *Molecular and Cellular Biology*, 8(9):3918 –3928. 25

Rupp, W. D. and Howard-Flanders, P. (1968). Discontinuities in the DNA synthesized in an excision-defective strain of escherichia coli following ultraviolet irradiation. *Journal of Molecular Biology*, 31(2):291–304. PMID: 4865486. 28

Russell, P. and Nurse, P. (1986). cdc25+ functions as an inducer in the mitotic control of fission yeast. *Cell*, 45(1):145–153. 3

Saitoh, S., Takahashi, K., Nabeshima, K., Yamashita, Y., Nakaseko, Y., Hirata, A., and Yanagida, M. (1996). Aberrant mitosis in fission yeast mutants defective in fatty acid synthetase and acetyl CoA carboxylase. *The Journal of Cell Biology*, 134(4):949–961. PMID: 8769419. 219

Saka, Y., Esashi, F., Matsusaka, T., Mochida, S., and Yanagida, M. (1997). Damage and replication checkpoint control in fission yeast is ensured by interactions of crb2, a protein with BRCT motif, with cut5 and chk1. *Genes & Development*, 11(24):3387–3400. PMID: 9407031. 15, 219

Salvati, E., Leonetti, C., Rizzo, A., Scarsella, M., Mottolese, M., Galati, R., Sperduti, I., Stevens, M. F. G., D'Incalci, M., Blasco, M., Chiorino, G., Bauwens, S., Horard, B., Gilson, E., Stoppacciaro, A., Zupi, G., and Biroccio, A. (2007). Telomere damage induced by the g-quadruplex ligand RHPS4 has an antitumor effect. *The Journal of Clinical Investigation*, 117(11):3236–3247. PMID: 17932567. 32

Sambrook, J., Fritsch, E., and Maniatis, T. (1989). *Molecular Cloning: A Laboratory Manual*. Second edition. Cold Spring Harbor Laboratory Press. 60

Sánchez-Gorostiaga, A., López-Estraño, C., Krimer, D. B., Schvartzman, J. B., and Hernández, P. (2004). Transcription termination factor reb1p causes two replication fork barriers at its cognate sites in fission yeast ribosomal DNA in vivo. *Molecular and Cellular Biology*, 24(1):398–406. PMID: 14673172. 37

Sandler, S. J. and Marians, K. J. (2000). Role of PriA in replication fork reactivation inEscherichia coli. *Journal of Bacteriology*, 182(1):9 –13. 91

Saparbaev, M., Prakash, L., and Prakash, S. (1996). Requirement of mismatch repair genes MSH2 and MSH3 in the RAD1-RAD10 pathway of mitotic recombination in saccharomyces cerevisiae. *Genetics*, 142(3):727–736. PMID: 8849883. 18

Sarkies, P., Reams, C., Simpson, L. J., and Sale, J. E. (2010). Epigenetic instability due to defective replication of structured DNA. *Molecular Cell*, 40(5):703–713. PMID: 21145480. 34, 114, 123, 129, 157, 159

Sarkies, P. and Sale, J. E. (2011). Propagation of histone marks and epigenetic memory during normal and interrupted DNA replication. *Cellular and Molecular Life Sciences*. 6

Saveson, C. J. and Lovett, S. T. (1997). Enhanced deletion formation by aberrant DNA replication in escherichia coli. *Genetics*, 146(2):457–70. PMID: 9177997. 82, 87

Schaffitzel, C., Berger, I., Postberg, J., Hanes, J., Lipps, H. J., and Plückthun, A. (2001). In vitro generated antibodies specific for telomeric guanine-quadruplex DNA react with stylonychia lemnae macronuclei. *Proceedings of the National Academy of Sciences of the United States of America*, 98(15):8572–8577. PMID: 11438689. 30, 32

Schlacher, K., Christ, N., Siaud, N., Egashira, A., Wu, H., and Jasin, M. (2011). Double-strand break repair-independent role for BRCA2 in blocking stalled replication fork degradation by MRE11. *Cell*, 145(4):529–542. PMID: 21565612. 27

Schürer, K. A., Rudolph, C., Ulrich, H. D., and Kramer, W. (2004). Yeast MPH1 gene functions in an error-free DNA damage bypass pathway that requires genes from homologous recombination, but not from postreplicative repair. *Genetics*, 166(4):1673–1686. PMID: 15126389. 89

Schvartzman, J. B. and Stasiak, A. (2004). A topological view of the replicon. *EMBO Reports*, 5(3):256–261. PMID: 14993926. 157

Segurado, M., de Luis, A., and Antequera, F. (2003). Genome-wide distribution of DNA replication origins at A+T-rich islands in schizosaccharomyces pombe. *EMBO Reports*, 4(11):1048–1053. PMID: 14566325. 40, 41, 93, 117

Segurado, M. and Diffley, J. F. X. (2008). Separate roles for the DNA damage checkpoint protein kinases in stabilizing DNA replication forks. *Genes & Development*, 22(13):1816–1827. PMID: 18593882. 17

Segurado, M. and Tercero, J. A. (2009). The s-phase checkpoint: targeting the replication fork. *Biology of the Cell / Under the Auspices of the European Cell Biology Organization*, 101(11):617–627. PMID: 19686094. 6, 12, 13, 15, 17, 27, 157

Sen, D. and Gilbert, W. (1988). Formation of parallel four-stranded complexes by guanine-rich motifs in DNA and its implications for meiosis. *Nature*, 334(6180):364–366. PMID: 3393228. 30

Sergeant, J., Taylor, E., Palecek, J., Fousteri, M., Andrews, E. A., Sweeney, S., Shinagawa, H., Watts, F. Z., and Lehmann, A. R. (2005). Composition and architecture of the schizosaccharomyces pombe rad18 (Smc5-6) complex. *Molecular and Cellular Biology*, 25(1):172–184. PMID: 15601840. 219

Sharma, S., Sommers, J. A., and Brosh, R. M. J. (2008). Processing of DNA replication and repair intermediates by the concerted action of RecQ helicases and rad2 structure-specific nucleases. *Protein and Peptide Letters*, 15(1):89–102. PMID: 18221018. 139, 151

Sheedy, D. M., Dimitrova, D., Rankin, J. K., Bass, K. L., Lee, K. M., Tapia-Alveal, C., Harvey, S. H., Murray, J. M., and O'Connell, M. J. (2005). Brc1-mediated DNA repair and damage tolerance. *Genetics*, 171(2):457–468. PMID: 15972456. 151, 154, 164

Shimmoto, M., Matsumoto, S., Odagiri, Y., Noguchi, E., Russell, P., and Masai, H. (2009). Interactions between Swi1-Swi3, mrc1 and s phase kinase, hsk1 may regulate cellular responses to stalled replication forks in fission yeast. *Genes to Cells: Devoted to Molecular & Cellular Mechanisms*, 14(6):669–682. PMID: 19422421. 16

Shor, E., Weinstein, J., and Rothstein, R. (2005). A genetic screen for top3 suppressors in saccharomyces cerevisiae identifies SHU1, SHU2, PSY3 and CSM2: four genes involved in error-free DNA repair. *Genetics*, 169(3):1275–1289. PMID: 15654096. 77

Siddiqui-Jain, A., Grand, C. L., Bearss, D. J., and Hurley, L. H. (2002). Direct evidence for a g-quadruplex in a promoter region and its targeting with a small molecule to repress c-MYC transcription. *Proceedings of the National Academy of Sciences of the United States of America*, 99(18):11593–11598. PMID: 12195017. 33

Sipiczki, M. (2000). Where does fission yeast sit on the tree of life? *Genome Biology*, 1(2):reviews1011.1–reviews1011.4. PMID: 11178233 PMCID: 138848. 2

Sofueva, S., Osman, F., Lorenz, A., Steinacher, R., Castagnetti, S., Ledesma, J., and Whitby, M. C. (2011). Ultrafine anaphase bridges, broken DNA and illegitimate recombination induced by a replication fork barrier. *Nucleic Acids Research*, 39(15):6568 –6584. 161

Sogo, J. M., Lopes, M., and Foiani, M. (2002). Fork reversal and ssDNA accumulation at stalled replication forks owing to checkpoint defects. *Science (New York, N.Y.)*, 297(5581):599–602. PMID: 12142537. 12, 27, 70

Solinger, J. A. and Heyer, W. (2001). Rad54 protein stimulates the postsynaptic phase of rad51

protein-mediated DNA strand exchange. *Proceedings of the National Academy of Sciences*, 98(15):8447 –8453. 23

Song, B. and Sung, P. (2000). Functional interactions among yeast rad51 recombinase, rad52 mediator, and replication protein a in DNA strand exchange. *Journal of Biological Chemistry*, 275(21):15895 –15904. 23

Stelter, P. and Ulrich, H. D. (2003). Control of spontaneous and damage-induced mutagenesis by SUMO and ubiquitin conjugation. *Nature*, 425(6954):188–91. PMID: 12968183. 70

Stewart, J. A., Campbell, J. L., and Bambara, R. A. (2010). Dna2 is a structure-specific nuclease, with affinity for 5-flap intermediates. 38(3):920–930. PMID: 19934252 PMCID: 2817469. 8

Stewart, J. A., Miller, A. S., Campbell, J. L., and Bambara, R. A. (2008). Dynamic removal of replication protein a by dna2 facilitates primer cleavage during okazaki fragment processing in saccharomyces cerevisiae. *The Journal of Biological Chemistry*, 283(46):31356–31365. PMID: 18799459. 8

Stillman, B. (2008). DNA polymerases at the replication fork in eukaryotes. *Molecular Cell*, 30(3):259–260. PMID: 18471969. 5, 7

Stokes, M. P., Van Hatten, R., Lindsay, H. D., and Michael, W. M. (2002). DNA replication is required for the checkpoint response to damaged DNA in xenopus egg extracts. *The Journal of Cell Biology*, 158(5):863–872. PMID: 12213834. 12

Streisinger, G., Okada, Y., Emrich, J., Newton, J., Tsugita, A., Terzaghi, E., and Inouye, M. (1966). Frameshift mutations and the genetic code. *Cold Spring Harbor Symposia on Quantitative Biology*, 31:77 –84. 69

Sugasawa, K. (2011). Multiple DNA damage recognition factors involved in mammalian nucleotide excision repair. *Biochemistry (Moscow)*, 76:16–23. 20

Sugasawa, K., Ng, J. M., Masutani, C., Iwai, S., van der Spek, P. J., Eker, A. P., Hanaoka, F., Bootsma, D., and Hoeijmakers, J. H. (1998). Xeroderma pigmentosum group c protein complex is the initiator of global genome nucleotide excision repair. *Molecular Cell*, 2(2):223–232. PMID: 9734359. 20

Sugawara, N. and Haber, J. E. (1992). Characterization of double-strand break-induced recombination: homology requirements and single-stranded DNA formation. *Molecular and Cellular Biology*, 12(2):563–575. PMID: 1732731 PMCID: 364230. 89

Sugawara, N., Ira, G., and Haber, J. E. (2000). DNA length dependence of the single-strand annealing pathway and the role of saccharomyces cerevisiae RAD59 in double-strand break repair. *Molecular and Cellular Biology*, 20(14):5300–5309. PMID: 10866686. 25

Sugawara, N., Pâques, F., Colaiácovo, M., and Haber, J. E. (1997). Role of saccharomyces cerevisiae msh2 and msh3 repair proteins in double-strand break-induced recombination. *Proceedings of the National Academy of Sciences of the United States of America*, 94(17):9214–9219. PMID: 9256462. 18, 25

Sugiyama, T. and Kantake, N. (2009). Dynamic regulatory interactions of rad51, rad52, and replication protein-a in recombination intermediates. *Journal of Molecular Biology*, 390(1):45–55. PMID: 19445949. 23

Sugiyama, T. and Kowalczykowski, S. C. (2002). Rad52 protein associates with replication protein a (RPA)-single-stranded DNA to accelerate rad51-mediated displacement of RPA and presynaptic complex formation. *The Journal of Biological Chemistry*, 277(35):31663–31672. PMID: 12077133. 23

Sugiyama, T., Zaitseva, E. M., and Kowalczykowski, S. C. (1997). A single-stranded DNA-binding protein is needed for efficient presynaptic complex formation by the saccharomyces cerevisiae rad51 protein. *The Journal of Biological Chemistry*, 272(12):7940–7945. PMID: 9065463. 23

Sung, P. (1997). Yeast rad55 and rad57 proteins form a heterodimer that functions with replication protein a to promote DNA strand exchange by rad51 recombinase. *Genes & Development*, 11(9):1111–1121. PMID: 9159392. 23

Symington, L. S. (1998). Homologous recombination is required for the viability of rad27 mutants. *Nucleic Acids Research*, 26(24):5589–5595. PMID: 9837987. 139

Symington, L. S. (2002). Role of RAD52 epistasis group genes in homologous recombination and Double-Strand break repair. *Microbiol. Mol. Biol. Rev.*, 66(4):630–670. 21, 26, 136

Szostak, J. W., Orr-Weaver, T. L., Rothstein, R. J., and Stahl, F. W. (1983). The double-strand-break repair model for recombination. *Cell*, 33(1):25–35. PMID: 6380756. 21, 22, 23

Szyjka, S. J., Viggiani, C. J., and Aparicio, O. M. (2005). Mrc1 is required for normal progression of replication forks throughout chromatin in s. cerevisiae. *Molecular Cell*, 19(5):691–697. PMID: 16137624. 9, 82, 87

Tak, Y., Tanaka, Y., Endo, S., Kamimura, Y., and Araki, H. (2006). A CDK-catalysed regulatory phosphorylation for formation of the DNA replication complex Sld2-Dpb11. *The EMBO Journal*, 25(9):1987–1996. PMID: 16619031. 4

Tanaka, K. (2010). Multiple functions of the s-phase checkpoint mediator. *Bioscience, Biotechnology, and Biochemistry*, 74(12):2367–2373. PMID: 21150122. 118

Tanaka, K. and Russell, P. (2001). Mrc1 channels the DNA replication arrest signal to checkpoint kinase cds1. *Nature Cell Biology*, 3(11):966–972. PMID: 11715017. 9

Tanaka, T., Umemori, T., Endo, S., Muramatsu, S., Kanemaki, M., Kamimura, Y., Obuse, C., and Araki, H. (2011). Sld7, an sld3-associated protein required for efficient chromosomal DNA replication in budding yeast. *EMBO J*, 30(10):2019–2030. 4

Tay, Y. D. and Wu, L. (2010). Overlapping roles for yen1 and mus81 in cellular holliday junction processing. *The Journal of Biological Chemistry*, 285(15):11427–11432. PMID: 20178992. 24, 141

Taylor, E. M., Cecillon, S. M., Bonis, A., Chapman, J. R., Povirk, L. F., and Lindsay, H. D. (2010). The Mre11/Rad50/Nbs1 complex functions in resection-based DNA end joining in xenopus laevis. *Nucleic Acids Research*, 38(2):441 –454. 21

Taylor, E. R. and McGowan, C. H. (2008). Cleavage mechanism of human Mus81-Eme1 acting on holliday-junction structures. *Proceedings of the National Academy of Sciences of the United States of America*, 105(10):3757–3762. PMID: 18310322. 135

Tercero, J. A. and Diffley, J. F. (2001). Regulation of DNA replication fork progression through damaged DNA by the Mec1/Rad53 checkpoint. *Nature*, 412(6846):553–557. PMID: 11484057. 17

Tercero, J. A., Longhese, M. P., and Diffley, J. F. (2003). A central role for DNA replication forks in checkpoint activation and response. *Molecular Cell*, 11(5):1323–1336. 9, 12, 17

Thorslund, T. and West, S. C. (2007). BRCA2: a universal recombinase regulator. *Oncogene*, 26(56):7720–7730. 26

Thuriaux, P., Nurse, P., and Carter, B. (1978). Mutants altered in the control co-ordinating cell division with cell growth in the fission yeast schizosaccharomyces pombe. *Molecular & General Genetics: MGG*, 161(2):215–220. PMID: 672898. 3

Tishkoff, D. X., Filosi, N., Gaida, G. M., and Kolodner, R. D. (1997). A novel mutation avoidance mechanism dependent on s. cerevisiae RAD27 is distinct from DNA mismatch repair. *Cell*, 88(2):253–263. PMID: 9008166. 158

Tong, A. H., Evangelista, M., Parsons, A. B., Xu, H., Bader, G. D., Pagé, N., Robinson, M., Raghibizadeh, S., Hogue, C. W., Bussey, H., Andrews, B., Tyers, M., and Boone, C. (2001). Systematic genetic analysis with ordered arrays of yeast deletion mutants. *Science (New York, N.Y.)*, 294(5550):2364–2368. PMID: 11743205. 24, 139, 151

Torigoe, H. and Furukawa, A. (2007). Tetraplex structure of fission yeast telomeric DNA and unfolding of the tetraplex on the interaction with telomeric DNA binding protein pot1. *Journal of Biochemistry*, 141(1):57–68. PMID: 17158862. 32

Torres-Rosell, J., Machín, F., Farmer, S., Jarmuz, A., Eydmann, T., Dalgaard, J. Z., and Aragón, L. (2005). SMC5 and SMC6 genes are required for the segregation of repetitive chromosome regions. *Nature Cell Biology*, 7(4):412–419. PMID: 15793567. 151

Tourrière, H., Versini, G., Cordón-Preciado, V., Alabert, C., and Pasero, P. (2005). Mrc1 and tof1 promote replication fork progression and recovery independently of rad53. *Molecular Cell*, 19(5):699–706. PMID: 16137625. 9

Tran, H. T., Degtyareva, N. P., Koloteva, N. N., Sugino, A., Masumoto, H., Gordenin, D. A., and Resnick, M. A. (1995). Replication slippage between distant short repeats in saccharomyces cerevisiae depends on the direction of replication and the RAD50 and RAD52 genes. *Molecular and cellular biology*, 15(10):5607–17. PMID: 7565712. 69

Tran, P. L. T., Mergny, J., and Alberti, P. (2011). Stability of telomeric g-quadruplexes. 39(8):3282–3294. PMID: 21177648 PMCID: 3082875. 32

Trowbridge, K., McKim, K., Brill, S. J., and Sekelsky, J. (2007). Synthetic lethality of drosophila in the absence of the MUS81 endonuclease and the DmBlm helicase is associated with elevated apoptosis. *Genetics*, 176(4):1993–2001. PMID: 17603121. 24, 138

Tsang, E. and Carr, A. M. (2008). Replication fork arrest, recombination and the maintenance of ribosomal DNA stability. *DNA Repair*, 7(10):1613–1623. PMID: 18638573. 35, 137

Tsuzuki, T., Fujii, Y., Sakumi, K., Tominaga, Y., Nakao, K., Sekiguchi, M., Matsushiro, A., Yoshimura, Y., and MoritaT (1996). Targeted disruption of the rad51 gene leads to lethality in embryonic mice. *Proceedings of the National Academy of Sciences of the United States of America*, 93(13):6236–6240. PMID: 8692798. 26

Ulrich, H. D. (2005). The RAD6 pathway: control of DNA damage bypass and mutagenesis by ubiquitin and SUMO. *Chembiochem: A European Journal of Chemical Biology*, 6(10):1735–1743. PMID: 16142820. 28, 29

Ulrich, H. D. (2011). Timing and spacing of ubiquitin-dependent DNA damage bypass. *FEBS Letters*, 585(18):2861–2867. PMID: 21605556. 11, 28, 29, 70

Umar, A., Risinger, J. I., Glaab, W. E., Tindall, K. R., Barrett, J. C., and Kunkel, T. A. (1998). Functional overlap in mismatch repair by human MSH3 and MSH6. *Genetics*, 148(4):1637–1646. PMID: 9560383. 18

Unsal-Kaçmaz, K., Mullen, T. E., Kaufmann, W. K., and Sancar, A. (2005). Coupling of human circadian and cell cycles by the timeless protein. *Molecular and Cellular Biology*, 25(8):3109–3116. PMID: 15798197. 16

van Hoffen, A., Natarajan, A. T., Mayne, L. V., van Zeeland, A. A., Mullenders, L. H., and Venema, J. (1993). Deficient repair of the transcribed strand of active genes in cockayne's syndrome cells. *Nucleic Acids Research*, 21(25):5890–5895. PMID: 8290349. 20

Venema, J., Mullenders, L. H., Natarajan, A. T., van Zeeland, A. A., and Mayne, L. V. (1990). The genetic defect in cockayne syndrome is associated with a defect in repair of UV-induced DNA damage in transcriptionally active DNA. *Proceedings of the National Academy of Sciences of the United States of America*, 87(12):4707–4711. PMID: 2352945. 20

Vengrova, S. and Dalgaard, J. Z. (2004). RNase-sensitive DNA modification(s) initiates s. pombe mating-type switching. *Genes & Development*, 18(7):794–804. PMID: 15059961. 37

Vialard, J. E., Gilbert, C. S., Green, C. M., and Lowndes, N. F. (1998). The budding yeast rad9 checkpoint protein is subjected to Mec1/Tel1-dependent hyperphosphorylation and interacts with rad53 after DNA damage. *The EMBO Journal*, 17(19):5679–5688. PMID: 9755168. 15

Voelkel-Meiman, K., Keil, R. L., and Roeder, G. S. (1987). Recombination-stimulating sequences in yeast ribosomal DNA correspond to sequences regulating transcription by RNA polymerase i. *Cell*, 48(6):1071–1079. PMID: 3548996. 35, 39

Voineagu, I., Freudenreich, C. H., and Mirkin, S. M. (2009a). Checkpoint responses to unusual structures formed by DNA repeats. *Molecular Carcinogenesis*, 48(4):309–318. PMID: 19306277. 88, 159

Voineagu, I., Surka, C. F., Shishkin, A. A., Krasilnikova, M. M., and Mirkin, S. M. (2009b). Replisome stalling and stabilization at CGG repeats, which are responsible for chromosomal

fragility. *Nature Structural & Molecular Biology*, 16(2):226–228. PMID: 19136957. 84, 118, 128, 159

Waddell, S. and Jenkins, J. R. (1995). arg3+, a new selection marker system for schizosaccharomyces pombe: application of ura4+ as a removable integration marker. *Nucleic Acids Research*, 23(10):1836–1837. PMID: 7784193. 116

Walworth, N., Davey, S., and Beach, D. (1993). Fission yeast chk1 protein kinase links the rad checkpoint pathway to cdc2. *Nature*, 363(6427):368–371. PMID: 8497322. 16

Ward, T. R., Hoang, M. L., Prusty, R., Lau, C. K., Keil, R. L., Fangman, W. L., and Brewer, B. J. (2000). Ribosomal DNA replication fork barrier and HOT1 recombination hot spot: shared sequences but independent activities. *Molecular and Cellular Biology*, 20(13):4948–4957. PMID: 10848619. 35, 39

Warren, C. D., Eckley, D. M., Lee, M. S., Hanna, J. S., Hughes, A., Peyser, B., Jie, C., Irizarry, R., and Spencer, F. A. (2004). S-phase checkpoint genes safeguard high-fidelity sister chromatid cohesion. *Molecular Biology of the Cell*, 15(4):1724–1735. PMID: 14742710. 9

Waters, L. S. and Walker, G. C. (2006). The critical mutagenic translesion DNA polymerase rev1 is highly expressed during G2/M phase rather than s phase. *Proceedings of the National Academy of Sciences*, 103(24):8971 –8976. 129

Watson, A. T., Garcia, V., Bone, N., Carr, A. M., and Armstrong, J. (2008). Gene tagging and gene replacement using recombinase-mediated cassette exchange in schizosaccharomyces pombe. *Gene*, 407(1-2):63–74. PMID: 18054176. 56, 116, 143

Watson, A. T., Werler, P., and Carr, A. M. (2011). Regulation of gene expression at the fission yeast schizosaccharomyces pombe urg1 locus. *Gene*, 484(1-2):75–85. PMID: 21664261. 25, 88, 219

Weinberg, G., Ullman, B., and Martin, D. W. (1981). Mutator phenotypes in mammalian cell mutants with distinct biochemical defects and abnormal deoxyribonucleoside triphosphate pools. *Proceedings of the National Academy of Sciences of the United States of America*, 78(4):2447–2451. PMID: 7017732 PMCID: 319363. 7, 18

Weinert, T. (1998). DNA damage checkpoints update: getting molecular. *Current Opinion in Genetics & Development*, 8:185–193. 12

Weinert, T. A. and Hartwell, L. H. (1988). The RAD9 gene controls the cell cycle response to DNA damage in saccharomyces cerevisiae. *Science (New York, N.Y.)*, 241(4863):317–322. PMID: 3291120. 12

Weinreich, M. and Stillman, B. (1999). Cdc7p-Dbf4p kinase binds to chromatin during s phase and is regulated by both the APC and the RAD53 checkpoint pathway. *The EMBO Journal*, 18(19):5334–5346. PMID: 10508166. 4

Whitby, M. C., Osman, F., and Dixon, J. (2003). Cleavage of model replication forks by fission yeast Mus81-Eme1 and budding yeast Mus81-Mms4. *The Journal of Biological Chemistry*, 278(9):6928–6935. PMID: 12473680. 24, 131, 135

Williams, D. R. and McIntosh, J. R. (2002). mcl1+, the schizosaccharomyces pombe homologue of CTF4, is important for chromosome replication, cohesion, and segregation. *Eukaryotic Cell*, 1(5):758–773. PMID: 12455694. 9, 126

Willson, J., Wilson, S., Warr, N., and Watts, F. Z. (1997). Isolation and characterization of the schizosaccharomyces pombe rhp9 gene: a gene required for the DNA damage checkpoint but not the replication checkpoint. *Nucleic Acids Research*, 25(11):2138–2146. PMID: 9153313. 15

Wood, V., Gwilliam, R., Rajandream, M., Lyne, M., Lyne, R., Stewart, A., Sgouros, J., Peat, N., Hayles, J., Baker, S., Basham, D., Bowman, S., Brooks, K., Brown, D., Brown, S., Chillingworth, T., Churcher, C., Collins, M., Connor, R., Cronin, A., Davis, P., Feltwell, T., Fraser, A., Gentles, S., Goble, A., Hamlin, N., Harris, D., Hidalgo, J., Hodgson, G., Holroyd, S., Hornsby, T., Howarth, S., Huckle, E. J., Hunt, S., Jagels, K., James, K., Jones, L., Jones, M., Leather, S., McDonald, S., McLean, J., Mooney, P., Moule, S., Mungall, K., Murphy, L., Niblett, D., Odell, C., Oliver, K., O'Neil, S., Pearson, D., Quail, M. A., Rabbinowitsch, E., Rutherford, K., Rutter, S., Saunders, D., Seeger, K., Sharp, S., Skelton, J., Simmonds, M., Squares, R., Squares, S., Stevens, K., Taylor, K., Taylor, R. G., Tivey, A., Walsh, S., Warren, T., Whitehead, S., Woodward, J., Volckaert, G., Aert, R., Robben, J., Grymonprez, B., Weltjens, I., Vanstreels, E., Rieger, M., Schäfer, M., Müller-Auer, S., Gabel, C., Fuchs, M., Düsterhöft, A., Fritzc, C., Holzer, E., Moestl, D., Hilbert, H., Borzym, K., Langer, I., Beck, A., Lehrach, H., Reinhardt, R., Pohl, T. M., Eger, P., Zimmermann, W., Wedler, H., Wambutt, R., Purnelle, B., Goffeau, A., Cadieu, E., Dréano, S., Gloux, S., Lelaure, V., Mottier, S., Galibert, F., Aves, S. J., Xiang, Z., Hunt, C., Moore, K., Hurst, S. M., Lucas, M., Rochet, M., Gaillardin, C., Tallada, V. A., Garzon, A., Thode, G., Daga, R. R., Cruzado, L., Jimenez, J., Sánchez, M., del Rey, F., Benito, J., Domínguez, A., Revuelta, J. L., Moreno, S., Armstrong, J., Forsburg, S. L., Cerutti, L.,

Lowe, T., McCombie, W. R., Paulsen, I., Potashkin, J., Shpakovski, G. V., Ussery, D., Barrell, B. G., Nurse, P., and Cerrutti, L. (2002). The genome sequence of schizosaccharomyces pombe. *Nature*, 415(6874):871–880. PMID: 11859360. 2

Wooster, R., Bignell, G., Lancaster, J., Swift, S., Seal, S., Mangion, J., Collins, N., Gregory, S., Gumbs, C., and Micklem, G. (1995). Identification of the breast cancer susceptibility gene BRCA2. *Nature*, 378(6559):789–792. PMID: 8524414. 26

Wu, L. and Hickson, I. D. (2003). The bloom's syndrome helicase suppresses crossing over during homologous recombination. *Nature*, 426(6968):870–874. PMID: 14685245. 24

Wu, P. J. and Nurse, P. (2009). Establishing the program of origin firing during s phase in fission yeast. *Cell*, 136(5):852–864. 4

Xu, H., Boone, C., and Klein, H. L. (2004). Mrc1 is required for sister chromatid cohesion to aid in recombination repair of spontaneous damage. *Mol. Cell. Biol.*, 24(16):7082–7090. 9

Xu, Y., Davenport, M., and Kelly, T. J. (2006). Two-stage mechanism for activation of the DNA replication checkpoint kinase cds1 in fission yeast. *Genes & Development*, 20(8):990–1003. PMID: 16618806. 13, 15, 16, 82, 87, 126, 128

Xu, Y. and Kelly, T. J. (2009). Autoinhibition and autoactivation of the DNA replication checkpoint kinase cds1. *The Journal of Biological Chemistry*, 284(23):16016–16027. PMID: 19357077. 15

Yoo, S. and Dynan, W. S. (1999). Geometry of a complex formed by double strand break repair proteins at a single DNA end: Recruitment of DNA-PKcs induces inward translocation of ku protein. *Nucleic Acids Research*, 27(24):4679 –4686. 21

Yoshizawa-Sugata, N. and Masai, H. (2007). Human Tim/Timeless-interacting protein, tipin, is required for efficient progression of s phase and DNA replication checkpoint. *The Journal of Biological Chemistry*, 282(4):2729–2740. PMID: 17102137. 16

Zampetti-Bosseler, F. and Scott, D. (1981). Cell death, chromosome damage and mitotic delay in normal human, ataxia telangiectasia and retinoblastoma fibroblasts after x-irradiation. *International Journal of Radiation Biology and Related Studies in Physics, Chemistry, and Medicine*, 39(5):547–558. PMID: 6972365. 12

Zegerman, P. and Diffley, J. F. X. (2007). Phosphorylation of sld2 and sld3 by cyclin-dependent kinases promotes DNA replication in budding yeast. *Nature*, 445(7125):281–285. PMID: 17167417. 4

Zegerman, P. and Diffley, J. F. X. (2009). DNA replication as a target of the DNA damage checkpoint. *DNA Repair*, 8(9):1077–1088. PMID: 19505853. 9, 16, 17

Zegerman, P. and Diffley, J. F. X. (2010). Checkpoint-dependent inhibition of DNA replication initiation by sld3 and dbf4 phosphorylation. *Nature*, 467(7314):474–478. PMID: 20835227. 17

Zhang, H. and Lawrence, C. W. (2005). The error-free component of the RAD6/RAD18 DNA damage tolerance pathway of budding yeast employs sister-strand recombination. *Proceedings of the National Academy of Sciences of the United States of America*, 102(44):15954–15959. PMID: 16247017. 29, 70, 87

Zhang, R., Sengupta, S., Yang, Q., Linke, S. P., Yanaihara, N., Bradsher, J., Blais, V., McGowan, C. H., and Harris, C. C. (2005). BLM helicase facilitates mus81 endonuclease activity in human cells. *Cancer Research*, 65(7):2526–2531. PMID: 15805243. 134, 139, 142, 151, 153

Zhao, H., Tanaka, K., Nogochi, E., Nogochi, C., and Russell, P. (2003). Replication checkpoint protein mrc1 is regulated by rad3 and tel1 in fission yeast. *Molecular and Cellular Biology*, 23(22):8395–8403. PMID: 14585996. 15

Zhao, X., Chabes, A., Domkin, V., Thelander, L., and Rothstein, R. (2001). The ribonucleotide reductase inhibitor sml1 is a new target of the Mec1/Rad53 kinase cascade during growth and in response to DNA damage. *The EMBO Journal*, 20(13):3544–3553. PMID: 11432841. 16

Zhao, X., Muller, E. G., and Rothstein, R. (1998). A suppressor of two essential checkpoint genes identifies a novel protein that negatively affects dNTP pools. *Molecular Cell*, 2(3):329–340. PMID: 9774971. 17

Zhu, Z., Chung, W., Shim, E. Y., Lee, S. E., and Ira, G. (2008). Sgs1 helicase and two nucleases dna2 and exo1 resect DNA double-strand break ends. *Cell*, 134(6):981–994. PMID: 18805091. 23

Zou, H. and Rothstein, R. (1997). Holliday junctions accumulate in replication mutants via a RecA homolog-independent mechanism. *Cell*, 90(1):87–96. PMID: 9230305. 137

Zou, L. and Elledge, S. J. (2003). Sensing DNA damage through ATRIP recognition of RPA-ssDNA complexes. *Science (New York, N.Y.)*, 300(5625):1542–1548. PMID: 12791985. 12

Zou, L., Liu, D., and Elledge, S. J. (2003). Replication protein a-mediated recruitment and activation of rad17 complexes. *Proceedings of the National Academy of Sciences of the United States of America*, 100(24):13827–13832. PMID: 14605214. 12

Appendix A

Proximity-dependent protein biotinylation

Biochemical procedures to identify interaction partners of a protein are well established. However, the strength of the interaction between the proteins is often a limiting factor for their purification. Choi-Rhee et al. (2004) proposed a new method, which involves proximity-dependent protein biotinylation by a mutated biotin protein ligase (BPL). Tagging of the protein of interest with this mutated BPL would allow us to take a snapshot of factors that are in close proximity by subsequent purification and identification by mass spectrometry (Choi-Rhee et al., 2004; Cronan, 2005).

A.1 Introduction and background

Biotin, also known as vitamin H, is essential for cell growth and a cofactor of enzymes involved in the cell metabolism. BPLs are enzymes that attach biotin to their target proteins with extraordinary specificity (Chapman-Smith and Cronan, 1999). There are usually less than five different target proteins in an organism and in *E. coli* there is only one, BCCP, the biotin carboxyl carrier protein subunit of acetyl-CoA carboxylase (Cronan, 1990).

Enzymatic biotinylation occurs via two steps: first, ATP and biotin are converted to the intermediate biotinoyl-AMP (bio-5'-AMP), which is then retained in the active site of the BPL. In the second part of the reaction, bio-5'-AMP is covalently bound to the biotin-accepting domain of a protein following a nucleophilic attack by the target lysine residue (McAllister and Coon, 1966; Chapman-Smith and Cronan, 1999). The active site of BPLs contains a conserved unstructured loop (GRGRXG, X; any amino acid), which was shown to be important for biotin and intermediate (bio-5'-AMP) binding (Kwon and Beckett, 2000). Choi-Rhee et al. (2004) proposed that mutations of the *E. coli* BPL, BirA, in this conserved motif, caused leakage of bio-5'-AMP from the

active site and would result in nonspecific biotinylation of lysine sidechains. This reaction is likely to be proximity-dependent based on the dilution of bio-5'-AMP as it diffuses away from BirA and its inactivation by hydrolysis (Choi-Rhee et al., 2004). Characterisation of BirA carrying the mutation R118G in the GRGRRG motif showed self-biotinylation and nonspecific biotinylation of a large number of cellular proteins *in vivo* (Choi-Rhee et al., 2004). *In vitro* experiments also confirmed that proteins fused to BirA-R118G are preferably biotinylated compared to proteins free in solution (Choi-Rhee et al., 2004).

Based on this data we decided to develop a method in *S. pombe* with which proteins in close proximity to a protein of interest can be biotinylated *in vivo*, purified with streptavidin-coated magnetic beads (Dynabeads) and subsequently identified by mass spectrometry (Figure A.1A). This purification method could then be used to identify proteins involved in replication fork collapse and restart at RTS1 or DNA repair pathways such as PRR.

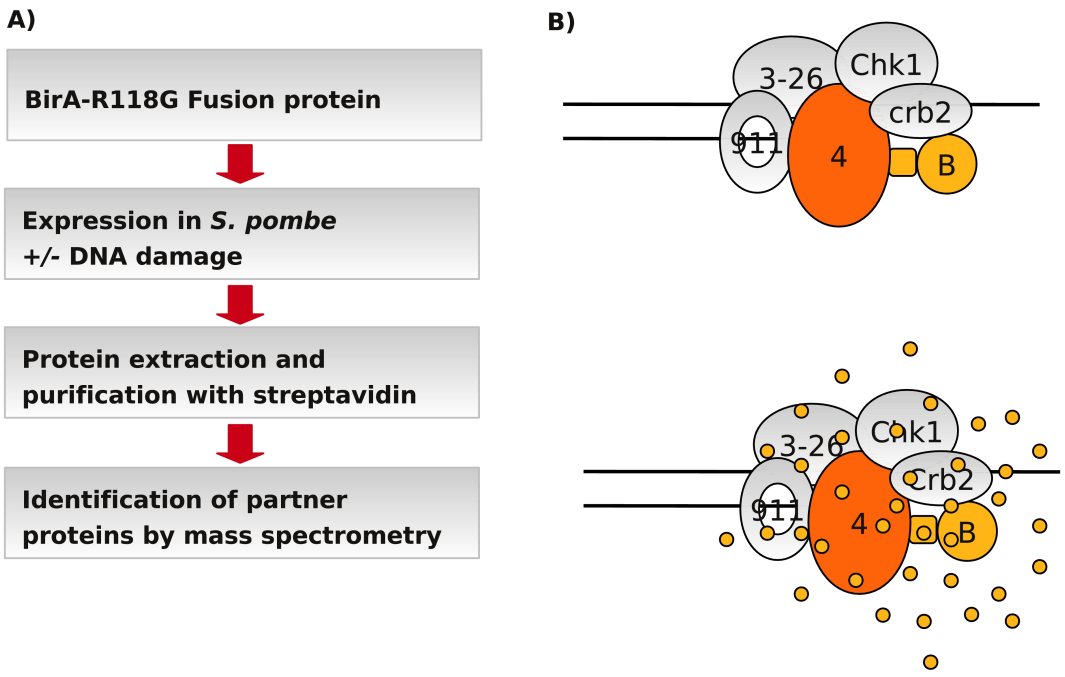

Figure A.1: A novel method for identification of interaction partners
A) Overview of the purification strategy.
B) Promiscous proximity-dependent biotinylation of proteins interacting with Rad4. 3-26; Rad3-Rad26, 911; Rad9-Rad1-Hus1, 4; Rad4; B; BirA-R118G. Small yellow circles; biotin-5'-AMP.

A.2 Initial protein tagging and expression of candidates (work done by R. Haigh)

Rhp18, Nse4, Rad4 and Cds1 were chosen as candidates in order to validate the method. These proteins are of interest to our institute and valuable information and constructs are available. *S. pombe* Nse4 (Rad62), the kleisin component of the Smc5-6 (Structural Maintenance of Chromosomes) complex, forms a subcomplex together with Nse3 and Nse1 and is thought to connect the head domains of Smc5 and Smc6 (Palecek et al., 2006). Smc5 and Smc6 form a complex with Nse2 and Nse5-Nse6 were also shown to interact (Sergeant et al., 2005; Pebernard et al., 2006). The essential protein Rad4 plays a role in the initiation of DNA replication and in the DNA damage checkpoint response (Garcia et al., 2005). It was shown to interact with Rad9, a component of the checkpoint clamp and Crb2 (Saka et al., 1997; Furuya et al., 2004). The interaction with Rad9 is strongly increased after treatment with Hydroxyurea (HU) or γ-radiation (Furuya et al., 2004). Cds1 (*h*Chk2) is a replication checkpoint kinase that stabilizes stalled replication forks and was shown to interact with Rad60 and Mus81 (Boddy et al., 2003; Kai et al., 2005). The ubiquitin ligase Rhp18 is recruited to stalled replication forks and initiates PRR together with Rhp6 by monoubiquitylation of PCNA (Hoege et al., 2002; Frampton et al., 2006). Other proteins involved in PRR, such as Rad8 and Ubc13-Mms2 are candidates for this assay (Frampton et al., 2006).

Fusion of the mutated BirA ligase (BirA-R188G, referred to as R118G) to Rhp18, Nse4, Cds1 and Rad4 should biotinylate interacting proteins and therefore allow to test the method and identify unknown and known interaction partners. An example for Rad4 is shown in Figure A.1B.

Rebecca Haigh, a project student in our lab under my supervision, carried out the initial work in this project. I will only summarise her results, most relevant for my subsequent work, as the experiments are presented and described in more details in her project report.

The BirA gene was amplified from *E. coli* genomic DNA and the mutation R118G was introduced by site-directed mutagenesis. *cds1*$^+$, *nse4*$^+$, *rhp18*$^+$ and *rad4*$^+$ were amplified from *S. pombe* genomic DNA. The fragments were cloned into a vector containing the *urg1*$^+$ promoter and a TGS linker, which are flanked by incompatible lox sites. Subsequent integration of these constructs by RMCE into the *urg1*$^+$ locus, allows induction of expression within 30 minutes after adding 0.25mg/ml of uracil to the media (Watson et al., 2011). These strains contain the overexpression construct tagged with R118G in addition to the endogenous copy of the gene.

Analysis of whole cell extracts for expression of these constructs by western blotting and probing with streptavidin-HRP conjugate (str-HRP), resulted in the detection of two strong bands in all the tested strains, even in the wild-type control. The sizes of the two bands are likely to correspond to the acetyl-CoA carboxylase Cut6 (256.8 kDa) (Saitoh et al., 1996) and the pyruvate

kinase Pyr1 (130.8 kDa), two suggested target proteins of the *S. pombe* BPL. From the four overexpressed constructs, only a band corresponding to Rad4-R118G (110 kDa), could be detected and was confirmed by probing with a phosphospecific anti-Rad4 antibody (532, V. Garcia). A time course of expression after the addition of uracil showed an increase of Rad4-R118G until up to 3 hours when detected with anti-Rad4 antibody, whereas the band detected with str-HRP only increased until up to 2 hours of expression. These experiments suggested that firstly Rad4-R118G is self-biotinylated and secondly that biotin might be limiting in the cell. The R118G tagged Nse4, Cds1 and Rhp18 were either not expressed or not biotinylated by R118G. The functionality of the tagged Rad4 protein was verified by suppression of temperature-sensitivity of the *rad4-T45M* mutant. R. Haigh subsequently carried out very valuable trial experiments trying to increase the concentration of biotin in the cell and also setting up the purification of biotinylated proteins using Dynabeads.

A.3 Biotinylation of the Rad4 interaction partner Rad9

The initial characterisation by R. Haigh suggested that random biotinylation, at least self-biotinylation, was detectable to a limited extent in cells expressing Rad4-R118G. Compared to the data of Choi-Rhee et al. (2004) in *E. coli*, the amount of biotinylated species appearing in whole cell extracts after overexpression of R118G, was much less in *S. pombe*. This might be due to the availability of biotin as a substrate in the nucleus or steric hindrance of the tagged R118G protein. Next, I wanted to test whether this limited biotinylation was sufficient to modify interacting proteins of Rad4, such as Rad9. Exponentially growing wild-type cells and cells expressing Rad4-R118G for 2 hours were lysed, dialysed for 6 hours and biotinylated proteins were purified using Dynabeads. Dialysis was necessary to wash out free biotin molecules that would saturate the Dynabeads. Figure A.2A shows the corresponding western blots. For detection, streptavidin-HRP and a phosphospecific anti-Rad4 antibody (532, V. Garcia) were used. The pulldown (P) fractions clearly showed an enrichment of biotinylated proteins, of which the two most intense bands correspond to the size of the previously observed Cut6 and Pyr1.

There is a band just below Pyr1, which would correspond to Rad4-R118G in size (red asterisk), but because of the high background, it is impossible to distinguish the band corresponding to Rad4-R118G. Furthermore, the P fraction in wild-type and Rad-R118G cells show the same pattern, although the band at the size of Rad4-R118G is less intense in the wild-type. The results suggest that the accumulation of biotinylated proteins is not due to R118G expression. Anti-Rad4 antibody was used for detection of the same samples and reacts with two specific bands in the input after dialysis (ad) and the unbound fraction after incubation with the Dynabeads (ab) in cells

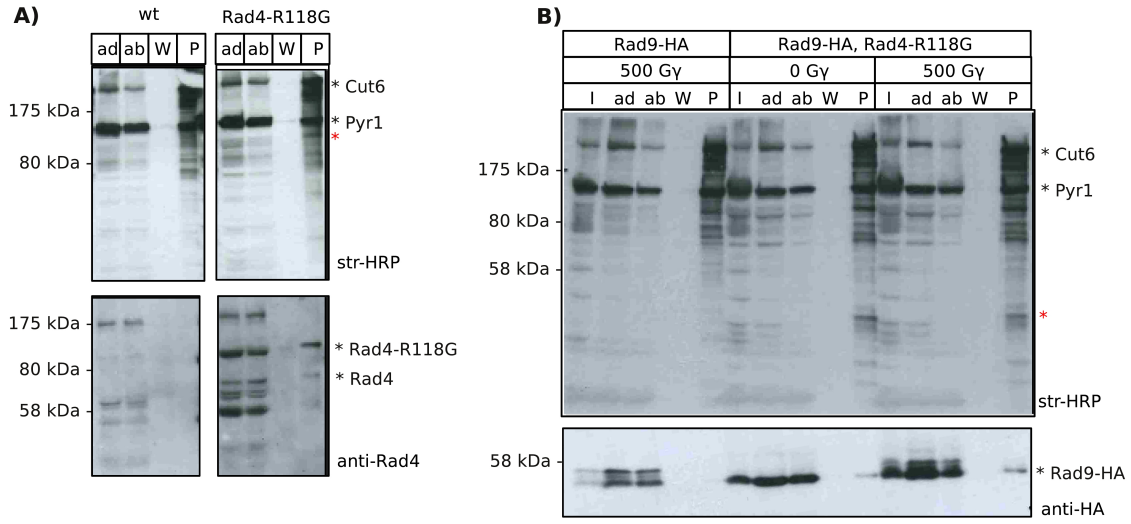

Figure A.2: Pulldown of Rad4-R118G by streptavidin-coated beads
A) Western blot of pulldowns. Wild-type cells and cells expressing Rad4-R118G were grown in YE. Full expression was ensured by addition of uracil to an end concentration of 0.25mg/ml for 2 hours. Cells were lysed with glass beads and extracts were dialysed, purified with streptavidin-coated magnetic beads, separated by 8% SDS-PAGE and analysed by western blotting (see Materials and Methods for details). Top: streptavidin-HRP conjugate (str-HRP), bottom: anti-Rad4 antibody (532). ad: after dialysis, ab: after beads (supernatant after incubation with magnetic beads), W: wash, P: purified elute. Samples taken during the experiment correspond to 10% of the total. Protein bands are indicated with asterisks. The red asterisk marks a band, possibly representing Rad4-R118G. Strain genotypes are listed in Materials and Methods. The molecular weight marker is indicated on the left. Strains used: wt; SAS362, Rad4-R118G; SAS372.
B) Pulldown of Rad4-R118G and Rad9-HA. Cells were grown in YE and expression was induced by adding 0.25mg/ml uracil for 2 hours. Cells were irradiated with 500 gray and lysed with glass beads. Cell extracts were dialysed and purified with streptavidin-coated beads. Fractions were separated by 8% SDS-PAGE and analysed by western blotting. Top: streptavidin-HRP conjugate (str-HRP), bottom: anti-HA antibody. I: input before dialysis, ad: after dialysis, ab: after beads (supernatant after incubation with magnetic beads), W: wash, P: purified elute. Samples taken during the experiment correspond to 10% of the total. Asterisks indicate the detected protein bands. The red asterisk marks a band of 46kDa. The molecular weight marker is indicated on the left. Strain genotypes are listed in Materials and Methods. Strains used: Rad9-HA; KAF1166, Rad4-R118G Rad9-HA; SAS419.

---

expressing Rad4-R118G. These bands correspond in size to Rad4-R118G (110kDa) and endogenous Rad4 (74kDa) protein. Endogenous Rad4 is absent in the pulldown from wild-type cells, which confirms that it is not biotinylated. The presence of Rad4-R118G and Rad4 in the pulldown fraction of the cells expressing Rad4-R118G could be due to interaction between Rad4 and Rad4-R118G proteins. Whether Rad4 is biotinylated as a result of this interaction is not known.

The relatively high amount of Rad4-R118G in the unbound fractions suggests that the pulldown of Rad4-R118G was not efficient, probably due to the high background of endogenous biotinylated proteins. I decided to express Rad9-HA in cells expressing Rad4-R118G and to purify the biotinylated species with Dynabeads. This enabled me to confirm the pulldown of Rad9-HA with

anti-HA antibody.

For this experiment, the cells were irradiated with 500 gray (Gy) to enhance the interaction between Rad4 and Rad9 (Furuya et al., 2004) and biotinylated proteins were pulled down using Dynabeads and detected with str-HRP and anti-HA antibody (Figure A.2B). Probing with str-HRP shows, as observed previously, that biotinylated proteins accumulate in the P fractions and this is irrespective of irradiation or strain background. The anti-HA antibody (bottom membrane) detects Rad9-HA. Rad9 is phosphorylated after DNA damage (Furuya et al., 2004) and the band-shift is clearly visible in the irradiated samples. The band-shift is also visible in P after irradiation, however the amount of protein loaded seems to be less compared to the input fraction (I) and therefore the band is faint. Furthermore, pulldown with streptavidin-coated beads in Rad4-R118G cells yields Rad9-HA. However, comparison of the P fraction to the input fraction (I, 10%) suggests that the reaction was not efficient.

Although Rad9-HA could be purified with Dynabeads, suggesting its biotinylation, this could be due to co-purification with Rad4-R118G, which is self-biotinylated. This experiment was carried out under native condition, which results in intact interaction of these proteins (Furuya et al., 2004). Therefore this experiment does not confirm the biotinylation of Rad9. Intriguingly, a band of lower molecular weight is detected by streptavidin-HRP specifically in Rad4-R118G cells. However, this band corresponds to about 46kDA and therefore runs at a different size as Rad9-HA (54kDa).

To clarify whether Rad9-HA was biotinylated, this experiment was repeated using anti-HA-coated beads (HA-beads) for the purification. Figure A.3 shows the results of an experiment, in which the cultures were split and biotinylated proteins were pulled down with Dynabeads (left) and Rad9-HA was purified by immunoprecipitation (IP) using HA-beads (right). Pulldown with Dynabeads shows enrichment of Rad9-HA in the P fraction of cells co-expressing Rad4-R118G and phosphorylation after DNA damage (left, lane 15, top). IP using HA-beads purified Rad9-HA to a weak intensity (right, lane 15, top). However, probing of these samples with str-HRP did not show any result indicating biotinylation of Rad9-HA, even after overexposure (right, lane 15, bottom).

These experiments suggest that either the fraction of biotinylated Rad9-HA is too small for detection under these conditions or Rad9-HA is not biotinylated by interaction with Rad4-R118G. Although Rad4-R118G is self-biotinylated, Rad9-HA might not be close enough for this reaction or maybe in an unfavourable conformation. Alternatively, Rad9-HA might not expose a suitable lysine residue as a target. The endogenous Rad4 protein is still expressed as well, which might cause some dilution of the over-expressed Rad4-R118G. The limited biotinylation in cells ex-

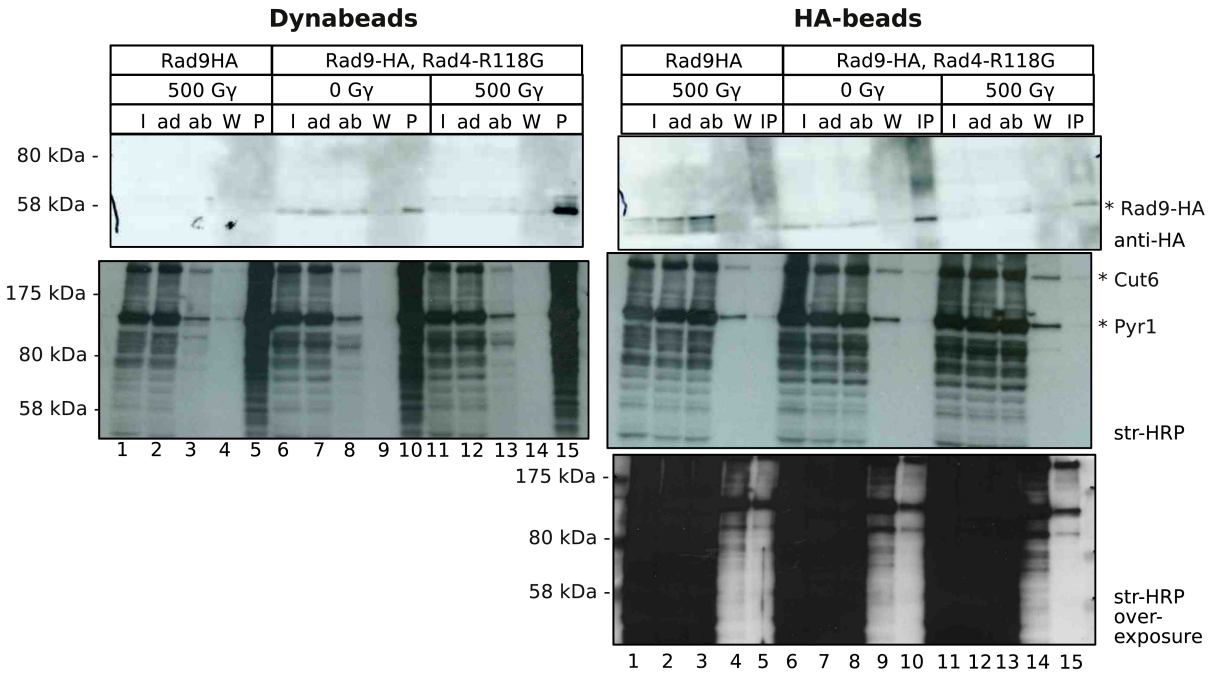

Figure A.3: Pulldown by streptavidin-coated beads and immunoprecipitation (IP) of Rad9-HA
Pulldown experiments shown on the left were performed as described in Figure A.2B. The IP experiment shown on the right was performed using anti-HA coated magnetic beads. The antibody was crosslinked to the beads. Streptavidin-HRP or anti-HA antibody was used for detection, as indicated. The molecular weight marker is indicated on the left. Strain genotypes are listed in Materials and Methods. Strains used: Rad9-HA; KAF1166, Rad4-R118G Rad9-HA; SAS419.

---

pressing Rad4-R118G compared to the work done in *E. coli* by Choi-Rhee et al. (2004), might also suggest that biotinylation is only efficient for the BPL itself. With all the uncertainties and variables, I decided to reproduce the ressults in *E. coli* first.

A.4 Overexpression of BirA and R118G in *E. coli* and *S. pombe*

Wild-type BirA and R118G were expressed in BL21 cells using a pET29b vector (Figure A.4A). The commassie staining shows expression of the two proteins at similar levels after induction by IPTG. The proteins run at about 30kDa, although the expected size is 35kDa. This might be due to the high levels of expression. The same samples were also run on SDS-PAGE and analysed by western blotting. Detection of the constructs by anti-His antibody shows the induction after addition of IPTG, which is completely absent in wild-type cells. A second membrane with these samples was probed with str-HRP which detected random biotinylation when R118G, but not BirA, was over-expressed. These results are comparable with the published data by Choi-Rhee et al. (2004). In these experiments, 5μM of biotin were added to the media. Initial experiments

with adding biotin to the media when growing *S. pombe* cells, did not show an effect on the biotinylation pattern. However, it was noted later that the biotin batch and its preparation was not optimal. For the experiments in *E. coli* a new stock was prepared and added.

BirA and BirA-R118G were also over-expressed in *S. pombe* cells using a pRep1 vector, which allows over-expression under the *nmt1*$^+$ promoter. This promoter in ON, after removal of thiamine from the media (Figure A.4B). The growth media contained 5μM of biotin. In parallel, a construct of the predicted *S. pombe* BPL (SPBC30D10.07c) mutated at the residue (R396G) corresponding to R118 in BirA was also overexpressed using pRep1 and adding a 6x His-tag on the C-terminus. In Figure A.4B, expression of the mutant BirA protein is detected by streptavidin-HRP and random biotinylation, as seen in *E. coli*, is dependent on R118G expression. Overexpression of the mutated *S. pombe* BPL did not show an effect.

Next, I tested, whether the random biotinylation is dependent on the addition of biotin to the media. For this experiment several constructs were used in addition to the *E. coli* BirA and R118G. Because *S. pombe* and *E. coli* differ in their codon usage, a construct was synthesised by the company GenScript (g), which consists of a 6x Flag tag and BirA-R118G adjusted to *S. pombe* codon usage and separated by a TGS linker (FgB). Furthermore, derivatives of this construct were used; the untagged (no Flag tag) R118G (gB) and a construct in which the Flag tag was placed at the C-terminus of R118G rather than the N-terminus (gBF). Figure A.5A shows the analysis of the expression of these constructs in *S. pombe*, comparing the presence and absence of additional biotin in the growth media. The pattern of random biotinylation seems to be similar in all constructs. However, this effect is strictly dependent on the presence of additional biotin. Self-biotinylation of the BirA constructs in the absence of additional biotin might still be detectable, but the intensity of the bands resulting from random biotinylation (on the same membrane) is too strong and prevents the detection of this band. Expression of the tagged constructs was confirmed by probing with anti-Flag and anti-His antibodies.

The ORF of *rad4*$^+$ was cloned into the pRep1 vector expressing FgB to yield the construct Rad4-TGS-6x Flag-TGS-R118G (Rad4-FgB). The results of expression of this fusion protein is depicted in Figure A.5B. Random biotinylation and over-expression was detected for all constructs with str-HRP and anti-Flag antibody, respectively. Cells expressing Rad9-HA and Rad4-R118G from pRep1, as well as cells expressing the Rad4-R118G construct from the *urg1* locus, as described previously, were used for an IP using HA-beads (Figure A.6). The cells were grown in the presence of additional biotin. Rad9-HA was enriched by IP in cells expressing Rad9-HA. Samples after irradiation show a slightly shifted band for Rad9-HA, consistent with phosphorylation. A membrane containing these samples was also probed with str-HRP, however no band

corresponding to Rad9-HA could be detected. These cells are expressing the endogenous Rad4 protein as well and the functionality of Rad4-FgB has to be tested further.

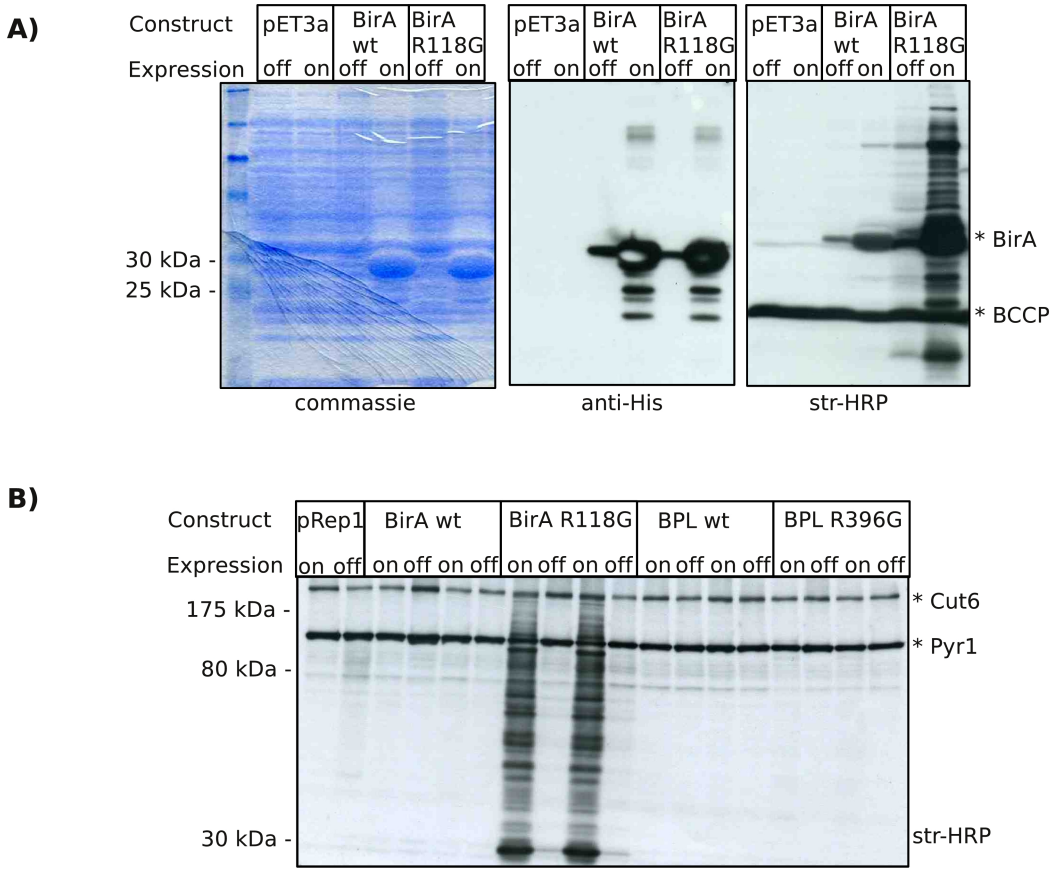

Figure A.4: Overexpression of BirA and R118G in *E. coli* and *S. pombe* cells
A) For overexpression in *E. coli*, the constructs were cloned into pET29b (*Nde*I, *Xho*I) resulting in a fusion to a 6x His tag. The vectors were transformed into BL21 cells. Cells were grown in LB supplemented with 5μM of biotin (d-biotin, Invitrogen, B1595). Expression in exponentially growing cells was induced by addition of 1mM isopropyl-beta-D-thiogalactopyranoside (IPTG) for 4 hours. As a negative control, cells containing the pET3a vector were used. The samples were separated by 12% SDS-PAGE and analysed by western blotting and commassie staining (left). Middle: anti-His antibody, right: streptavidin-HRP conjugate (str-HRP). The molecular weight marker is indicated on the left. Asterisks indicate the detected protein bands.
B) For overexpression in *S. pombe*, the constructs were cloned into pRep1 (*Nde*I, *Bam*HI). The vectors were transformed into *S. pombe* 501 wild-type cells. Cells were grown in minimal media supplemented with 5μM biotin and 15μM thiamine. Expression in exponentially growing cells was induced by removal of the thiamine and growth for 24 hours. The samples were separated by 8% SDS-PAGE and analysed by western blotting. Biotinylated proteins were detected with streptavidin-HRP conjugate (str-HRP). The molecular weight marker is indicated on the left. Asterisks indicate the detected protein bands. Strain genotypes are listed in Materials and Methods. Strains used: BirA wt; SAS477, BirA-R118G; SAS478, BPL wt (*S. pombe* BPL); SAS480, BPL-R396G; SAS479.

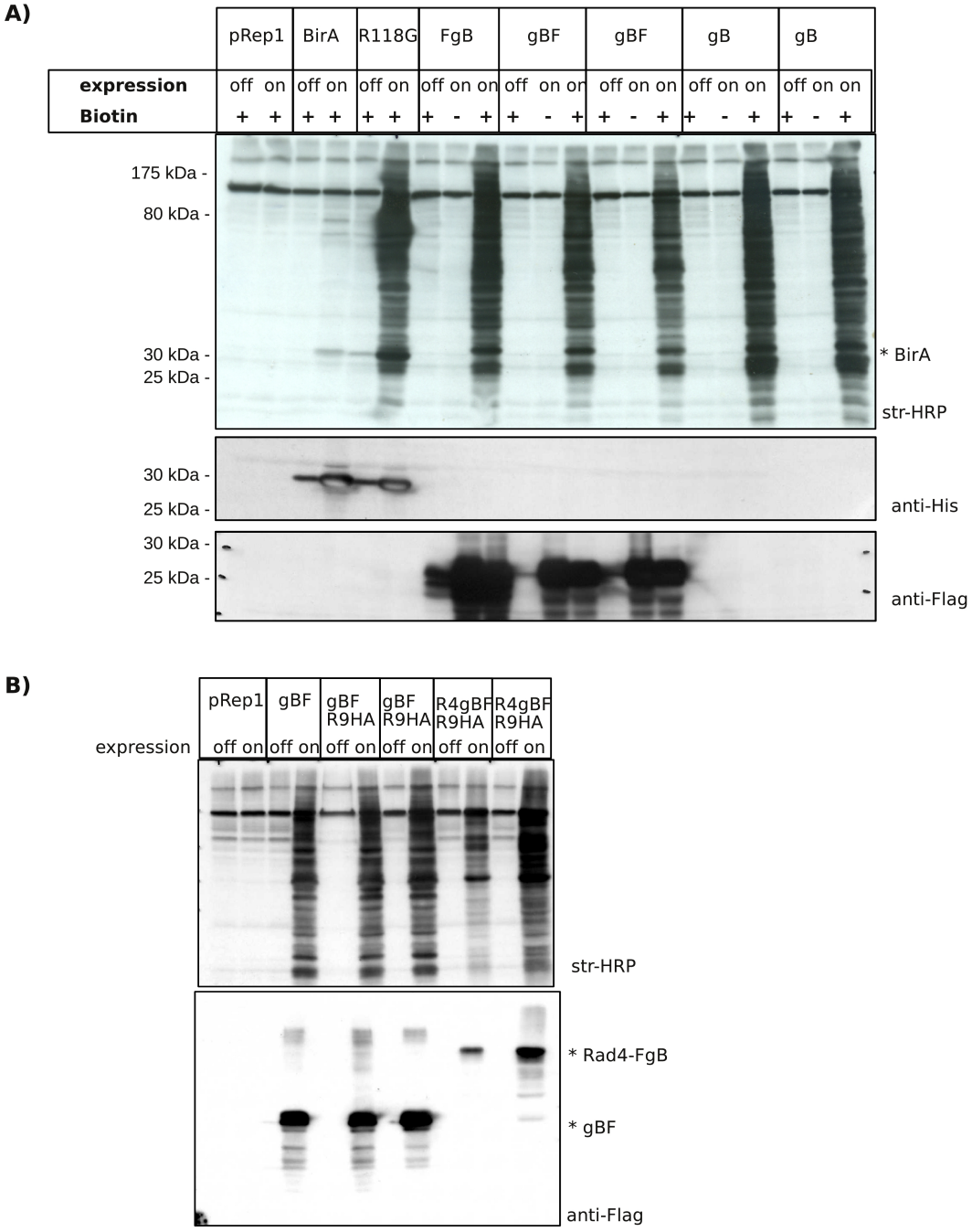

Figure A.5: Random biotinylation is dependent on the presence of additional biotin
A) Cells were grown in the presence or absence of 15μM thiamine and 5μM biotin for 20 hours, as indicated. Expression of the BirA constructs in exponentially growing cells was induced by removal of the thiamine and growth for 24 hours. The samples were separated by 10% SDS-PAGE and analysed by western blotting. Top: streptavidin-HRP conjugate (str-HRP), middle: anti-His, bottom: anti-Flag antibody. Asterisks indicate the detected protein bands. Strain genotypes are listed in Materials and Methods. Strains used: pRep1; SAS424, BirA; SAS477, BirA-R118G; SAS478, FgB (6x Flag-genscript-R118G); SAS426, gBF (genscript-R118G-6x Flag); SAS514/515, gB; SAS523/524 (genscript-R118G).
B) As in **A**. Strain genotypes are listed in Materials and Methods. Strains used: pRep1; SAS424, gBF; SAS514, gBF Rad9-HA; SAS525/526, R4gBF Rad9-HA; SAS527/528.

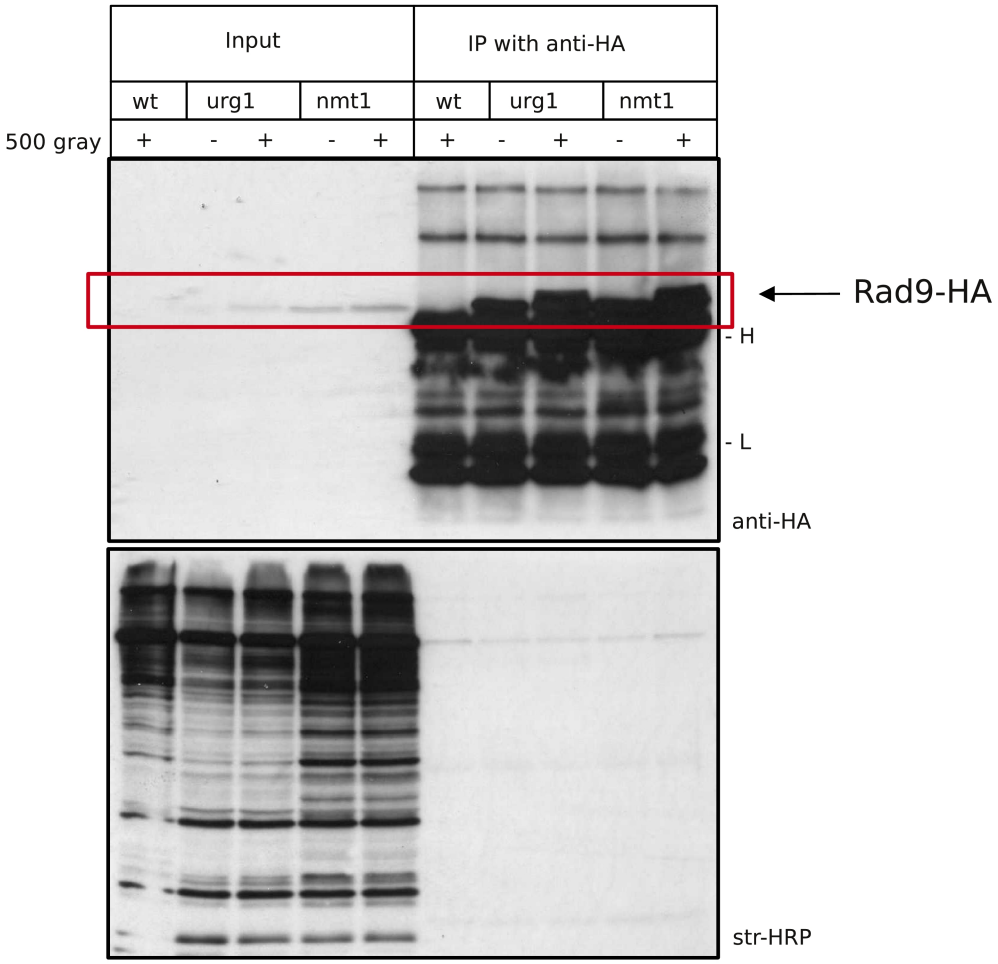

Figure A.6: IP of Rad9-HA and detection with streptavidin-HRP conjugate
Cells were grown in the presence of 5μM biotin and expression of Rad4-R118G was induced by addition of 0.25mg/ml uracil (urg1) or removal of thiamine for 20 hours (nmt1). Cells were irradiated as indicated, lysed and the extracts were used for IP with HA-beads. The samples were separated by 10% SDS-PAGE and analysed by western blotting. The antibody was not crosslinked to the beads, the detected heavy and light chains of the antibody are marked with H and L, respectively. Top: anti-HA antibody, bottom: streptavidin-HRP conjugate (str-HRP). The input corresponds to 1% of the total fraction. Strain genotypes are listed in Materials and Methods. Strains used: urg1 (co-expression of Rad4-R118G from the *urg1* promoter and Rad9-HA from the endogenous promoter); SAS419, nmt1 (co-expression of Rad4-R118G from the *nmt1* promoter and Rad9-HA from the endogenous promoter); SAS527.

A.5 Discussion

These results could not verify the use of promiscuous biotinylation for the identification of interaction partners. Further experiments are required to clarify whether this biotinylation reaction takes place in the nucleus and whether the high background of endogenously biotinylated proteins can be minimised. Chromatin extracts, as shown in Chapter 6 (Figure 6.3C), could be used for fractionation and replacing the endogenous copy of *rad4*$^{+}$ with the R118G tagged construct might help to improve this method.

Appendix B

Analysis of the short PCR product amplified from rura(inv)R

The PCR product of PP5 of 1250bp was gel purified and sent for sequencing to confirm which elements it contained. The sequencing results confirmed the presence of the rDNA RFB, RTS1 and part 'a'. However, sequencing from both ends resulted in an abrupt loss of signal after revealing a few bases of 'b' (Figure B.1A). This suggests that there might be some secondary structure which prevents the sequencing, but did not abort the PCR reaction. Consultation with the sequencing company (GATC Biotech) confirmed that the sequencing reaction was carried out at lower temperature (50°C) than the melting temperature (55°C) in the PCR reaction. In order to analyse this result further, the PCR was repeated with DMSO, which facilitates the disruption of hydrogen-bonds and secondary structures (Hentges et al., 2005; Jensen et al., 2010). This reaction still yielded a fragment of approximately 1250bp (Figure B.1B). Furthermore, an aliquot of the purified DNA which was sent for sequencing was separated by agarose gel electrophoresis using denaturing (alkaline) conditions and probed for either 'a' or 'cb' by Southern blot analysis. Under these conditions still no change in fragment size could be detected (Figure B.1C). However, probe 'a' was present in all fragments, whereas probe 'cb' only hybridised to the rura(dir)R samples, confirming the sequencing results. Taken together, the analysis of the 1250bp fragment suggests that it consists of rDNA RFB-ura(a)R, where a few basepairs of an inverted repeat ('b-b') could be detected between the rDNA RFB and 'a' (see Figure B.1A). This fragment is likely to be an artefact, considering that it shows the same band intensity in the PCR analysis in the parental sample and in clones 1-6 in Figure 4.3B (PP5).

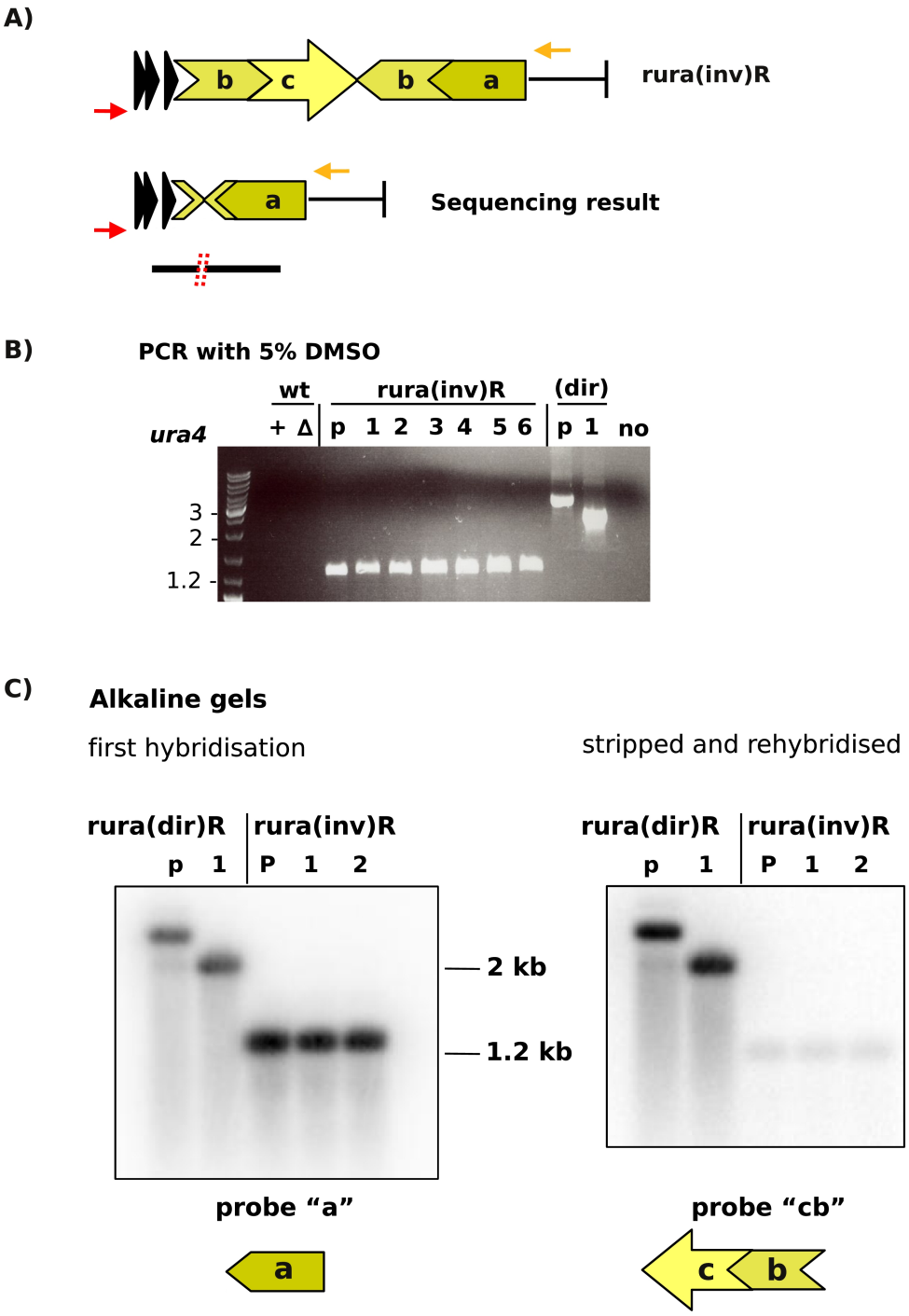

Figure B.1: Analysis of the short PCR fragment resulting from rura(inv)R PP5
A) The 1.25kb PCR fragment resulting from the reaction with PP5 on rura(inv)R (Figure 4.3B) was gel purified and send for sequencing. The black bars underline the sequencing results and the red dashed line indicates an abrupt loss of signal in the sequencing reaction.
B) The PCR with PP5 on rura(inv)R was repeated with 5% DMSO to facilitate denaturation of the template DNA. The template DNA used was the same as in Figure 4.3B. The sizes of the marker DNA are shown in kb.
C) PCR fragments were analysed by denaturing (alkaline) gel electrophoresis. The DNA was transferred onto a membrane by alkaline transfer and hybridised with radioactively labelled probes ’a’ and ’cb’, as indicated below the membranes. The faint bands in the three lanes of rura(inv)R are likely due to incomplete removal of probe ’a’ during stripping of the membrane.